University of California
Santa Barbara

The Many Facets of Black Hole Physics in AdS/CFT

A dissertation submitted in partial satisfaction
of the requirements for the degree

Doctor of Philosophy
in
Physics

by

Robinson Mancilla

Committee in charge:

Professor David Berenstein, Chair
Professor Gary Horowitz
Professor David Caratelli

June 2025

The Dissertation of Robinson Mancilla is approved.

Professor Gary Horowitz

Professor David Caratelli

Professor David Berenstein, Committee Chair

June 2025

The Many Facets of Black Hole Physics in AdS/CFT

Copyright © 2025

by

Robinson Mancilla

Para las Carmenes

Acknowledgements

First, I want to say a heartfelt thank you to my advisor, David Berenstein. You profoundly changed the way I think about physics—opening my eyes well beyond gravity—and gave me the freedom to follow my curiosity wherever it led. I deeply admire the way you understand physics; sometimes I wonder if I'll ever get close to that level myself. I've always enjoyed your sociological takes on how academia works. On the days when I felt lost or anxious, your advice meant more to me than I can express. It helped me focus, breathe, and return to the simple joy of doing physics.

Alejandra Castro, academia can be a difficult place for minorities. That's why I truly admire your strength—and the way you balance it with such warmth and generosity. Halfway through my PhD, I felt like I was struggling to find my place in the HEP community. Getting to know you—not just as a collaborator, but as a person—has meant a great deal to me and to my path in academia. I've learned so much from you—not only about physics, but also about what it means to be a professional physicist. The way I approach physics has been deeply influenced by you.

I would also like to thank my collaborators: Anayelli and Elliot—who would have thought that calculating geodesics numerically could be so time-consuming? And Ioannis Papadimitriou—our project with Alejandra has been long and, at many points, very confusing; thank you for your patience with all my questions and confusion.

To Gabriel Treviño, Adolfo Holguin, David Grabovsky, Jesse Held, Sean McBride, and Henry Leung—thank you for making me feel welcome and part of the group during the early years of my PhD. To Wayne W. Weng, Kwinten Fransen, Xiaoyi Liu, Leonel Quemeida, Peter Thomas Lloyd, Zhencheng Wang, Chih-Hung Wu, Diandian Wang, Jiuci Xu, Xuyang Yu, Zi-Yue Wang, Hiroki Kawai, Ziyi Li, Marija Tomašević, Carlos Perez-Pardavila, and Suzanne Bintaja—thank you for sharing with me a deep love for

physics. A special thanks to my TASI roommate, Henry, with whom I've shared, over the years, many meaningful conversations—about politics, physics, and the little things in life.

I would also like to thank Don Marolf, who was the only person in the world to reply to my emails when I was searching for PhD opportunities. To Gary Horowitz, Steve Giddings, Xi Dong, Mark Srednicki, David Berenstein, Don Marolf, and Clifford Johnson—thank you for all the physics I learned from your classes and from the gravity lunch discussions.

I spent many hours of my PhD engaged in teaching activities. I would like to thank David Caratelli and Andrea Young for their efficiency and their understanding of how busy we are as graduate students. To Sathya Guruswamy, thank you so much for spreading kind words about me across campus—it truly meant a lot. I'm deeply grateful to all the undergraduate students who have expressed such thoughtful and encouraging words about my role as a TA.

My physics journey began long before UCSB. To Nelson Zamorano—thank you for patiently listening to me talk about my dream of one day becoming an expert in quantum gravity, back when I barely knew any math or physics. To Jorge Alfaro, my master's advisor—thank you for always encouraging us to believe in ourselves and in the quality of our work. To Alberto Faraggi—one of the most beautiful moments of my life was during the Fulbright interview where I met you. For the first time, I felt that a professor truly recognized my potential in physics, despite the unfairness of my circumstances.

I'm truly proud of my Beauchef gang: Diego García, Bruno Scheihing, Ernesto Bianchi, and Nico Valdés. Our undergraduate physics department didn't have a HEP group, but we still found our own paths into HEP across different places in the US and Europe. Thank you also to my master's degree gang—Kevin Araya, Diego Tancara, Daniel Bonilla, Matias Briceño, and Anthony Canazas—for all the physics and spon-

taneous conversations we've had together. And to the Grav UC crew—Felipe, Nico, Camilo, and Mai—I just want to say that your efforts to promote quantum gravity at UC are truly admirable.

Since I was a child, I dreamed of building a better future for my family. Despite the injustice of our circumstances and the systemic barriers imposed by society, I never stopped pursuing that childhood dream. My mother's selflessness instilled in me an unwavering determination to overcome it all—alcoholism, socioeconomic hardship, physical and emotional violence, and every obstacle society placed in my path. In my twenties, during the darkest moments of my life, I never imagined that my childhood dream would one day come true—through the unlikely path of physics. The goddess of Fortune bowed to my determination in the most unexpected way.

Above all, I want to thank Paulina Peña, my girlfriend and partner in this journey, with all my heart. Over the past four years, distance has never weakened the deep emotional bond we share—a bond that has given me the stability I needed to face the challenges of a PhD. When things in academia weren't going the way I had hoped, and madness felt close, I thought of you—of the wonderful person you are—and I remembered what truly matters. Together, we are stronger.

Curriculum Vitæ

Robinson Mancilla

Education

2025	Ph.D. in Physics, University of California, Santa Barbara.
2020	M.A. in Physics, Pontificia Universidad Católica de Chile.
2017	B.A. in Physics, Universidad de Chile.

Publications

1. Alejandra Castro, **Robinson Mancilla**, and Ioannis Papadimitriou, *Near-extremal dynamics away from the horizon*, arXiv:2506.XXXXX [hep-th].
2. **Robinson Mancilla**, *Generalized Euler Equation from Effective Action: Implications for the Smarr Formula in AdS Black Holes*, arXiv:2410.06605 [hep-th].
3. David Berenstein, Elliot Maderazo, **Robinson Mancilla**, Anayeli Ramirez, *Chaotic LLM billiards*, JHEP 08 (2024) 056, arXiv:2305.19321 [hep-th].
4. David Berenstein, **Robinson Mancilla**, *Aspects of thermal one-point functions and response functions in AdS black holes*, Phys. Rev. D 107 (2023) 12, arXiv:2211.05144 [hep-th].

Abstract

The Many Facets of Black Hole Physics in AdS/CFT

by

Robinson Mancilla

The AdS/CFT correspondence offers a powerful framework for addressing fundamental questions in quantum gravity, enabling the study of strongly coupled quantum systems via semiclassical gravity. Simultaneously, non-perturbative quantum field theory techniques provide tools to probe the quantum nature of gravity. Over the years, numerous entries in the holographic dictionary have been uncovered; one particularly relevant to this work is the correspondence between thermal states in the boundary theory and black hole geometries in the bulk.

This thesis presents four distinct studies on key aspects of AdS black holes and their holographic implications for the dual CFT. The first analyzes the pole structure of thermal one-point functions for light operators, revealing nontrivial mixing between light modes and the stress tensor. The second, inspired by the AdS Smarr formula, establishes a generalized Euler relation for perfect fluids on curved spatial manifolds. The third investigates the emergence of Schwarzian dynamics from the perspective of higher-dimensional CFTs and their Ward identities, via a novel off-shell decoupling limit. Finally, the fourth explores whether LLM geometries with many droplets exhibit incipient black hole behavior, focusing on null geodesics trapped in regions of high droplet density.

Taken together, these studies illuminate diverse facets of AdS black hole physics in the holographic context, spanning thermal correlators, hydrodynamics, low-energy effective actions, and bubbling geometries.

Contents

Curriculum Vitae viii

Abstract ix

1 Introduction 1
- 1.1 Gravity . . . 1
- 1.2 Black Holes as a window into Quantum Gravity . . . 7
- 1.3 String theory . . . 14
- 1.4 Gauge/Gravity duality . . . 29
- 1.5 Organization of this thesis . . . 39
- 1.6 Permissions and attributions . . . 42

2 Thermal one-point function in AdS black holes 43
- 2.1 Introduction to the chapter . . . 44
- 2.2 The flat black brane case . . . 47
- 2.3 Some simple generalizations . . . 57
- 2.4 Conclusion . . . 74

3 A fluid perspective of Smarr formula 76
- 3.1 Introduction to the chapter . . . 76
- 3.2 Smarr formula for AdS black holes . . . 79
- 3.3 Effective action for perfect fluids . . . 84
- 3.4 Smarr formula as a particular case of the generalized Euler equation . . . 94
- 3.5 Comments on cosmological constant as a thermodynamic variable . . . 100
- 3.6 Discussion . . . 102

4 Near-extremal dynamics away from the horizon 105
- 4.1 Introduction to the chapter . . . 106
- 4.2 Aspects of $\mathrm{nAdS}_2/\mathrm{nCFT}_1$ . . . 108
- 4.3 Near-extremality at the boundary of $\mathrm{AdS}_3/\mathrm{CFT}_2$ . . . 129
- 4.4 Near-extremality at the boundary of TMG . . . 141
- 4.5 Near-extremality at the boundary of $\mathrm{AdS}_4/\mathrm{CFT}_3$ . . . 155

4.6 Discussion 174

5 Chaotic LLM Billiards **178**
5.1 Introduction to the chapter 179
5.2 LLM geometries 184
5.3 General dynamics of the system 188
5.4 The global $AdS_5 \times S^5$ geometry 191
5.5 Numerical results and graphs for one example: three disks 194
5.6 Conclusion 202
5.7 Appendix: Small Lyapunov exponents 204

Bibliography **207**

Chapter 1

Introduction

This introductory chapter aims to provide context and motivation for the research presented in this thesis, which lies within the field of quantum gravity. I envision this introduction as a conceptual roadmap, guiding the reader from classical aspects of gravity to the AdS/CFT correspondence. Rather than focusing on detailed derivations, the emphasis is placed on the overarching ideas and insights that have shaped my understanding throughout the course of my PhD.

1.1 Gravity

Before we delve into the intricate landscape of higher dimensions, dualities, and black holes, it is worth pausing to reflect on two foundational insights from Galileo Galilei:

1. The laws of physics are the same in all inertial frames of reference.

2. In free fall, all objects experience the same gravitational acceleration, regardless of their mass.

Regarding the first lesson, we recall that Newton's second law is covariant under spatial

diffeomorphisms and invariant under Galilean transformations. However, when formulated in a non-inertial reference frame, Newton's second law requires modification by the introduction of fictitious forces. This unaesthetic adjustment arises from the treatment of space and time as separate entities. In contrast, special relativity unifies space and time into a single geometric entity — spacetime — where the geodesic equation is inherently covariant. This allows it to naturally handle accelerating reference frames without the need for ad hoc corrections.[1]

The second lesson follows directly from the weak equivalence principle, which states that inertial mass is equivalent to gravitational mass.[2] As a result, over small regions of space and short time intervals, the effects of gravitational acceleration can be effectively canceled by moving to an accelerated frame. This insight was central to Einstein's revolutionary realization: gravity is not a force in the traditional sense, but a manifestation of spacetime curvature.

Understanding gravity in this way naturally leads to a profound conclusion: locally, accelerating frames are indistinguishable from inertial ones. This enhances our interpretation of Galileo's lessons, transforming them into statements about the nature of spacetime itself.

In Einstein's view of spacetime, a particle moving in a gravitational background follows a geodesic, governed by the equation:

$$u^\mu \nabla_\mu u^\nu = 0, \quad \nabla_\mu u^\nu = \partial_\mu u^\nu + \Gamma^\nu_{\mu\alpha} u^\alpha \ , \tag{1.1}$$

where $u^\xi = \frac{dx^\xi}{d\lambda}$ represents the particle's velocity, and λ is the affine parameter along the geodesic. The curvature of the spacetime is codified in the commutator of covariant

[1] In Minkowski spacetime, the Christoffel symbols encode two distinct effects: (i) the use of non-curvilinear coordinate systems and (ii) the description of accelerating frames.

[2] This principle is, in fact, an experimental fact verified to a precision of one part in 10^{15} [1].

derivatives:

$$[\nabla_\mu, \nabla_\nu]k_\alpha = R_{\mu\nu\alpha\xi}k^\xi \ , \tag{1.2}$$

where $R_{\mu\nu\alpha\xi}$ is the Riemann curvature tensor, and k^ξ is an arbitrary vector field.

The natural next step is to determine the background spacetime dynamically by introducing the field equations. To this end, we promote the spacetime geometry from a fixed background to a dynamical entity governed by the Einstein–Hilbert action:

$$S = \frac{1}{2\kappa^2}\int_{\mathcal{M}} d^4x\sqrt{-g}(R-2\Lambda) + \frac{1}{8\pi G}\int_{\partial\mathcal{M}} dx^3\sqrt{|h|}K + S_{matter} \ . \tag{1.3}$$

Here, Λ is the cosmological constant, $\kappa^2 = 8\pi G$ and G is Newton's constant. A remarkable property of the Einstein-Hilbert Lagrangian, $\mathcal{L}_{EH} = \sqrt{-g}(R-2\Lambda)$, is that the Ricci scalar behaves like $R \sim \partial^2 g$. Therefore, to ensure a well-defined variational principle, we must include the Hawking-Gibbons boundary term $\mathcal{L}_{HG} = \sqrt{|h|}K$, where K_{mn} is the extrinsic curvature, and h_{mn} is the induced metric of the boundary manifold $\partial\mathcal{M}$. The Einstein equation is then given by:

$$R_{\alpha\beta} - \frac{1}{2}Rg_{\alpha\beta} + \Lambda g_{\alpha\beta} = 8\pi G T_{\alpha\beta} \ . \tag{1.4}$$

The most compelling aspect of the Einstein equation is its *universal character*: all forms of matter and energy influence the geometry of spacetime through the energy-momentum tensor $T_{\alpha\beta}$. More precisely, one must solve the Einstein equation—a highly non-linear system of partial differential equations—coupled with the equations governing the dynamics of matter fields. Of course, this is much easier said than done.

Observables in gravity: The derivation of the Einstein–Hilbert action exhibits structural parallels with that of the Yang–Mills action coupled to charged matter. To illustrate

this analogy, consider a complex scalar field ϕ propagating in flat spacetime, minimally coupled to a background gauge field A_μ in the fundamental representation of a gauge group. The dynamics of the scalar field are governed by the action

$$S_{\text{scalar}} = \int d^4x (D_\mu \phi)^\dagger D^\mu \phi \ , \tag{1.5}$$

where the covariant derivative is defined as $D_\mu = \partial_\mu + iA_\mu$. The corresponding gauge field strength arises from the commutator of covariant derivatives:

$$[D_\mu, D_\nu] = iF_{\mu\nu} \ , \tag{1.6}$$

with $F_{\mu\nu}$ denoting the non-Abelian field strength tensor. By promoting the background gauge field A_μ to a dynamical variable, we are naturally led to the Yang–Mills action, constructed from a gauge-invariant quantity:

$$S_{\text{YM}} = -\frac{1}{2g_{\text{YM}}^2} \int d^4x \, \text{Tr}(F_{\mu\nu} F^{\mu\nu}) \ . \tag{1.7}$$

Observables in gauge theory are defined through gauge-invariant combinations, typically involving traces over products of field operators.[3] This construction relies on the internal gauge symmetry and the availability of a natural trace operation over the gauge group.

In gravity, however, the situation is markedly different. There is no direct analogue of a trace to construct local diffeomorphism-invariant observables. Instead, gravitational theories rely on the presence of boundaries—particularly at asymptotic infinity—to define meaningful, diffeomorphism-invariant quantities. These boundaries break certain diffeomorphisms, promoting them to physical symmetries of the system known as *asymptotic symmetries*. A key example is the notion of energy: locally, gravitational energy is mean-

[3] In gauge theory, there are local observables but also non-local observables such as Wilson Loops.

ingless, as one can always adopt an accelerating frame to eliminate the effects of gravity. Nonetheless, asymptotic symmetries yield conserved charges, enabling a well-defined, global notion of gravitational energy associated with a given spacetime.

Another way to illustrate the difference between gauge theory and general relativity is through a canonical analysis à la Dirac of gauge symmetries and diffeomorphisms. In Yang-Mills theory, the gauge generators $G^a(x)$ satisfy the following algebra:

$$\{G^a(x), G^b(y)\} = f_c^{ab}\,\delta(x-y)G^c(x)\ , \tag{1.8}$$

where f_c^{ab} are the structure constants of the gauge group, which remain the same at every point in spacetime.

In contrast, the algebra of diffeomorphisms in general relativity is more involved. It is constructed from the Hamiltonian constraint $H(x)$ and the momentum constraint $P_m(x)$, which generate time and space diffeomorphisms, respectively. These constraints are given by

$$\begin{aligned} H &= K^{mn}K_{mn} - K^2 - {}^{(3)}R\ , \\ P^m &= \nabla_n\left(K^{mn} - h^{mn}K\right)\ , \end{aligned} \tag{1.9}$$

where ${}^{(3)}R$ is the Ricci scalar and ∇_n is the covariant derivative associated with the induced spatial metric h_{mn}. The algebra of these generators takes the following form [2]:

$$\begin{aligned} \{H(x), H(y)\} &= \left(h^{mn}P_n\right)(x)\frac{\delta}{\delta x^m}\delta(x-y) - \left(h^{mn}P_n\right)(y)\frac{\delta}{\delta y^m}\delta(x-y)\ , \\ \{P_m(x), H(y)\} &= H(y)\frac{\delta}{\delta x^m}\delta(x-y)\ , \\ \{P_m(x), P_n(y)\} &= P_m(y)\frac{\delta}{\delta x^n}\delta(x-y) - P_n(x)\frac{\delta}{\delta y^m}\delta(x-y)\ . \end{aligned} \tag{1.10}$$

Unlike Yang-Mills theory, these generators do not form a Lie algebra due to the presence of structure functions, rather than constant structure coefficients. As a consequence,

gravity cannot be described in terms of fiber bundles in which spacetime is the base manifold and the symmetry group defines the fibers.[4]

Moreover, the bulk Hamiltonian in general relativity vanishes, $\mathcal{H}_{\text{bulk}} = 0$, reducing the bulk phase space action to a combination of the Hamiltonian and momentum constraints given in (1.9). In addition to the bulk dynamics, there exists a boundary canonical action that allows for the canonical definition of *surface charges*[5] associated with asymptotic symmetries for spacetime with boundaries. This is, for example, how the ADM mass is defined in asymptotically flat spacetime [3].

The globally well-defined symmetries within the asymptotic symmetry group typically leave the vacuum solutions of a gravity theory invariant. For example, asymptotically flat spacetimes in four dimensions possess the BMS algebra [4, 5], whose vacuum solution is Minkowski spacetime. The global part of the BMS algebra corresponds to the Poincaré group. Similarly, asymptotically AdS spacetimes in three dimensions exhibit a Virasoro algebra of charges [6], with AdS_3 as the vacuum solution. In this case, the global part of the Virasoro algebra matches the $SL(2,\mathbb{R}) \times SL(2,\mathbb{R})$ isometry group of AdS_3.

There is, however, an important exception to this rule: the isometries of de Sitter spacetime cannot be promoted to asymptotic symmetries. This is because asymptotically de Sitter spacetimes do not possess a boundary. Without a boundary, there is no mechanism to break certain diffeomorphisms, which is essential for defining asymptotic symmetries. Consequently, the physics of de Sitter spacetimes is conceptually more challenging than in the asymptotically flat or AdS cases.

[4] In the first-order formulation of gravity, where the spin connection $\omega^a_{\ b\mu}$ and frame fields e^a_μ are treated as independent variables, the spin connection transforms under the principal G-bundle over $\mathcal{M}$, with G being the (non-compact) Lorentz group. In this regard, the first-order formulation is closer to standard gauge theories, although these do not involve a metric structure [2].

[5] These surface charges can be viewed as an early indication of the holographic principle.

1.2 Black Holes as a window into Quantum Gravity

A natural starting point for discussing quantum gravity is to ask: Why should we even consider a quantum version of gravity? The short answer lies in the universality of Einstein's equations. While classical gravity accurately describes the behavior of spacetime at large scales, matter at very short distances is governed by the laws of quantum physics. Since, according to general relativity, spacetime is shaped by the matter content, this mismatch suggests that gravity itself must be subject to quantum principles in order to maintain a consistent description across all scales.

However, there are fundamental conceptual conflicts between the geometrical description of general relativity and the probabilistic nature of quantum mechanics. According to the uncertainty principle, probing shorter distances requires higher energy. For a particle of mass m, quantum mechanics associates a Compton wavelength $\lambda_C \sim \hbar/(mc)$, which sets the scale below which localization becomes uncertain. On the other hand, general relativity tells us that concentrating energy in a small region leads to the formation of a black hole when the energy is confined within its Schwarzschild radius $r_s \sim Gm/c^2$.

As we increase the energy to probe smaller distances, the Schwarzschild radius grows while the Compton wavelength shrinks. At the Planck scale—where $\lambda_C \sim r_s$—these two characteristic lengths become comparable. Equating them gives a natural energy scale known as the *Planck mass*, defined by

$$M_P = \sqrt{\frac{\hbar c}{G}}. \tag{1.11}$$

At this scale, quantum and gravitational effects become equally significant, and our current theories—quantum field theory and general relativity—cease to be adequate. This thought experiment suggests that the principle of locality may need to be abandoned

in a complete theory of quantum gravity. It strongly points to the need for a new framework that consistently unifies quantum physics and gravity at very high energies.

However, constructing such a framework is deeply challenging. Einstein's theory is highly non-linear and features non-trivial constraints: the Hamiltonian constraint and the momentum constraint, which satisfy the open algebra given in (1.10). As a result, a canonical quantization of gravity is notoriously difficult to implement.[6] For this reason, understanding the quantization of the linearized Einstein theory provides a natural starting point for exploring quantum gravity.

Yet even at the level of the linearized theory, a major obstacle arises: in four dimensions, pure gravity is famously non-renormalizable because the Newton constant has dimensions of length squared, $G \sim \ell_p^2 = \frac{1}{M_p^2}$.[7] This difficulty historically led to the view that gravity was fundamentally incompatible with quantum mechanics. However, from the modern Wilsonian perspective, such theories are perfectly valid as effective field theories (EFT), as long as they are applied at energy scales below a physical cutoff—in the case of gravity, the Planck mass M_p [8].

Moreover, the universal coupling of gravity to energy and momentum implies that any quantum field theory, including the Standard Model, must eventually couple to gravity. As a result, the Standard Model cannot remain decoupled from gravitational effects at arbitrarily high energies. Even though it is a renormalizable gauge theory, it must be viewed as an effective theory that breaks down before reaching the Planck scale, where new degrees of freedom are expected to emerge.

Numerically, the Planck scale is extraordinarily large: $M_p \sim 10^{19}$ GeV. In stark contrast, the electroweak scale is around 10^2 GeV. This enormous separation of scales

[6] Loop Quantum Gravity (LQG) is a canonical quantization approach formulated in terms of loop variables. However, a complete implementation of the constraint algebra remains elusive, and its status within the EFT paradigm continues to be a subject of debate [7].

[7] Power counting reveals potential divergences, but symmetries like supersymmetry can forbid certain counterterms, leading to cancellations and improved UV behavior [9].

suggests that gravity is, in fact, the most successful effective field theory, remaining valid over a vast range of energies before reaching its natural cutoff at the Planck scale [9].

At the same time, the large hierarchy between the electroweak and Planck scales remains deeply mysterious.[8] One possibility is that no new physics appears between these scales, and the Standard Model remains valid all the way up to the Planck scale. Alternatively, new physics—such as gauge coupling unification or other mechanisms—could emerge at intermediate energies.[9] From a theoretical standpoint, the latter scenario is widely regarded as more plausible, as it offers potential resolutions to the hierarchy problem and opens pathways toward the unification of gauge forces with gravity.

In summary, it is not accurate to claim that we know nothing about quantum gravity. Perturbative quantum gravity below the Planck scale can make meaningful predictions—for instance, quantum corrections to Newton's law [8]. Moreover, as in any EFT, one should include higher-derivative corrections to the Einstein-Hilbert action, accompanied by arbitrary Wilson coefficients. These corrections are highly suppressed at large distances, consistent with current experimental data. A central challenge in quantum gravity, however, is the absence of a known UV completion that determines the precise values of these coefficients—unlike in QCD, where the underlying theory uniquely fixes the coefficients of the low-energy pion Lagrangian.[10]

That said, the analogy between QCD and quantum gravity has important limitations. In particular, the presence of black holes gives rise to fundamentally new phenomena that lie beyond the scope of conventional QFT. As we will discuss, this is precisely why black holes serve as such a valuable window for exploring the principles of quantum gravity.

[8] If the Planck scale is used as the cutoff for the electroweak gauge theory, the Higgs mass would naturally be expected to be of the same order as the cutoff.

[9] In particular, in many extensions of the Standard Model, the gauge couplings are expected to unify at a scale around $M_{\rm GUT} \sim 10^{16}$ GeV, well below the Planck scale but still extraordinarily high [10].

[10] This statement holds in principle; however, due to confinement and the strongly coupled nature of QCD in the infrared, the low-energy coefficients cannot be derived analytically and must instead be obtained through other methods, such as experimental input or lattice QCD.

1.2.1 Black holes and the holographic principle

Up to this point, we have barely defined the main protagonists of this PhD work: black holes. For illustrative purposes, let us consider the AdS–Schwarzschild black hole in five dimensions, whose line element is given by

$$ds^2 = -f(r)dt^2 + f(r)^{-1}dr^2 + r^2 d\Omega_3^2 \ , \tag{1.12}$$

where the lapse function $f(r)$ is

$$f(r) = 1 - \frac{M}{r^2} + \frac{r^2}{\ell^2} \ . \tag{1.13}$$

Here, ℓ is the AdS radius, and M is proportional to the energy of the spacetime. The singularity of a black hole lies at $r = 0$, where the curvature diverges. In contrast, the horizon of the black hole is defined by the condition $f(r_h) = 0$, which specifies a null hypersurface in the geometry. According to the equivalence principle, locally near the horizon, no dramatic physical effects occur: the curvature remains finite and, for sufficiently large black holes, it becomes negligible. In this regime, the near-horizon geometry is well-approximated by the Rindler metric of flat spacetime. However, the global structure of the black hole spacetime is significantly different. The horizon acts as a surface of no return—signals originating from within the black hole, beyond the horizon, cannot reach an external observer, as the exterior lies in the causal past of such signals. As a consequence, black holes do not radiate in classical general relativity.

As Bekenstein first argued, black holes must possess entropy; otherwise, the infall of matter into a black hole would lead to a violation of the second law of thermodynamics [11]. Initially, Hawking was skeptical of this idea. However, through a groundbreaking calculation, he derived the black hole temperature and showed that black holes indeed

obey the laws of thermodynamics. Rather than reproducing Hawking's original derivation [12], we will instead employ the Euclidean approach [13], which highlights both the similarities and differences between a black hole and a *piece of coal*.

In statistical physics, thermal effects are studied by transitioning to *Euclidean time* and compactifying it. Specifically, consider a scalar or spinor field propagating in Euclidean spacetime $\mathbb{R}^4$. To introduce a finite temperature T, we compactify the Euclidean time direction as $t_E \sim t_E + \beta$, where $\beta = \frac{1}{T}$. This results in the manifold $S^1 \times \mathbb{R}^3$.

The compactification gives rise to a discrete spectrum of Kaluza-Klein (KK) modes, known as *Matsubara frequencies*. For bosonic and fermionic free fields, these frequencies are respectively given by

$$\omega_n^{(\text{boson})} = \frac{2\pi n}{\beta} = 2\pi n T \ , \quad \omega_n^{(\text{fermion})} = \frac{2\pi(n+\frac{1}{2})}{\beta} = 2\pi\left(n+\tfrac{1}{2}\right) T \ , \quad n \in \mathbb{Z} \ . \tag{1.14}$$

These discrete modes arise from the periodic (for bosons) or antiperiodic (for fermions) boundary conditions imposed along the compact Euclidean time circle. The inverse temperature $\beta = 1/T$ sets the compactification radius, which can be adjusted continuously.

In a similar fashion, we can apply this strategy to fields propagating on black hole spacetimes. However, black holes exhibit a distinctive feature: their temperature cannot be adjusted arbitrarily. Instead, there is a unique relation between the temperature and the event horizon radius. If this relation is not satisfied, a conical singularity would appear in the Euclidean geometry. This marks a fundamental difference between black holes and ordinary thermal systems, such as a piece of coal (see Figure 1.1).

For the AdS–Schwarzschild black hole, the Hawking temperature is given by

$$T = \frac{\hbar}{4\pi}\left(\frac{2}{r_h} + \frac{4r_h}{\ell^2}\right) \ , \tag{1.15}$$

where r_h is the event horizon radius. The proportionality of the temperature to $\hbar$ is consistent with the fact that, in the classical limit $\hbar \to 0$, black holes do not radiate.

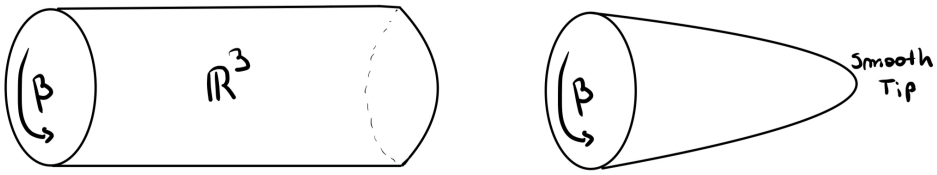


Figure 1.1: On the left-hand side is an illustration of how I visualize a piece of coal; on the right-hand side, we see a Euclidean black hole. In Lorentzian signature, the smooth tip of the Euclidean geometry corresponds to the location of the event horizon. In the jargon of black hole physics, we say that the black hole has a *contractible thermal circle*.

Furthermore, by analytically continuing the Matsubara frequencies to real time, one obtains complex frequencies whose real part corresponds to the physical oscillation frequency, and whose imaginary part captures the decay rate. These imaginary contributions are known as quasi-normal modes (QNMs), and they reflect how perturbations of the field dissipate into the black hole horizon.[11]

Returning to black hole thermodynamics: given the Hawking temperature, one can derive the entropy of a black hole, known as the *Bekenstein–Hawking entropy*:

$$S_{\text{BH}} = \frac{A}{4G} \,, \tag{1.16}$$

where A is the area of the black hole horizon, and we use natural units: $\hbar = c = k_b = 1$.

There are two important remarks about this result:

1. The mass of the black hole at the center of our galaxy, *Sagittarius A**, is approximately $M \sim 10^{36}$ kg, which corresponds to an entropy of $S_{\text{BH}} \sim 10^{90}$. This is vastly larger than the entropy of the Sun, which is approximately $\sim 10^{57}$. A natural ques-

[11] This claim relies on insights from the AdS/CFT correspondence. In particular, the AdS boundary is timelike, which allows for a well-controlled analytic continuation from Euclidean to Lorentzian signature for fluctuations around the background geometry.

tion arises: in the microcanonical ensemble, the entropy is given by $S = \ln \Omega$, where Ω is the number of accessible microstates. What, then, are the microstates that the black hole entropy is counting?

2. In conventional thermodynamic systems, entropy typically scales with volume.[12] However, for black holes, entropy scales with the *area* of the event horizon. What is the underlying reason for this unusual property of black holes?

Not only is black hole entropy a surface quantity, but the energy of a black hole also arises as a surface charge as we discussed before. In fact, for large AdS–Schwarzschild black holes where $r_h \gg \ell$, the entropy scales with temperature as [14]

$$S(T) \sim \frac{\ell^6}{2\ell_p^3} T^3 \ . \tag{1.17}$$

On the other hand, the entropy of a conformal field theory (CFT) in d spacetime dimensions scales as[13]

$$S_{\text{CFT}} \sim T^{d-1} \ . \tag{1.18}$$

Therefore, a CFT in four spacetime dimensions exhibits qualitatively similar entropy scaling to that of a five-dimensional large AdS–Schwarzschild black hole. However, the CFT_4 lives in one fewer dimension! In this way, black hole physics leads naturally to the holographic principle: the degrees of freedom associated with the black hole entropy can be encoded in a boundary quantum theory [15, 16].

In summary, black hole physics offers profound insights into quantum gravity. On one hand, black holes act as natural regulators of very high-energy processes, as discussed in

[12] This is true under the assumption that the spatial volume is non-compact. For compact volumes, finite-size corrections can modify this behavior even in the thermodynamic limit (large number of degrees of freedom). In chapter 3, this point will be fundamental.

[13] This result holds in flat space. If the CFT is placed in a curved space, there are additional corrections, which become especially important at low temperatures.

the introduction to this section. On the other hand, they reveal a fundamental limitation on the number of degrees of freedom that can be accommodated within a given region of spacetime, as implied by the holographic principle. Consequently, any UV completion of perturbative general relativity must not only reproduce the full set of Wilson coefficients associated with higher-derivative corrections to the Einstein–Hilbert action—governing graviton scattering at low energies—but also account for the microscopic origin of black hole entropy in a manner consistent with holography.[14]

1.3 String theory

In this section, we briefly introduce string theory, emphasizing its gravitational aspects. One might envision a modern version of the renowned Landau-Lifshitz series—a "theoretical minimum"—in which the classical string is left as an exercise for the reader, since it introduces no fundamentally new principles. The true marvel emerges upon quantization: the consistency of two-dimensional quantum gravity on the worldsheet requires that the target spacetime satisfy the Einstein equations, supplemented by specific matter content. Incorporating supersymmetry further enriches the structure of string theory, giving rise to new non-perturbative states: D-Branes. It also leads to five consistent superstring theories, all formulated in ten dimensions and intricately connected through a web of dualities, ultimately pointing toward a unifying framework known as M-theory.[15]

[14] Asymptotic safety program posits a non-trivial UV fixed point for gravity [9], but this seems to conflict with holographic principle [17].

[15] One of the most pedagogical resources for beginners in string theory is the lecture notes by David Tong [18]. Another excellent set of lecture notes is [19], where BRST quantization is explained in a clear and pedagogical manner.

1.3.1 Perturbative Strings

Classical aspects: A relativistic string is a one-dimensional extended object propagating through a D-dimensional spacetime. As it evolves in time, it traces out a two-dimensional surface called the *worldsheet*, denoted by Σ. The ambient spacetime, $\mathcal{M}$, is known as the *target space* and appears, from the worldsheet's point of view, as an internal space. The classical dynamics of the string are governed by the Nambu–Goto action, which is given by

$$S_{\mathrm{NG}}[X] = -T \int_{\Sigma} d^2\sigma \, \sqrt{-\det\left(\partial_a X^\mu \partial_b X_\mu\right)} \ , \tag{1.19}$$

where σ^a with $a = \{0, 1\}$ are the coordinates on the worldsheet.[16] The scalar fields $X^\mu = X^\mu(\sigma^0, \sigma^1)$ describe the embedding of the worldsheet into the target space, that is, they define a map $X : \Sigma \to \mathcal{M}$. The parameter T represents the string tension, which is historically related to the Regge slope α' by

$$T = \frac{1}{2\pi\alpha'} \ . \tag{1.20}$$

A classically equivalent formulation of the Nambu–Goto action is the Polyakov action:

$$S_P[X;\gamma] = -\frac{T}{2} \int d^2\sigma \, \sqrt{-\gamma}\, \gamma^{ab} \, \partial_a X^\mu \partial_b X_\mu \ , \tag{1.21}$$

where γ_{ab} is the intrinsic metric on the worldsheet. Integrating out γ_{ab} brings the action back to the Nambu–Goto form. The corresponding worldsheet stress-energy tensor is

$$T_{ab} = \partial_a X^\mu \partial_b X_\mu - \frac{1}{2} \gamma_{ab} \gamma^{cd} \partial_c X^\mu \partial_d X_\mu \ . \tag{1.22}$$

[16] Spacetime indices are denoted by Greek letters, $\mu = \{0, \ldots, D-1\}$ as in previous sections.

Invariance under two-dimensional diffeomorphisms, $\sigma^a \to \sigma'^a(\sigma)$, implies the covariant conservation of the stress-energy tensor, $\nabla^a T_{ab} = 0$. Since the Polyakov action is classically equivalent to the Nambu–Goto action, an additional gauge symmetry under Weyl transformations, $\gamma_{ab} \to e^{2\omega(\sigma)}\gamma_{ab}$, emerges to eliminate the extra, unphysical degrees of freedom associated with the worldsheet metric γ_{ab}. As a consequence, the stress-energy tensor must also be traceless, $T^a_{\ a} = 0$.

In two dimensions, the metric γ_{ab} possesses three local degrees of freedom, all of which can be eliminated *locally* by a combination of diffeomorphism and Weyl symmetries. However, this gauge-fixing can be *globally* obstructed by the nontrivial topology of the worldsheet—an aspect that becomes crucial in the quantum theory. Moreover, fixing the worldsheet metric γ_{ab} does not eliminate all redundancies; the residual symmetry is encoded in the emergence of the two-dimensional conformal group, governed by the conformal Killing equation:

$$(\delta_\xi + \delta_\omega)\gamma_{ab} = 0 \ , \tag{1.23}$$

where δ_ξ denotes an infinitesimal diffeomorphism, and δ_ω an infinitesimal Weyl transformation. By choosing the conformal gauge, $\gamma_{ab} = \eta_{ab}$, the conformal Killing equations yield an infinite-dimensional symmetry algebra known as the Witt algebra, the classical counterpart of the Virasoro algebra.

Quantum aspects: Quantizing the closed string in flat spacetime reveals a tachyonic mode,[17] a massless sector consisting of the graviton $h_{\mu\nu}$, the dilaton Φ, and the 2-form called Kalb–Ramond field $B_{\mu\nu}$, along with an infinite tower of massive higher-spin excitations. Similarly, the open string spectrum contains a tachyon, a massless vector field A_u, and an infinite tower of massive higher-spin states.

[17] A particle with negative mass squared signals an instability of the perturbative bosonic string vacuum.

Since strings are extended objects, they probe spacetime in a fundamentally different way than point particles. In fact, the quantum consistency of the two-dimensional gravity theory on the worldsheet requires the target spacetime to satisfy the Einstein equations coupled to matter fields, and this constraint is only satisfied in a specific number of dimensions. This condition arises naturally from the gauge-like nature of conformal symmetry in string theory. To understand this in detail, recall that in two dimensions, Weyl symmetry is anomalous, as expressed by the relation

$$\langle T^a_{\ a} \rangle = \frac{c}{24\pi} R \ , \tag{1.24}$$

where R is the Ricci scalar on the worldsheet and c is the central charge. However, a gauge symmetry cannot suffer from an anomaly without rendering the theory inconsistent. Thus, when considering the string partition function,

$$Z = \int \mathcal{D}\gamma \, \mathcal{D}X \, e^{iS_P[X,\gamma]} \ , \tag{1.25}$$

we must properly account for the gauge redundancy under diffeomorphisms and Weyl transformations. This is achieved by applying the Faddeev–Popov procedure, which introduces ghost fields into the path integral. Their contribution to the central charge must cancel that of the matter fields to preserve quantum conformal invariance:

$$c_{\text{ghost}} + c_{\text{matter}} = 0 \quad \Longrightarrow \quad c_{\text{matter}} - 26 = 0 \ . \tag{1.26}$$

Since each scalar field X^μ contributes with $c = 1$, we require 26 dimensions to ensure the consistency of the critical string in flat spacetime. Moreover, when considering the Polyakov action for a closed string in a curved background with additional massless fields,

the action takes the form

$$S = \frac{1}{4\pi\alpha'} \int d^2\sigma \, \sqrt{\gamma} \left[\gamma^{ab} G_{\mu\nu}(X) \, \partial_a X^\mu \partial_b X^\nu + \epsilon^{ab} B_{\mu\nu}(X) \, \partial_a X^\mu \partial_b X^\nu + \alpha' R^{(2)} \Phi(X) \right] . \tag{1.27}$$

We see that the string couples electrically to the two-form field $B_{\mu\nu}$ through its two-dimensional worldsheet, in direct analogy with how a charged particle couples electrically to a one-form gauge potential along its worldline.[18] The physical interpretation of the dilaton Φ will be discussed later. For now, let us simply note that, at the classical level, Φ breaks Weyl invariance unless it is constant.

The absence of conformal anomaly for the non-linear sigma model (1.27) leads to the following one-loop beta functions:

$$\begin{aligned} \beta^G_{\mu\nu} &= R_{\mu\nu} - \frac{1}{4} H_{\mu\lambda\rho} H_\nu{}^{\lambda\rho} + 2\nabla_\mu \nabla_\nu \Phi + \mathcal{O}(\alpha') = 0 \ , \\ \beta^B_{\mu\nu} &= -\frac{1}{2} \nabla^\lambda H_{\lambda\mu\nu} + \nabla^\lambda \Phi \, H_{\lambda\mu\nu} + \mathcal{O}(\alpha') = 0 \ , \\ \beta^\Phi &= \frac{D-26}{6} - \alpha' \left(R - \frac{1}{12} H_{\mu\nu\rho} H^{\mu\nu\rho} + 4\nabla^2 \Phi - 4(\nabla\Phi)^2 \right) + \mathcal{O}(\alpha'^2) = 0 \ . \end{aligned} \tag{1.28}$$

In this way, the classical breaking of Weyl invariance induced by the dilaton Φ is canceled by one-loop contributions involving the background fields $G_{\mu\nu}$ and $B_{\mu\nu}$. The corresponding 3-form field strength associated with the antisymmetric tensor field $B_{\mu\nu}$ is defined as: $H_{\mu\nu\rho} = \partial_\mu B_{\nu\rho} + \partial_\nu B_{\rho\mu} + \partial_\rho B_{\mu\nu}$. The action that encodes these beta functions is nothing other than the Einstein–Hilbert action coupled to matter fields:

$$S_{\text{eff}} = \frac{1}{2\kappa^2} \int d^{26}x \, \sqrt{-G} \, e^{-2\Phi} \left(R + 4(\nabla\Phi)^2 - \frac{1}{12} H_{\mu\nu\rho} H^{\mu\nu\rho} \right) + \mathcal{O}(\alpha') \ . \tag{1.29}$$

In conclusion, the internal consistency of bosonic string theory requires a 26-dimensional

[18] The ends of the open string can be thought of as point particles that couple electrically to the vector potential A_μ.

spacetime that satisfies the Einstein equations.[19] In this way, the graviton, initially appearing as a perturbative excitation of the closed string, is promoted to the fully non-linear theory of gravity described by Einstein's equations.

The mass gap between the massless sector and the first massive excitations of the higher-spin tower is $m^2_{\text{gap}} \sim \frac{1}{\alpha'} = \frac{1}{\ell_s^2}$. Consequently, at long distances $L \gg \ell_s$, only the massless modes survive and appear in (1.29). This regime corresponds to the point-particle limit, where the finite extension of the string becomes negligible. To gain further intuition, we note that the string length is given by $\ell_s = \sqrt{\alpha'}$, implying that the combination $\alpha'^n \partial^{2n}$ is dimensionless. Thus, the α' expansion corresponds to a derivative expansion, organized by the number of spacetime derivatives acting on the background fields.

One simple solution to the equations of motion (1.28) is a vanishing Kalb-Ramond field $B_{\mu\nu} = 0$, flat spacetime $g_{\mu\nu} = \eta_{\mu\nu}$, and a constant dilaton $\Phi(x) = \Phi_0$. At the level of the non-linear sigma model (1.27), this background introduces an additional contribution to the Polyakov action:

$$S = S_P[X;\gamma] + S_\chi[\gamma] \ , \quad S_\chi = \frac{\Phi_0}{4\pi}\int d^2\sigma\sqrt{\gamma}R^{(2)} = \chi \ , \tag{1.30}$$

where χ is the Euler characteristic of the worldsheet, given in terms of the genus h as $\chi = 2-2h$.[20] In other words, the 2d quantum gravity on the worldsheet is a topological theory. In string theory, interactions — corresponding to the joining and splitting of strings — are naturally captured by changes in the topology of the worldsheet. The perturbative expansion thus organizes into a topological expansion, with the string coupling controlled by the v.e.v of the dilaton field, $g_s = e^{\Phi_0}$. The corresponding partition function takes

[19] Instead of thinking in terms of extra dimensions, it is more appropriate to think in terms of central charge. This point is well illustrated in alternative background solutions—such as the linear dilaton model—where the spacetime dimension can differ from $d = 26$, as it can infer from equation (1.28).

[20] $h = 0$ corresponds to the sphere, $h = 1$ to the torus, and so on.

the form

$$Z_{\text{closed string}} = \sum_{h=0}^{\infty} g_s^{2h-2} Z_h \ , \tag{1.31}$$

where Z_h denotes the contribution from closed worldsheet geometries of genus h. Consequently, higher-loop corrections are suppressed by powers of g_s^{2h-2}. Remarkably, string theory predicts its own coupling through the dynamics of the dilaton field.

We now turn to the relation between string parameters and the 26-dimensional Newton constant, $G_N \sim \ell_p^{24}$. On dimensional grounds, the constant appearing in the effective action (1.29) in the string frame is $\kappa \sim \ell_s^{24}$. This leads to the following relation:[21]

$$8\pi G_N \equiv \kappa^2 e^{-2\Phi_0} \quad \Longrightarrow \quad \ell_p^{24} \sim \ell_s^{24} g_s^2 \ . \tag{1.32}$$

In the weak coupling regime $g_s \ll 1$, there is a parametric separation between the Planck and string scales:

$$g_s \ll 1 \quad \Longrightarrow \quad \ell_p \ll \ell_s \ . \tag{1.33}$$

This illustrates that the regime where perturbative string theory is under control is well-separated from the strongly coupled regime of gravity.

Let us now connect the current discussion to the broader expectations for a quantum theory of gravity, as outlined in Section 1.2. Perturbative string theory provides a UV completion of the non-renormalizable linearized Einstein theory. Roughly speaking, the extended nature of strings softens interactions near Planckian energies, rendering the theory UV finite. Moreover, the α' expansion naturally generates higher-derivative corrections to the Einstein theory, with the coefficients of these corrections playing the role of Wilson coefficients in an effective field theory description.[22]

[21] The Newton constant G_N is defined in the Einstein frame, while κ is defined in the string frame.

[22] This statement holds strictly in 26 dimensions; after compactification, the structure of higher-

However, up to this point, bosonic string theory says little about black holes. This is where supersymmetry becomes essential—not only to address black hole physics but also because our universe contains chiral fermions.

1.3.2 Superstring theory

The subject of superstring theory is vast, and our discussion will necessarily be brief due to constraints of space and time. The dynamics on the string worldsheet are governed by a 2d supergravity theory, in which the ghost fields contribute a central charge of $c_{\text{ghost}} = -15$. Consistency of the quantum theory requires the total central charge to vanish, leading to the condition

$$c_{total} = c_{\text{bosons}} + c_{\text{fermions}} + c_{\text{ghost}} = \frac{3}{2}(D-10) \ . \tag{1.34}$$

Here, each bosonic coordinate contributes $c_{\text{boson}} = 1$, while each worldsheet fermion contributes $c_{\text{fermion}} = \frac{1}{2}$. The requirement $c_{\text{total}} = 0$ then implies that the theory is consistent only in $D = 10$ spacetime dimensions—this defines the critical dimension for superstrings. Within this framework, there exist five consistent superstring theories:

- **Type I:** A $\mathcal{N} = 1$ supersymmetric theory that includes both open and closed unoriented strings. The antisymmetric two-form field $B_{\mu\nu}$ is projected out at tree level. Anomaly cancellation via the Green–Schwarz mechanism restricts the gauge group to $SO(32)$ [20].

- **Heterotic strings:** These are $\mathcal{N} = 1$ supersymmetric closed string theories constructed by combining the left-moving sector of the 26d bosonic string with the right-moving sector of the 10d superstring. Anomaly cancellation via the

derivative corrections must be reanalyzed in four dimensions.

Green–Schwarz mechanism requires the gauge group to be either $SO(32)$ or $E_8 \times E_8$ [21].

- **Type IIA and IIB:** These are $\mathcal{N} = 2$ supersymmetric closed string theories with independent left- and right-moving sectors. Type IIA is non-chiral, with opposite chiralities, while type IIB is chiral, with matching chiralities. Both include Ramond–Ramond (RR) potentials: type IIA has $C^{(1)}$ and $C^{(3)}$; type IIB has $C^{(0)}$, $C^{(2)}$, and a self-dual $C^{(4)}$.

Each of the five superstring theories[23] admits, in the low-energy limit, a corresponding supergravity (SUGRA) theory bearing the same name. In what follows, we focus only on type IIB SUGRA.[24]

Type IIB SUGRA: This theory features 128 fermionic degrees of freedom, as required by maximal $\mathcal{N} = 2$ supersymmetry in 10d. However, the bosonic sector consisting of the NS-NS sector given by the metric $G_{\mu\nu}$, the Kalb–Ramond field $B_{\mu\nu}$, and the dilaton Φ contributes only $35 + 28 + 1 = 64$ degrees of freedom. Supersymmetry thus demands an additional set of 64 bosonic degrees of freedom, which will play a central role in the discussion that follows. The bosonic part of the action is

$$S_{\text{IIB}} = \frac{1}{2\kappa^2} \int d^{10}x \, \sqrt{-G} \, e^{-2\Phi} \left(R + 4(\nabla\Phi)^2 - \frac{1}{12} H_{\mu\nu\rho} H^{\mu\nu\rho} \right) + S_{\text{RR}} + S_{\text{CS}} \ , \tag{1.35}$$

where the Ramond-Ramond sector is described by the following actions

$$\begin{aligned} S_{\text{RR}} &= -\frac{1}{4\kappa^2} \int d^{10}x \sqrt{-G} \Big(F_{(1)}^2 + \tilde{F}_{(3)}^2 + \frac{1}{2} \tilde{F}_{(3)}^{+2} \Big) \ , \\ S_{\text{CS}} &= -\frac{1}{4\kappa^2} \int C^{(4)+} \wedge H \wedge F_{(3)} \ . \end{aligned} \tag{1.36}$$

[23] The tachyonic mode present in bosonic string theory is absent in superstring theories.
[24] We follow the references [22, 23, 24] for the discussions on supergravity.

We adopt the convention that the kinetic term for a p-form RR field strength is normalized as $F^2_{(p)} = \frac{1}{p!} F_{\mu_1 \cdots \mu_p} F^{\mu_1 \cdots \mu_p}$. We also have introduced the following definitions

$$\begin{aligned} \tilde{F}_3 &= dC^{(2)} - C^{(0)} \wedge H \ , \\ \tilde{F}_5^+ &= dC^{(4)+} + \frac{1}{2} C^{(2)} \wedge H \ + \frac{1}{2} B \wedge F_{(3)} \ . \end{aligned} \tag{1.37}$$

The main feature of type IIB SUGRA action is the inclusion of the RR potentials $C^{(0)}, C^{(2)}, C^{(4)}$ which precisely contribute with $1 + 28 + \frac{1}{2} \cdot 70 = 64$ degrees of freedom after imposing the self-dual condition in $\tilde{F}_5$:

$$* \tilde{F}^+_{(5)} = \tilde{F}^+_{(5)} \ , \tag{1.38}$$

thereby matching the fermionic content of the theory and ensuring supersymmetry is preserved.

Classical duality symmetry: The type IIB SUGRA action has a $SL(2, \mathbb{R})$ duality group. To see this explicitly, we rewrite the action as follows

$$S_{IIB} = \frac{1}{16 \pi G_N} \int d^{10} x \sqrt{-g} \Big(R - \frac{1}{2} \mathcal{M}_{ab} \mathcal{F}^a \mathcal{F}^b - \frac{1}{4} \tilde{F}^{2+}_{(5)} - \frac{\partial_u \bar{\tau} \partial^u \tau}{2 (\mathrm{Im}(\tau))^2} \Big) + S_{CS} \ . \tag{1.39}$$

To get this expression, we went from the string frame to the Einstein frame $g_{\mu\nu} = e^{-\Phi/2} G_{\mu\nu}$, and we introduced the following field redefinitions

$$\tau \equiv C^{(0)} + i e^{-\Phi} \ , \quad \mathcal{F}^a_{(3)} \equiv \begin{pmatrix} H \\ F_{(3)} \end{pmatrix} \ . \tag{1.40}$$

In this context, $C^{(0)}$ is called an axion field since it is a pseudo-scalar field. The period matrix $\mathcal{M}_{ab}$ for the 2-form doublet $\mathcal{F}^a_{(3)}$ is given by

$$\mathcal{M}_{ab} = \frac{1}{\mathrm{Im}(\tau)} \begin{pmatrix} |\tau|^2 & -\mathrm{Re}(\tau) \\ -\mathrm{Re}(\tau) & 1 \end{pmatrix} . \tag{1.41}$$

In this way, the $SL(2,\mathbb{R})$ transformations act on the complex scalar field τ and 2-form doublet $\mathcal{F}^a_{(3)}$ as

$$\tau \to \frac{a\tau + b}{c\tau + d} , \quad \mathcal{F}^a_{(3)} \to \Lambda^a_b \mathcal{F}^b_{(3)}, \quad ad - bc = 1, \quad a, b, c, d \in \mathbb{R} . \tag{1.42}$$

while the metric g_{ab}, and self-dual 5-form $\tilde{F}^+_{(5)}$ remain the same. In the full string theory, quantum effects break the continuous $SL(2,\mathbb{R})$ symmetry down to its discrete subgroup $SL(2,\mathbb{Z})$. In particular, type IIB SUGRA is self-dual under S-duality, which maps $g_s \to 1/g_s$, implying that the strong-coupling limit of type IIB is again type IIB.[25]

1.3.3 D-Branes

Let's reverse the logic in how we think about string theory. In the NS–NS sector, we encounter the B-field, which is a generalization of the standard vector field A_μ, under which point particles are charged. A natural question then arises: what kind of object is charged under the B-field? The answer is a one-dimensional string, whose quantization gives rise to the massless NS–NS sector consisting of the fields $h_{\mu\nu}$, $B_{\mu\nu}$, and Φ plus an infinite tower of massive higher-spin quanta.

An interesting question now arises. Under S-duality, the B-field of the NS-NS sector

[25] The T-generator of $SL(2,\mathbb{Z})$ is not the T-duality of perturbative string.

is exchanged with the RR potential $C^{(2)}$, as seen from the transformation:

$$\tau \longrightarrow -\frac{1}{\tau}, \quad \begin{pmatrix} H \\ F_{(3)} \end{pmatrix} \longrightarrow \begin{pmatrix} F_{(3)} \\ -H \end{pmatrix} . \tag{1.43}$$

This implies that the low-energy effective theory cannot distinguish between fields that, in perturbative string theory, have entirely different origins. Notably, the fundamental string is neutral under the RR potential $C^{(2)}$ because it does not couple to it. This observation naturally leads to the conclusion that there must exist an object charged under $C^{(2)}$, which is invisible to the perturbative closed string spectrum. Moreover, since S-duality maps $g_s \to 1/g_s$, it suggests that this new object arises as a non-perturbative effect from the viewpoint of perturbation theory.

In the supergravity limit, these new objects are **p-branes** which are half-BPS states [25].[26] These (p+1)-dimensional extended objects are electrically charged under the RR potentials $C^{(p+1)}$, and are singular since they solve the equation of motion with delta function sources. The isometry of these solutions is $SO(9-p) \times \text{Poincare}(1,p)$. In the Einstein frame, the solutions are

$$\begin{aligned} ds^2 &= H_p^{-(7-p)/8} d\vec{x}^2 + H_p^{(p+1)/8} d\vec{y}^2 \ , \\ C^{(p+1)}_{0\ldots p} &= H_p^{-1} - 1 \ , \\ e^{\Phi} &= H_p^{-(p-3)/4} \ , \\ H_p = 1 + \frac{k^{7-p}}{r^{7-p}} \ , &\quad p < 7 \ , \quad r = \sqrt{y^2} \ . \end{aligned} \tag{1.44}$$

Here, x^a, $a = \{0, ..., p\}$ and y^m, $a = \{p, ..., 9\}$ are the coordinates along and perpendicular

[26] P-branes preserve 16 out of the 32 supercharges.

to the brane. The constant k in terms of string parameters is

$$k^{7-p} = c_p g_s N l_s^{7-p} \ , \quad c_p = \frac{(2\pi)^{5-p}\Gamma\left(\frac{7-p}{2}\right)}{(7-p)\Omega_{8-p}} \ . \tag{1.45}$$

The tension T_p of a single p-brane is

$$T_p = \frac{1}{(2\pi)^p l_s^{p+1} g_s} \ . \tag{1.46}$$

The p-brane saturates the BPS bound, $q_p = T_p$. These solutions obey the superposition principle, so that for a stack of N branes, the total charge and total tension are given by $Q_p = N q_p$ and $T_p^{\text{total}} = N T_p$, respectively. Since BPS states belong to short multiplets, they cannot continuously evolve into long multiplets under adiabatic deformations. This rigidity ensures that the BPS bound remains protected from quantum corrections.[27] Furthermore, the scaling $T_p \sim 1/g_s$ indicates that p-branes are non-perturbative objects exhibiting soliton-like behavior.

Non-perturbative p-branes play a central role in string theory, even though, at the perturbative level, type II string theories contain only closed strings. Remarkably, T-duality relates type IIA and type IIB by exchanging their Ramond–Ramond sectors. Nevertheless, open strings can be introduced into type II theories via non-perturbative effects. For open strings, T-duality acts on the worldsheet boundary conditions, transforming Neumann into Dirichlet conditions along compact directions. This mechanism gives rise to D-branes—hypersurfaces on which open strings can end. These D-branes are half-BPS objects, preserving 16 supercharges, and mirror the supersymmetry properties of supergravity p-branes.

[27] In extended supersymmetric theories with $\mathcal{N} \geq 2$, states annihilated by a subset of supercharges form short multiplets with reduced degrees of freedom. In contrast, long multiplets are generic representations in which all supercharges act non-trivially, yielding the maximal number of components.

The physical picture is as follows. At finite g_s, in the supergravity regime, one finds half-BPS p-brane solutions—extended objects carrying RR charge. Owing to their BPS nature, these p-branes can be reliably extrapolated to the weak-coupling limit $g_s \to 0$, where they appear as D-branes in perturbative string theory. In this limit, D-branes decouple from the closed string sector and behave as non-dynamical hypersurfaces imposing Dirichlet boundary conditions on open strings. The precise agreement in RR charges and tensions between supergravity p-branes and perturbative D-branes confirms that they are the same physical objects, described from complementary perspectives within string theory [26].

As we previously saw in the case of closed strings, the requirement of worldsheet conformal invariance—interpreted as a gauge symmetry—imposes constraints on the background fields, leading to Einstein's equations as consistency conditions for closed string propagation. We now turn to the analogous question for open strings ending on D-branes. In the perturbative open string spectrum, one finds gauge fields localized on the D-brane worldvolume, to which the endpoints of open strings are charged. Additionally, scalar fields arise, corresponding to fluctuations of the D-brane in directions transverse to its worldvolume. Requiring Weyl invariance of the open string sigma model in the presence of a background gauge field A_a leads to the vanishing of the beta function, whose solution is captured by the Dirac–Born–Infeld (DBI) action:

$$S_{D_p} = -T_p \int d^{p+1}\xi \, e^{-\Phi} \sqrt{-\det\left(G_{ab} + B_{ab} + 2\pi\alpha' F_{ab}\right)} \,, \tag{1.47}$$

where G_{ab} and B_{ab} are the pullbacks of the spacetime metric and the NS–NS 2-form field to the worldvolume swept out by the Dp-brane, and F_{ab} is the field strength associated with the gauge field A_a. This action resums all orders in α' in the field strength expansion, but is valid only for slowly varying F_{ab}. Derivative corrections involving ∂F appear

beyond the leading order.

In flat spacetime, we take $G_{ab} = \eta_{ab}$, $B_{ab} = 0$, and a constant dilaton $\Phi = \Phi_0$. Expanding the DBI action to leading order in α' (point-particle limit), one recovers the Maxwell action:

$$S_{\text{DBI}} = -T_p \int d^{p+1}\xi \, e^{-\Phi_0} + \int d^{p+1}\xi \, \frac{1}{4g_{\text{YM}}^2} F_{ab}F^{ab} + \mathcal{O}(\alpha'^4) \ , \tag{1.48}$$

where the effective Yang–Mills coupling on the Dp-brane is defined by[28]

$$\frac{1}{g_{\text{YM}}^2} = (2\pi)^{p-2}\alpha'^{(p-3)/2}e^{-\Phi_0} \ . \tag{1.49}$$

In particular, for a D3-brane, this reduces to

$$g_{\text{YM}}^2 = \frac{g_s}{2\pi} \ , \tag{1.50}$$

where we have used $g_s = e^{\Phi_0}$. For a stack of N coincident D3-branes, the low-energy effective theory is $\mathcal{N} = 4$ Super Yang–Mills (SYM) theory with gauge group $U(N)$, a topic we will return to later.

Black hole microstate: Strominger and Vafa gave the first microscopic account of black hole entropy by analyzing a D1–D5–P bound state [27]. This setup involves D1-branes along (x^0, y), D5-branes wrapping $(x^0, y, x^6, x^7, x^8, x^9)$, and momentum modes along $y = x^5$. The configuration is asymptotically flat, but near the horizon, it approaches an $\text{AdS}_3 \times S^3 \times K3$ geometry. Compactifying on $S^1 \times K3$ yields a five-dimensional BPS black hole.

At weak coupling, the system is described by a $(1 + 1)$-dimensional superconformal

[28] To derive this expression, one must use the D-brane tension expressed in terms of string parameters, as given in equation (1.46).

field theory. The momentum modes excite only the left-moving sector, as required by the BPS condition. The Cardy formula then counts the degeneracy of states, reproducing the black hole entropy. Roughly speaking, at weak coupling, the D1–D5–P system behaves as a gas of strings with momentum excitations, while at strong coupling, the same configuration manifests as a BPS black hole with a finite horizon area.

In summary, string theory provides a microscopic derivation of entropy for certain classes of BPS black holes by exploiting the non-renormalization properties of BPS states. In doing so, it meets several key criteria expected of a consistent theory of quantum gravity, as discussed in Section 1.2. However, string theory is not manifestly background-independent. The explicit quantization of perturbative strings is only feasible in specific background geometries, such as flat spacetime or pp-wave solutions, where enough symmetry is present to control the theory. This limitation may seem unsatisfactory from the perspective of gravitational physics, where background independence is a foundational principle. To address this issue, we now turn to an explicit realization of the holographic principle within string theory, where a gauge theory provides a background-independent formulation via a duality.

1.4 Gauge/Gravity duality

There are three important roads that lead to the holographic principle:

1. The asymptotic symmetries of gravitational theories with boundaries allow for the definition of conserved charges as surface quantities. Famously, the asymptotic symmetries of AdS_3 reproduce the Virasoro algebra with the following central charge:

$$c = \frac{3\ell_3}{2G_3} \,, \tag{1.51}$$

where $c \gg 1$ encodes a large number of degrees of freedom [6].

2. The fact that black hole entropy scales with the area of the horizon rather than its volume: $S = \frac{A}{4\ell_p^2}$, where $S \gg 1$ corresponds to a large number of microstates. Historically, it was this property of black holes that led to the formulation of the holographic principle [15, 16].

3. In the large-N limit, $SU(N)$ Yang-Mills theories exhibit a topological expansion:

$$\log(Z) = \sum_{h=0}^{\infty} N^{2-2h} F_h(\lambda) \ , \quad \lambda = g_{\rm YM}^2 N \ . \tag{1.52}$$

Here, λ is the 't Hooft coupling, which serves as an effective loop parameter for fixed topology in the large-N limit. The index h denotes the genus of a given two-dimensional surface. This expansion resembles the topological genus expansion of closed string theory, as given in (1.31), which describes a quantum theory of gravity [28].

To provide a concrete realization of the holographic principle, the dual nature of D-branes plays a fundamental role, as it serves as a bridge between gauge theories and gravity. Let's consider N-stack D3-branes with the following supergravity solution

$$\begin{aligned} ds^2 = \left(1+\frac{k^4}{r^4}\right)^{-1/2} \eta_{\nu\mu} dx^\nu dx^\mu + \left(1+\frac{k^4}{r^4}\right)^{1/2} (dr^2 + r^2 d\Omega_5^2) \ , \\ F_{0123r} = \frac{4k^4}{r^5} \ , \\ e^{\Phi} = g_s \ , \quad C^{(0)} = \frac{\theta}{2\pi} \ . \end{aligned} \tag{1.53}$$

Here, $k^4 = 4\pi g_s N \alpha'^2$. This solution is asymptotically flat, and the near-horizon approximation becomes

$$ds^2 = \frac{\ell_5^2}{u^2}\left(du^2 + \eta_{\mu\nu} dx^\mu dx^\nu\right) + \ell_5^2 d\Omega_5^2 \ , \tag{1.54}$$

where we introduced a new radial variable $u = \frac{k^2}{r^2}$ before expanding near $r \sim 0$. In this way, a stack of N D3-branes behaves like a soliton that interpolates between 10-dimensional Minkowski spacetime and the near-horizon geometry $\mathrm{AdS}_5 \times S^5$, where the AdS radius is identified as $\ell_5 = k$. The isometry group of this near-horizon background is $SO(2,4) \times SO(6)$, corresponding respectively to the conformal symmetry in four spacetime dimensions and the rotational symmetry of the internal five-dimensional space.

The near-horizon approximation of the D3-brane corresponds, in fact, to a decoupling limit in which only low-energy modes survive. To understand why this is the case, recall that the presence of a D3-brane backreacts on the spacetime geometry, leading to the metric given in equation (1.53). Now, we can relate the energy at infinity E_∞ and the energy of a local observer at r as follows

$$E_\infty = \left(1 + \frac{k^4}{r^4}\right)^{1/4} E_{local} \Longrightarrow E_\infty \sim \frac{\ell_5}{r} E_{local} \ , \quad r \to 0 \ . \tag{1.55}$$

Therefore, due to the redshift factor, the low-energy physics is described by the near-horizon region. Due to the strong gravitational redshift in the bulk, a mode localized near the horizon would require increasingly high energy to escape to infinity. As a result, low-energy excitations are effectively trapped in the near-horizon region, where they remain decoupled from the asymptotic bulk geometry. This is why the near-horizon limit isolates the low-energy sector of the theory.

Now that we have identified the AdS radius, we can construct two dimensionless parameters:

$$\frac{\ell_5^4}{\ell_s^4} \sim g_s N, \qquad \frac{\ell_5^4}{\ell_p^4} \sim N \ , \tag{1.56}$$

where ℓ_s is the string length, ℓ_5 is the AdS radius, and ℓ_p is the 10-dimensional Planck length. The supergravity approximation is valid in the regime where $\ell_5 \gg \ell_s$ and $\ell_5 \gg \ell_p$,

which corresponds to the double limit $g_sN \gg 1$ and $N \gg 1$. We can now extend this discussion to type IIB supergravity with asymptotically $AdS_5 \times S^5$ boundary conditions. In this context, the near-horizon geometry given in (1.54) is identified as the vacuum solution, and other solutions of the theory can be interpreted as "excited" states. Moreover, the isometry group $SO(2,4) \times SO(6)$ becomes the asymptotic symmetry group of the theory, playing a central role in defining observables in gravity as we emphasize at the end of section 1.1.

On the other hand, we also know that the low-energy effective description of a stack of N D3-branes is given by $\mathcal{N} = 4$ SYM theory, whose bosonic part of the action is:

$$S_{\rm YM} = \frac{1}{2g^2_{\rm YM}} \int d^4x {\rm Tr}\Big(- F_{\mu\nu}F^{\mu\nu} + 2D_\mu X^i D^\mu X^i - [X^i, X^j]^2\Big) + \frac{\theta}{8\pi^2} \int d^4x {\rm Tr}\Big(F_{\mu\nu}\tilde{F}^{\mu\nu}\Big) \ . \quad (1.57)$$

Here, the gauge group is $U(N)$. Furthermore, this theory is conformal invariant both at the classical and quantum level with conformal group $SO(2,4)$. Associated with the $\mathcal{N} = 4$ supersymmetry, there is also an R-symmetry given by $SO(6)_R \cong SU(4)_R$. In the D3-brane picture: Greek letters $\mu \in \{0, .., 3\}$ describe the worldvolume indices while Latin letters $i \in 1, .., 6$ are the indices describing the transverse fluctuations given by the six real scalar fields X^i.

In the large-N limit, it is natural to define the effective one-loop coupling—known as the 't Hooft coupling—as $\lambda = g^2_{\rm YM}N$, which, using equation (1.50), scales as $\lambda \sim g_sN$. This leads us to interpret equation (1.56) as an identification of parameters between the two theories:

$$\frac{\ell_5^4}{\ell_s^4} \sim \lambda, \qquad \frac{\ell_5^4}{\ell_p^4} \sim N \ . \quad (1.58)$$

At low energies, the system of N D3-branes admits two dual descriptions: A semiclassical type IIB supergravity description with asymptotically $AdS_5 \times S^5$ geometry, valid in the regime $\ell_5 \gg \ell_s$ (the point-particle limit) and $\ell_5 \gg \ell_p$ (weakly coupled gravity); An

equivalent description in terms of $\mathcal{N} = 4$ SYM theory with gauge group $U(N)$, valid in the strongly coupled regime $\lambda \gg 1$ and large number of degrees of freedom $N \gg 1$. This duality represents a strong–weak correspondence between a gauge theory and a gravitational theory.

The AdS/CFT correspondence is a conjectured duality between type IIB superstring theory on asymptotically $AdS_5 \times S^5$ spacetime and $\mathcal{N} = 4$ SYM theory with gauge group $U(N)$ and 't Hooft coupling λ, proposed to hold for all values of N and λ [29].

It is important to emphasize that the derivation presented above is valid in the regime where $N \gg 1$ and $\lambda \gg 1$, where the string theory side admits a reliable classical supergravity description. But why should one conjecture that the duality holds for all values of N and λ, beyond the low-energy limit of the D3-brane stack that originally motivated it? The key motivation lies in the fact that large-N gauge theories exhibit a topological expansion reminiscent of closed string perturbation theory, suggesting a deeper connection that may persist beyond the supergravity limit. Extending the correspondence to this more general regime, however, would require a full quantization of closed strings in the $AdS_5 \times S^5$ background—a notoriously difficult problem due to the nontrivial RR 5-form flux that supports the geometry. To date, a complete quantization in this background remains an open challenge.

Nonetheless, compelling evidence for the validity of the correspondence at finite N and λ comes from studying the Penrose limit of $AdS_5 \times S^5$, which yields a maximally supersymmetric pp-wave background. In this limit, string theory becomes exactly solvable. On the gauge theory side, this corresponds to taking a large R-charge limit in $\mathcal{N} = 4$ SYM theory, isolating a closed subsector known as the BMN sector. Remarkably, this sector reproduces the spectrum of string excitations in the pp-wave background [30], offering strong evidence in support of the AdS/CFT correspondence beyond the supergravity approximation.

1.4.1 Holographic dictionary

To date, the holographic dictionary contains numerous entries; here, we focus on those most relevant to this work, particularly those concerning symmetries and correlation functions.

Symmetries: The "zeroth entry" of the holographic dictionary states that the asymptotic symmetries of AdS spacetime correspond to the global symmetries of the dual field theory. The canonical example is the duality between $\mathcal{N} = 4$ SYM theory and type IIB superstring theory on asymptotically $AdS_5 \times S^5$, both of which share the conformal symmetry group $SO(2,4)$ and the R-symmetry/rotational symmetry group $SO(6)_R$.

A natural way to test the AdS/CFT correspondence is to ask whether gravity can reproduce the quantum anomalies of the dual field theory—highly non-trivial features of quantum dynamics. Remarkably, it can. A celebrated example is AdS_3, where the asymptotic symmetry algebra forms two copies of the Virasoro algebra with a large central charge $c \gg 1$, as given by the Brown–Henneaux formula (1.51). This result aligns with the expectation that any holographic CFT must have a large number of degrees of freedom to accommodate the extra dimensions in the gravitational dual. More generally, it was shown in [33] that the gravitational theory correctly accounts for the presence—or absence—of Weyl anomalies across dimensions. An explicit realization of the diffeomorphism anomaly in a boundary CFT_2 was later provided in [34]. In short, gravity knows about quantum anomalies.

Let us now turn to the role of asymptotic symmetries in defining a quantum theory of gravity. At low energies, quantum gravity can be formulated using a path integral approach which, in the spirit of Feynman, involves summing over all geometries—both on-shell and off-shell. In this framework, the diffeomorphism invariance of gravity implies that local observables are not well-defined: in a theory without a fixed background space-

time, the very notion of a spacetime event loses meaning. Instead, physically meaningful observables must be defined at the boundary, where asymptotic symmetries provide a natural structure for identifying diffeomorphism-invariant quantities.

This perspective, where boundary conditions are essential to defining the theory, naturally leads to a broader insight: a background-independent formulation of string theory may emerge through its boundary dual. Specifically, type IIB superstring theory on asymptotically $AdS_5 \times S^5$ is fully defined, in a manifestly background-independent way, by $\mathcal{N} = 4$ SYM theory "living" on the boundary.

GKPW dictionary: AdS spacetime has a timelike boundary, which means that any propagating field in this background requires specified boundary conditions to define a well-posed dynamical problem. More generally, one can consider spacetimes that are asymptotically AdS, potentially with nontrivial matter content, provided that appropriate boundary data are assigned to all fields in the theory. The key insight of Gubser, Klebanov, Polyakov, and Witten (GKPW) is that these boundary data correspond, in the dual field theory, to sources for specific operators [35, 36].

In this way, the GKPW dictionary provides a simple yet powerful statement: the partition function of the CFT equals that of quantum gravity in AdS,

$$Z_{\text{CFT}}[J, g_{ik}, A_k] = Z_{\text{AdS}}[\phi^{(0)}, g_{ik}^{(0)}, A_k^{(0)}] \ . \tag{1.59}$$

In this correspondence:

- J is the source for a generic operator $\mathcal{O}_J$ in the CFT, g_{ik} and A_k are the background metric and background gauge field of the CFT with boundary indices $\{i, k\}$,
- $\phi^{(0)}$, $g_{ik}^{(0)}$, and $A_k^{(0)}$ are the boundary values of the bulk matter field, metric, and gauge field, respectively. Here, the bulk indices are $\{i, k, r\}$ where r is the radial

coordinate.

These quantities are identified as follows: $J = \phi^{(0)}, g_{ik} = g^{(0)}_{ik}, A_k = A^{(0)}_k$. This implies that one-point functions of the dual CFT operators can be computed by functional differentiation of the gravitational generating functional $W = \log Z$ with respect to the boundary sources:

$$\begin{aligned} \langle T_{ik}(x)\rangle_g &= -\frac{2}{\sqrt{-g^{(0)}}}\frac{\delta W}{\delta g^{(0)}_{ik}(x)} \ , \\ \langle J_i(x)\rangle_A &= -\frac{1}{\sqrt{-g^{(0)}}}\frac{\delta W}{\delta A^{(0)}_i(x)} \ , \\ \langle \mathcal{O}_J(x)\rangle_J &= -\frac{1}{\sqrt{-g^{(0)}}}\frac{\delta W}{\delta \phi^{(0)}(x)} \ . \end{aligned} \tag{1.60}$$

Higher-point correlation functions can be obtained by successive functional differentiation with respect to the corresponding sources.

To carry out this holographic procedure explicitly, one must solve the bulk equations of motion and expand the solutions near the AdS boundary. Mathematically, this becomes a Dirichlet boundary problem for the radial coordinate: the boundary condition near the AdS boundary is universal across all geometries, while the condition in the interior of the bulk depends on the specific geometry under consideration. To illustrate this, consider a massive scalar field propagating in a fixed geometry, expanded near the AdS boundary:

$$\phi(x,r) = \phi^{(0)}(x)\Big(\frac{r}{\ell}\Big)^{\Delta} + \frac{2\ell}{d}\langle \mathcal{O}_J(x)\rangle_J \Big(\frac{r}{\ell}\Big)^{d-\Delta} + ... \tag{1.61}$$

This expansion defines the boundary source as $J = \phi^{(0)}(x)$. The relation between $\phi^{(0)}$ and $\langle \mathcal{O}_J(x)\rangle_J$ is then determined by solving the Dirichlet problem subject to an appropriate boundary condition in the interior of the bulk geometry. For instance, in the vacuum solution—AdS spacetime—the appropriate boundary condition corresponds to regularity at the center of AdS. In the case of black holes, the second boundary condition is imposed at the horizon, where one can choose among several options, such as ingoing or outgoing

boundary conditions, which lead to retarded or advanced Green's functions, respectively [31, 32].

It is important to note that, in evaluating the partition function, holographic renormalization must be performed to regulate IR divergences arising from the infinite volume of AdS spacetime. In the dual field theory, these IR divergences correspond to the familiar UV divergences [33, 37]. Similar expansions to (1.61) must be carried out for the bulk metric and gauge field in order to compute their corresponding dual operators.

Furthermore, this asymptotic expansion allows one to extract the scaling behavior of the dual operator, thereby identifying its conformal dimension. In particular, the conformal dimensions of the operators considered in (1.60) are:

- The boundary stress-energy tensor, dual to the bulk metric, has conformal dimension $\Delta = d$.
- The boundary $U(1)$ current, dual to a bulk gauge field, has conformal dimension $\Delta = d - 1$.
- For a scalar field of mass m, the dual operator has conformal dimension $\Delta = \frac{d}{2} + \sqrt{\frac{d^2}{4} + m^2 \ell_{\text{AdS}}^2}$.

This correspondence between bulk asymptotics and boundary operator dimensions is a central feature of the holographic dictionary. Moreover, given the asymptotic symmetries of the theory, one can verify that the one-point functions in equation (1.60) satisfy the corresponding CFT Ward identities, including possible anomalies, as previously discussed—with details depending on the spacetime dimension.

Black holes: As discussed in Section 1.2, the thermodynamic properties of black holes can be studied by examining their Euclidean counterparts. In this formulation, a bulk geometry describing a Euclidean eternal AdS black hole is holographically dual to

a thermal state in the boundary theory, and the correlators in equation (1.60) are interpreted as thermal one-point functions. Alternatively, in Lorentzian signature, thermal correlators are computed using the Schwinger–Keldysh formalism, which involves doubling the sources to obtain advanced, retarded, and Feynman propagators. Remarkably, this doubling has a geometric counterpart: it aligns precisely with the boundary data defined on the left and right asymptotic regions of an eternal black hole [31]. As a result, the QNMs of the black hole manifest as poles of the retarded Green's function [32].

As a final remark on the holographic dictionary, it is generally expected that the entropy of $\mathcal{N} = 4$ SYM theory scales as $S \sim N^2$ in the large-N limit. From the gravity side, black hole thermodynamics yields a prediction for this entropy, as presented in equation (1.17). When expressed in terms of field theory parameters using the holographic identifications in equation (1.58), this result becomes

$$S \sim \frac{N^2}{2} T^3 \mathrm{Vol}(\mathbb{R}^3) \ . \tag{1.62}$$

Here, $\mathrm{Vol}(\mathbb{R}^3)$ is the spatial volume on which $\mathcal{N} = 4$ SYM is defined, thereby providing a full conceptual realization of the holographic principle envisioned by 't Hooft and Susskind around 1993 [15, 16].

Final remarks: We began this introductory chapter with a simple observation: in free fall, all objects experience the same gravitational acceleration, regardless of their mass. Just a few pages later, the discussion naturally led us to extra dimensions, unexpected dualities, extended objects, and black holes. This mirrors the arc of my own journey in physics—what began as a fascination with gravitational acceleration culminates in a PhD exploring its deepest mysteries. Gravity, indeed, works in mysterious ways.

1.5 Organization of this thesis

In this chapter, we have outlined a roadmap that begins with Galileo Galilei's elementary observations on inertia and gravitational acceleration and leads to our modern understanding of quantum gravity, as described by string theory and the AdS/CFT correspondence. Having now established the key concepts of holography, we are equipped to explain the structure and interconnections of the chapters that follow in this thesis.

In Chapter 2, we study a probe scalar field propagating in a black hole background, interacting with the Weyl factor of the geometry. In the dual CFT, this corresponds to a light operator with conformal dimension $\Delta \sim O(N^0)$ in a thermal state. The thermal one-point function can be interpreted in the microcanonical ensemble, via the ETH hypothesis [38, 39], in terms of heavy–light–heavy configuration $\langle H|\mathcal{O}_L|H\rangle$, where $|H\rangle$ is a state with $\Delta \sim O(N^2)$ corresponding to the black hole. In the large-N limit, light operators behave as generalized free fields, so their thermal one-point functions vanish, as they correspond to OPE coefficients. This makes the interaction with the Weyl factor essential: it can be viewed as an α' correction that generates a non-trivial one-point function [40, 41]. As we will study analytically, this coupling also induces operator mixing between the light operator and the stress tensor.

In Chapter 3, we investigate the physical meaning of the Smarr formula for AdS black holes through the lens of fluid/gravity duality. Thanks to recent developments in this duality, we now understand that strongly coupled quantum field theories in the long-wavelength regime are governed by the laws of hydrodynamics [42]. In particular, the gradient expansion of the Ward identities around a local thermal state gives rise to a relativistic generalization of the Navier–Stokes equations, potentially modified by quantum anomalies. From this modern perspective, constructing an effective action for the fluid is essential—not only for capturing the classical hydrodynamic behavior but

also for systematically computing thermal and quantum fluctuations [43, 44].

To elucidate the physical content of the Smarr formula in the dual theory, we construct an effective action for a perfect fluid that generalizes the standard Euler relation by incorporating the effects of spatial curvature into the fluid description. This generalization is derived purely from effective field theory techniques, rendering it independent of the AdS/CFT correspondence. As such, the resulting Euler relation may find applications beyond holography, including astrophysical contexts or $(2+1)$-dimensional condensed matter systems in the hydrodynamic regime with non-trivial spatial geometry. When embedded within AdS/CFT, this effective framework naturally recovers the Smarr formula for AdS black holes as a particular instance of a broader thermodynamic identity. Moreover, since this construction holds off-shell, it opens the door to further questions, such as the derivation of the Schwarzian action from a perfect fluid effective theory.

In Chapter 4, our goal is to understand the emergence of the Schwarzian theory in the low-temperature regime of holographic CFTs. The Schwarzian theory is a universal low-energy effective action that appears in a broad class of systems, including the SYK model and near-extremal charged or rotating black holes [45, 46]. In the latter case, and guided by our confidence in the AdS/CFT correspondence, it is natural to expect that holographic CFTs must exhibit a Schwarzian sector at low temperatures. Our aim is to make this expectation precise and to address a gap in the existing literature.

To this end, we exploit the fact that, although the Schwarzian action transforms anomalously under one-dimensional Weyl transformations, this anomaly is not a genuine quantum anomaly. This observation motivates the construction of a gravitational phase space dual to the Ward identities of the holographic CFT. By carefully analyzing the bulk decoupling limit, we systematically map it to a 'gradient' expansion of the boundary Ward identities, thereby reproducing the Schwarzian Ward identities in the boundary theory. We explicitly demonstrate this construction for both CFT_3 and CFT_2, including

scenarios with equal and unequal left- and right-moving central charges.

In Chapter 5, we study specific classes of null geodesics in LLM geometries to draw analogies with the fuzzball proposal. In gravity, there exist smooth, horizonless BPS geometries that are asymptotically indistinguishable from black holes and share the same quantum numbers. The distinction between black holes and horizonless geometries becomes apparent only when probing the region near where the horizon would be located. The fuzzball proposal asserts that a black hole is a coarse-grained description of an ensemble of possible microstate geometries [47, 48]. In this context, several natural questions arise: Can an individual microstate geometry behave qualitatively like a black hole? Do signals generally take a very long time to escape from the center of the geometry? Are there large tidal forces that tear objects apart?

To explore these questions, we turn to LLM geometries, which provide a concrete and tractable setting that shares key features with fuzzball geometries. These are 1/2 BPS solutions of type IIB supergravity on $AdS_5 \times S^5$ [49]. In $\mathcal{N} = 4$ SYM, they correspond to a simple sector described by two-dimensional incompressible droplets of free fermions [50]. In particular, numerical studies of in-plane null geodesics in LLM geometries with many droplets reveal chaotic behavior. In regions of high droplet density, these geodesics become effectively trapped for extended periods, offering a mechanism through which signals may be lost in the putative black hole.

Overall, each chapter of this thesis investigates a distinct aspect of black hole physics within the broader framework of the AdS/CFT correspondence. The variety of topics reflects the central role black holes have played in shaping modern theoretical physics. Our overarching goal is to refine and deepen the entries of the holographic dictionary and, in doing so, illuminate the fundamental nature of black holes.

1.6 Permissions and attributions

1. The content of Chapter 2 is based on work done in collaboration with David Berenstein and has previously appeared in Physical Review D [51]. These materials are reproduced in accordance with the copyright policy of the American Physical Society.

2. The content of Chapter 3 is based on the preprint [52], available on the arXiv.

3. The content of Chapter 4 is the result of a collaboration with Alejandra Castro and Ioannis Papadimitriou, and is adapted from a forthcoming preprint [53].

4. The content of chapter 5 is the result of a collaboration with David Berenstein, Elliot Maderazon, and Anayelli Ramirez, and has previously appeared in the Journal of High Energy Physics [54]. It is reproduced here with the permission of the International School of Advanced Studies (SISSA): Open Access and Copyright Terms

Chapter 2

Thermal one-point function in AdS black holes

In this chapter, we revisit the problem of analytically computing the one point functions for scalar fields in planar AdS black holes of arbitrary dimension, which are sourced by the Weyl squared tensor. We analyze the problem in terms of power series expansions around the boundary using the method of Frobenius. We clarify the pole structure of the final answer in terms of operator mixing, as argued previously by Grinberg and Maldacena. We generalize the techniques to also obtain analytic results for slowly modulated spatially varying sources to first non-trivial order in the wave vector for arbitrary dimension. We also study the first order corrections to the one point function of the global AdS black hole at large mass, where we perturb in terms that correspond to the curvature of the horizon.

2.1 Introduction to the chapter

The AdS/CFT correspondence [29] provides information about field theories at strong coupling by performing gravity calculations. Correlators of the field theory can be expressed as boundary correlators of the AdS geometry [35, 36]. In particular an AdS black hole corresponds to a thermal state in the field theory. Usually, one uses the eigenstate thermalization hypothesis (ETH) [38, 39] to argue that it does not matter if the state in question is pure (with the right energy, charge, etc) or mixed: their average properties will be the same. It is important that if the state in question is pure, some correlation functions that can be studied can also be interpreted as OPE coefficients or four point functions of primary operators in conformal field theory, whereas in a mixed state, they are averages of OPE coefficients, or four point functions. The ETH tells us that both results will be almost identical to each other with exponentially suppressed differences.

Non-trivial one point functions in a thermal background can be interpreted as OPE coefficients if we work on the sphere times time. These should be finite. Models introduced by Myers et al. in [40] produce a non-trivial expectation of a scalar operator of dimension Δ by having an interaction in the bulk that couples the dual scalar field to the curvature squared in the bulk. Such couplings can be argued to arise directly from string theory (the associated particle can decay to two gravitons, similar to dilaton couplings). The model has been solved in the flat brane case, with an expression that only converges if Δ is bounded above by a number of order one [40]. Grinberg and Maldacena [41] argued that the computation admits an analytic continuation that gives rise to an expression whose dependence on Δ has the functional form

$$\langle O \rangle \propto \frac{(d-2)(d-1)^2}{d} \frac{h(1-h)}{\sin(\pi h)} \frac{\Gamma(h)^2}{\Gamma(2h)} \ , \tag{2.1}$$

where $h = \Delta/d$ is a normalized dimension of the operator, where d is the dimension of the conformal field theory. In their paper, they argued that the poles in h arise from operator mixing. We want to understand this issue better.

In this chapter we extract the same information by using the Frobenius method to solve the problems. In this case, the method itself does not require an analytic continuation and the answer is finite, except for the presence of the poles. The analysis readily produces generalized hypergeometric functions from the source that need to be expanded carefully around the horizon, where we extract a logarithmic divergence. Regularity at the horizon cancels the logarithm with the normalizable (at the boundary) solution of the unsourced equation, that has a similar singularity at the horizon.

The end result is similar to what occurs in conformal perturbation theory, where the gravity answer is automatically finite in calculations that usually require an analytic continuation in the conformal dimension of the operator [56].

The presence of the poles that appear in the finite answer can be explained by the theory of how differential equations are solved around the boundary of AdS, given by a theorem of Fuchs. We will give a way to see this effect more explicitly by converting the radial direction into a fictitious time. The pole can be interpreted as arising from a forced harmonic oscillator driven at resonance, just like certain logarithmic behaviors can be interpreted as resonances in conformal perturbation theory [57]. With a little more care, one can check that the picture of operator mixing of [41] can be understood explicitly.

Other problems, like the determination of response functions to the presence of a modulated scalar source at finite temperature are also interesting (see for example [59, 60, 61, 62]). They are very hard to solve analytically, even in the linear regime. These response functions are usually solved numerically. In the special case of two dimensional conformal field theories (AdS_3 black holes), the classic computation [63] solved this linear

problem. Recently, the retarded Green's function of AdS_5 black holes has also been computed [64, 65] by converting the problem into solutions of the Heun equation. Some progress has also been made in the computation of quasinormal modes for these setups [66] (see also [67]). The main insight is to relate the problem in gravity in AdS_5 to other problems in mathematical physics [68]. In particular, these analytic computations require the "connection formulae" for Heun functions expanded around different singularities of the equation.. For Kerr black holes, it is found here [69]. A more general study of some of the connection formulae for Heun functions can be found in [70].

In this chapter we make progress on some of these questions by using a perturbative method for small momenta. At first order the problem reduces to understanding singularities of more complicated sums of generalized hypergeometric functions.

We use the same techniques to solve the one point function problem with a Weyl squared tensor source in global AdS black holes, rather than the flat Poincare black holes by using perturbation theory in the curvature of the sphere for large mass black holes. Here, the analysis of the singular behavior near the horizon is complicated by the fact that pieces of the perturbation term are more singular than in other examples. We show how to deal with these in detail and are able to obtain a first order correction.

The chapter is organized as follows. In section 2.2 we study the response function at zero momentum and the one point function sourced by the Weyl term using the method of Frobenius around infinity. In section 2.3 we study a slight generalization of this problem to arbitrary powers of the Weyl curvature. This calculation can be used to solve more generally the problem of response functions and one point functions in a perturbative treatment that we perform. This includes the study of the spherical black hole. Additional issues arise in this case because the horizon gets shifted. In a perturbative treatment, we show how to deal with these to find a finite answer. We then conclude.

2.2 The flat black brane case

The metric of the AdS flat black brane in $d+1$ dimensions is

$$ds^2 = \frac{L^2}{z^2}\left[-f(z)dt^2 + \frac{1}{f(z)}dz^2 + d\vec{x}^2\right] , \tag{2.2}$$

where the function f is given by

$$f(z) = 1 - \left(\frac{z}{z_0}\right)^d . \tag{2.3}$$

We want to study the static solution of a massive scalar field in this background, which is sourced by the square of the Weyl tensor. This coupling arises from the action

$$S = -\frac{1}{16\pi G_N}\int\left[\frac{1}{2}(\nabla\phi)^2 + \frac{1}{2}m^2\phi^2 + \alpha\phi W^2\right] \tag{2.4}$$

as studied by Myers at al. and Grinberg and Maldacena. Our goal is to solve this problem using different techniques than what has been used so far. This will help understand in more detail why certain singularities can appear in the answer. The solution to this problem is straightforward from theorems in the study of linear differential equations. What is important is that the physics can be attributed to operator mixing with the background stress tensor.

We need the Weyl tensor squared as a source. In these coordinates it is simple to write and given by

$$W^2 = \frac{d(d-2)(d-1)^2}{L^4}\left(\frac{z}{z_0}\right)^{2d} . \tag{2.5}$$

Also, notice that when $z_0 = \infty$ we get the metric of AdS in the Poincaré patch. The region $z \simeq 0$ is the AdS boundary. Whereas $z = z_0$ is the horizon: the locus where g_{tt}

vanishes with a single regular zero. The temperature can be related to z_0 as follows

$$z_0^{-\Delta} = \left(\frac{4\pi T}{d}\right)^{\Delta} \ . \tag{2.6}$$

The expectation value of the stress tensor is proportional to the deviation away from the AdS metric near $z \sim 0$. The subleading difference is captured by the decay of g_{tt} near $z \sim 0$

$$\langle T_{00} \rangle \simeq \frac{1}{z_0^d} \ . \tag{2.7}$$

This metric is not in Fefferham-Graham coordinates, which would require that $g_{zz} = L^2/z^2$ for all z, but it is in a set of coordinates that make the analysis simpler to perform. In part this is because the determinant factor is simple

$$\sqrt{-g} = \left(\frac{L}{z}\right)^{d+1} \tag{2.8}$$

as it is only a power of z.

When we consider the action of the scalar field, we get the following equation of motion

$$\frac{1}{\sqrt{-g}}\partial_\mu \left(\sqrt{-g} g^{\mu\nu} \partial_\nu \phi\right) - m^2 \phi = \alpha W^2. \tag{2.9}$$

We now want to consider a position and time independent solution of this equation, for various values of the mass m^2, or equivalently, using the dimension of the associated operator $m^2 L^2 = \Delta(\Delta - d)$, the equation we need to solve is

$$z^{d+1} \frac{d}{dz}\left(z^{-d+1} f(z) \frac{d\phi}{dz}\right) - \Delta(\Delta - d)\phi = \alpha L^2 W^2 \tag{2.10}$$

This equation depends explicitly on d, but we can eliminate any dimensional dependence

after using the following change of variables

$$\omega \equiv \left(\frac{z}{z_0}\right)^d, \quad h \equiv \frac{\Delta}{d} \ . \tag{2.11}$$

This way we obtain the following differential equation

$$\omega^2 \frac{d^2\phi}{d\omega^2} - \omega \left[\omega^2 \frac{d^2\phi}{d\omega^2} + \omega \frac{d\phi}{d\omega}\right] + (1-h)h\phi = B\omega^2 \ , \tag{2.12}$$

where the constant B is given by

$$B \equiv \frac{\alpha(d-2)(d-1)^2}{dL^2} \ . \tag{2.13}$$

Notice that the term in square brackets is proportional to $\rho = \langle T_{00} \rangle$. That is, dimensional analysis in the variable ω is equivalent to counting powers of the expectation value ρ (the energy density). In the coordinate ω, there is a singularity of the differential equation at $\omega = 0$ and another one at $\omega = 1$ which is inherited from the coordinate singularity of the horizon. There is also a singularity at $\omega = \infty$. In a problem of linear differential equations, with three singularities in the complex plane at $\omega = 0, \omega = 1, \omega = \infty$, the solution is closely related to hypergeometric functions.

We will now solve the differential equation by the method of Frobenius. We need the homogeneous solution with regular boundary conditions at $z = 0$ (the boundary of AdS) and a solution of the inhomogenous problem (also called the particular solution for the differential equation). We then combine both of these by requiring regularity at the horizon.

Let us start with the homogeneous solution (the one where the source is ignored).

We write it as

$$\phi_H = \omega^\lambda \sum_{n=0}^{\infty} a_n \omega^n \tag{2.14}$$

and we normalize the solution so that $a_0 = 1$. The method of Frobenius will produce two results. First, it will solve for the value of λ and then it gives a recurrence relation for the a_n.

The most singular term in the differential equation is the one of dimension 0 in powers of ω. The eigenvalue condition for λ is given by

$$\lambda(\lambda - 1) - h(h - 1) = 0 \ , \tag{2.15}$$

which has two clear solutions: $\lambda = h$ and $\lambda = 1 - h$. We assume for simplicity that $\lambda = h > 0$. When $\lambda < 0$ the solution diverges at $\omega = 0$ and is considered unphysical from the point of view of the problem we are considering (more generally a source has been added for the field ϕ on the boundary of AdS).

We also obtain the following recurrence relation

$$\frac{a_{n+1}}{a_n} = \frac{(n+h)^2}{(n+2h)(n+1)} \ . \tag{2.16}$$

We recognize the general coefficient a_n as

$$a_n = \frac{1}{n!} \frac{(h)_n (h)_n}{(2h)_n} \ . \tag{2.17}$$

Here we have introduced the Pochhammer symbol defined as

$$(y)_n \equiv \frac{\Gamma(y+n)}{\Gamma(y)} = y(y+1)...(y+n-1) \ . \tag{2.18}$$

The solution of the homogeneous term is

$$\phi_{H1} = \omega^h \sum_{n=0}^{\infty} \frac{1}{n!} \frac{(h)_n (h)_n}{(2h)_n} \omega^n = \omega^h {}_2F_1(h, h, 2h, \omega) \ , \tag{2.19}$$

that we immediately recognize as a ${}_2F_1$ hypergeometric function. Since the horizon is located at $\omega = 1$, it is convenient to understand the large n limit of the terms in the series, to get at the structure of the possible divergence at $\omega = 1$. We find that since

$$\lim_{n\to\infty} \frac{\Gamma(n+h)^2}{\Gamma(n)\Gamma(n+2h)} = 1 \tag{2.20}$$

the series for large n looks like

$$\phi_{H_1} \sim \frac{\Gamma(2h)}{\Gamma(h)^2} \sum_{n}^{\infty} \frac{1}{n} \omega^n \sim -\frac{\Gamma(2h)}{\Gamma(h)^2} \log(1-w) \tag{2.21}$$

so that it diverges logarithmically. The series expansion around $\omega = 1$ that uses the full analytic properties of the hypergeometric function is

$$\begin{aligned} \phi_{H_1} \approx & -\frac{\Gamma(2h)}{\Gamma(h)^2}(2\psi^{(0)}(h) + \log(1-\omega) + 2\gamma) \\ & + \frac{(h-1)h\Gamma(2h)}{\Gamma(h)^2}(2\psi^{(0)}(h) + \log(1-\omega) + 2\gamma - 2)(\omega - 1) + O\left((\omega-1)^2\right) \ . \end{aligned} \tag{2.22}$$

Here γ is the Euler-Mascheroni constant and $\psi^{(0)}(h)$ is the first Polygamma Function (Digamma Function). These extra finite pieces are not relevant for the computation of the one point function of the boundary.

One can similarly consider the $h \to 1-h$ homogeneous solution that diverges at the boundary. In that case the logarithmic term diverging at the horizon will be given by

$$\phi_{H_2} \sim -\frac{\Gamma(2-2h)}{\Gamma(1-h)^2} \log(1-w) \ . \tag{2.23}$$

The most general solution of the homogeneous differential equation part of (2.12) is given by

$$\phi_T = c_1\phi_{H1} + c_2\phi_{H2} \ . \tag{2.24}$$

We require that the linear combination of ϕ_{H_1} and ϕ_{H_2} is regular at $\omega = 1$ (the logarithmic divergence cancels between them). This is how regularity at the horizon is imposed. Basically, the divergent piece of the stress tensor for the scalar field ϕ that is proportional $(\partial_w\phi)^2 \sim \frac{1}{(1-w)^2}$ is absent.

The response function for a source at the boundary, at finite temperature will be proportional to $-c1/c2$. In this case

$$\langle \delta\phi_{H_1} \rangle_{\delta\phi_{H_2}} = -\frac{\Gamma(h)^2}{\Gamma(1-h)^2}\frac{\Gamma(2-2h)}{\Gamma(2h)} \ . \tag{2.25}$$

The temperature dependence (dependence on ρ, or equivalently z_0) is fixed by dimensional analysis and a correction factor from normalization $d(2h-1) = 2\Delta - d$ (see the discussion in [55, 56]). This way

$$\left\langle \frac{\delta\phi}{\delta J} \right\rangle = -\frac{\Gamma(h)^2}{\Gamma(1-h)^2}\frac{\Gamma(2-2h)}{\Gamma(2h)}(2\Delta - d)z_0^{d-2\Delta} \ . \tag{2.26}$$

Notice that the answer can be divergent when h is a half-integer. Then $\Gamma(2-2h)$ is divergent while the terms in the denominator are regular. The divergence appears already from the Pochhammer symbol in equation (2.19) where we find a denominator $n + 2(1-h) = 0$. The power of ω appearing for this term is $\omega^{(1-h)+n+1} = \omega^h$ and it coincides with the positive root for λ, namely h. This has nothing to do with the horizon. Instead, it indicates that there is a naïve failure of the Frobenius method. In that case the two roots $h, 1-h$ differ by an integer. This is resolved by having a series with an additional $\phi_{H_1}\log(w)$ starting at this term. This case is a special example of

Fuchs' theorem. For h integer, the denominator will have a double pole at $n = h$, which cancels the pole in the numerator and makes the answer vanish. What happens is that the recurrence relation (2.16) terminates when $n+1-h = 0$, before we hit the singularity $n+2-2h = 0$. In that case, the solution with the boundary source is already regular at the horizon and one can not turn on a non-trivial response function. The normalization of the field in AdS is more subtle, but one can compare the field theory two point function and the AdS bulk two point function to do that [58, 56], resulting in an extra factor of

$$\mathcal{N} = \frac{\Gamma(\Delta)}{2\pi^{d/2}\Gamma(\Delta - d/2 + 1)} \tag{2.27}$$

that has no additional poles in h, as $\Delta > 1 - d/2$. From our point of view, this is a global rescaling factor that has nothing to do with the details of the differential equation, so we can drop it.

We now want to consider the bulk source, rather than the boundary source. The techniques for solving the problem are essentially identical, except that we will not get a ${}_2F_1$, but more complicated functions.

2.2.1 Particular solution ϕ_P

Now, we focus on obtaining the particular solution ϕ_P of the differential equation (2.12) with the squared Weyl tensor as a source. We look for a series solution

$$\sum_{n=0}^{\infty} a_n \omega^{n+\lambda}[(1-h)h + (n+\lambda)(n+\lambda-1)] - \sum_{n=0}^{\infty} a_n \omega^{n+\lambda+1}(n+\lambda)^2 = B\omega^2 \ . \tag{2.28}$$

To match the ω^2 dependence of $B\omega^2$, we need to start with $\lambda = 2$. The coefficient a_0 is given by

$$a_0 = \frac{B}{(2-h)(1+h)} \ . \tag{2.29}$$

The recurrence relation is

$$a_{n+1} = \frac{(n+2)^2}{(n+2+h)(n+3-h)} a_n \tag{2.30}$$

and it is a ratio of polynomials of n. The answer is written in terms of a ${}_3F_2$ series, as follows

$$a_n = \frac{(2)_n (2)_n}{(3-h)_n (h+2)_n} a_0 = \frac{1}{n!} \frac{(1)_n (2)_n (2)_n}{(3-h)_n (h+2)_n} a_0 \ , \tag{2.31}$$

where we use $(1)_n = n!$. The solution is explicitly written as

$$\phi_P = \frac{B\omega^2}{(2-h)(h+1)} {}_3F_2([1,2,2],[3-h,h+2],\omega) \ . \tag{2.32}$$

Again, we can look at the asymptotic behavior of the coefficients by using the limit

$$\lim_{n\to\infty} \frac{\Gamma(n+1)\Gamma(n+2)\Gamma(n+2)}{\Gamma(n)\Gamma(n+3-h)\Gamma(n+h+2)} = 1 \tag{2.33}$$

to find that

$$\begin{aligned} \phi_P &\sim \frac{B\omega^2}{(2-h)(h+1)} \left[\frac{\Gamma(n+2)\Gamma(n+2)}{\Gamma(n+3-h)\Gamma(n+h+2)}\right]^{-1}\Bigg|_{n=0} \sum \frac{w^n}{n} \\ &\sim -\frac{B\omega^2}{(2-h)(h+1)} \left[\frac{\Gamma(2)\Gamma(2)}{\Gamma(3-h)\Gamma(2+h)}\right]^{-1} \log(1-\omega) \\ &\sim -B\Gamma(2-h)\Gamma(1+h)\log(1-\omega)] \ . \end{aligned} \tag{2.34}$$

We want to reexpress this limit in a more illuminating way, so we recall the following identity for Gamma functions

$$\Gamma(1-z)\Gamma(z) = \frac{\pi}{\sin(\pi z)} \ . \tag{2.35}$$

Therefore, we obtain the following expression

$$\lim_{\omega\to 1-\epsilon}\phi_P = -B\frac{\pi(1-h)h}{\sin(\pi h)}\log(\epsilon)\ . \tag{2.36}$$

The most general solution of the differential equation (2.12) is given by

$$\phi_T = c_1\phi_{H1} + \phi_P\ . \tag{2.37}$$

The thermal one-point function is proportional to c_1, and we can determine this constant by demanding regularity for ϕ_T at the horizon. So, taking the $\omega \to 1$ limit we obtain that the divergent pieces must cancel

$$\lim_{\omega\to 1-\epsilon}\phi_T|_{sing} = -c_1\frac{\Gamma(2h)}{\Gamma(h)^2}\log(\epsilon) - B\frac{\pi(1-h)h}{\sin(\pi h)}\log(\epsilon)\ . \tag{2.38}$$

Demanding that this limit is regular (that is, the logarithmic divergences cancel), we obtain that

$$c_1 = -B\pi\frac{h(1-h)}{\sin(\pi h)}\frac{\Gamma(h)^2}{\Gamma(2h)}\ . \tag{2.39}$$

Finally, we take into account the physical scale (2.6) to obtain the following thermal one-point function

$$\langle O\rangle \propto -\left(\frac{4\pi T}{d}\right)^{\Delta}\frac{\alpha\pi(d-2)(d-1)^2}{dL^2}\frac{h(1-h)}{\sin(\pi h)}\frac{\Gamma(h)^2}{\Gamma(2h)}\ . \tag{2.40}$$

Except for some overall factors associated with the normalization of the massive scalar action and the normalization of the one-point function, we have replicated the result of Maldacena-Grinberg [41], which generalized results from Myers et al. [40] that were computed using the Green's function method by analytic continuation. Here we see that in this treatment the answer does not need additional regularization or analytic

continuation.

Notice that there can be singularities in the answer: poles when h is integer appearing from $\sin(\pi h)$. These can be traced to the $\Gamma(2-h)$ appearing in (2.34), or equivalently, to the $(3-h)_n$ symbol appearing in (2.31). These indicate a pole at some finite value of n: again, these are indicative of the naive failure of the Frobenius method as an expansion around $\omega = 0$ when we are studying the problem at finite order. These have nothing to do with the singular behavior at the horizon. The fix requires a logarithmic correction proportional to $\log(\omega)$ times ϕ_{H_1} to the answer. These occur when h is a positive integer greater than or equal to 3, and render the one point function ambiguous: $\log(\omega)$ can be replaced by $\log\left(\omega\tilde{\Lambda}\right)$ for any $\tilde{\Lambda}$, thus shifting the value of c_1 by a finite amount.

If we think of $\log\left(\tilde{\Lambda}\right)$ as a cutoff in quantum field theory (it determines a surface in the UV by $\log\left(\omega\tilde{\Lambda}\right) = 0$), we see that the answer bears close similarity to logarithmic divergences in quantum field theory. Where can these arise from? The answer suggested in [41] is that they arise from mixing between a power of the stress tensor $:T^s:$ and $\mathcal{O}$. We would like to explain this intuition in more detail.

The idea is the following. Consider a new coordinate σ defined by $\omega = \exp(i\sigma)$. The differential equation (2.12) becomes

$$-\partial_\sigma^2\phi + i\partial_\sigma\phi + (1-h)h\phi = B\exp(2i\sigma) + \exp(i\sigma)\left[-\partial_\sigma^2\right]\phi\ . \tag{2.41}$$

The σ coordinate is behaving like a time, rather than a position, because we added the factor of i. This coordinate lets us interpret the radial direction ω as a flow in a fictitious time.

The left hand side is translation invariant in σ. The right hand side has two pieces: a source at constant frequency $\exp(2i\sigma)$, and a field dependent source that adds one unit to the frequency. This second term is the one that is proportional to the energy density

ρ. The particular solution is

$$\sum a_n \exp(i(n+2)\sigma) \ . \tag{2.42}$$

We see that the singularity arises from a resonance condition, when $(n+2)^2-(n+2)+h(1-h)=(n+2-h)(n+1+h)=0$. This is the condition to be on-shell for the σ independent part of the differential equation: if we are driving at resonance, the solution must grow linearly in the time σ on top of the oscillating piece. This is the $\log(\omega)$ we had before. The precise solution depends on "initial conditions". Notice that this occurs on a term that behaves as ρ^{n+2}, since the Weyl tensor squared also counts as two powers of ρ. The resonance is between a quantity proportional to $\langle : T_{00} :^{n+2} \rangle$ and the operator dual to the field ϕ: they both have the same dimension when h is a positive integer greater than or equal to 2. The normal ordering here indicates that we have the naive dimension of the composite operator T_{00}^{n+2}. Basically, the terms in the series expansion of the particular solution, with the source W^2 seeding the solution are oscillating at integer frequencies. When h is not an integer there is no resonance condition and in principle there is no operator mixing ambiguity that needs to be considered. This is very similar to how logarithmic divergences from mixing appear in other settings [57]

2.3 Some simple generalizations

In our next step, we consider the following action for a massive scalar field

$$S=-\frac{1}{16\pi G_N}\int\left[\frac{1}{2}(\nabla\phi)^2+\frac{1}{2}m^2\phi^2+\alpha\phi W^{2\beta}\right] \ . \tag{2.43}$$

Basically, we are writing a solution with a source that has a different power of z than the one that arises from the Weyl squared tensor W^2. Many other similar problems can be

analyzed if we have a better understanding of solutions to the modified source as a more general power of z. In the w variables, the differential equation is the following

$$(1-\omega)\omega^2\frac{d^2\phi}{d\omega^2}-\omega^2\frac{d\phi}{d\omega}+(1-h)h\phi=K\omega^{2\beta}\ , \tag{2.44}$$

where we have defined the constant K as follows

$$K\equiv\left(\frac{\alpha R^2}{d^2}\right)\left(\frac{d(d-2)(d-1)^2}{R^4}\right)^{\beta}\ . \tag{2.45}$$

Again, at this stage, what we are really doing is solving for an arbitrary power of ω in the right hand side of equation (2.44). The inhomogeneous solution will start with a power of $\omega^{2\beta}$, rather than ω^2. The result for the first term is very similar to (2.29), giving

$$a_0=\frac{K}{(h+2\beta-1)(2\beta-h)}\ . \tag{2.46}$$

The full result, after following the method of Frobenius is:

$$\phi_{P_\beta}=\frac{K\omega^{2\beta}}{(2\beta-h)(h+2\beta-1)}\sum_{n=0}^{\infty}\frac{1}{n!}\frac{(1)_n(2\beta)_n(2\beta)_n}{(1+2\beta-h)_n(h+2\beta)_n}\omega^n\ . \tag{2.47}$$

This is, again, a ${}_3F_2$ function with different parameters:

$$\phi_{P_\beta}=\frac{K\omega^{2\beta}}{(2\beta-h)(h+2\beta-1)}{}_3F_2([1,2\beta,2\beta],[1+2\beta-h,h+2\beta],\omega)\ . \tag{2.48}$$

Using the same methods as before, we get that the near horizon limit logarithmic behavior is given by

$$\lim_{\omega\to1-\epsilon}\phi_{P_\beta}=-K\frac{\Gamma(2\beta-h)\Gamma(h+2\beta-1)}{\Gamma(2\beta)^2}\log(\epsilon)\ . \tag{2.49}$$

It is then straightforward to find the one point function by requiring that the logarithmic divergence of the inhomogeneous solution cancels with the homogeneous piece as well.

2.3.1 Response function to a weakly modulated source

We now consider a solution that apart from the radial variable z also has dependence on the spatial variables x^i, so that $\phi = \phi(z, x)$. We notice that we still consider a static solution, but allow for modulation (slow variation in x). The equation of motion in this case is

$$\frac{1}{\sqrt{-g}}\partial_z\left(\sqrt{-g}g^{zz}\partial_z\phi\right) + g^{ii}\partial_i^2\phi - m^2\phi = \alpha W^2 \ . \tag{2.50}$$

By doing a Fourier transformation in the variables x^i, and using a spatial profile $\exp\left(i\vec{k}\cdot\vec{x}\right)$, we can decompose into momentum modes. The x dependence becomes trivial and we get a slight modification of the equation

$$\omega^2\frac{d}{d\omega}\left((1-\omega)\frac{d\tilde{\phi}}{d\omega}\right) + (1-h)h\tilde{\phi} - q^2\omega^{2/d}\tilde{\phi} = B_W\omega^2\delta^{d-1}(k) \ , \tag{2.51}$$

where q is the momentum variable in dimensionless units $q \equiv \frac{k}{4\pi T}$. The idea is to expand perturbatively in q, in the presence of a weakly modulated source. We have also used the radial variable ω defined in (2.11). Since we are interested in the case $k \neq 0$, we can safely ignore the Weyl source. Now, we assume the regime $q << 1$ in order to solve the previous equation perturbatively $\tilde{\phi}_{Hi}(u, q) = \phi^{(0)}_{Hi}(u) + \delta\tilde{\phi}_{Hi}(u, q)$ where we notice that $\tilde{\phi}^{(0)}_{Hi}(u) = \phi^{(0)}_{Hi}(u)$. Thus, the differential equation becomes

$$\omega^2\frac{d}{d\omega}\left((1-\omega)\frac{d(\delta\tilde{\phi}_{Hi})}{d\omega}\right) + (1-h)h(\delta\tilde{\phi}_{Hi}) = q^2\omega^{2/d}\phi^{(0)}_{Hi} \ . \tag{2.52}$$

We can write the homogeneous solutions given in (2.19) in terms of series as follows,

for both h and $1-h$ (so that we have the two solutions without a source in the bulk)

$$\phi^{(0)}_{H1} = \omega^h \sum a_n \omega^n \ , \quad a_n = \frac{1}{n!}\frac{(h)_n (h)_n}{(2h)_n} \ , \tag{2.53}$$

$$\phi^{(0)}_{H2} = \omega^{1-h} \sum b_n \omega^n \ , \quad b_n = \frac{1}{n!}\frac{(1-h)_n (1-h)_n}{(2-2h)_n} \ . \tag{2.54}$$

From here, we notice that the equation (2.52) becomes exactly the same differential equation given by (2.44) (on a term by term basis) by the identification of parameters: $\beta_{H1} = n + h + 2/d$, $K_{\beta_{H1}} = q^2 a_n$ and $\beta_{H2} = n + 1 - h + 2/d$, $K_{\beta_{H2}} = q^2 b_n$. We can just write sums of the corresponding solutions (2.47) to get the answer at this order. Now, we use the near horizon limit given in (2.49) term by term to get the logarithmic divergence

$$\begin{aligned} \lim_{\omega\to 1-\epsilon} \delta\tilde{\phi}_{H1}(u,q) &= -q^2 \sum a_n \frac{\Gamma(n+2/d)\Gamma(n+2h-1+2/d)}{\Gamma(n+h+2/d)^2} \log(\epsilon) \equiv -q^2 \sum A_n \log(\epsilon) \ , \\ \lim_{u\to 1-\epsilon} \delta\tilde{\phi}_{H2}(u,q) &= -q^2 \sum b_n \frac{\Gamma(n+2/d)\Gamma(n-2h+1+2/d)}{\Gamma(n+1-h+2/d)^2} \log(\epsilon) \equiv -q^2 \sum B_n \log(\epsilon) \ . \end{aligned} \tag{2.55}$$

We have ignored in both limits an infinite sum of finite terms that could potentially diverge. This can be analyzed more carefully from (2.52). The idea is that the right hand side is smooth for $\omega < 1$ and decays rapidly for $\omega \sim 0$ (faster than $\phi^{(0)}_{H_i}$). The most dangerous part of the analysis is that $\phi^{(0)}_{H_i}$ diverges at $\omega \to 1$ logarithmically, so $\delta\phi$ might be more singular than we originally thought. It can be checked by expanding directly around $\omega = 1$ that if $\phi^{(0)}_{H_i}$ behaves logarithmically, then the terms of $\delta\phi$ near $\omega \to 1$ grow at most logarithmically. This will come from the $h(1-h)$ term. Basically, the second order differential equation is elliptic in the region $\omega \in (0,1)$, so the solution will not be more singular than the singularity of the source.

The derivative terms in fact kill a logarithmic divergence of $\delta\phi$. To get a log on the left hand side from the second derivative would require a term $(1-\omega)\log(1-\omega)$, which has a zero limit when $\omega \to 1$ and is less singular than the right hand side. The term with $h(1-h)$ would then be the one that dominates the first term in the expansion around $\omega \sim 1$. We conclude that in practical terms we can ignore those finite terms safely. Thus,

the limit of the total homogeneous solution is

$$\lim_{\omega\to 1-\epsilon}\tilde{\phi}(u,k)=\left[-c_1\left(\frac{\Gamma(2h)}{\Gamma(h)^2}+q^2\sum A_n\right)-c_2\left(\frac{\Gamma(2-2h)}{\Gamma(1-h)^2}+q^2\sum B_n\right)\right]\log(\epsilon)\ . \tag{2.56}$$

Demanding the regularity condition at the horizon, we obtain the following response function (which is given by $-\frac{c_1}{c_2}$ times certain normalization factors independent of k)

$$-\frac{c_1}{c_2}=\frac{\Gamma(h)^2}{\Gamma(2h)}\frac{\Gamma(2-2h)}{\Gamma(1-h)^2}\left[1+q^2\left(\frac{\Gamma(1-h)^2}{\Gamma(2-2h)}\sum B_n-\frac{\Gamma(h)^2}{\Gamma(2h)}\sum A_n\right)\right]\ . \tag{2.57}$$

These sums can be re-expressed in terms of regularized hypergeometric functions of type ${}_4\tilde{F}_3$ given by

$$\mathcal{A}(h,d)\equiv\frac{\Gamma(h)^2}{\Gamma(2h)}\sum A_n=\Gamma(2/d)\Gamma(h)^2\Gamma(2/d+2h-1)$$
$${}_4\tilde{F}_3[(h,h,2/d,2/d+2h-1),(2h,h+2/d,h+2/d);1]\ , \tag{2.58}$$

and

$$\mathcal{B}(h,d)\equiv\frac{\Gamma(1-h)^2}{\Gamma(2-2h)}\sum B_n=\Gamma(2/d)\Gamma(1-h)^2\Gamma(2/d+1-2h)$$
$${}_4\tilde{F}_3[(1-h,1-h,2/d,2/d-2h+1),(2-2h,1-h+2/d,1-h+2/d);1]\ . \tag{2.59}$$

By analyzing the parameters of these hypergeometric functions, one can infer that these functions are regular at 1. Therefore, by removing the logarithm divergence we are assured to get a finite result. Finally, the response function is given by

$$\left\langle\frac{\delta\phi}{\delta J}\right\rangle=-(2\Delta-d)z_0^{d-2\Delta}\frac{\Gamma(h)^2}{\Gamma(2h)}\frac{\Gamma(2-2h)}{\Gamma(1-h)^2}\left[1+q^2\left(\mathcal{B}(h,d)-\mathcal{A}(h,d)\right)\right]\ . \tag{2.60}$$

We also notice that in this computation, we didn't use the Weyl source which is defined

only for $d \geq 3$. Therefore, we can evaluate the answer at $d = 2$ to obtain that

$$\left\langle \frac{\delta\phi}{\delta J} \right\rangle^{d=2} \propto \frac{\Gamma(h)^2}{\Gamma(2h)} \frac{\Gamma(2-2h)}{\Gamma(1-h)^2} \left[1 + q^2 \left(\psi^{(1)}(1-h) - \psi^{(1)}(h)\right)\right] \ .$$

On the other hand, for the planar BTZ black hole, the retarded Green function (See for instance [63, 71, 72]) is given by

$$G_r(q,\nu) \propto \frac{\Gamma(2-2h)}{\Gamma(2h)} \frac{\Gamma(h+i(\nu-q))\Gamma(h+i(\nu+q))}{\Gamma(1-h+i(\nu-q))\Gamma(1-h+i(\nu+q))} \ , \tag{2.61}$$

where $\nu \equiv \frac{\omega}{4\pi T}$. Expanding for small momenta, we obtain

$$G_r(q,\nu=0) \propto \frac{\Gamma(2-2h)\Gamma(h)^2}{\Gamma(2h)\Gamma(1-h)^2} \left[1 + q^2 \left(\psi^{(1)}(1-h) - \psi^{(1)}(h)\right)\right] + O(q^3) \ .$$

Therefore, our method reproduces at first order in q^2 the pure spatial part of the retarded Green function of the planar BTZ black hole. This is a consistency check that our result in (2.60) is correct and provides the first order term in any dimension d of the purely spatial response function.

One can ask, from our point of view, what makes the case $d = 2$ simple? When $d = 2$, the exponent of ω on the q^2 term is $\gamma = 2/d = 1$ produces an additional term in $\exp(i\sigma)$ at the same frequency than the term that arises from the metric. In that sense, if one does not use a perturbation approach, one finds instead a modified quadratic numerator in the recurrence (2.16) given by

$$\frac{a_{n+1}}{a_n} = \frac{(h+n)^2 + q^2}{(n+2h)(n+1)} \tag{2.62}$$

whose numerator can be easily factorized into $(h+n+iq)(h+n-iq)$. The solution of

the recursion is

$$a_n = \frac{(h+iq)_n (h-iq)_n}{n!(2h)_n} \tag{2.63}$$

and the answer is in terms of hypergeometric functions, where the parameters are modified by q

$$\phi_h \sim \omega^h \, {}_2F_1(h+iq, h-iq, 2h, \omega) \ . \tag{2.64}$$

It is easy to check that all the poles in q in the numerator and denominator at finite q appearing in equation (2.61) are captured this way: the logarithmic behavior at $\omega \to 1$ cancels in the same way as when we work with $q = 0$. In principle, one should be able to argue that the dependence on the frequency also comes automatically. The linear combinations $\nu \pm q = const$ are related to traveling at the speed of light, as $\partial_q \nu = \pm 1$, splitting into products of left and right moving modes. Moreover, the poles in the numerator (quasinormal modes) should occur for a fixed sign of the imaginary part of ν, $\mathrm{Im}\, m(\nu)$ at real momentum q. If one can argue that the left and right movers must be split this way, the full result should immediately follow from just the spatial modulation dependence.

2.3.2 One point function in global AdS black holes in the large mass limit.

We are going to consider again a massive scalar field but this time in a AdS_{d+1} spherical black hole background rather than a black brane. We do not know how to make the full calculation exactly. What we can do is a perturbative expansion in inverse powers of the mass (expanding around large black holes). In this case, in the equation of motion we are going to consider the horizon curvature as a small parameter so as to be able to use perturbation theory around the black brane solution.

The AdS_{d+1} spherical black hole metric is

$$ds^2 = -H(r)dt^2 + \frac{1}{H(r)}dr^2 + r^2 d\Omega^2 \ , \tag{2.65}$$

where $H(r)$ is defined as follows

$$H(r) = 1 + \frac{r^2}{L^2} - \frac{2M}{r^{d-2}} \ . \tag{2.66}$$

These coordinates are convenient as the determinant of the metric is

$$\sqrt{-g} \propto r^{d-1} \tag{2.67}$$

and the Weyl tensor squared is given by a simple expression

$$W^2 = \frac{d(d-2)(d-1)^2}{r^{2d}} (2M)^2 \ . \tag{2.68}$$

If we compare with the flat black brane, we would use instead $H(r) = \frac{r^2}{L^2} - \frac{2M}{r^{d-2}}$, and the boundary of spacetime is located at $r \to \infty$. The natural z coordinate that we used before is simply $z = L^2/r$. In this way, we find that

$$H(z) = L^2 \left(\frac{1}{z^2} + \frac{1}{L^2} - \frac{1}{z^2} \left[\frac{z}{z_0} \right]^d \right) \ , \tag{2.69}$$

where z_0 is determined by looking at the flat brane factor without the curvature correction. Namely, we first define $r_0^d = 2ML^2$. In this sense, r_0 is a notion of the radius of the black hole, and then we take $z_0 \to L^2/r_0$. This is equivalent to having an adjusted value

of $f(z)$ in equation (2.3), given by

$$f(z) = 1 - \left(\frac{z}{z_0}\right)^d + \frac{z^2}{L^2} \ . \tag{2.70}$$

and the idea of a large mass black hole is that the additional term is very small still when $z \sim z_0$, that is, we take $z_0/L \ll 1$ so the horizon is very close to the boundary. Notice that large r_0 is equivalent to large M, and that large r_0 becomes a small z_0 after the inversion. We can now introduce the dimensionless $\omega = (z/z_0)^d$ coordinate that we used before. In this coordinate system we have that $z^2 = z_0^2\omega^{2/d}$. After some algebra, the differential equation becomes

$$\omega^2\left(s^2\omega^\gamma + 1 - \omega\right)\frac{d^2\phi}{d\omega^2} + \omega\left(\gamma s^2\omega^\gamma - \omega\right)\frac{d\phi}{d\omega} + (1-h)h\phi = B\omega^2 \ , \tag{2.71}$$

where

$$\gamma \equiv \frac{2}{d} \ , \quad s^2 \equiv \frac{L^2}{r_0^2} = \frac{L^2}{(2ML^2)^\gamma} \ . \tag{2.72}$$

We now treat s as a small parameter in which we can do perturbation theory. We notice that if we take $s \to 0$ we recover our previous differential equation with the source, so s can indeed be treated perturbatively.

It is important to understand at this point why the general problem is going to be hard to solve: the equation (2.71) has more singularities in the complex plane than the corresponding planar problem. These occur at $\omega = 0, \infty$ and at the non trivial roots of $(s^2\omega^\gamma + 1 - \omega) = 0$. There is one that is perturbatively close to $\omega = 1$, but there are new singularities. In practice this means that the problem can not be handled with hypergeometric functions. An exact solution becomes very hard in that case. This is why we will attempt to do a perturbative expansion in s^2. This is actually a non-trivial expansion.

Perturbative computation for the homogeneous solution

We write down the total homogeneous solution ϕ_H^{Tot} as follows

$$\phi_H^{Tot} = \phi_H + \delta\phi_H \ , \tag{2.73}$$

where ϕ_H is the homogeneous solution of the black brane that we already computed and is given by

$$\phi_H = \omega^h {}_2F_1(h,h,2h,\omega) = \omega^h \sum_{n=0}^{\infty} a_n \omega^n \ , \quad a_n = \frac{1}{n!}\frac{(h)_n (h)_n}{(2h)_n} \ ,$$

and where $\delta\phi$ is a first order correction proportional to s^2. We plug the solution we already know, equation (2.19) into the differential equation (2.71) to obtain

$$\omega^2(1-\omega)\delta\phi_H'' - \omega^2\delta\phi_H' + h(1-h)\delta\phi_H = -s^2\omega^\gamma(\gamma\omega\phi_H' + \omega^2\phi_H'') \ . \tag{2.74}$$

In this last expression, we have dropped terms of higher order $s^2\delta\phi_H'$ and $s^2\delta\phi_H''$, and used the homogeneous differential equation for ϕ_H. Let us use the information we have about how $\phi_H(\omega)$ behaves as $\omega \to 1$. It depends on ω as $\phi_H \sim C\omega^h \log(1-\omega) + \omega^h C' + \omega^h O(1-\omega)$. The second derivative of ϕ_H gives a double pole in $(1-\omega)$ on the right hand side. This needs to be cancelled by the most singular term in the differential equation for $\delta\phi$. This requires a divergence of $\delta\phi_H$ that behaves as $\Theta(1-\omega)^{-1}$, whose coefficient is uniquely determined by C. Since C has already been computed, this most singular term is simple.

At the next order, we get a single pole in $1-\omega$ on the right hand side. This extra pole can arise from a $\log(1-\omega)^2$ in $\delta\phi_H$ (a double logarihtmic singularity). The rest of the terms on the right hand side are at most log divergent and we have already seen that

these are not a problem in the previous example. A similar structure arises from the inhomogeneous solution and since the $\phi_H + \phi_P$ is regular at $\omega = 1$.

Now, we compute the following quantities

$$\omega\phi'_H = \sum_{n=0}^{\infty} a_n(n+h)\omega^{n+h} , \tag{2.75}$$

$$\omega^2\phi''_H = \sum_{n=0}^{\infty} a_n(n+h)(n+h-1)\omega^{n+h} , \tag{2.76}$$

as power series in ω. Each term essentially corresponds to a source with a different coefficient K and a different β in (2.44), so we can use those results term by term, finding that

$$-s^2\omega^\gamma(\gamma\omega\phi'_H + \omega^2\phi''_H) = -s^2\sum_{n=0}^{\infty} a_n(n+h)(n+h+\gamma-1)\omega^{n+h+\gamma} . \tag{2.77}$$

To simplify this expression, we define $\bar{A}_n$ as

$$\bar{A}_n \equiv \frac{1}{n!}\frac{(h)_n(h)_n}{(2h)_n}(n+h)(n+h+\gamma-1) \tag{2.78}$$

so that the problem to solve is the following differential equation

$$\omega^2(1-\omega)\delta\phi''_H - \omega^2\delta\phi'_H + h(1-h)\delta\phi_H = -s^2\sum_{n=0}^{\infty}\bar{A}_n\omega^{n+h+\gamma} . \tag{2.79}$$

Notice that the $\bar{A}_n$ coefficients are more divergent when $n \to \infty$ than the ones for a_n. This is the source of the different singular behavior as $\omega \to 1$.

We now need to sum over the solutions we already know to find that the modified homogeneous solution is

$$\delta\phi_H = -s^2\sum_{n=0}^{\infty}\frac{\bar{A}_n\omega^{n+h+\gamma}}{(n+\gamma)(n+\gamma+2h-1)}{}_3F_2([1, n+h+\gamma, n+h+\gamma], [1+n+\gamma, n+2h+\gamma], \omega) . \tag{2.80}$$

Notice that this is a double series, with n dependence on the ${}_3F_2$. To understand the divergent behavior in ω, as $\omega \to 1$, it needs to be resummed.

Perturbative computation for the inhomogeneous (particular) solution

The calculation is very similar to what we just did. We start with the particular solution ϕ_P^{Tot} expanded as a perturbation series as follows

$$\phi_P^{Tot} = \phi_P + \delta\phi_P \ , \tag{2.81}$$

where ϕ_P is the particular solution of the planar black hole given by

$$\phi_P = \frac{B\omega^2}{(2-h)(h+1)} \sum_{n=0}^{\infty} j_n \omega^n \ , \quad j_n \equiv \frac{1}{n!} \frac{(1)_n (2)_n (2)_n}{(3-h)_n (h+2)_n} \ ,$$

The differential equation for the first order perturbation $\delta\phi_p$ is

$$\omega^2(1-\omega)\delta\phi_p'' - \omega^2\delta\phi_p' + h(1-h)\delta\phi_p = -s^2\omega^\gamma(\gamma\omega\phi_p' + \omega^2\phi_p'').\tag{2.82}$$

Computing the source gives

$$\omega^2(1-\omega)\delta\phi_P'' - \omega^2\delta\phi_P' + h(1-h)\delta\phi_P = -s^2 \frac{B}{(2-h)(h+1)} \sum_{n=0}^{\infty} \bar{J}_n \omega^{n+2+\gamma} \ ,$$

where we have defined the constant $\bar{J}_n$ as follows

$$\bar{J}_n \equiv \frac{1}{n!} \frac{(1)_n (2)_n (2)_n}{(3-h)_n (h+2)_n} (n+2)(n+1+\gamma) \ . \tag{2.83}$$

The solution we need is

$$\delta\phi_P = \frac{-Bs^2}{(2-h)(h+1)} \sum_{n=0}^{\infty} \frac{\bar{J}_n \omega^{n+2+\gamma}}{(n+\gamma+2-h)(n+\gamma+h+1)} \\ {}_3F_2([1, n+\gamma+2, n+\gamma+2], [n+\gamma+3-h, n+\gamma+2+h], \omega) \ . \quad (2.84)$$

Again, it should be noted that this is also a double series expansion, with n dependence on the ${}_3F_2$, so one needs to do a resummation before one can understand the details of the divergent pieces.

Double limit series

Now, instead of doing a resummation, we will consider the expression

$$\delta\phi_H = -s^2 \sum_{n=0}^{\infty} \frac{\bar{A}_n \omega^{n+h+\gamma}}{(n+\gamma)(n+\gamma+2h-1)} {}_3F_2([1, n+h+\gamma, n+h+\gamma], [1+n+\gamma, n+2h+\gamma], \tilde{\omega}) \ , \quad (2.85)$$

where we have a new variable $\tilde{\omega}$. We want to take $\tilde{\omega} \to 1, \omega \to 1$ independently to understand the structure of the singularities. In the end we will make $\omega = \tilde{\omega}$ once we have cured the problems. Because the double sum is not being done in standard form, this way of dividing the problem into two different variables might cause an order of limits problem. Essentially, if we take $\tilde{\omega} = \omega < 1$, then the series is absolutely convergent and both ways of doing calculations give the same answer. Because there are singularities in $\tilde{\omega} = 1$, independent of ω, when we take the double limit, the behavior can change. We will see that this happens in practice.

The idea is as follows. In (2.85) we get a clear divergence in $\tilde{\omega} \to 1$ that we have already computed that is logarithmic in nature. We find that

$$\delta\phi_H = -s^2 \sum_{n=0}^{\infty} \bar{A}_n \omega^{n+h+\gamma} \frac{\Gamma(n+2h+\gamma-1)\Gamma(n+\gamma)}{\Gamma(n+h+\gamma)\Gamma(n+h+\gamma)} \log(1-\tilde{\omega}) \ . \quad (2.86)$$

The sum over n behaves as if the coefficients are approximately constant

$$\mathcal{N}\sum_n \omega^n \sim \frac{\mathcal{N}}{(1-\omega)} \tag{2.87}$$

times a normalization factor. This is because $a_n \sim 1/n$, the additional product of the Gamma functions also behaves exactly as $1/n$ when n is large, and we're multiplying by a quadratic polynomial in n. The normalization factor was already found in (2.21)

$$\mathcal{N} = \frac{\Gamma(2h)}{\Gamma(h)^2} \ . \tag{2.88}$$

Doing a similar analysis for the other terms, we find that

$$\begin{aligned}\phi &= \left[c_1\frac{\Gamma(2h)}{\Gamma(h)^2}\left(1+s^2\left(\mathcal{E}(d,h)+\frac{1}{1-\omega}\right)\right)+\right.\\ &\left.\frac{B_W(1-h)h\pi}{\sin(\pi h)}\left(1+s^2\left(\mathcal{F}(d,h)+\frac{1}{1-\omega}\right)\right)\right]\log(1-\tilde{\omega}) \ .\end{aligned} \tag{2.89}$$

where

$$\begin{aligned}\mathcal{E}(d,h) &\equiv \lim_{\omega\to 1}\left[h\Gamma(h)^2\Gamma\left(2h-1+\frac{2}{d}\right)\Gamma\left(\frac{2}{d}\right)\right.\\ &\left.{}_4\tilde{F}_3\left(\left[h,h+1,\frac{2}{d},2h+\frac{2}{d}-1\right],\left[2h,h+\frac{2}{d},h+\frac{2}{d}-1\right],\omega\right)-\frac{1}{1-\omega}\right] \ ,\end{aligned} \tag{2.90}$$

and

$$\begin{aligned}\mathcal{F}(d,h) &\equiv \lim_{\omega\to 1}\left[\frac{-2\pi}{\sin\left[\pi(h-2/d)\right]}\frac{\Gamma\left(h+1+\frac{2}{d}\right)}{\Gamma\left(h-1-\frac{2}{d}\right)}\right.\\ &\left.{}_5\tilde{F}_4\left(\left[1,2,3,\frac{2}{d}+2-h,\frac{2}{d}+1+h\right],\left[3-h,h+2,\frac{2}{d}+2,\frac{2}{d}+1\right],\omega\right)-\frac{1}{1-\omega}\right]\end{aligned} \tag{2.91}$$

are subtracted versions of the functions that appear in our problem. The hypergeometric functions are regularized hypergeometric functions. It can be checked numerically that these regularized functions with the pole substracted actually have a limit. This indicates

the absence of the double logarithmic divergence in our treatment of the sums.

It turns out that the single pole contribution that could in principle give rise to the double logarithmic behavior cancels between all the terms for the homogeneous problem by itself, which include the $h(1-h)$ term in the unperturbed differential operator, plus the expansion of the derivatives of the hypergeometric function on the source from the original problem. There are no such double logarithms generated in any intermediate step. This seems to be required so that the log divergences are unambiguous.

One can ask more generally, what is the source of the additional singular behavior? The idea is that the horizon is not longer at $\omega = 1$, but that it has been shifted. The solution of the location of the horizon can be written as $\omega_h = 1+\sum k_n s^{2n}$. The singularity is always logarithmic in terms of

$$f(\omega)\log(\omega_h - \omega) \tag{2.92}$$

as follows from the analysis of the singular points of the differential equation. We can expand the logarithm as a power series in s^2, and we get

$$\log(\omega_0 - \omega) = \log\Big(1 + \sum k_n s^{2n} - \omega\Big) \sim \log(1-\omega) - \frac{\sum k_n s^{2n}}{1-w} + O(1/(1-\omega)^2)\ , \tag{2.93}$$

which gives an expansion in terms of a single logarithm and poles determined as a power series in s^2 by the shift of the horizon and the computation of f to lower orders. There is no double logarithm ever.

Also, for non-extremal black holes is well-known that a field on a fixed background will be split into outgoing and infalling modes. These modes are mixed in the static limit

$\nu \to 0$, and develop a logarithmic divergence

$$C_{\pm}(\nu)(\omega_h - \omega)^{\pm i\nu} \approx \tilde{C}_{\pm}(\nu)(1 \pm i \log(\omega_h - \omega)) + O(\nu^2) \ .$$

In this expression, $C_{\pm}(\nu)$ and $\tilde{C}_{\pm}(\nu)$ are constants with some dependence on the frequency ν. This logarithmic divergence basically comes from the coordinate singularity of the black hole. In fact, this expression is a remnant of Tortoise coordinate near the horizon $u^* = \frac{1}{2\kappa}\log(u_h - u)$. From this point of view, the natural Boundary condition for the scalar field ϕ in any non-extremal black hole in static limit at the horizon is

$$\phi \approx A \log(\omega_h - \omega) \ , \tag{2.94}$$

where A is a constant to determine from the exact solution of ϕ and where we have ignored some finite terms. In our perturbative treatment, we expand $A = A^{(0)} + s^2 A^{(1)} + O(s^2)$ and $\omega_h = 1 + s^2 + O(s^2)$, so the boundary condition becomes

$$\phi \approx A^{(0)} \log(1-\omega) + A^{(1)} s^2 \log(1-\omega) + \frac{A^{(0)} s^2}{1-\omega} + O(s^4) \ . \tag{2.95}$$

In this expansion in s^2, the boundary condition has picked an extra divergence coming from $\frac{A^{(0)}s^2}{1-\omega}$. This is an artifact of the perturbative treatment since the natural boundary condition is always (2.94). We can check explicitly that this expansion of the boundary condition in s^2 (2.95) solves the differential equation (2.71) up to order $O(1-\omega)$ with the appropriate choice of $A^{(0)}$ given by $\frac{\Gamma(h)^2}{\Gamma(2h)}$ and $\frac{h(1-h)\pi}{\sin(\pi h)}$ for the homogeneous and particular solution respectively. We notice that the extra divergence is completely determined by the zeroth order solution which means that we can safely ignore it at order s^2. Our task is reduced to find explicitly $A^{(1)}$ to find the leading correction to the thermal one-point function. This behavior is similar to analysis of the renormalization group, where higher

order singularities are completely determined by the leading logarithmic singularity.

When we impose the first order result we already had, we see that the pole in $1-\omega$ cancels between the homogeneous solution and the inhomogeneous solution. We are left with a strict logarithmic singularity at order s^2. A correction of order s^2 in the homogeneous solution can cancel this extra singularity. The only possible source of this logarithmic singularity is the one that arises from the limits of the ${}_3F_2$ series that we computed. Hence, the calculation in this order is actually the correct calculation.

Notice also that the $\tilde{F}$ regularized hypergeometric functions are always well defined as functions of their parameters. There are additional poles that can appear in $\tilde{F}(d,h)$ arising from the $\sin(\pi(h-2/d))$ in the denominator. The poles occur when $h-2/d$ is an integer (except zero and one, where the $\Gamma(h-1-2/d)$ cancels them). These additional poles should also be interpreted as mixing, with operators that include the curvature of the background metric (which always has dimension 2 and at least two powers of $:T:^2$).

The final result is

$$\langle O\rangle_{J=0} = -N z_0^{-\Delta} B_W \frac{\Gamma(h)^2}{\Gamma(2h)} \frac{\pi h(1-h)}{\sin(\pi h)} \left(1 - s^2[\mathcal{F}(d,h) - \mathcal{E}(d,h)]\right) \ . \tag{2.96}$$

Notice that this is written in terms of z_0, which denotes the energy density.

If one wants to use the temperature instead, one needs to notice that that the temperature is given by a computation on the horizon

$$T_{sbh} = \frac{d}{4\pi}\left(\frac{r_h}{L^2}\right) + \frac{d-2}{8\pi r_h} \ , \tag{2.97}$$

where r_h is the radius of the horizon. In the large mass limit, the horizon is close to $r_h \sim r_0 = L^2 z_0^{-1}$. The correction is small and the temperature of the black hole can be

written as

$$T_{sbh} \approx T_{bb}\left(1+\frac{(d-3)}{d}\frac{L^2}{r_0^2}\right) \ , \quad T_{bb}=\frac{dr_0}{4\pi L^2} \ , \tag{2.98}$$

where we compare to the black brane temperature. This introduces an additional correction of order s^2 in (2.96).

$$\langle O\rangle_{J=0} = -N\left(\frac{4\pi T_{sbh}}{d}\right)^{\Delta} B_W \frac{\Gamma(h)^2}{\Gamma(2h)}\frac{\pi h(1-h)}{\sin(\pi h)}\left(1-s^2[\mathcal{F}(d,h)-\mathcal{E}(d,h)]-s^2(d-3)h\right) \ . \tag{2.99}$$

2.4 Conclusion

The problem of linear response in AdS black holes and its relation to conformal field theory correlators is an important problem on which a lot of recent progress has been made, especially for AdS_5 black holes.

Our results, by contrast, are valid for arbitrary dimension, but we are only able to make a perturbative analysis order by order. The zero-th order problem of a black brane at zero momentum is relatively simple. Already, the first non-trivial order is rather complicated. Our answers are given in terms of infinite sums of Γ functions, which we showed could be matched to the AdS_3 setup, giving us confidence in our methods.

Solutions in terms of other methods for AdS_5 give very complicated answers as well, in terms of solutions to the Heun differential equations. It would be interesting to understand the relation between these methods more carefully. Perhaps there is a way to simplify the final computations, which in our case get harder as we increase the order of the perturbation.

More generally, we plan to study the problem of retarded Green's function at arbitrary dimension, perturbing around the zero frequency, zero momentum result.

In regards to the one point function in AdS spherical black holes, we also found a

complicated answer. It would be interesting if there is a better solution for the case of AdS_5 related to the other recent developments in the computation of retarded Green's functions, perhaps by understanding how solutions of Heun's equation with sources generate generalized solutions (similar to generalized hypergeometric functions). This is something we're currently looking into as well.

Our method, which is perturbative, is probably also useful to study non-linear equations in the bulk, even at zero momentum. It would be interesting to also generalize our results beyond scalar fields.

On some other issues, like computing the time to the singularity by looking at the one point functions, as suggested in [41], we have nothing useful to say. We believe understanding this issue will require solving the exact equation in detail. The presence of additional singularities that can appear in the differential makes the analysis of such a problem a lot harder to undertake than in the flat brane case.

Chapter 3

A fluid perspective of Smarr formula

We derive a generalized Euler equation, $\epsilon + p = sT + \mu q + y\frac{\partial p}{\partial y}$, using the effective field theory formulation of perfect fluids. This generalization was achieved by introducing a new variable y into the effective action, which encodes a geometrical scale of the space-time where the fluid is on. Notably, the generalized Euler equation is independent of the AdS/CFT correspondence. However, when applied to a holographic perfect fluid, this equation naturally recovers the Smarr formula for AdS black holes, thus situating the physical interpretation of the Smarr formula within the framework of well-established physics. Finally, our findings raise important questions regarding the validity of treating the cosmological constant Λ as a thermodynamic variable, as proposed in certain frameworks within the literature.

3.1 Introduction to the chapter

The AdS/CFT correspondence [29] has greatly advanced our understanding of quantum field theory in the strong coupling regime, in part by geometrizing abstract concepts from quantum physics in gravitational terms. For instance, a thermal state in field the-

ory is dual to an eternal AdS black hole [73]. Moreover, the Hawking-Page transition between thermal AdS spacetime and a "large" AdS black hole [74] is interpreted as the confinement/deconfinement transition in a gauge theory on $S^1 \times S^3$ [14]. Within this holographic framework, [75] derived the Smarr formula for AdS black holes, providing further insight into its thermodynamic interpretation.

In this chapter, we revisit the physical meaning of the Smarr formula within the context of gauge/gravity duality. Our goal is to explore the Smarr formula from the perspective of fluid/gravity duality [76, 77, 42]. It is well-established that the boundary stress tensor of many AdS black holes takes the form of a perfect fluid in global equilibrium [78, 79]. From this perspective, the thermodynamics of the holographic fluid directly corresponds to black hole thermodynamics. This connection establishes a natural bridge between the Smarr formula and the theory of perfect fluids, which we explore in detail.

A significant development relevant to this work is the recent construction of effective actions for perfect fluids [80, 81, 82, 85, 86, 43, 87, 88, 89, 90]. Within this framework, the effective action not only reproduces the perfect fluid stress tensor but also ensures the validity of the Euler equation, with the effective Lagrangian acting as a local thermodynamic potential. As we will explore in Section 3.2, the Smarr formula, when suitably reformulated, bears a close resemblance to the Euler equation—with an additional correction term. This resemblance motivates the pursuit of a generalized Euler equation, which we establish via an explicit derivation from the effective action for perfect fluids. Crucially, this derivation introduces a new variable into the local thermodynamic potential—one that is invariant under both spacetime diffeomorphisms and the emergent low-energy gauge symmetries of the fluid. As we will show, this variable admits a natural

geometric interpretation and leads directly to the central result of this work:

$$\epsilon + p = sT + \mu q + y\frac{\partial p}{\partial y} \ . \tag{3.1}$$

We refer to this as the generalized Euler equation, with the additional term $y\frac{\partial p}{\partial y}$ representing an extra contribution mentioned earlier. Importantly, this result is independent of black hole physics and the AdS/CFT correspondence. We then apply this equation to the case of a holographic perfect fluid, from which the Smarr formula is naturally reproduced.

Another prominent context in which the Smarr formula has been extensively discussed is extended black hole thermodynamics (EBHT). This framework provides a specific interpretation of the Smarr formula by introducing a thermodynamic variable associated with the cosmological constant Λ [91, 92, 93, 94, 95]. Initially, this variable was identified as a pressure term, $p_\Lambda \sim \frac{1}{l^2}$. However, more recent formulations of EBHT reinterpret it as the central charge, $C \sim N^2$, where N represents the number of degrees of freedom in the dual field theory [96, 97, 98, 99]. This shift was primarily motivated by [75], which aimed to align EBHT with holography. However, the central result of this chapter, (3.1), challenges these interpretations of the Smarr formula, as we shall discuss later.

This chapter is organized as follows: In Section 3.2, we review the Smarr formula and highlight its preliminary similarities with the Euler equation. In Section 3.3, we examine the standard construction of the effective action for perfect fluids and introduce a new variable into the effective action, which enables us to derive a generalized Euler equation. In Section 3.4, we demonstrate that the Smarr formula is a specific instance of the generalized Euler equation. Section 3.5 discusses why our results are inconsistent with the proposal for extended black hole thermodynamics. Finally, in Section 3.6, we present our conclusions and suggest potential directions for future research.

3.2 Smarr formula for AdS black holes

In this section, we will review the Smarr formula for the AdS_d Reissner-Nordström black hole, closely following the conventions in [75]. The Einstein-Maxwell action, with a negative cosmological constant, is given by

$$S = \frac{1}{16\pi G_N} \int d^d x \sqrt{-g} \left(R - 2\Lambda - F^2 \right) \ , \tag{3.2}$$

where G_N is the d-dimensional Newton's constant. The negative cosmological constant Λ can be expressed in terms of the AdS radius l as follows: $\Lambda = -\frac{(d-2)(d-1)}{2l^2}$. For the spherical AdS_d Reissner-Nordström black hole with $d > 3$, the metric and gauge field are, respectively,

$$ds^2 = -f(r)dt^2 + f(r)^{-1}dr^2 + r^2 d\Omega_{d-2}^2 \ , \quad f(r) = \frac{r^2}{l^2} + 1 - \frac{\tilde{m}}{r^{d-3}} + \frac{\tilde{q}^2}{r^{2d-6}} \ , \tag{3.3}$$

$$A = \left(\mu l - \frac{1}{\gamma} \frac{\tilde{q}}{r^{d-3}} \right) dt \ , \quad \gamma = \sqrt{\frac{2(d-3)}{(d-2)}} \ . \tag{3.4}$$

The constant μ is the chemical potential, and it is defined such that the gauge field A vanishes at the event horizon located at r_h

$$\mu = \frac{1}{\gamma} \frac{\tilde{q}}{l r_h^{d-3}} \ . \tag{3.5}$$

The black hole energy M and charge Q are related to the parameters $\tilde{m}$ and $\tilde{q}$ as follows:

$$M = \frac{(d-2)A_{d-2}\tilde{m}}{16\pi G_N} \ , \quad Q = \frac{l\gamma(d-2)A_{d-2}\tilde{q}}{8\pi G_N} \ , \tag{3.6}$$

where A_D is the area of the D-dimensional unit sphere S^D. The black hole entropy S and the Hawking temperature T are given, respectively, by

$$S = \frac{A_{d-2} r_h^{d-2}}{4G_N} \ , \tag{3.7}$$

$$T = \frac{(d-1) r_h}{4\pi l^2} + \frac{(d-3)(1-\gamma^2 l^2 \mu^2)}{4\pi r_h} \ . \tag{3.8}$$

The Smarr formula is traditionally derived either by applying Euler's theorem for homogeneous functions to the "bulk" scaling of thermodynamic quantities[1] or by evaluating the Komar integral at spatial infinity and the horizon [102, 103, 104, 105, 106]. In this work, we adopt a different perspective, interpreting black hole thermodynamics as the thermodynamics of the dual field theory in the strongly interacting regime, in accordance with the AdS/CFT correspondence. Consequently, we derive the Smarr formula using thermodynamic considerations and the Euclidean action [75]. To this end, let us consider the grand canonical potential, Ω:

$$\Omega(T, \mu, V) = U - TS - \mu Q \ . \tag{3.9}$$

In our context, M represents the internal energy U of the system. For what is coming it is important to note that, in principle, Ω is a function of the volume V, which, in the case of black holes in AdS spacetimes, corresponds to the spatial volume of the boundary metric where the dual field theory resides. For the AdS_d Reissner-Nordström black hole, we compute the grand canonical potential Ω using the Euclidean on-shell action

$$\Omega = \frac{A_{d-2}}{8\pi G_N} r_h^{d-3} - \frac{M}{(d-2)} \ . \tag{3.10}$$

[1]Scaling arguments have been widely used in black hole thermodynamics to derive Smarr formulas, accommodating various matter contents and asymptotic behaviors (see, e.g., [100, 101]).

Equating the definition of Ω in (3.9) with the "on-shell value" of Ω (3.10), we obtain the Smarr formula for AdS black holes:

$$(d-1)M = (d-2)(TS + \mu Q) + \frac{(d-2)A_{d-2}}{8\pi G_N} r_h^{d-3} \ . \tag{3.11}$$

In the last term of this expression, the radius of the event horizon r_h should be understood as a function of the thermodynamic variables. In summary, the Smarr formula is an unusual relation among thermodynamic quantities.

Our objective is to develop a deeper physical understanding of the Smarr formula within the broader framework of the AdS/CFT correspondence. In particular, we are going to recast the Smarr formula (3.11) into a form that naturally generalizes the standard Euler relation, $U + pV = TS + \mu Q$, by incorporating an additional correction term arising from a geometric scale inherent to the system. As previously noted in [75], this correction captures the fact that the dual field theory lives on a sphere rather than a flat plane. Our analysis will go beyond purely thermodynamic reasoning by incorporating insights from the fluid/gravity correspondence.

In thermodynamics, the Euler equation arises in the thermodynamic limit, where the volume V and the number of particles N both tend to infinity while maintaining a fixed ratio $\frac{N}{V}$. In this limit, the grand canonical potential becomes $\Omega = -pV$, and the Euler equation follows as $-pV = U - TS - \mu Q$. We seek to extend this reasoning to the Smarr formula. However, in the context of black hole thermodynamics, defining the thermodynamic volume V and pressure p is far from straightforward. This is where fluid/gravity duality offers crucial insight. To define the pressure p for AdS black holes, we observe that the boundary stress-energy tensor associated with these black holes takes the form of a perfect fluid stress tensor [78, 79]. The boundary stress tensor for any given

gravitational solution can be calculated using the formula provided in [107, 108, 109]:

$$T_{ab} = \frac{1}{8\pi G_N}\left(h_{ab}\left(K - \frac{(d-2)}{l}\right) + K_{ab} + \frac{lG_{ab}}{(d-3)} + ...\right) \ , \tag{3.12}$$

where h_{ab} is the induced metric, K_{ab} is the extrinsic curvature, and G_{ab} is the Einstein tensor for a fixed value of the radial direction r. The counterterms explicitly written in (3.12), are valid for $d < 6$; for higher dimensions, see [108]. As a reminder, d is the bulk dimension, so $(d-1)$ is the boundary dimension. In our case, the boundary metric is

$$ds^2|_{\partial\mathcal{M}} = -dt^2 + l^2 d\Omega^2_{d-2} \ . \tag{3.13}$$

Thus, the volume of the spatial section of the boundary spacetime is $V = l^{d-2}A_{d-2}$ where the AdS radius l is acting as the radius of the $(d-2)$-dimensional sphere. For even-dimensional boundary spacetime, the conformal anomaly and Casimir energy appear [107, 109]. Since these effects are not relevant to the present discussion, we restrict our analysis to odd-dimensional boundary spacetime. For $(d-1) = 2n+1$ dimensions, the components of the boundary stress tensor are

$$-T^t_{\ t} = \frac{(d-2)\tilde{m}}{16\pi G_n l^{d-2}} = \frac{M}{l^{d-2}A_{d-2}} = \frac{M}{V} \ , \tag{3.14}$$

$$T^{\phi_j}_{\ \phi_j} = \frac{\tilde{m}}{16\pi G_n l^{d-2}} = \frac{M}{(d-2)V} \ . \tag{3.15}$$

where we denoted by ϕ_j an arbitrary angle of the sphere. We can recast these components of T_{ab} as a perfect fluid stress tensor

$$T_{ab} = pg_{ab} + (p+\epsilon)u_a u_b \ , \tag{3.16}$$

where g_{ab} denotes the boundary metric, and u_a is a unit timelike vector. The pressure p and the energy density ϵ are

$$p = \frac{\epsilon}{(d-2)} \ , \quad \epsilon = \frac{M}{V} \ . \tag{3.17}$$

This holographic perfect fluid in certain sense is dual to the AdS_d Reissner-Nordström black hole. Clearly, this fluid satisfies the conformal equation of state $\epsilon = (d-2)p$. The thermodynamics of this fluid is the same than the black hole thermodynamics since the fluid is at global thermal equilibrium.

Returning to the Smarr formula, substituting the conformal equation of state $M = (d-2)pV$ into (3.11) provides a more suggesting expression:

$$M + pV = TS + \mu Q + \frac{A_{d-2}}{8\pi G_N} r_h^{d-3} \ , \tag{3.18}$$

which resembles the Euler equation plus an additional correction term. As mentioned earlier, the traditional Euler equation arises in the thermodynamic limit, where $V \to \infty$. However, in our case, the volume V occupied by the fluid is finite, and thus the standard derivation of the Euler equation no longer applies. In the gravitational context, the limit $V \to \infty$ corresponds to a charged black brane, for which the Smarr formula reduces to the Euler equation $p + \epsilon = Ts + \mu q$ [110], as the dual field theory lives in a plane.

In the analysis leading to equation (3.18), we relied on the idea that a perfect fluid in global thermal equilibrium provides an equivalent description of global thermodynamics. However, perfect fluids are typically used to describe local thermodynamics, where the Euler equation is assumed to hold universally—a point that seems at odds with our intuitive understanding of the Smarr formula developed in this section. To fully grasp the physical significance of the Smarr formula, it is essential to extend the Euler equation

beyond its conventional domain. Therefore, in the next section, we will set aside the discussion of black holes and focus solely on the Euler equation and its generalization in the context of perfect fluids.

3.3 Effective action for perfect fluids

In this section, we begin by reviewing the standard construction of the effective action for perfect fluids, which naturally leads to the Euler equation. We then extend this framework by introducing a new variable into the effective action, capturing the fluid's response to the presence of a geometrical scale. With this extension, we derive a generalized form of the Euler equation.

3.3.1 Review standard effective action for perfect fluids

Formal constructions of effective actions for hydrodynamics have been developed using techniques such as the Schwinger-Keldysh formalism [85, 86, 43, 87] and superspace methods [88, 89, 90]. Comprehensive reviews can be found in [44, 111]. Although these advanced techniques will not be explicitly employed in this chapter, they highlight the significant progress and depth this field has achieved. Instead, we revisit the foundational constructions presented in [80, 81, 82], informed by a more modern understanding of the subject. Moreover, we focus exclusively on perfect fluids, leaving aside considerations of dissipation and hydrodynamic anomalies.

Hydrodynamics provides a valid effective description in the long-wavelength limit. For this reason, we assume that the curvature of the manifolds under consideration is much larger than the mean free path of the fluid. To construct the effective action for perfect fluids, two key components are required:

- **Auxiliary Scalar Fields:** To ensure that the covariant conservation of the stress tensor becomes a second-order equation (as it is initially a first-order equation with respect to the fluid variables), auxiliary scalar fields are introduced as the low-energy dynamical variables of the effective action.

- **Symmetry Organization:** To organize the potential terms that can appear in the action principle, the symmetries of the fluid must be known. In this case, the relevant symmetries are low-energy gauge symmetries, which imply that the auxiliary scalar fields can be interpreted as Stueckelberg fields [85, 44].

Given the dynamical variables and symmetries of the effective action, we should, in principle, include all gauge-invariant terms in the theory. However, since our focus is on perfect fluids, we will disregard higher-derivative terms in the effective action. Moreover, as stated in the introduction, we assume that the bulk spacetime has d dimensions. Consequently, in this section, we consider a perfect fluid in an odd $(d-1) = 2n+1$ dimensional manifold, ensuring that anomalies and Casimir energy do not play a role in our discussion. Finally, we limit this section to field-theoretical aspects, deferring the connection between these results and gravity to the next section.

Let's begin by establishing the notation: the background metric for the perfect fluid is

$$ds^2 = g_{ab}dx^a dx^b \ , \quad a, b \in \{0, 1, ..., d-2\} \ . \tag{3.19}$$

The low-energy dynamical variables for the effective action are $(d-2)$ spatial scalar fields σ^I that describe the fluid element, plus a temporal scalar field σ^0 that acts as an internal clock for the fluid element:

$$\sigma^I = \sigma^I(x^a) \ , \quad \sigma^0 = \sigma^0(x^a) \ , \quad I \in \{1, ..., d-2\} \ . \tag{3.20}$$

The fluid dynamics possess the following emergent low-energy internal symmetries:

$$\sigma^0 \to \sigma^0 + f^0(\sigma^I) \ , \tag{3.21}$$

$$\sigma^I \to \sigma^I + f^I(\sigma^J) \ . \tag{3.22}$$

These symmetry transformations can be motivated by the observation that σ^I represents spatial coordinates describing the fluids. As such, σ^I must satisfy the comoving condition

$$\frac{d}{d\tau}\sigma^I(x^a(\tau)) = 0 \Longleftrightarrow u^a\partial_a\sigma^I = 0 \ , \tag{3.23}$$

where x^a in the position in the spacetime, and the fluid velocity is $u^a = \frac{dx^a}{d\tau}$. The second expression in (3.23) employs the directional derivative along the fluid velocity u^a. Notably, this condition is preserved by the symmetry transformations (3.21) and (3.22). It is also important to highlight that, unlike σ^I, the temporal scalar field satisfies $\frac{d}{d\tau}\sigma^0(x^a(\tau)) \neq 0$, yet it remains gauge-invariant under these symmetry transformations.

In essence, the perfect fluid is characterized by a target metric $G_{MN}(\sigma^M)$, where the fluid coordinates are $\sigma^M = (\sigma^0, \sigma^I)$. In this framework, the internal symmetries (3.21) and (3.22) correspond to the isometries of a degenerate metric [81]:

$$ds^2 = G_{MN}d\sigma^M d\sigma^N \ , \quad G_{NM}n^M = 0 \ , \quad M, N \in \{0, 1, ..., d-2\} \ , \tag{3.24}$$

where n^N is a null-like eigenvector associated with the zero eigenvalue of G_{MN}. An explicit parameterization of this degenerate target metric in terms of spatial target metric[2]

[2]In the context of fluid/gravity duality, the target metric G_{MN} is essentially the horizon metric. In this way, the horizon asymptotic symmetry becomes the emergent low-energy gauge symmetries of the effective action for hydrodynamics [112].

is

$$ds^2 = 0 \cdot (d\sigma^0)^2 + G_{IJ}(d\sigma^I - v^I d\sigma^0)(d\sigma^J - v^J d\sigma^0) \ , \quad I, J \in \{1, ..., d-2\} \ , \tag{3.25}$$

where v^J denotes boosts. The null normal vector n^M is then given by

$$n^M = \frac{1}{\gamma}(1, v^J) \ , \quad \gamma^{-1} = \sqrt{1 - G_{IJ} v^I v^J} \ . \tag{3.26}$$

Thus, the fluid coordinates σ^M are Stueckelberg fields associated with a sub-class of diffeomorphisms of the target metric. Further discussion of this point is found in [85, 44].

So far, we have provided the description for neutral fluids. To describe charged fluids, a Stueckelberg field associated with a $U(1)$ symmetry must be introduced [82]

$$\varphi = \varphi(x^a) \ , \tag{3.27}$$

with the following internal transformation, dubbed chemical shift symmetry:

$$\varphi \to \varphi + g(\sigma^I) \ . \tag{3.28}$$

Given the low-energy dynamical variables σ^M and φ, along with the corresponding low-energy gauge symmetries, we proceed to construct the effective action for a charged perfect fluid. To achieve this, we must identify scalar quantities that remain invariant under diffeomorphisms of the physical metric g_{ab} and are also gauge-invariant under the fluid symmetry transformations (3.21) and (3.22).

One such scalar is the entropy density s of the system, which is defined in terms of

the spatial target metric G_{IJ} (3.25) as follows [81]:

$$s = \sqrt{\mathrm{Det}(B^{IJ}G_{JK})} \ , \quad B^{IJ} = g^{ab}e^I_a e^J_b \ , \tag{3.29}$$

$$e^I_a \equiv \partial_a \sigma^I - v^I \partial_a \sigma^0 \ . \tag{3.30}$$

Another scalar is the chemical potential μ associated with the $U(1)$ symmetries [82] which reads

$$\mu = u^a \partial_a \varphi \ . \tag{3.31}$$

We note that both s and μ are local functions of the physical spacetime where fluids is on, and they take constant values only at global thermal equilibrium.

The low-energy fields σ^M, φ are auxiliary variables that allow the description of perfect fluids and their local thermodynamics in terms of an action principle. To zero-order in the derivative expansion, the effective action for a perfect fluid is:

$$I = -\int d^{d-1}x\sqrt{-g}\zeta(s,\mu) \ , \tag{3.32}$$

where ζ is a local thermodynamic potential function of the entropy density s and the chemical potential μ. By taking the variation with respect to the background metric g_{ab}, one obtains the stress tensor:

$$T_{ab} = \left(-\zeta + s\frac{\partial\zeta}{\partial s}\right) g_{ab} + \left(-\mu\frac{\partial\zeta}{\partial\mu} + s\frac{\partial\zeta}{\partial s}\right) u_a u_b \ . \tag{3.33}$$

Comparing this result with the stress tensor of a perfect fluid $T_{ab} = pg_{ab} + (p+\epsilon)u_a u_b$, one deduces the pressure p

$$p = -\zeta + s\frac{\partial\zeta}{\partial s} \ , \tag{3.34}$$

and the local energy density ϵ

$$\epsilon = \zeta - \mu \frac{\partial \zeta}{\partial \mu} \ . \tag{3.35}$$

The local thermodynamic potential ζ is essentially a Legendre transformation: $\zeta = \epsilon - \mu q$, where the charge density is $q = -\frac{\partial \zeta}{\partial \mu}$. Then, the temperature is simply $T = -\frac{\partial \zeta}{\partial s}$. In this way, the consistency of the effective action (3.32) and the stress tensor (3.33) with the standard thermodynamic relation implies the Euler equation:

$$p + \epsilon = sT + \mu q \ . \tag{3.36}$$

Thus, the Euler equation is an unavoidable consequence of the effective action (3.32). Note that the equation of state for the fluid is not used at all in this derivation.

For completeness, we mention that due to the comoving condition (3.23), the entropy current s^a is conserved off-shell:

$$\nabla_a s^a = 0, \quad s^a = s u^a \ . \tag{3.37}$$

This conservation law reflects the non-dissipative nature of the fluid. In addition, the chemical shift symmetry (3.28) implies the on-shell conservation of the charge current:

$$\nabla_a q^a = 0, \quad q^a = q u^a \ . \tag{3.38}$$

With this, we conclude our review of the effective action formulation for perfect fluids. In the following section, we will use this framework to derive a generalized Euler equation.

3.3.2 Generalized Euler equation

To generalize the Euler equation, we introduce a new variable into the effective action for perfect fluids. This variable must be a diffeomorphism-invariant scalar with respect to g_{ab} and must remain gauge-invariant under the symmetry transformations defined in (3.21), (3.22). Furthermore, as discussed at the end of Section 3.2, there are scenarios in which the standard scaling argument to derive the Euler equation fails, particularly when the volume of the system is compact. In such cases, the compact space's radius introduces an additional geometric scale to the problem. This observation suggests that the new variable in the effective action should have a geometric origin.

The gauge-invariant quantity that satisfies these criteria is

$$y = u^a \partial_a \sigma^0 \ . \tag{3.39}$$

The definition of this variable closely resembles the definition of the chemical potential μ presented in (3.31). However, the temporal scalar field σ^0, which represents the clock for the fluid element, differs in nature from the Stueckelberg field φ associated with U(1) symmetry.[3] Given the definition of y, its physical meaning may not be immediately clear. Therefore, let us first derive the generalized Euler equation and subsequently discuss the physical meaning of y.

The effective action for perfect fluids is now

$$I = -\int d^{d-1}x\sqrt{-g}\chi(s,\mu,y) \ , \tag{3.40}$$

where χ represents a new local thermodynamic potential that depends on entropy density s, chemical potential μ, and the new variable y. Taking the variation with respect to the

[3]The variable y has been previously studied in the literature, but [113] did not clearly distinguish between the temporal scalar field σ^0 and the gauge scalar field φ.

background metric g_{ab}, the stress tensor follows

$$T_{ab} = \left(-\chi + s\frac{\partial\chi}{\partial s}\right) g_{ab} + \left(-y\frac{\partial\chi}{\partial y} - \mu\frac{\partial\chi}{\partial\mu} + s\frac{\partial\chi}{\partial s}\right) u_a u_b \ . \tag{3.41}$$

The next step is to compare this expression with the stress tensor of a perfect fluid: $T_{ab} = pg_{ab} + (p+\epsilon)u_a u_b$. Thus, we can identify the pressure p and energy density ϵ as:

$$p = -\chi + s\frac{\partial\chi}{\partial s} \ , \quad \epsilon = \chi - y\frac{\partial\chi}{\partial y} - \mu\frac{\partial\chi}{\partial\mu} \ . \tag{3.42}$$

The following combination will be relevant later:

$$\epsilon + p = -y\frac{\partial\chi}{\partial y} - \mu\frac{\partial\chi}{\partial\mu} + s\frac{\partial\chi}{\partial s} \ . \tag{3.43}$$

As a second step, we need to properly identify the rest of the thermodynamic variables. We note that the energy density has the following dependence: $\epsilon = \epsilon(s, q, y)$. Thus, if we perform the Legendre transformation $\tilde{\epsilon} = \epsilon - \mu q$, we find that $\tilde{\epsilon} = \tilde{\epsilon}(s, \mu, y)$. In this way, the temperature T and charge density q are given by:

$$T = \left.\frac{\partial\tilde{\epsilon}}{\partial s}\right|_{y,\mu} \ , \quad q = \left.\frac{\partial\tilde{\epsilon}}{\partial\mu}\right|_{y,s} \ . \tag{3.44}$$

From these expressions, we deduce how to compute the local temperature T and charge density q from the thermodynamic potential χ:

$$T = \frac{\partial\chi}{\partial s} - y\frac{\partial^2\chi}{\partial y\partial s} \ , \quad q = -\frac{\partial\chi}{\partial\mu} \ . \tag{3.45}$$

Inserting these results into (3.43), we obtain the relation

$$\epsilon + p = sT + \mu q + y\partial_y \left(-\chi + s\frac{\partial \chi}{\partial y} \right) \ . \tag{3.46}$$

In parentheses of the last term, we recognize the local pressure p given in (3.42). Therefore, we obtain a new relation among thermodynamic variables:

$$\epsilon + p = sT + \mu q + y\frac{\partial p}{\partial y} \ . \tag{3.47}$$

This expression is the generalized Euler equation that we were seeking. The additional correction involves a derivative of the pressure p with respect to y. Therefore, if the thermodynamics of a fluid in a given spacetime does not respond to variations in y, the additional correction $\frac{\partial p}{\partial y}$ vanishes recovering the standard Euler identity.

Another important aspect of the generalized effective action for a perfect fluid (3.40) is the emergence of a new conserved current. In addition to the off-shell conservation of the entropy current (3.37) and the on-shell conservation of the charge current (3.38), we now also have:

$$\nabla_a J^a_{(y)} = 0, \quad J^a_{(y)} = u^a \partial_y p \ . \tag{3.48}$$

This conservation law arises from the fact that the variable y, defined in (3.39), is invariant under spatial diffeomorphisms of the target space, $\sigma^I \to \sigma^I + f^I(\sigma^J)$. Mathematically, the pair $(y, \partial_y p)$ is analogous to the chemical potential μ and the charge density q associated with the $U(1)$ symmetry. However, it is important to emphasize that the variable y was introduced to capture a geometric scale imposed by the underlying spacetime on the thermodynamics of the fluid. For this reason, unlike conventional thermodynamic variables, y is not expected to admit a microscopic interpretation.

To further explore the meaning of the variable y, let us consider a scenario of global

thermal equilibrium, where the fluid clock can be aligned with physical time; that is, $\sigma^0 = x^0$. In this case, we find that $y = u^0$, a result that may appear somewhat opaque at first glance. To build intuition, let us perform a Weyl transformation of the physical metric, $g' = Wg$, where W is a conformal factor. Under this transformation, the fluid velocity transforms as $u'^a = \frac{u^a}{W}$. This leads to the following relation:

$$y = u'^0 = \frac{u^0}{W} \ . \tag{3.49}$$

This expression suggests that the variable y is naturally associated with the inverse of the conformal factor W. Alternatively, rather than performing an explicit Weyl transformation, one can express the physical metric as a conformal rescaling of a reference metric, $g = W\bar{g}$, leading to the same conclusion that $y \sim \frac{1}{W}$.

To facilitate comparison between the central result of this work and existing literature, we rewrite the generalized Euler identity (3.47) in the following form:

$$\omega = \epsilon - sT - \mu q \Longrightarrow \omega = -p + y\frac{\partial p}{\partial y} \ , \tag{3.50}$$

where ω denotes the density of the grand canonical potential. This expression highlights that the presence of an additional scale in the system, encoded by the variable y, challenges the conventional assumption that, in the thermodynamic limit, the grand canonical potential ω is simply proportional to the pressure p.

The relation in (3.50) bears a notable resemblance to earlier results in the literature on effective actions for fluids [83, 84].[4] However, a key distinction lies in the construction of our effective action, which is formulated at zeroth order in the derivative expansion. In contrast, the works cited in [83, 84] incorporate higher-order derivative corrections,

[4]We thank Kristan Jensen for bringing these references to our attention.

which modify the form of the free energy accordingly.

3.4 Smarr formula as a particular case of the generalized Euler equation

As discussed around equation (3.18), the Smarr formula can be viewed as a generalization of the Euler equation. Traditionally, however, the thermodynamics of black holes is examined using Euclidean methods. Unfortunately, these methods do not readily define the thermodynamic volume V and pressure p of a thermal system within the context of gravity. This limitation motivates our use of fluid dynamics to analyze the Smarr formula. We will now demonstrate the generalized Euler equation (3.47), derived in the previous section, reduces to a local version of the Smarr formula when applied to holographic fluids. Subsequently, the standard form of the Smarr formula emerges by considering the fluid in global thermal equilibrium, which encapsulates the same thermal information as the first law of thermodynamics.

In this section, we extend the discussion from section 3.2 by examining the AdS_d Reissner-Nordström black hole with arbitrary horizon topology. We adopt Eddington-Finkelstein coordinates, as this gauge simplifies the analysis of Weyl transformations compared to the Fefferman-Graham gauge. Moreover, we restrict the boundary dimension $(d-1)$ to be odd; otherwise, the conformal anomaly and the Casimir energy would need to be accounted for in the effective action. The line element is:

$$ds^2 = -f(r)du^2 - 2dudr + r^2 d\Sigma_k^2 \ , \quad f(r) = \frac{r^2}{l^2} + k - \frac{\tilde{m}}{r^{d-3}} + \frac{\tilde{q}^2}{r^{2d-6}} \ . \tag{3.51}$$

Here, the gauge field A is still given by equation (3.4). The constant k represents the unit-normalized curvature of the transverse space Σ_k. Thus, the black brane is recovered

for $k = 0$, the spherical black hole for $k = 1$, and the hyperbolic black hole for $k = -1$. In all cases, the black hole energy M and charge Q are related to the parameters $\tilde{m}$ and $\tilde{q}$ as follows:

$$M = \frac{(d-2)\Sigma_{k,d-2}\tilde{m}}{16\pi G_N} , \quad Q = \frac{\gamma l(d-2)\Sigma_{k,d-2}\tilde{q}}{8\pi G_N} . \tag{3.52}$$

The entropy of the black holes is given by:

$$S = \frac{\Sigma_{k,d-2} r_h^{d-2}}{4G_N} , \tag{3.53}$$

where $\Sigma_{k,d-2}$ represents the volume of the transverse space with unit radius. It is important to note that for flat and hyperbolic spaces, $\Sigma_{k,d-2}$ is formally infinite. Additionally, hyperbolic space has negative curvature, introducing an extra scale into the physical problem.

The Hawking temperature T and the chemical potential μ are

$$T = \frac{(d-1)r_h}{4\pi l^2} + \frac{(d-3)(k - l^2\gamma^2\mu^2)}{4\pi r_h} , \quad \mu = \frac{\tilde{q}}{\gamma l r_h^{d-3}} . \tag{3.54}$$

Note that the chemical potential μ is the same as in equation (3.5). The Smarr formula is now given by:

$$M + pV = TS + \mu Q + \frac{k\Sigma_{k,d-2}}{8\pi G_N} r_h^{d-3} . \tag{3.55}$$

For for $k = 0$ the last term vanishes, thereby recovering the standard Euler equation for a charged black brane. This is because, in flat space, there are no additional scales to consider.

We will now compute the thermodynamic potential χ (3.40) which is associated with the effective action for the holographic perfect fluid dual to the AdS_d Reissner-Nordström black hole. Our objective is to place the holographic fluid in a boundary spacetime

that exhibits spacetime dependence, allowing us to mimic a state that is near out of equilibrium.[5] As a consequence, the thermodynamic variables now will become local functions of the spacetime. To obtain the boundary metric with the desired properties, we perform the following radial diffeomorphism in the bulk line element (3.51):

$$r \to W(x^a) r \ , \tag{3.56}$$

where $W(x^a)$ is an arbitrary function independent of the radial variable r. The new line element is

$$ds^2 = -f(Wr)du^2 - 2W du dr - 2r\partial_a W du dx^a + W^2 r^2 d\Sigma_k^2 \ , \tag{3.57}$$

$$f(r) = \frac{W^2 r^2}{l^2} + k - \frac{\tilde{m}}{(Wr)^{d-3}} + \frac{\tilde{q}^2}{(Wr)^{2d-6}} \ . \tag{3.58}$$

Therefore, the boundary metric is

$$ds^2|_{\partial\mathcal{M}} = -\frac{W^2}{l^2} du^2 + W^2 d\Sigma_k^2 \ . \tag{3.59}$$

This line element describes a non-homogeneous, time-dependent background in which the fluid resides. The radial diffeomorphism (3.56) consequently induces a Weyl transformation on the boundary metric,[6] leading to the following expression for the fluid velocity:

$$u_a = -\frac{W}{l}\delta_a^0 \ . \tag{3.60}$$

Let's focus now on the target metric G_{MN} that describes the fluid space. Using the unitary gauge embedding $\sigma^0 = x^0$ and $\sigma^I = x^i$ [81], the target metric G_{MN} takes a very

[5] This step is purely for illustrative purposes and carries no additional meaning, as we are disregarding dissipation, and anomalies.

[6] In other words, the Weyl transformation is induced by a PBH transformation of the bulk metric. A detailed discussion of the consequences of this transformation in the thermodynamics of asymptotically locally AdS black holes is given in [114].

simple form:

$$ds^2_{fluid} = -0 \cdot du^2 + r_h^2 d\Sigma_k^2 \ , \tag{3.61}$$

that matches the horizon metric.[7] Given the target metric and the fluid velocity, we can use the formulas (3.29), (3.31), and (3.39) to compute the entropy density s, the chemical potential μ, and the variable y, respectively:

$$s = \frac{\Sigma_{k,d-2}}{4G_N} \frac{r_h^{d-2}}{W^{d-2}} \ , \quad \mu = \frac{\tilde{q}}{\gamma r_h^{d-3}} \frac{1}{W} \ , \quad y = \frac{l}{W} \ , \tag{3.62}$$

which are the variables that the thermodynamic potential χ depends on. We note that the entropy density satisfies its conservation law (3.37) as expected. We will utilize these variables to derive the explicit expression for the new thermodynamic potential χ from the energy density ϵ using equation (3.42). Our next step involves computing the boundary stress tensor via the formula (3.12) and the boundary metric given in (3.59). The components of the stress tensor are

$$-T^t_{\ t} = \frac{lM}{W^{d-1}\Sigma_{k,d-2}} \ , \tag{3.63}$$

$$T^{\phi_j}_{\ \phi_j} = \frac{lM}{(d-2)W^{d-1}\Sigma_{k,d-2}} \ . \tag{3.64}$$

Similar to section 3.2, these components can be expressed in the form of a perfect fluid stress tensor $T_{ab} = pg_{ab} + (p+\epsilon)u_a u_b$, from which we read the energy density ϵ:

$$\epsilon = \frac{(d-2)}{16\pi G_N l} \left[\left(\frac{4G_N s}{\Sigma_{k,d-2}} \right)^{\frac{d-3}{d-2}} (ky^2 + (\gamma l)^2 \mu^2) + \left(\frac{4G_N s}{\Sigma_{k,d-2}} \right)^{\frac{d-1}{d-2}} \right] \ , \tag{3.65}$$

where M has been expressed in terms of r_h as an intermediate step, and then in terms of the variables s, μ, and y given in equation (3.62). One can also verify that the conformal

[7] More precisely, the horizon metric before the Weyl transformation.

equation of state: $p = \frac{\epsilon}{d-2}$ is satisfied.

As a final step, using equation (3.42) that connects ϵ and p with the thermodynamic potential χ, we can infer the effective action for this holographic fluid

$$I = -\int d^{d-1}x\sqrt{-g}\chi(s,\mu,y) \ , \tag{3.66}$$

with the thermodynamic potential χ given by

$$\chi = \frac{(d-2)}{16\pi G_N l}\left[-\left(\frac{4G_N s}{\Sigma_{k,d-2}}\right)^{\frac{d-3}{d-2}}(ky^2+(\gamma l)^2\mu^2)+\left(\frac{4G_N s}{\Sigma_{k,d-2}}\right)^{\frac{d-1}{d-2}}\right] \ . \tag{3.67}$$

We note that all thermodynamic variables involved in χ are local functions of the space-time where the fluid resides. Certainly, we have derived χ in this case through inverse engineering, as we already knew some of the thermodynamic variables and the geometrical variable y. This approach is not an inconvenience for us; rather, it allows us to treat the thermodynamic potential χ as a starting point, as it encodes all the thermal information of the fluid. Finally, using equation (3.45), we compute respectively the local temperature T and charge density q as follows:

$$T = \frac{(d-1)}{4\pi l}\left(\frac{4G_N s}{\Sigma_{k,d-2}}\right)^{\frac{1}{d-2}} + \frac{(d-3)(ky^2-(\gamma l)^2\mu^2)}{4\pi l}\left(\frac{4G_N s}{\Sigma_{k,d-2}}\right)^{\frac{-1}{d-2}} \ , \tag{3.68}$$

$$q = \frac{(d-2)\gamma^2 l\mu}{8\pi G_N}\left(\frac{4G_N s}{\Sigma_{k,d-2}}\right)^{\frac{d-3}{d-2}} \ . \tag{3.69}$$

Furthermore, we notice that $\frac{\partial p}{\partial y}$ is proportional to k:

$$\frac{\partial p}{\partial y} = \frac{ky}{8\pi G_N l}\left(\frac{4G_N s}{\Sigma_{k,d-2}}\right)^{\frac{d-3}{d-2}} \ . \tag{3.70}$$

Consequently, this term vanishes for a charged black brane, as expected, since flat space-

time does not introduce any additional geometrical scale. Through straightforward algebraic manipulations, one can verify that the generalized Euler equation holds:

$$\epsilon + p = sT + \mu q + y\frac{\partial p}{\partial y} \ . \tag{3.71}$$

Furthermore, substituting the expressions for y and μ from (3.62), one can confirm that q[8] and $\partial_y p$ satisfy their respective conservation laws, given by (3.38) and (3.48).

To this point, we have utilized an arbitrary conformal factor to represent a curved physical background, simulating a state near out of equilibrium for the fluid. The usual global thermal state is obtained by selecting $W = Rl$, where R is a constant factor, reducing equation (3.71) to the Smarr formula given in (3.55). Strictly speaking, the last statement is true for $R = 1$; however, the extra scale allows us to distinguish the radius Rl of the transverse space Σ_k from the AdS radius l.

In conclusion, we have demonstrated that the Smarr formula is a specific instance of the generalized Euler equation (3.71). This result implies that holographic fluids satisfying the Smarr formula are not fundamentally distinct from more conventional fluids. The key insight is that when an additional scale arises from the underlying geometry of the thermal system, the standard scaling argument used to derive the Euler equation no longer holds, necessitating a generalized formulation. For a system with a compact volume, the physical interpretation is quite clear: the correction term $y\frac{\partial p}{\partial y}$ in the Euler equation naturally accounts for a finite-volume effect, as previously noted by [75]. In summary, there is nothing intrinsically special about the Smarr formula for AdS black holes; it emerges naturally from general thermodynamic and fluid considerations.

[8]Let us emphasize that $\tilde{q}$ denotes the constant appearing in the black hole line element, whereas $q = q(x)$ is a local function defined on the boundary spacetime. We apologize for any notational inconvenience this may cause.

3.5 Comments on cosmological constant as a thermodynamic variable

In the previous sections, we argued and demonstrated that the Smarr formula is a specific case of the generalized Euler equation, particularly in the context of black holes in AdS. In this sense, the Smarr formula naturally fits within the framework of the AdS/CFT correspondence, as its origins are rooted in well-established physics. This conclusion is supported by the fact that we derived the generalized Euler equation using effective field theory techniques applied to fluids. Only after establishing this result did we invoke the AdS/CFT correspondence to interpret the Smarr formula.

Extended black hole thermodynamics was initially proposed outside the context of gauge/gravity duality to provide an interpretation of the Smarr formula. In the original version of this proposal, the cosmological constant Λ was identified with a thermodynamic pressure [91, 92, 93, 94, 95] as follows:

$$p_\Lambda = -\frac{\Lambda}{8\pi G_N} = \frac{(d-1)(d-2)}{16\pi G_N l^2} \,, \tag{3.72}$$

where d is the dimension of the bulk spacetime.[9] Clearly, the notion of pressure p_Λ does not correspond to the pressure of the dual field theory. For this reason, the physical interpretation of the Smarr formula was investigated from a holographic perspective in [75].

Following the work of [75], a revised version of extended black hole thermodynamics was proposed to reinterpret the Smarr formula consistently with the AdS/CFT correspondence. To understand this new proposal, we recall the holographic identification

[9] For reviews on extended black hole thermodynamics, see [116, 117]. Other relevant literature on the subject includes [118, 119, 120, 121].

between the parameters of gravity and those of the dual field theory:

$$N^2 \sim \frac{l^{d-2}}{G_N} \ . \tag{3.73}$$

Here, N represents the number of degrees of freedom on field theory side of the duality. For instance, in $\mathcal{N} = 4$ SYM, N corresponds to the rank of the gauge group $SU(N)$, which is also the size of a matrix A in the adjoint representation. In the revised version of extended black hole thermodynamics, the so-called central charge $C \sim N^2$ is treated as a thermodynamic variable associated with the cosmological constant Λ [96, 97, 98, 99]. In this view, a variation in the cosmological constant induces a flow in theory space, affecting the thermodynamics of black holes in AdS. This proposal is supported by a possible origin of extended black hole thermodynamics in higher-dimensional physics [115].

The main result of this chapter—that the Smarr formula is a specific instance of the generalized Euler equation—conflicts this new interpretation for extended black hole thermodynamics. The reasoning is as follows: perfect fluids, a particular case of hydrodynamics, differs fundamentally from renormalization group (RG) physics. While the number of degrees of freedom N can indeed change with the energy scale in RG flow (as is well understood in the context of AdS/CFT, see [122, 123]), this cannot explain the Smarr formula. In a perfect fluids, thermodynamic variables must be functions of spacetime to describe local thermal equilibrium, something that the number of degrees of freedom N cannot do. The point is that we should not confuse a flow in a physical space where the fluid is on with a flow in theory space where an RG flow takes place. Finally, it is crucial to recognize that global equilibrium is merely a special case of local equilibrium. As a result, there is no justification for treating $C \sim N^2$ as a thermodynamic variable.

As a final remark for this section, the standard techniques for studying AdS black hole thermodynamics—such as the Euclidean method or your preferred method for com-

puting conserved charges—struggle to clarify the meaning of the Smarr formula. One reason for this difficulty is the double role played by the AdS radius l. On one hand, l can be interpreted as the radius of the transverse space at the boundary, while on the other, it sets the scale for constructing dimensionless quantities in holography, such as in equation (3.73). This point can be a source of confusion. However, in our construction, this issue is resolved because the variable y (as defined in equation (3.39) is diffeomorphism-invariant with respect to physical metric g_{ab} and gauge-invariant under the fluid transformations (3.21), (3.22) from the outset. Thus, there is no ambiguity. Ultimately, the insights gained from fluid/gravity duality were instrumental in revealing the correct understanding of the Smarr formula within holography.

3.6 Discussion

In this work, we derived a generalized Euler equation (3.47) using effective field theory techniques, granting our result a broader range of applicability independent of the AdS/CFT correspondence. We then applied the generalized Euler equation to a specific case: a holographic fluid derived from the boundary stress tensor associated with an AdS_d Reissner-Nordström black hole, from which we recovered the Smarr formula. Based on these findings, we further argue that treating the cosmological constant as a thermodynamic variable is not physically justified. This is because any thermodynamic variable associated with the AdS radius l cannot become a function of the boundary spacetime, as required for local thermodynamic equilibrium.

It has been demonstrated that evaluating the on-shell action of spacetimes with a future event horizon (featuring a planar horizon topology) can reproduce the standard effective action presented in (3.32). This was achieved by setting up a double-Dirichlet boundary problem to evaluate the on-shell action [124, 125]. It would be intriguing

to extend this construction to the more general effective action (3.40) discussed in our chapter. For this purpose, it is necessary to gain a deeper understanding of the variable y introduced in this work.

Another intriguing avenue for exploration is the explicit construction of the thermodynamic potential χ for rotating black holes, which also exhibit a boundary stress tensor with a perfect fluid form [78, 79]. In this work, we focused on even boundary dimensions d to avoid the complications arising from conformal anomalies. It would be valuable to develop the most general effective action for perfect fluids that can incorporate such conformal anomalies. In lower-dimensions, a notable example is the Schwarzian action, which can be interpreted as the effective action of an anomalous perfect fluid in 1d [126]. A similar structure appears in the boundary action of a non-rotating BTZ black hole with external sources [127, 128].

It's well-known that the Schwarzian action captures the near-horizon dynamics of near-extremal black holes [149, 45]. In contrast, our effective action given in (3.40) is an off-shell formulation that captures not only the one-point functions (the stress tensor), but also the Ward identities (the Navier-Stokes equations without dissipation). In this way, following closely the work of [53], it should be possible to derive a decoupling limit from the action (3.67), which encodes the dynamics of a holographic charged fluid, and connect it to the one-dimensional anomalous perfect fluid of [126]. In fact, the author of [53] already achieved this decoupling limit for a restricted class of CFT_3, although using a different set of variables from the fluid variables.

The Smarr formula remains valid in gravity theories with higher-order curvature corrections [104]. This raises an important question: can the generalized Euler equation (3.47) accommodate these theories? If not, it would suggest that the Smarr formula once again indicates the need for further generalizations of the Euler equation. Similar questions arise in the context of the dyonic AdS black holes with a non-trivial scalar

profile discussed in [129, 130], which constitute solutions to gauged supergravity.

It is worth emphasizing that the isometries of the target metric G_{MN}, as defined in (3.24), correspond to the emergent low-energy gauge symmetries of the hydrodynamic effective action. More broadly, asymptotic symmetries at the horizon [131, 132, 133, 134, 135] can be interpreted as manifestations of these emergent gauge symmetries of the boundary theory. Consequently, any generalization of horizon symmetries implies the presence of new gauge symmetries in holographic effective actions. Exploring potential connections between the present work and the novel symmetries identified in [112] would be a compelling direction for future research.

Similarly, the isometries of the degenerate target metric G_{MN} given in (3.24) are closely related to Carrollian diffeomorphisms. Motivated by this, it should be possible to formulate an effective action for Carrollian fluids [136, 137, 138, 139, 140, 141, 142, 143]. In this context, Carrollian diffeomorphisms would serve both as gauge symmetries of the effective action and as spacetime symmetries of the fluid's background.[10] With this action principle in place, the Smarr formula for asymptotically flat black holes should follow in a manner similar to the derivation presented in this chapter.

[10]This perspective aligns naturally with the Gauge/Gravity duality [112], as it likely follows from taking a flat limit of the fluid. There is also a body of work exploring the connection between Carrollian fluids and horizon symmetries [144, 145, 146, 147, 148].

Chapter 4

Near-extremal dynamics away from the horizon

In this chapter, we investigate the emergence of Schwarzian dynamics at low energies from a higher-dimensional holographic CFT. We focus on matching the Ward identities and their generating functional of the Schwarzian theory with those of the parent CFT, using an off-shell decoupling limit based on a gravitational phase space rather than a particular black hole solution. Through an explicit construction, we demonstrate that the anomalous dynamics characteristic of the Schwarzian theory can originate from a three-dimensional CFT that is free of a Weyl anomaly. This is enabled by exploiting the inherent ambiguities in defining the Weyl anomaly in one dimension. For comparison, we also apply our construction to the AdS_3/CFT_2 correspondence, considering both equal and unequal left and right central charges, thereby establishing connections with previous results in the literature.

4.1 Introduction to the chapter

Asymptotically AdS_2 quantum gravity plays a fundamental role in our understanding of black hole physics, as an AdS_2 factor naturally arises in the near-horizon geometry of higher-dimensional extremal black holes, typically of the form $AdS_2 \times \mathcal{M}$. A notable example is the quantum entropy function in AdS_2/CFT_1 [153, 154], which captures both classical and quantum aspects of extremal black holes and successfully matches the microscopic entropy computed in string theory [155]. However, pure AdS_2 gravity is topological: in Euclidean signature, its on-shell action is proportional to the Euler characteristic. As a result, the theory lacks both local and boundary excitations, precluding the construction of a standard holographic dictionary for AdS_2/CFT_1—a limitation already noted in the original formulation of the AdS/CFT correspondence [29], and further emphasized from different yet complementary perspectives in [156, 157].

For many years, this posed a paradox: the simplest instance of quantum gravity, realized in two dimensions, remained less understood from a holographic perspective than its higher-dimensional counterparts. This paradox began to be resolved around 2016, when attention shifted from extremal to near-extremal black holes. In this regime, the relevant near-horizon degrees of freedom are effectively described by Jackiw–Teitelboim (JT) gravity, a two-dimensional theory of gravity coupled to a dilaton. While pure AdS_2 gravity admits no local or boundary modes, JT gravity supports nontrivial boundary dynamics. The dilaton plays a central role in realizing the nearly AdS_2/nearly CFT_1 ($nAdS_2/nCFT_1$) correspondence. The resulting one-dimensional boundary theory is governed by the Schwarzian action, which encodes the dynamics of time reparametrizations [149, 45, 150].

The Schwarzian dynamics can be understood as the effective theory of a one dimensional anomalous perfect fluid [126], fitting naturally within the broader context of the

fluid/gravity correspondence [76, 77]. This interpretation is further clarified by a complementary formulation in terms of Ward identities, which makes the role of the Weyl anomaly more transparent [158]. It is this latter perspective that aligns most closely with the approach taken in the present work.

The emergence of JT gravity as an effective description of near-horizon dynamics in higher-dimensional gravitational theories is well understood. In contrast, its dual counterpart—the emergence of Schwarzian dynamics from higher-dimensional holographic CFTs—remains far less clear. The goal of this work is to advance our understanding of this emergence from the boundary field theory perspective. In particular, the structure of the Ward identities in the Schwarzian theory makes it evident that its dynamics is anomalous. This raises a natural question: how can a one-dimensional Weyl anomaly emerge at low energies from a UV CFT such as CFT_3, which is free of Weyl anomalies?

This is precisely the question we address in this work by constructing a generalization of the standard decoupling limit, which typically leads to the near-horizon region of a black hole. Unlike the conventional approach, which focuses on specific black hole solutions, our generalization begins with the gravitational phase space, thereby capturing the UV Ward identities from the outset. Applying the decoupling limit to the full gravitational phase space then allows for a clean derivation of the Ward identities of the Schwarzian theory. As a result, we can explicitly track the origin of the one-dimensional Weyl anomaly.

This approach stands in contrast to other versions of the decoupling limit that focus on the s-wave sector of the Einstein equations, which are particularly effective in three dimensions [158]. These constructions support the intuition that, in the dual field theory, the decoupling limit corresponds to an RG flow from a UV CFT_2 to an nCFT_1, with an effective number of degrees of freedom reduced by half.[1] However, in dimensions higher

[1]This resembles the C-theorem in two dimensions, and bootstrap arguments in CFT_2 provide support

than three, this method encounters difficulties due to the mismatch in the Weyl factor between the UV and IR descriptions, as well as complications arising from rotating black holes. Furthermore, the approach is not fully off-shell, since the UV Ward identities are solved from the outset, making it difficult to track their evolution along the RG flow. In contrast, our construction overcomes these limitations by providing a more general framework that remains fully off-shell on the field theory side.

This chapter is organized as follows: In Section 4.2, we review the formulation of the $\text{nAdS}_2/\text{nCFT}_1$ correspondence in terms of Ward identities and provide a careful analysis of the one-dimensional Weyl anomaly, revealing an inherent ambiguity in its definition that will play a fundamental role in this work. In Section 4.3, we construct an off-shell generalization of the decoupling limit in the context of the $\text{AdS}_3/\text{CFT}_2$ correspondence, which allows us to match the two-dimensional Ward identities with those of the nCFT_1. In Section 4.4, we consider topologically massive gravity (TMG), which is dual to a CFT_2 with unequal left and right central charges. We then apply our off-shell decoupling limit to connect the corresponding Ward identities to those of the nCFT_1. Section 4.5 addresses the most important case: the $\text{AdS}_4/\text{CFT}_3$ correspondence, where no Weyl anomaly is present on the field theory side. Our off-shell construction of the decoupling limit provides an explicit derivation of the anomalous Schwarzian dynamics from a parent CFT that is anomaly-free. Finally, in Section 4.6, we summarize our conclusions and discuss the main results of this work.

4.2 Aspects of $\text{nAdS}_2/\text{nCFT}_1$

In this section, we revisit JT gravity as a prototype for near extremal dynamics. By decomposing the dynamics along and transverse to the radial coordinate using a suitable

for this perspective [170, 172].

Bondi gauge, and explicitly solving the radial evolution, we obtain a description that is off-shell in the transverse direction. The transverse equations of motion can be identified with Ward identities in the holographic dual quantum mechanics and lead to Schwarzian dynamics. As we will see later on, the variables that describe the transverse dynamics of JT gravity naturally arise in a specific IR limit of higher dimensional CFTs dual to higher dimensional AdS black holes. The conventions and analysis in this section follow mainly [158]; other useful references include [149, 45, 126], as well as the reviews [46, 159, 160].

JT gravity couples the two-dimensional metric g_{ab} to a dilaton ϕ through the action [45]

$$S_{\rm JT} = \frac{1}{2\kappa_2^2}\int_{\mathcal{M}_2} \mathrm{d}^2x\sqrt{-g}\,\phi\left(\mathcal{R}+\frac{2}{\ell_2^2}\right) + \frac{1}{\kappa_2^2}\int_{\partial\mathcal{M}_2}\mathrm{d}x\sqrt{-h}\,\phi\left(K-\frac{1}{\ell_2}\right). \tag{4.1}$$

Here, κ_2^2 is the dimensionless Newton's constant in two dimensions and ℓ_2 is the AdS_2 radius. The surface terms are the standard Gibbons-Hawking-York term that involves the trace, K, of the extrinsic curvature of the induced metric h on the one-dimensional boundary $\partial\mathcal{M}_2$, and the local volume counterterm proportional to $1/\ell_2$.

The field equations following from the action (4.1) are

$$\begin{aligned} \mathcal{R}+\frac{2}{\ell_2^2} &= 0\,, \\ (\nabla_a\nabla_b - g_{ab}\Box)\phi + \frac{g_{ab}}{\ell_2^2}\phi &= 0\,. \end{aligned} \tag{4.2}$$

These equations do not describe any propagating degrees of freedom. In particular, the first equation fixes the two-dimensional metric to be locally AdS_2.

4.2.1 Reduced phase space and local symmetries

The field equations (4.2) can be completely integrated by selecting a suitable gauge [45, 150]. For our present analysis, it will be convenient to parameterize the solutions in the so-called Bondi gauge,[2]

$$ds^2 = -f(u,r)\mathrm{d}u^2 - 2\alpha(u)\mathrm{d}u\mathrm{d}r\,, \tag{4.3}$$

where $\alpha(u)$ is an arbitrary function of the time coordinate, u, unrestricted by the equations of motion. Demanding that the metric (4.3) is locally AdS_2 requires the radial profile of the lapse function $f(u,r)$ to be at most quadratic in r, i.e.,

$$f(u,r) = \alpha(u)^2\frac{r^2}{\ell_2^2} + f_1(u)\frac{r}{\ell_2} + f_0(u)\,, \tag{4.4}$$

where $f_1(u)$ and $f_0(u)$ are arbitrary functions of u. Moreover, the rr component of the second equation in (4.2) determines that the dilaton ϕ must be linear in r, namely

$$\phi(u,r) = \nu(u)\frac{r}{\ell_2} + \phi_0(u)\,, \tag{4.5}$$

where $\nu(u)$ and $\phi_0(u)$ are arbitrary functions.[3]

The relations (4.4) and (4.5) fully determine the radial dependence of the Bondi gauge solution and, therefore, parameterize a reduced phase space. However, there exist three different local transformations that modify the functions $\alpha(u)$, $\nu(u)$, $f_1(u)$, $f_2(u)$ and

[2]The Bondi gauge has been employed in JT gravity to explore various boundary conditions and their associated asymptotic symmetries [151, 152].

[3]There exists a diffeomorphism that relates the Bondi gauge (4.3) with the Fefferman-Graham gauge $ds^2 = d\bar{r}^2 + \gamma_{tt}(\bar{r},t)dt^2$ used in [158]. The general solutions in these two gauges are related by an asymptotic diffeomorphism of the form $e^{\bar{r}/\ell_2} = r/\ell_2 + \mathcal{O}(1)$, $t = u - \frac{\ell_2^2}{\alpha(u)r} + \mathcal{O}(1/r^2)$. Under this transformation, the functions $\alpha(u)$ and $\nu(u)$ here coincide respectively with the functions $\alpha(t)$ and $\nu(t)$ that parameterize the running dilaton solutions in [158].

$\phi_0(u)$, but preserve the form of the radial solution:

i) Time reparameterizations, $u \to \bar{u}(u)$, under which:

$$\begin{aligned} &\alpha(u) \to \bar{\alpha}(\bar{u}) = \Big(\frac{d\bar{u}}{du}\Big)^{-1}\alpha(u)\,, \qquad f_{1,0}(u) \to \bar{f}_{1,0}(\bar{u}) = \Big(\frac{d\bar{u}}{du}\Big)^{-2} f_{1,0}(u)\,, \\ &\nu(u) \to \bar{\nu}(\bar{u}) = \nu(u)\,, \qquad \phi_0(u) \to \bar{\phi}_0(\bar{u}) = \phi_0(u)\,. \end{aligned} \tag{4.6}$$

ii) Local rescalings of the radial coordinate, $r \to e^{\sigma(u)} r$, under which:

$$\begin{aligned} &\alpha \to e^{\sigma}\alpha\,, \qquad f_1 \to e^{\sigma}\big(f_1 + 2\alpha\sigma'\big)\,, \qquad f_0 \to f_0\,, \\ &\nu \to e^{\sigma}\nu\,, \qquad \phi_0 \to \phi_0\,. \end{aligned} \tag{4.7}$$

iii) Local shifts of the radial coordinate, $r \to r + \zeta(u)$, under which:

$$\begin{aligned} &\alpha \to \alpha\,, \qquad f_1 \to f_1 + 2\alpha^2\zeta/\ell_2\,, \qquad f_0 \to f_0 + \alpha^2\zeta^2/\ell_2^2 + f_1\zeta/\ell_2 + 2\alpha\zeta'\,, \\ &\nu \to \nu\,, \qquad \phi_0 \to \phi_0 + \nu\zeta/\ell_2\,. \end{aligned} \tag{4.8}$$

The fact that $f_1(u)$ and $\phi_0(u)$ transform additively under this transformation implies that either of the two can be viewed as a compensator. In particular, taking $\phi_0(u)$ as the compensator, we can dress each of the variables with an appropriate function of $\phi_0(u)$ so that the resulting composite variable is invariant. Since $\alpha(u)$ and $\nu(u)$ are already invariant we need only consider $f_1(u)$ and $f_0(u)$. It is straightforward to verify that the variables

$$\widetilde{f}_1 = f_1 - 2\alpha^2\frac{\phi_0}{\nu}\,, \qquad \widetilde{f}_0 = f_0 + \alpha^2\frac{\phi_0^2}{\nu^2} - \frac{\phi_0}{\nu}f_1 - 2\ell_2\alpha\partial_u\Big(\frac{\phi_0}{\nu}\Big)\,, \tag{4.9}$$

are invariant under the transformations (4.8).

Using $\phi_0(u)$ as a compensator of the radial shift symmetry allows us to parameterize

the reduced phase space in terms of the four shift invariant functions $\alpha(u)$, $\nu(u)$, $\widetilde{f}_1(u)$ and $\widetilde{f}_0(u)$. As we will see next, it is precisely these variables that can be mapped to the sources and one-point functions of the dual quantum mechanics.

4.2.2 Holographic dictionary and Ward identities

The remaining equations of motion impose differential relations among the functions that parameterize the reduced phase space. These relations take the form

$$\widetilde{f}_1 = 2\ell_2\alpha\frac{\partial_u\nu}{\nu}\,, \qquad \partial_u\left(\frac{\nu^2}{\alpha^2}\widetilde{f}_0\right) = 0\,, \tag{4.10}$$

and correspond to first class constraints that generate the local symmetries i) and ii) above. In order to identify these constraints with Ward identities in the dual quantum mechanics, it is necessary to choose a suitable parameterization of the reduced phase space.

Examining the leading asymptotic form of the radial solutions (4.4) and (4.5), we identify $-\alpha(u)^2$ with the boundary metric and $\log\nu(u)$ with the source of the scalar operator dual to the dilaton (see footnote 3) [158]. We expect, therefore, that the shift-invariant functions $\widetilde{f}_1(u)$ and $\widetilde{f}_2(u)$ are related to the one-point functions of the stress tensor $\mathcal{O}_u$ and the scalar operator dual to the dilaton $\mathcal{O}_\phi$. The precise relation between the variables $\widetilde{f}_1(u)$, $\widetilde{f}_2(u)$ and $\mathcal{O}_u$, $\mathcal{O}_\phi$ is dictated by the requirement that the constraints imposed by the remaining equations of motion take the standard form of conformal Ward identities when expressed in terms of the operators $\mathcal{O}_u$, $\mathcal{O}_\phi$. This requirement determines that

$$\begin{aligned}\widetilde{f}_1(u) &= 2\kappa_2^2\gamma^2\frac{\alpha^2}{\nu}\int \mathrm{d}u\,\alpha(\mathcal{O}_u+\mathcal{O}_\phi) + 2(1-\omega^2\gamma^2)\ell_2\alpha\frac{\partial_u\nu}{\nu}\,,\\ \widetilde{f}_0(u) &= 2\kappa_2^2\frac{\alpha^2}{\nu}\ell_2\mathcal{O}_u - \omega^2\ell_2^2\frac{(\partial_u\nu)^2}{\nu^2}\,,\end{aligned} \tag{4.11}$$

where γ and ω are arbitrary constants that reflect an ambiguity in the identification of the dual quantum mechanics operators from the reduced phase space variables. As we will see, ω is related to a local counterterm in the effective action of the dual conformal quantum mechanics and will play a key role in the subsequent analysis.

In terms of the variables $\mathcal{O}_u$, $\mathcal{O}_\phi$ introduced via (4.11) the remaining equations of motion become

$$\mathcal{O}_u + \mathcal{O}_\phi = \frac{\omega^2 \ell_2}{\kappa_2^2 \alpha} \partial_u \left(\frac{\partial_u \nu}{\alpha} \right) , \tag{4.12a}$$

$$\partial_u \mathcal{O}_u - \mathcal{O}_\phi \frac{\partial_u \nu}{\nu} = 0 . \tag{4.12b}$$

These match exactly the Ward identities in the dual conformal quantum mechanics [158], with the r.h.s. of (4.12a) identified with a "conformal anomaly". It is not a genuine conformal anomaly, since, as we mentioned above and we will review below, the value of the parameter ω can be modified by a local counterterm. These equations are also independent of the arbitrary parameter γ in equation (4.11).

Unlike in higher dimensions, the Ward identities (4.12a), (4.12b) can be integrated to obtain the form of the variables $\mathcal{O}_u$ and $\mathcal{O}_\phi$. In particular, the general solution of the Ward identities is [158]

$$\begin{aligned} \mathcal{O}_u &= -\frac{m}{\nu} + \frac{\omega^2 \ell_2}{2\kappa_2^2 \nu} \left(\frac{\partial_u \nu}{\alpha} \right)^2 , \\ \mathcal{O}_\phi &= \frac{m}{\nu} + \frac{\omega^2 \ell_2}{2\kappa_2^2} \left(\frac{2}{\alpha} \partial_u \left(\frac{\partial_u \nu}{\alpha} \right) - \frac{1}{\nu} \left(\frac{\partial_u \nu}{\alpha} \right)^2 \right) , \end{aligned} \tag{4.13}$$

where m is an integration constant. These variables may be expressed as variations of the action

$$I_\omega[\alpha, \nu] = \int \mathrm{d}u \, \alpha \left[-\frac{m}{\nu} - \frac{\omega^2 \ell_2}{2\kappa_2^2} \frac{1}{\nu} \left(\frac{\partial_u \nu}{\alpha} \right)^2 \right] , \tag{4.14}$$

with respect to α and ν, respectively. Namely,

$$\delta I_\omega = \int \mathrm{d}u \Big(\mathcal{O}_u \, \delta\alpha + \frac{\alpha}{\nu} \mathcal{O}_\phi \, \delta\nu \Big) \,. \tag{4.15}$$

The effective action $I_\omega[\alpha, \nu]$ allows us to exhibit the direct relation between the Ward identities (4.12a), (4.12b) and the reduced phase space symmetries i) and ii), which we can now recognize, respectively, as boundary diffeomorphisms and Weyl transformations. Taking ϵ as the parameter of an infinitesimal boundary diffeomorphism and σ of an infinitesimal boundary Weyl transformation, the sources $\alpha(u)$ and $\nu(u)$ transform as

$$\delta_{\epsilon,\sigma}\alpha = \partial_u(\epsilon\alpha) + \alpha\sigma \ , \quad \delta_{\epsilon,\sigma}\nu = \epsilon\partial_u\nu + \nu\sigma \,. \tag{4.16}$$

Applying these transformations to the expressions (4.13), we can also determine the transformation of the variables $\mathcal{O}_u$ and $\mathcal{O}_\phi$, which we will need later on. A direct calculation gives

$$\begin{aligned} \delta_{\epsilon,\sigma}\mathcal{O}_u &= \epsilon\, \partial_u \mathcal{O}_u - \sigma \mathcal{O}_u + \frac{\omega^2 \ell_2}{\kappa_2^2} \frac{\partial_u \nu \partial_u \sigma}{\alpha^2} \,, \\ \delta_{\epsilon,\sigma}\mathcal{O}_\phi &= \epsilon\, \partial_u \mathcal{O}_\phi - \sigma \mathcal{O}_\phi + \frac{\omega^2 \ell_2}{\kappa_2^2} \frac{\nu}{\alpha} \partial_u \left(\frac{\partial_u \sigma}{\alpha} \right) \,. \end{aligned} \tag{4.17}$$

In particular, both operators transform as scalars under boundary diffeomorphisms, but possess an anomalous Weyl transformation when $\omega \neq 0$.[4]

Returning to the relation between the Ward identities (4.12a), (4.12b) and the symmetry transformations (4.16), let us first consider boundary diffeomorphisms. The transformations (4.16) lead us to identify $h_b = -\alpha^2$ with the metric on the one-dimensional boundary and ν with a boundary scalar. The effective action can then be expressed in

[4]Note that the transformation of $\mathcal{O}_\phi$ in eq. (5.8b) of [158] contains two typos.

the manifestly covariant form

$$I_\omega = \int \mathrm{d}u \sqrt{-h_b}\, \nu^{-1} \left(-m + \frac{\omega^2 \ell_2}{2\kappa_2^2} h_b^{-1} (\partial_u \nu)^2 \right) . \tag{4.18}$$

It follows that I_ω is invariant under boundary diffeomorphisms. This means that specializing (4.15) to boundary diffeomorphisms we have

$$\delta_\epsilon I_\omega = - \int \mathrm{d}u\, \epsilon\, \alpha \left(\partial_u \mathcal{O}_u - \mathcal{O}_\phi \frac{\partial_u \nu}{\nu} \right) = 0 . \tag{4.19}$$

Since this must hold for arbitrary $\epsilon(u)$, we recover the Ward identity (4.12b).

This argument can be repeated for boundary Weyl transformations. However, the effective action is not invariant in this case. In particular, under an infinitesimal Weyl transformation

$$\delta_\sigma I_\omega = \frac{\omega^2 \ell_2}{\kappa_2^2} \int \mathrm{d}u\, \sigma \partial_u \Big(\frac{\partial_u \nu}{\alpha} \Big) . \tag{4.20}$$

From (4.15) follows that

$$\delta_\sigma I_\omega = \int \mathrm{d}u\, \sigma\, \alpha (\mathcal{O}_u + \mathcal{O}_\phi) = \frac{\omega^2 \ell_2}{\kappa_2^2} \int \mathrm{d}u\, \sigma \partial_u \Big(\frac{\partial_u \nu}{\alpha} \Big) , \tag{4.21}$$

which implies the trace Ward identity (4.12a).

Let us now consider a combined boundary diffeomorphism and Weyl transformation such that the boundary metric remains unchanged. The parameters ϵ_o and σ_o of such a transformation satisfy

$$\delta_{\epsilon_o, \sigma_o} \alpha = \partial_u (\epsilon_o \alpha) + \alpha \sigma_o = 0 . \tag{4.22}$$

This condition reduces the local parameters from two to one. In particular, the two

parameters satisfying the constraint (4.22) can be chosen as

$$\epsilon_o = \frac{\xi}{\alpha}\,, \qquad \sigma_o = -\partial_\tau \xi\,, \tag{4.23}$$

where $\xi(u)$ is an arbitrary function and

$$\tau(u) = \int^u \mathrm{d}u'\, \alpha(u')\,, \tag{4.24}$$

is the proper time on the boundary. Under generic ξ-transformations ν transforms as

$$\delta_\xi \nu = \epsilon_o \partial_u \nu + \nu \sigma_o = \epsilon_o \partial_u \nu - \frac{\nu}{\alpha}\partial_u(\epsilon_o \alpha) = -\nu^2 \partial_\tau(\nu^{-1}\xi)\,, \tag{4.25}$$

or

$$\delta_\xi \nu^{-1} = \partial_\tau(\nu^{-1}\xi)\,. \tag{4.26}$$

Finite ξ-transformations play a central role in the dynamics of JT gravity and take the form

$$\nu(\tau) \to \nu_{\mathcal{F}}(\tau) = \frac{1}{\partial_\tau \mathcal{F}(\tau)} \nu(\mathcal{F}(\tau))\,, \tag{4.27}$$

where $\mathcal{F}(\tau)$ is an arbitrary function with $\partial_\tau \mathcal{F}(\tau) \neq 0$. Indeed, inserting $\mathcal{F}(\tau) = \tau + \xi(\tau)$ in (4.27) and expanding for small $\xi(\tau)$ we recover the infinitesimal transformation (4.26). If $\omega \neq 0$, a specific finite ξ-transformation can be used to set $\omega = 1$, at the expense of introducing an overall factor of ω in the effective action, I_ω, and in the variables $\mathcal{O}_u$ and $\mathcal{O}_\phi$. In particular, a finite ξ-transformation with $\mathcal{F}(\tau) = \omega\,\tau$ amounts to the rescaling $\nu \to \nu/\omega$. Accordingly, $I_\omega \to \omega I_{\omega=1}$, $\mathcal{O}_u^\omega \to \omega\, \mathcal{O}_u^{\omega=1}$ and $\mathcal{O}_\phi^\omega \to \omega\, \mathcal{O}_\phi^{\omega=1}$. In particular, the Ward identities (4.12a) and (4.12b), as well as the operator transformations (4.17) become independent of ω.

Applying two successive infinitesimal ξ-transformations on ν we can determine the

corresponding algebra. Using (4.26), we obtain

$$[\delta_{\xi_1}, \delta_{\xi_2}]\nu^{-1} = \delta_\xi \nu^{-1}\,, \qquad \xi = \xi_2\partial_\tau\xi_1 - \xi_1\partial_\tau\xi_2\,. \tag{4.28}$$

The representation of the algebra of ξ-transformations on the phase space of JT gravity solutions requires a Poisson bracket. The variation (4.15) of the effective action defines the symplectic form

$$\Omega_{\rm JT} = \int \mathrm{d}u\Big(\delta\mathcal{O}_u \wedge \delta\alpha + \frac{\alpha}{\nu}\delta\mathcal{O}_\phi \wedge \delta\nu\Big)\,. \tag{4.29}$$

Inverting this leads to the Poisson bracket

$$\{A, B\} = \int du\left(\frac{\delta A}{\delta\alpha}\frac{\delta B}{\delta\mathcal{O}_u} + \frac{\nu}{\alpha}\frac{\delta A}{\delta\nu}\frac{\delta B}{\delta\mathcal{O}_\phi} - A \leftrightarrow B\right)\,, \tag{4.30}$$

where A, B are arbitrary functions of the phase space variables, α, ν, $\mathcal{O}_u$, and $\mathcal{O}_\phi$.

Boundary diffeomorphisms and Weyl transformations are generated through this Poisson bracket by the Ward identities (4.12a), (4.12b). In particular, introducing the phase space functional

$$\mathcal{L}(\epsilon,\sigma) = \int du\,\alpha\left[\epsilon\left(\partial_u\mathcal{O}_u - \mathcal{O}_\phi\frac{\partial_u\nu}{\nu}\right) - \sigma\left(\mathcal{O}_u + \mathcal{O}_\phi - \frac{\omega^2\ell_2}{\kappa_2^2\alpha}\partial_u\left(\frac{\partial_u\nu}{\alpha}\right)\right)\right]\,, \tag{4.31}$$

the transformation of any phase space variable A is given by

$$\delta_{\epsilon,\sigma}A = \{\mathcal{L}(\epsilon,\sigma), A\}\,. \tag{4.32}$$

ξ-transformations are generated by (4.31) with the parameters given in (4.23), namely

$$\mathcal{L}(\xi) = \int du\left[\xi\left(\partial_u\mathcal{O}_u - \mathcal{O}_\phi\frac{\partial_u\nu}{\nu}\right) + \partial_u\xi\left(\mathcal{O}_u + \mathcal{O}_\phi - \frac{\omega^2\ell_2}{\kappa_2^2\alpha}\partial_u\left(\frac{\partial_u\nu}{\alpha}\right)\right)\right]\,. \tag{4.33}$$

Dropping total derivative terms, this can be simplified to

$$\mathcal{L}(\xi) = -\int d\tau\, \xi\nu^{-1}\,\partial_\tau\left(\nu\mathcal{O}_\phi - \frac{\omega^2\ell_2}{\kappa_2^2}\Big(\nu\partial_\tau^2\nu - \frac{1}{2}(\partial_\tau\nu)^2\Big)\right). \tag{4.34}$$

It is straightforward to verify that the ξ-transformations of α and ν we found above, namely $\delta_\xi\alpha = 0$, $\delta_\xi\nu = -\nu^2\partial_\tau(\nu^{-1}\xi)$, are generated by (4.34) through the Poisson bracket (4.30). Similarly, the ξ-transformation of the variables $\mathcal{O}_u$ and $\mathcal{O}_\phi$ may be obtained either by specializing the transformations (4.17) to ξ-transformations, or via the Poisson bracket. Either way, one obtains

$$\begin{aligned}\delta_\xi\mathcal{O}_u &= \partial_\tau\left(\xi\mathcal{O}_u\right) - \frac{\omega^2\ell_2}{\kappa_2^2}\partial_\tau\nu\partial_\tau^2\xi\,,\\ \delta_\xi\mathcal{O}_\phi &= \partial_\tau\left(\xi\mathcal{O}_\phi\right) - \frac{\omega^2\ell_2}{\kappa_2^2}\nu\partial_\tau^3\xi\,.\end{aligned} \tag{4.35}$$

In particular, the combination $\nu^{-1}\mathcal{O}_\phi$ transforms as [158]

$$\delta_\xi(\nu^{-1}\mathcal{O}_\phi) = \{\mathcal{L}(\xi), \nu^{-1}\mathcal{O}_\phi\} = 2\nu^{-1}\mathcal{O}_\phi\partial_\tau\xi + \xi\partial_\tau\left(\nu^{-1}\mathcal{O}_\phi\right) - \frac{\omega^2\ell_2}{\kappa_2^2}\partial_\tau^3\xi\,, \tag{4.36}$$

which corresponds to the coadjoint representation of the Virasoro algebra with central charge proportional to $\omega^2\ell_2/\kappa_2^2$ [162]. However, the combination $\nu^{-1}\mathcal{O}_\phi - \frac{\omega^2\ell_2}{\kappa_2^2}\nu^{-2}\big(\nu\partial_\tau^2\nu - \frac{1}{2}(\partial_\tau\nu)^2\big)$ that enters in the generating function (4.34) possesses a homogeneous ξ transformation. As a result, the algebra of ξ-symmetry generators on the phase space closes without a central element, namely

$$\{\mathcal{L}(\xi_1), \mathcal{L}(\xi_2)\} = \delta_{\xi_1}\mathcal{L}(\xi_2) = \mathcal{L}(\xi_2\partial_\tau\xi_1 - \xi_1\partial_\tau\xi_2)\,. \tag{4.37}$$

Finally, let us consider the special case of ξ-transformations that preserve ν, besides α. From the ξ-transformation of ν in (4.26) we see that ν is preserved provided $\xi = k\nu$,

where k is constant. In that case, ϵ_o in (4.23) corresponds to the unique conformal Killing vector (CKV) of JT gravity solutions. The existence of CKVs implies the existence of associated conserved charges, which can be constructed using the Ward identities (4.12b) and (4.12a).[5] Multiplying the diffeomorphism Ward identity (4.12b) with ϵ_o we obtain

$$\frac{1}{\alpha}\big(\partial_u(\nu\mathcal{O}_u) - (\mathcal{O}_u + \mathcal{O}_\phi)\partial_u\nu\big) = 0\,. \tag{4.38}$$

Using the trace Ward identity (4.12a), this in turn can be written as

$$\partial_\tau(\nu\mathcal{O}_u) - \frac{\omega^2\ell_2}{\kappa_2^2}\partial_\tau^2\nu\partial_\tau\nu = 0\,, \tag{4.39}$$

or

$$\partial_\tau\left(\nu\mathcal{O}_u - \frac{\omega^2\ell_2}{2\kappa_2^2}(\partial_\tau\nu)^2\right) = 0\,. \tag{4.40}$$

It follows that the conserved charge associated with the unique CKV corresponding to constant ξ is

$$\mathcal{Q} \equiv -\left(\nu\mathcal{O}_u - \frac{\omega^2\ell_2}{2\kappa_2^2}(\partial_\tau\nu)^2\right) = m\,, \tag{4.41}$$

where in the second equality we have used the form of $\mathcal{O}_u$ in (4.13). It follows that the integration constant, m, parameterizing the variables $\mathcal{O}_u$ and $\mathcal{O}_\phi$ is the conserved charge associated with the timelike CKV, i.e. the mass or energy of the solution.

4.2.3 On-shell action and Schwarzian dynamics

Let us next compute the on-shell value of the JT action (4.1). The equations of motion (4.2) imply that the bulk integral vanishes on-shell and so there is only a boundary

[5] In higher dimensions, not all CKVs lead to a conserved charge in the presence of a conformal anomaly [114]. However, due to the form of the conformal anomaly in one dimension, a conserved charge always exists.

contribution to the action

$$S_{\rm JT}\Big|_{\rm on-shell} = \frac{1}{\kappa_2^2}\int_{\partial\mathcal{M}_2} \mathrm{d}x\sqrt{-h}\,\phi\left(K-\frac{1}{\ell_2}\right)\,. \tag{4.42}$$

Writing the Bondi gauge metric (4.3) in the ADM form

$$ds^2 = (N^2+N_uN^u)\mathrm{d}r^2 + 2N_u\mathrm{d}u\mathrm{d}r + h_{uu}\mathrm{d}u\mathrm{d}u\,, \tag{4.43}$$

we identify $N_u=-\alpha$, $h_{uu}=-f$, and $N=\alpha f^{-\frac{1}{2}}$. It follows that the extrinsic curvature is given by

$$K_{uu} = \frac{1}{2N}(\partial_r h_{uu} - 2D_uN_u) = \frac{1}{2N}(\partial_r h_{uu} - 2\partial_u N_u + h_{uu}^{-1}\partial_u h_{uu}N_u)\,, \tag{4.44}$$

where D_u is the covariant derivative with respect to the induced metric h_{uu}. Evaluating the trace of the extrinsic curvature, $K=h_{uu}^{-1}K_{uu}$, inserting it in (4.42), and taking the limit $r\to\infty$ we obtain (see also appendix B of [161])

$$S_{\rm JT}\Big|_{\rm on-shell} = \int \mathrm{d}u\,\alpha\left[\frac{m}{\nu}+\frac{\ell_2}{2\kappa_2^2}\left(\frac{2}{\alpha}\partial_u\left(\frac{\partial_u\nu}{\alpha}\right)-\frac{1}{\nu}\left(\frac{\partial_u\nu}{\alpha}\right)^2\right)\right]\,. \tag{4.45}$$

As expected, the on-shell action is independent of the parameters ω or γ introduced in (4.11), since the invariant functions $\widetilde{f}_{0,1}$ do not depend on these parameters once the explicit form of the operators in (4.13) is taken into account. More importantly, the on-shell action is also independent of the function $\phi_0(u)$, which reflects the fact that the boundary theory is inert under the local symmetry iii).

Comparing the on-shell action (4.45) and the effective action I_ω in (4.14), we observe that they contain exactly the same terms, but with different coefficients. In particular,

the two are related by

$$S_{\rm JT}\Big|_{\rm on-shell} = I_\omega + 2\int {\rm d}u\sqrt{-h_b}\,\nu^{-1}\mathcal{Q} + (1-\omega^2)\,\frac{\ell_2}{2\kappa_2^2}\int {\rm d}u\sqrt{-h_b}\,\nu^{-1}h_b^{-1}(\partial_u\nu)^2\,, \quad (4.46)$$

where $h_b = -\alpha^2$ is the metric on the one-dimensional boundary and $\mathcal{Q} = m$ is the conserved charge in (4.41). Each of the additional terms on the right-hand side of (4.46) plays an important role which is worth discussing separately:

1. The last term in (4.46) is a local counterterm that modifies the value of ω. This is why ω is not a conformal anomaly as mentioned below (4.12). To make this more manifest, we write

$$S_{\rm ct} = \frac{\ell_2}{2\kappa_2^2}\int {\rm d}u\sqrt{-h}\,\phi^{-1}h^{uu}(\partial_u\phi)^2\,, \quad (4.47)$$

and

$$S_{\rm ct}\Big|_{\rm on-shell} = \frac{\ell_2}{2\kappa_2^2}\int {\rm d}u\sqrt{-h_b}\,\nu^{-1}h_b^{-1}(\partial_u\nu)^2\,. \quad (4.48)$$

The addition of this boundary counterterm will play a crucial role in our subsequent analysis. As we will see in the coming sections, the UV completion of JT gravity determines ω.

2. The term proportional to $\mathcal{Q}$ in (4.46) is simply the Gibbons-Hawking-York term evaluated on the surface of minimum radius [163, 164]. This term is state-dependent, since it involves the mass parameter m, which places it in a different footing to $S_{\rm ct}$. Adding such contribution to I_ω leads to some useful properties. We define

$$\widetilde{I}_\omega = I_\omega + 2\int {\rm d}u\sqrt{-h_b}\,\nu^{-1}\mathcal{Q} = \int {\rm d}u\,\alpha\,\mathcal{O}_\phi\,. \quad (4.49)$$

Since the integrand of $\widetilde{I}_\omega$ is proportional to $\mathcal{O}_\phi$, its ξ-transformation is related to the

transformation of a Virasoro current, and therefore to Schwarzian dynamics. To render this connection manifest, let us begin by writing the effective action (4.49) in the form

$$\widetilde{I}_\omega = \frac{\ell_2}{\kappa_2^2}\int \mathrm{d}\tau\ \nu\,\mathcal{S}_\omega\,, \tag{4.50}$$

where $\mathcal{S}_\omega$ is given by

$$\mathcal{S}_\omega[\nu;\tau] = \frac{\kappa_2^2}{\ell_2}\nu^{-1}\mathcal{O}_\phi = \frac{s_0}{2\nu^2} + \frac{\omega^2}{2}\left(\frac{2}{\nu}\partial_\tau^2\nu - \frac{1}{\nu^2}\left(\partial_\tau\nu\right)^2\right)\,, \qquad s_0 = \frac{2\kappa_2^2}{\ell_2}m\,. \tag{4.51}$$

The Ward identities in (4.12) imply that $\mathcal{S}_\omega$ satisfies the differential constraint

$$\partial_\tau(\nu^2\mathcal{S}_\omega) - \omega^2\nu\partial_\tau^3\nu = 0\,. \tag{4.52}$$

Moreover, (4.36) implies that $\mathcal{S}_\omega$ transforms as a Virasoro current under ξ transformations, namely

$$\delta_\xi\mathcal{S}_\omega = 2\mathcal{S}_\omega\partial_\tau\xi + \xi\partial_\tau\mathcal{S}_\omega - \omega^2\partial_\tau^3\xi\,. \tag{4.53}$$

As we will see shortly, $\widetilde{I}_\omega$ and $\mathcal{S}_\omega$ will be central in decoding thermodynamical properties.

To close, we find that $\widetilde{I}_\omega$ coincides with the on-shell value of $S_{\rm JT}$ plus the local covariant counterterm, namely

$$S_{\rm JT} + (\omega^2 - 1)S_{\rm ct}\,. \tag{4.54}$$

Schwarzian dynamics

The analysis so far has not revealed that the gravitational aspects of JT gravity can be described in terms of a Schwarzian effective action, as shown in [45]. In the following, we

will show how this description is derived in our notation. The main idea is to characterize appropriately our reduced phase space under the boundary condition that ν is constant.

We will start by being more explicit about the solutions to the equations of motion in the Bondi gauge by writing out explicitly (4.3)-(4.5). With a convenient choice of the function ϕ_0, the general solution to (4.2) is

$$ds^2 = -\left(\frac{r^2}{\ell_2^2} - 2\ell_2^2\,\mathcal{S}_{\omega=1}\right)\mathrm{d}\tau^2 - 2\,\mathrm{d}\tau\,\mathrm{d}r\,, \qquad \phi = \nu\frac{r}{\ell_2} - \ell_2\partial_\tau\nu\,, \tag{4.55}$$

where $\mathcal{S}_{\omega=1}$ stands for (4.51) with $\omega = 1$ and the proper time τ is defined in (4.24); we also used (4.9), (4.11), and (4.13). Recall that even though intermediate steps have ω-dependence, all solutions are independent of the parameter ω.

Vacuum solutions correspond to configurations with $\mathcal{S}_{\omega=1} = 0$. Via (4.52), this provides an equation for $\nu(\tau)$, whose general solution takes the form

$$\nu(\tau) = -a(\tau-\tau_0)^2 + b(\tau-\tau_0) + \frac{s_0 - b^2}{4a}\,, \tag{4.56}$$

where a, b and τ_0 are integration constants.

Analogously, a black hole solution with temperature T corresponds to configurations with $\mathcal{S}_{\omega=1} = 2\pi^2T^2$. The general solution to (4.52) in this case that reduces to (4.56) as $T \to 0$ is

$$\nu(\tau) = -\frac{a}{\pi^2T^2}\sinh^2\left(\pi T(\tau-\tau_0)\right) + \frac{b}{2\pi T}\sinh\left(2\pi T(\tau-\tau_0)\right) + \frac{\sqrt{a^2 + (s_0-b^2)\pi^2T^2} - a}{2\pi^2T^2}\,, \tag{4.57}$$

where again a, b and τ_0 are integration constants. A static solution is obtained by setting $a = b = 0$, in which case $\nu = \sqrt{s_0}/2\pi T$ or $s_0 = (2\pi T\nu)^2$. This is in agreement with (4.51), which implies that $\mathcal{S}_{\omega=1} = s_0/2\nu^2$ for static solutions .

Both (4.56) and (4.57) are solutions of the condition $\partial_\tau \mathcal{S}_{\omega=1} = 0$. Importantly, this equation is not a consequence of the JT equations of motion, since (4.55) solves these for any function $\nu(\tau)$. However, $\partial_\tau \mathcal{S}_{\omega=1} = 0$ enforces the regularity of JT gravity solutions – that is smooth AdS_2 or existence of a horizon – and can be derived from the on-shell action of JT gravity as follows [45]. Consider the finite ξ-transformation (4.27), where we will reparametrize the proper time via $\tau \to t = t(\tau)$. It is convenient to cast this as an inverse transform, i.e., take $\tau(t)$, and hence we write

$$\nu(t) \to \nu_\tau(t) = \frac{\nu(\tau(t))}{\tau'(t)}\,, \tag{4.58}$$

and then functional $\mathcal{S}_\omega[\nu;\tau]$ transforms as

$$\mathcal{S}_\omega[\nu;\tau] \to \mathcal{S}_\omega[\nu_\tau;t] = \tau'^2 \mathcal{S}_\omega[\nu;\tau] - \omega^2\{\tau,t\}\,. \tag{4.59}$$

This is the finite version of (4.53), where we have introduced the Schwarzian derivate,

$$\{\tau,t\} = -\frac{1}{2}\left(\frac{\tau''}{\tau'}\right)^2 + \left(\frac{\tau''}{\tau'}\right)'\,. \tag{4.60}$$

Primes here are derivatives with respect to t. Taking the initial $\nu(\tau)$ to be the vacuum solution (4.56), this transformation reduces to

$$\mathcal{S}_{\omega=1}[\nu_\tau] = -\{\tau,t\}\,. \tag{4.61}$$

The corresponding value of the effective action (4.50) for $\omega = 1$ is

$$\widetilde{I}_{\omega=1}[\alpha,\nu_\tau] = \frac{\ell_2}{\kappa_2^2}\int \mathrm{d}t\,\nu_\tau\,\mathcal{S}_{\omega=1}[\nu_\tau] = -\frac{\ell_2}{\kappa_2^2}\int \mathrm{d}t\,\nu_\tau\,\{\tau,t\}\,. \tag{4.62}$$

The equation $\partial_\tau \mathcal{S}_{\omega=1} = -\partial_\tau\{\tau, t\} = 0$ follows by varying this action with respect to $\tau(t)$, keeping ν_τ fixed and constant. In fact, keeping ν_τ a fixed constant and the equation $\partial_\tau\{\tau, t\} = 0$ are not independent. Equations (4.56) and (4.58) imply that in order for ν_τ to be constant, $\tau(t)$ must satisfy the first order equation

$$\nu_\tau = \frac{-a\big(\tau(t) - \tau_0\big)^2 + b\big(\tau - \tau_0\big) + \frac{s_0 - b^2}{4a}}{\tau'(t)} \,. \tag{4.63}$$

The general solution of this equation is

$$\tau(t) = \frac{\sqrt{s_0}}{2a} \tanh\left(\frac{\sqrt{s_0}}{2\nu_u}(t - t_0)\right) + \frac{b}{2a} + \tau_0 \,, \tag{4.64}$$

where t_0 is an integration constant. Moreover, the solution of the condition $\{\tau, t\} = -2\pi^2 T^2$ is

$$\tau(t) = a_1 \tanh\left(\pi T(t - t_0)\right) + a_2 \,, \tag{4.65}$$

where again a_1, a_2 and t_0 are integration constants. Clearly, the two solutions coincide provided we identify $s_0 = (2\pi T \nu_\tau)^2$, $a_1 = \pi T \nu_\tau / a$ and $a_2 = b/2a + \tau_0$.

The analysis of the regular static solutions above was based on the effective action (4.50) for $\omega = 1$. Interestingly, the same results follow for any $\omega \neq 0$. In particular, for generic ω we find

$$\widetilde{I}_\omega[\alpha, \nu_\tau] = \frac{\ell_2}{\kappa_2^2} \int \mathrm{d}t\, \nu_\tau\, \mathcal{S}_\omega[\nu_\tau] = \frac{\ell_2}{\kappa_2^2} \int \mathrm{d}t\, \nu_\tau \left((1 - \omega^2)\frac{s_0}{2\nu_\tau^2} - \omega^2\{\tau, t\}\right) . \tag{4.66}$$

Varying this with respect to $\tau(t)$ keeping ν_τ fixed leads to the same constraint, $\partial_\tau\{\tau, t\} = 0$. Moreover, on-shell $\{\tau, t\} = -2\pi^2 T^2$ and $s_0 = (2\pi T \nu_\tau)^2$, which implies that for any ω

the on-shell value of the effective action is

$$\widetilde{I}_{\omega}[\alpha,\nu_\tau]=\frac{\ell_2}{\kappa_2^2}\int \mathrm{d}t\,\nu_\tau\,2\pi^2T^2\,. \tag{4.67}$$

It is worth pointing out that for $\omega=1$, which is the value appearing naturally in JT gravity, we have

$$S_{\rm JT}\Big|_{\rm on-shell}=\widetilde{I}_{\omega=1}[\alpha,\nu_\tau]=-\frac{\ell_2}{\kappa_2^2}\int \mathrm{d}t\,\nu_\tau\,\{\tau,t\}\,. \tag{4.68}$$

In this scheme, everything is encoded in the Schwarzian effective action. What our analysis here shows is that the local counterterm (4.47) modifies the normalization of this piece of the effective action, as reflected in (4.66), without tampering with the final answer in (4.67) which is ω independent. From this perspective, the Schwarzian effective action is a scheme-dependent contribution.

Thermodynamics

Since the value of the effective action (4.50) on the static black hole solution is independent of the of ω, its Euclidean version can be identified with the Helmholtz free energy of the 2D black hole. Wick rotating to Euclidean time, $t_E\sim t_E+T^{-1}$, the Euclidean on-shell action is given by

$$\widetilde{I}^E_{\omega}[\alpha,\nu_\tau]=\frac{\ell_2}{\kappa_2^2}\int \mathrm{d}t_E\left(-\frac{s_0}{2\nu_\tau}\right)=-\frac{2\pi^2\ell_2}{\kappa_2^2}\nu_\tau T\,. \tag{4.69}$$

From (4.55) we read off the location of the horizon, $r_h=2\pi\ell_2^2T$, as well as the corresponding value of the scalar field, $\phi(r_h)=\nu_\tau r_h/\ell_2$. It follows that the black hole entropy is given by

$$S=\frac{2\pi}{\kappa_2^2}\phi(r_h)=\frac{4\pi^2\ell_2}{\kappa_2^2}\nu_\tau T\,, \tag{4.70}$$

while the heat capacity is

$$C = \frac{\partial S}{\partial T} = \frac{4\pi^2 \ell_2}{\kappa_2^2} \nu_\tau \,. \tag{4.71}$$

Identifying the energy with the conserved charge (4.41), modified by the appropriate normalization of the timelike Killing vector for the static solution [164], we have

$$E = \frac{m}{\nu_\tau} = \frac{\ell_2}{2\kappa_2^2} \frac{s_0}{\nu_\tau} = \frac{2\pi^2 \ell_2}{\kappa_2^2} \nu_\tau T^2 \,. \tag{4.72}$$

Putting everything together, we verify that the Euclidean on-shell action for any ω is indeed proportional to the Helmholtz free energy, i.e.,

$$\widetilde{I}_\omega^E[\alpha, \nu_\tau] = T^{-1} \left(E - TS\right) \,. \tag{4.73}$$

4.2.4 Key results

To facilitate comparison with subsequent sections, let us define $I_{\rm JT} \equiv I_{\omega=1}$ as the generating functional obtained via a canonical transformation from the on-shell action of JT gravity given in (4.45). This allows us to express the relation:

$$I_{\rm JT} = I_\omega + (1-\omega^2) \frac{\ell_2}{2\kappa_2^2} \int du \sqrt{-h_b} \nu^{-1} h_b^{-1} (\partial_u \nu)^2 \,, \tag{4.74}$$

where $h_b = -\alpha^2$. The two generating functionals are related by a covariant counterterm. The key insight of this section is that, in one dimension, the concept of a Weyl anomaly is inherently ambiguous because such a counterterm can always be added. In sharp contrast, in higher dimensions, no covariant counterterm exists to alter the coefficient of the Weyl anomaly, making it a robust quantity. As a result, the following Ward identity

in one dimension is ambiguous:

$$\mathcal{O}_u + \mathcal{O}_\phi = \frac{\omega^2 \ell_2}{\kappa_2^2 \alpha} \partial_u \left(\frac{\partial_u \nu}{\alpha} \right) , \tag{4.75}$$

On the other hand, the Ward identity associated with diffeomorphism invariance remains unchanged:

$$\partial_u \mathcal{O}_u - \mathcal{O}_\phi \frac{\partial_u \nu}{\nu} = 0 \, . \tag{4.76}$$

In parallel, let us define the operators generated by $I_{\rm JT}$ as $\mathcal{O}_u^{\rm JT} \equiv \mathcal{O}_u^{\omega=1}$ and $\mathcal{O}_\phi^{\rm JT} \equiv \mathcal{O}_\phi^{\omega=1}$. The boundary counterterm (4.74) then induces the following field redefinitions:

$$\begin{aligned} \mathcal{O}_u^{\rm JT} &= \mathcal{O}_u + \frac{(1-\omega^2)}{2} \frac{\ell_2}{\kappa_2^2} \frac{(\partial_u \nu)^2}{\nu \alpha^2} \, , \\ \mathcal{O}_\phi^{\rm JT} &= \mathcal{O}_\phi - \frac{(1-\omega^2)}{2} \frac{\ell_2}{\kappa_2^2} \frac{(\partial_u \nu)^2}{\nu \alpha^2} + (1-\omega^2) \frac{\ell_2}{\kappa_2^2 \alpha} \partial_u \left(\frac{\partial_u \nu}{\alpha} \right) \, . \end{aligned} \tag{4.77}$$

This mapping preserves the diffeomorphism Ward identity while modifying the Weyl anomaly identity in (4.75), thereby yielding the standard JT Ward identities:

$$\begin{aligned} \mathcal{O}_u^{\rm JT} + \mathcal{O}_\phi^{\rm JT} &= \frac{\ell_2}{\kappa_2^2 \alpha} \partial_u \left(\frac{\partial_u \nu}{\alpha} \right) \, , \\ \partial_u \mathcal{O}_u^{\rm JT} - \mathcal{O}_\phi^{\rm JT} \frac{\partial_u \nu}{\nu} &= 0 \, . \end{aligned} \tag{4.78}$$

The Lagrangian version of the Schwarzian action, which is the form that usually appears in the literature, is simply a canonical transformation of $I_{\rm JT}$:

$$\tilde{I}_{\rm JT} = I_{\rm JT} + 2 \int \mathrm{d}u \sqrt{-h_b} \, \nu^{-1} \mathcal{Q} = -\frac{\ell_2}{\kappa_2^2} \int dt \nu_t \{\tau, t\} \, , \tag{4.79}$$

where $\mathcal{Q}$ is the conserved charge defined in (4.41). Finally, we summarize the three-level thermodynamics in a convenient form for future comparison:[6]

$$E = 2\pi^2 C_H \ell_2^2 T^2 \ , \quad S = \frac{2E}{T} \ , \quad C_H = \frac{1}{\kappa_2^2} \tag{4.80}$$

In the following sections, we will make use of the operator mapping in (4.77), derived from the counterterm in (4.74), to relate a particular low-energy limit of higher-dimensional CFTs to the Ward identities of Schwarzian dynamics. In this context, we will focus primarily on the generating function $I_{\rm JT}$, rather than its Lagrangian form $S_{\rm JT}$, since they are related in a straightforward way by equation (4.79). Finally, the three-level thermodynamics (4.80) will serve as a consistency check for the off-shell construction of the decoupling limit, which we will develop in the following sections.

4.3 Near-extremality at the boundary of $\mathbf{AdS_3/CFT_2}$

This section will describe the emergence of near-extremal dynamics in the context of $\mathrm{AdS}_3/\mathrm{CFT}_2$. This task has two aspects worth highlighting. First, we will work partially off-shell in a reduced phase space: concretely, the radial dependence of the metric component is fully solved, and the remaining conditions to be fully on-shell are equivalent to imposing the Ward identities in the CFT_2. This approach will show how the phase space and dynamics of Sec. 4.2 enter AdS_3 gravity in the appropriate limit without tampering with the radial direction and identifying the variables off-shell appropriately. Second, the parametrization of the metric functions will make explicit how variables of the CFT_2 are related to those in the nCFT_1. With this, we will show the connection between the Ward identities of the two systems.

[6] In comparison with equations (4.70), (4.71), and (4.72), we have set $\nu_\tau = \ell_2$.

4.3.1 CFT$_2$ Ward identities on curved backgrounds

Our starting point is to consider a CFT$_2$ on a non-trivial two-dimensional background. A useful characterization of this background will be

$$ds^2_{\text{2D}} = -\alpha^2 \mathrm{d}u^2 + \nu^2(\mathrm{d}\theta + \mu \mathrm{d}u)^2 \ , \tag{4.81}$$

where here $\alpha(u)$, $\nu(u)$ and $\mu(u)$ are three arbitrary functions.[7] With this parametrization of the background metric, it is convenient to decompose the stress tensor such that its components tie directly to the appropriate source we have introduced: (α, ν, μ). For this reason, we write

$$\begin{aligned} T_{\theta\theta} &= \nu\, \mathcal{O}^{\text{2D}}_{\theta} \ , \\ T_{u\theta} &= \alpha\, \mathcal{O}^{\text{2D}}_{j} + \mu\, T_{\theta\theta} \ , \\ T_{uu} &= \mu^2 \nu\, \mathcal{O}^{\text{2D}}_{\theta} + 2\mu\alpha\, \mathcal{O}^{\text{2D}}_{j} - \frac{\alpha^2}{\nu} \mathcal{O}^{\text{2D}}_{u} \ , \end{aligned} \tag{4.82}$$

where we have traded the three components of the stress tensor for the operators $\mathcal{O}^{\text{2D}}_{s} \equiv (\mathcal{O}^{\text{2D}}_{u}, \mathcal{O}^{\text{2D}}_{j}, \mathcal{O}^{\text{2D}}_{\theta})$. Now it is simple to verify the pairing between sources and operators, which reads

$$\delta I = -\frac{1}{2} \int d^2x \sqrt{-g_{\text{2D}}}\, T_{ab}\, \delta g^{ab}_{\text{2D}} = \int d^2x (-\mathcal{O}^{\text{2D}}_{j} \nu \delta\mu + \mathcal{O}^{\text{2D}}_{\theta} \frac{\alpha}{\nu} \delta\nu + \mathcal{O}^{\text{2D}}_{u} \delta\alpha) \ . \tag{4.83}$$

The Ward identity and the trace anomaly for a CFT$_2$ are

$$\nabla_a T^{ab} = 0 \ , \quad T^a_{\ a} = \frac{c}{24\pi} R^{(2)} \ , \tag{4.84}$$

where c is the central charge, and $R^{(2)}$ is the Ricci scalar of the background geometry. For the moment, we are considering CFTs with no gravitational anomalies, i.e., $c_L = c_R = 2c$,

[7] We could also consider α, ν and μ to be functions of θ. However, it suffices to have time-dependent sources for our analysis.

but we will generalize this discussion in Sec. 4.4.1. In terms of the operators introduced in (4.82), and for the background in (4.81), these equations take a simple form. Assuming that the sources in (4.81) have only u-dependence, the Ward identity reads

$$\begin{aligned}(\partial_u - \mu\partial_\theta)\mathcal{O}_j^{\text{2D}} + \mathcal{O}_j^{\text{2D}}\frac{\partial_u\nu}{\nu} + \frac{\alpha}{\nu}\partial_\theta\mathcal{O}_u^{\text{2D}} = 0 \ , \\ (\partial_u - \mu\partial_\theta)\mathcal{O}_u^{\text{2D}} - \mathcal{O}_\theta^{\text{2D}}\frac{\partial_u\nu}{\nu} + \frac{\alpha}{\nu}\partial_\theta\mathcal{O}_j^{\text{2D}} = 0 \ ,\end{aligned} \tag{4.85}$$

while the trace anomaly is

$$\mathcal{O}_\theta^{\text{2D}} + \mathcal{O}_u^{\text{2D}} = \frac{c}{24\pi}\frac{2}{\alpha}\partial_u\left(\frac{\partial_u\nu}{\alpha}\right) \ , \tag{4.86}$$

where we used that the Ricci scalar is given by

$$R^{(2)} = \frac{2}{\alpha\nu}\partial_u\left(\frac{\partial_u\nu}{\alpha}\right) \ . \tag{4.87}$$

Finally, there are two charges that are important to highlight: the total energy (E) and angular momentum (J) of the system. In our conventions, they read

$$\begin{aligned}E &= -\int \mathrm{d}\theta\left(\nu\,\mathcal{O}_u^{\text{2D}} - \frac{c}{24\pi}\left(\frac{\partial_u\nu}{\alpha}\right)^2\right) \ , \\ J &= \int \mathrm{d}\theta\,\nu\,\mathcal{O}_j^{\text{2D}} \ .\end{aligned} \tag{4.88}$$

From (4.85), we can see that these charges are conserved when the operators are independent of θ.

4.3.2 AdS_3 reduced phase space

In this portion, guided by Sec. 4.3.1, we will construct a geometry whose boundary metric is (4.81) and supported by a boundary stress tensor (4.82). We will be working

with a three-dimensional Einstein-Hilbert action, supplemented with a negative cosmological constant, i.e.,

$$S_{\text{AdS}_3} = \frac{1}{2\kappa_3^2}\int_{\mathcal{M}} \mathrm{d}^3x\sqrt{-g}\left(R+\frac{2}{\ell_3^2}\right) + \frac{1}{\kappa_3^2}\int_{\partial\mathcal{M}} \mathrm{d}^2x\sqrt{-h}\left(K-\frac{1}{\ell_3}\right) \ , \tag{4.89}$$

where $\kappa_3^2 = 8\pi G_3$, ℓ_3 is the AdS_3 radius, and K is the extrinsic curvature.

It is well known how to describe asymptotically AdS_3 backgrounds for pure AdS_3 gravity, with one key fact being that the Fefferman-Graham expansion terminates [33]. Here, we will describe these geometries in the Bondi-gauge,[8] where we start by characterizing the metric as

$$ds^2_{\text{3D}} = -F(u,r,\theta)\mathrm{d}u^2 - 2\alpha(u)\mathrm{d}u\mathrm{d}r + \Phi^2(u,r)\left(\mathrm{d}\theta + A(u,r,\theta)\mathrm{d}u\right)^2 \ . \tag{4.90}$$

One can determine the radial dependence of these functions such that they comply with the equations of motion. Concretely, we have

$$\Phi(u,r) = \nu(u)\frac{r}{\ell_3} + \Phi_0 \ , \tag{4.91}$$

where Φ_0 is constant, and the remaining metric functions are

$$\begin{aligned} F(u,r,\theta) &= \frac{\alpha^2}{\nu^2}\,\Phi^2 + F_1(u,\theta)\,\Phi + F_0(u,\theta) + \frac{F_{-2}(u,\theta)^2}{\Phi^2} \ , \\ A(u,r,\theta) &= \mu(u) + \frac{F_{-2}(u,\theta)}{\Phi^2} \ . \end{aligned} \tag{4.92}$$

In relation to the CFT_2 setup, the boundary metric of this spacetime is given by (4.81) as desired; note that the coordinate u is null in the bulk, but on the boundary, it becomes time-like. Φ controls the size of S^1, and hence we can use this field as a dial to get close to

[8] The Bondi gauge has been employed in AdS_3 to explore various boundary conditions and their associated asymptotic symmetries [152, 165, 166]

the UV (asymptotic AdS_3 region) or close to the IR (near horizon region). The functions $F_i(u,\theta)$ control the one-point functions of the stress tensor. In relation to the notation in (4.82), we find

$$\begin{aligned} F_1(u,\theta) &= 2\kappa_3^2 \frac{\alpha^2}{\nu^2} \int \mathrm{d}u\, \alpha \left(\mathcal{O}_\theta^{\text{2D}} + \mathcal{O}_u^{\text{2D}}\right) , \\ F_0(u,\theta) &= 2\ell_3\kappa_3^2 \frac{\alpha^2}{\nu}\mathcal{O}_u^{\text{2D}} - \ell_3^2 \left(\frac{\partial_u \nu}{\nu}\right)^2 - \Phi_0 F_1(u,\theta) , \\ F_{-2}(u,\theta) &= \ell_3\kappa_3^2\, \alpha(u)\, \mathcal{O}_j^{\text{2D}} . \end{aligned} \tag{4.93}$$

Here the operators $(\mathcal{O}_\theta^{\text{2D}}, \mathcal{O}_u^{\text{2D}}, \mathcal{O}_j^{\text{2D}})$ depend on the variables u and θ. As stated, the background is still not a solution to Einstein's equations. Imposing that the (4.90) solves the equations of motion requires that

$$\begin{aligned} (\partial_u - \mu\partial_\theta)\mathcal{O}_j^{\text{2D}} + \mathcal{O}_j^{\text{2D}} \frac{\partial_u \nu}{\nu} + \frac{\alpha}{\nu}\partial_\theta \mathcal{O}_u^{\text{2D}} &= 0 , \\ (\partial_u - \mu\partial_\theta)\mathcal{O}_u^{\text{2D}} - \mathcal{O}_\theta^{\text{2D}} \frac{\partial_u \nu}{\nu} + \frac{\alpha}{\nu}\partial_\theta \mathcal{O}_j^{\text{2D}} &= 0 , \\ \mathcal{O}_\theta^{\text{2D}} + \mathcal{O}_u^{\text{2D}} = \frac{c}{24\pi}\frac{2}{\alpha}\partial_u \left(\frac{\partial_u \nu}{\alpha}\right) &, \end{aligned} \tag{4.94}$$

where the central charge is given in terms of gravitational parameters by

$$c = \frac{3\ell_3}{2G_3} . \tag{4.95}$$

These are exactly the Ward identities of the CFT_2: the covariant conservation equation (4.85) and trace anomaly (4.86). Hence, imposing that (4.90)-(4.93) is locally AdS_3 is equivalent to imposing the Ward identities of the CFT.

It is important to note that (4.90)-(4.93) generalizes the Bañados phase space introduced in [167]. Here, we have parametrized the solution for a time-dependent boundary metric, and in contrast to [167], the trace anomaly is not solved for. Our parametrization

of AdS_3 is an adaptation of [33, 37] where we are working in the Bondi gauge, rather than a Fefferman-Graham gauge. The advantage of working in the Bondi gauge, relative to Fefferman-Graham, is that Φ in (4.91) is independent of the operators $(\mathcal{O}_\theta^{\text{2D}}, \mathcal{O}_u^{\text{2D}}, \mathcal{O}_j^{\text{2D}})$; for this reason the decoupling limit will not tamper with a redefinition of the radial direction.

BTZ black hole

It is useful to describe the BTZ black hole [168, 169] in our parameterization of the phase space (4.90). First, we set $\nu = \ell_3$ and $\Phi_0 = 0$ so that Φ is simply the radial variable. The remaining sources are chosen as $\alpha = 1$ and $\mu = 0$. Then, the metric is given by

$$ds^2_{\text{BTZ}} = -\left(\frac{r^2}{\ell_3^2} - m + \frac{j^2}{4r^2}\right) \mathrm{d}u^2 - 2\mathrm{d}u\mathrm{d}r + r^2 \left(\mathrm{d}\theta + \frac{j}{2r^2}\mathrm{d}u\right)^2 , \tag{4.96}$$

where m and j are constants and are related to the inner (r_-) and outer (r_+) horizon via

$$m = \frac{r_+^2 + r_-^2}{\ell_3^2} , \quad j = \frac{2r_+ r_-}{\ell_3} . \tag{4.97}$$

The energy and angular momentum of the black hole are given by $M_{\text{BTZ}} = \frac{m}{8G_3}$ and $J_{\text{BTZ}} = \frac{j}{8G_3}$, respectively. In our parameterization, this standard metric follows after making the following identifications with the operators $(\mathcal{O}_\theta^{\text{2D}}, \mathcal{O}_u^{\text{2D}}, \mathcal{O}_j^{\text{2D}})$

$$\begin{aligned} \mathcal{O}_u^{\text{2D}} &= -\mathcal{O}_\theta^{\text{2D}} = -\frac{1}{2\pi} M_{\text{BTZ}} , \\ \mathcal{O}_j^{\text{2D}} &= \frac{1}{2\pi\ell_3} J_{\text{BTZ}} . \end{aligned} \tag{4.98}$$

The Hawking temperature T, angular velocity Ω and black hole entropy S are

$$T = \frac{r_+^2 - r_-^2}{2\pi\ell_3^2 r_+} , \quad \Omega = \frac{r_+}{\ell_3 r_-} , \quad S = \frac{\pi r_+}{2G_3} . \tag{4.99}$$

Near-extremal thermodynamics: For an extremal black hole, the temperature vanishes, and the energy is set by the angular momentum, satisfying the condition $\ell_3 M_{\rm BTZ} = J_{\rm BTZ}$, which is equivalent to the horizons coinciding, i.e., $r_+ = r_- \equiv r_0$. To study the low-temperature regime, we expand around extremality as $r_\pm = r_0 \pm \delta r$, while keeping $J_{\rm BTZ}$ fixed. This gives at leading order in δr

$$T = \frac{2\delta r}{\pi \ell_3^2} \ , \tag{4.100}$$

and the response in the energy $\Delta M_{\rm BTZ}$ and the entropy ΔS to leading order is given respectively by[9]

$$\Delta M_{\rm BTZ} = \pi^2 \frac{c}{12} \ell_3 T^2 \ , \qquad \Delta S = \pi^2 \frac{c}{6} \ell_3 T \ . \tag{4.101}$$

For future reference, we note that the extremal condition in terms of the operators $(\mathcal{O}_\theta^{\rm 2D}, \mathcal{O}_u^{\rm 2D}, \mathcal{O}_j^{\rm 2D})$ can be expressed as

$$\mathcal{O}_\theta^{\rm 2D,*} + \mathcal{O}_u^{\rm 2D,*} = 0 \ , \quad \mathcal{O}_u^{\rm 2D,*} + \mathcal{O}_j^{\rm 2D,*} = 0 \ . \tag{4.102}$$

Here, the asterisk in the operators is to emphasize that these relations hold only at extremality. Strictly speaking, the first condition is the absence of anomaly for the stationary solution. In addition, we notice that in terms of the parameter r_0, we can express $\mathcal{O}_j^{\rm 2D,*}$ as follows

$$\mathcal{O}_j^{\rm 2D,*} = \frac{r_0^2}{\kappa_3^2 \ell_3^2} \ . \tag{4.103}$$

[9]For brevity, we are only stating the naive semi-classical expressions for entropy and mass in the near-extremal regime. Quantum corrections can be large, see [170, 171, 172], but will not impact the subsequent analysis. We will discuss briefly quantum corrections in Sec. 4.6.

4.3.3 Off-shell decoupling limit

In this portion, we construct the decoupling limit that implements the near-extremal limit of the reduced phase space in (4.90)-(4.93). We refer to our approach as an off-shell decoupling limit, since it does not require imposing the equations of motion (4.94) on our procedure.

To gain physical insight into our construction, let us recall that the radial coordinate r roughly corresponds to the energy scale along the holographic renormalization flow. In this context, the linear form of the UV dilaton,

$$\Phi(u,r) = \nu \frac{r}{\ell_3} + \Phi_0 \ . \tag{4.104}$$

can be interpreted as follows. The source ν acts as a scaling factor for the energy scale r, while the constant Φ_0 serves as a reference energy. By redefining ν as $\nu = \lambda\tilde{\nu}$ and taking the limit $\lambda \to 0$ while keeping $\tilde{\nu}$ fixed, we effectively zoom in on the reference energy Φ_0.

Another important aspect of the decoupling limit is to keep the angular momentum J, defined in (4.88), finite as λ goes to zero. Concretely, this means

$$\mathcal{O}_j^{\text{2D}} = \frac{\mathcal{O}_j^{(-1)}}{\lambda} \ , \tag{4.105}$$

where $\mathcal{O}_j^{(-1)}$ is fixed. Therefore, the defining feature of the decoupling limit is to take

$$\nu = \lambda\tilde{\nu} \ , \qquad \lambda \to 0 \ , \tag{4.106}$$

while keeping $\tilde{\nu}$ fixed combined with (4.105). By itself, this limit introduces divergences in the line element (4.90)-(4.93). To make the limit well defined in the metric functions

in (4.92), we therefore expand our operators in terms of λ as

$$\mathcal{O}_i^{\text{2D}} = \frac{\mathcal{O}_i^{(-1)}}{\lambda} + \mathcal{O}_i^{(0)} + \mathcal{O}_i^{(1)}\lambda + \cdots \ , \tag{4.107}$$

for $\mathcal{O}_i^{\text{2D}} = \{\mathcal{O}_u^{\text{2D}}, \mathcal{O}_\theta^{\text{2D}}\}$. For a geometric perspective, the expansion of $\mathcal{O}_i^{\text{2D}}$ starts with λ^{-1} because of the dependence on ν in (4.92); from a a CFT_2 perspective, this will lead to a finite energy and angular momentum as $\lambda \to 0$ in (4.88). Demanding regularity of $F(r, u, \theta)$ in the limit $\lambda \to 0$ gives

$$\begin{aligned} \mathcal{O}_j^{(-1)} = \mathcal{O}_\theta^{(-1)} = -\mathcal{O}_u^{(-1)} = \frac{\Phi_0^2}{\ell_3 \kappa_3^2 \tilde{\nu}} \ , \\ \mathcal{O}_\theta^{(0)} = -\mathcal{O}_u^{(0)} = 0 \ . \end{aligned} \tag{4.108}$$

Here, we recognize the regularity conditions as the extremality condition of thermodynamics, given in (4.103), upon setting $\tilde{\nu} = \ell_3$ and $\Phi_0 = r_0$.

Next, demanding regularity of $A(r, u, \theta)$ requires, in addition to (4.108), the implementation of the shift

$$\mu = \tilde{\mu} - \frac{\alpha}{\lambda \tilde{\nu}} \ . \tag{4.109}$$

With the redefintions (4.106)-(4.109) the limit $\lambda \to 0$, where $(\tilde{\nu}, \tilde{\mu}, \alpha)$, Φ_0 and $\mathcal{O}_i^{\text{2D}}$ are held fixed, the line element (4.90) is smooth and well defined. In particular, we find

$$ds^2_{\text{3D}} \underset{\lambda \to 0}{=} -f_{\text{IR}}(u, r, \theta)\text{d}u^2 - 2\alpha(u)\text{d}u\text{d}r + \Phi_0^2 \left(\text{d}\theta - \frac{2\alpha(u)}{\ell_3 \kappa_3^2 \Phi_0} r \text{d}u\right)^2 + O(\lambda) \ , \tag{4.110}$$

where

$$\begin{aligned} f_{\text{IR}}(u, r, \theta) &:= \lim_{\lambda \to 0} F(r, u, \theta) \\ &= \frac{\alpha^2 r^2}{(\ell_3/2)^2} + 2r \frac{\alpha^2}{\tilde{\nu}} \frac{\kappa_3^2}{\ell_3} \int \text{d}u \, \alpha (\mathcal{O}_\theta^{(1)} + \mathcal{O}_u^{(1)}) + 2 \frac{\alpha^2}{\tilde{\nu}} \ell_3 \kappa_3^2 \mathcal{O}_u^{(1)} - \ell_3^2 \left(\frac{\partial_u \tilde{\nu}}{\tilde{\nu}}\right)^2 \ . \end{aligned} \tag{4.111}$$

From here, we already recognize that the geometry, at fixed θ, becomes locally AdS_2.

It is important to stress that in (4.105)-(4.111) the equations of motion (4.94) are *not* used. We now turn to the effect of this decoupling limit on the dynamics of the system. Replacing the decoupling limit in (4.94), to leading order in λ, we find

$$\begin{aligned} \partial_\theta \mathcal{O}_i^{(-1)} = \partial_u(\tilde{\nu}\mathcal{O}_i^{(-1)}) = 0 \ , \quad i \in \{u, \theta, j\} \ , \\ \partial_\theta \mathcal{O}_i^{(1)} = 0 \ , \quad i \in \{u, \theta\} \ . \end{aligned} \tag{4.112}$$

Hence, the decoupling limit drops all the θ-dependence of our ansatz. Note that the conditions for $\mathcal{O}_i^{(-1)}$ in (4.112) are compatible with the regularity condition in (4.106). With this, the geometry (4.111) becomes an S^1 fibration over AdS_2 with $\ell_2 = \ell_3/2$. To order λ, which is the first backreaction of the system, the equations of motion reduce to

$$\begin{aligned} \mathcal{O}_\theta^{(1)} + \mathcal{O}_u^{(1)} = \frac{c}{24\pi}\frac{2}{\alpha}\partial_u\left(\frac{\partial_u\tilde{\nu}}{\alpha}\right) \ , \\ \partial_u\mathcal{O}_u^{(1)} - \mathcal{O}_\theta^{(1)}\frac{\partial_u\tilde{\nu}}{\tilde{\nu}} = 0 \ . \end{aligned} \tag{4.113}$$

Hence, the Ward identities of the CFT_2 have a well-defined behavior as we take $\lambda \to 0$.

Finally, applying the decoupling limit directly to the generating functional (4.83) yields[10]

$$\begin{aligned} \delta I^{\mathrm{IR}} = \int dx^2 \left(\left(\frac{\mathcal{O}_\theta^{(-1)} - \mathcal{O}_j^{(-1)}}{\lambda\tilde{\nu}}\right)\frac{\alpha}{\tilde{\nu}}\delta\tilde{\nu} + \left(\frac{\mathcal{O}_u^{(-1)} + \mathcal{O}_j^{(-1)}}{\lambda\tilde{\nu}}\right)\delta\alpha\right) \\ + \lambda\int dx^2 \left(\mathcal{O}_\theta^{(1)}\frac{\alpha}{\tilde{\nu}}\delta\tilde{\nu} + \mathcal{O}_u^{(1)}\delta\alpha\right) \ . \end{aligned} \tag{4.114}$$

Invoking the regularity conditions given in (4.108), this variation remains finite as $\lambda \to 0$.

[10] To derive this expression, We performed a Legendre transformation to switch from the source $\tilde{\mu}$ to the operator $\tilde{\nu}\mathcal{O}_j^{(-1)}$, which is held fixed in the limit $\lambda \to 0$. As a result, the term $\tilde{\mu}\delta(\tilde{\nu}\mathcal{O}_j^{(-1)})$ is omitted.

Therefore, to leading order in λ, we obtain the simplified expression:

$$\delta I^{\rm IR} = 2\pi \int du \left(\mathcal{O}_\theta^{(1)} \frac{\alpha}{\tilde{\nu}} \delta\tilde{\nu} + \mathcal{O}_u^{(1)} \delta\alpha \right) , \tag{4.115}$$

which defines the effective variation of the generating functional in the decoupled, low-energy limit. In the final expression, we have set $\lambda = 1$, as it does not affect the analysis that follows.

Comparison with JT gravity. We can see now that many portions of our decoupling limit reproduce the features of JT gravity described in Sec. 4.2. In particular, the blackening factor (4.111) resembles (4.4), and the equations of motion (4.113) are compatible with (4.12a)-(4.12b). We will now make the map precise, taking into account the ambiguities that we encountered in Sec. 4.2.

Our first step is to identify the JT dilaton as follows:

$$\Phi - \Phi_0 = \frac{\tilde{\nu}}{l_3} r \equiv \phi \Longrightarrow \phi = \frac{\nu}{l_2} r \ , \tag{4.116}$$

where ℓ_2 and ν denote the AdS radius and the source of JT gravity, respectively. These are related to the corresponding quantities in AdS_3 via:

$$l_2 = \frac{l_3}{2} \ , \quad \nu = \frac{\tilde{\nu}}{2} \ . \tag{4.117}$$

With this identification, the IR lapse function $f_{\rm IR}$ from equation (4.111) can be rewritten as:

$$f_{\rm IR}(u,r) = \frac{\alpha^2 r^2}{\ell_2^2} + 2r \frac{\alpha^2}{4\nu} \frac{\kappa_3^2}{\ell_2} \int \mathrm{d}u \, \alpha(\mathcal{O}_\theta^{(1)} + \mathcal{O}_u^{(1)}) + 2\frac{\alpha^2}{\nu} \ell_2 \kappa_3^2 \mathcal{O}_u^{(1)} - 4\ell_2^2 \left(\frac{\partial_u \nu}{\nu} \right)^2 \ . \tag{4.118}$$

By comparing this expression with equations (4.11) in Section 4.2, we recognize that the

decoupling limit in AdS_3 yields the identifications $\omega^2 = \gamma^{-2} = 4$, provided we relate the operators as:

$$\kappa_2^2 \mathcal{O}_u = \kappa_3^2 \mathcal{O}_u^{(1)} \ , \quad \kappa_2^2 \mathcal{O}_\phi = \kappa_3^2 \mathcal{O}_\theta^{(1)} \ . \tag{4.119}$$

Applying this relation to the IR generating functional I_{3D}^{IR} defined in (4.115), we find:

$$\delta I^{IR} = 2\pi \frac{\kappa_2^2}{\kappa_3^2} \int \mathrm{d}u \Big(\mathcal{O}_u \, \delta\alpha + \frac{\alpha}{\nu} \mathcal{O}_\phi \, \delta\nu \Big) = \delta I_\omega \ . \tag{4.120}$$

Here we used the fact that $2\pi\kappa_2^2/\kappa_3^2 = 1$, in accordance with thermodynamic considerations.[11] Thus, we obtain the following mapping:

$$I_{JT} = I_{\omega=2} - 3\frac{\ell_2}{2\kappa_2} \int du \sqrt{-h_b} \nu^{-1} h_b^{-1} (\partial_u \nu)^2 \ . \tag{4.121}$$

From this point, the Schwarzian action can be derived via the canonical transformation given in (4.79). In conclusion, we have recovered the Schwarzian dynamics as the outcome of our off-shell construction of the decoupling limit.

In the case of AdS_3/CFT_2, it is well known that the effective outcome of the decoupling limit is a flow of the central charge, $c \to c/2$, as half of the degrees of freedom become frozen near extremality (see, for instance, [170]). For this reason, AdS_3/CFT_2 serves as a warm-up exercise for the more challenging scenarios to be explored in the following sections, where our off-shell construction of the decoupling limit will reveal its full power.

[11] The relation $2\pi\kappa_2^2/\kappa_3^2 = 1$ also follows directly from dimensional reduction. However, this procedure fails when the parent theory includes higher-derivative terms, as in the case of topologically massive gravity, which we will discuss next.

4.4 Near-extremality at the boundary of TMG

In this section, we generalize the analysis of Sec. 4.3 to situations where the CFT_2 has both a conformal and gravitational anomaly, inducing independent left and right central charges, c_L and c_R, respectively. From the gravitational perspective, we will introduce c_L and c_R by considering Topologically Massive Gravity (TMG) with boundary conditions suitable for $\text{AdS}_3/\text{CFT}_2$ as done in [173, 174, 175, 176, 177, 178].

The main appeal of this situation is to track further the imprint of the CFT_2 data in the near-extremal dynamics. This will reinforce some aspects already encountered in Sec. 4.3, related to how we implement the decoupling limits, and it will also illustrate the role of the left and right moving sectors of the CFT_2 in the near-extremal dynamics. With this in mind, we will only consider the minimal modifications to the analysis of Sec. 4.3 such that the effects of $c_L \neq c_R$ are manifest.

It is important to mention that TMG, as a semi-classical gravitational theory, suffers instabilities and unitarity violations; see, for example, [179, 180, 181]. Although these are important dynamical aspects of the theory, our reduced phase space does not contain these pathological modes; hence, instabilities will not influence the analysis here.

4.4.1 CFT_2 Ward identities on curved backgrounds

In analogy to Sec. 4.3.1, we want to place a two-dimensional CFT with unequal left and right central charges, i.e., $c_R \neq c_L$, on a curved background. However, the CFT_2 cannot be consistently coupled to dynamical gravity due to the presence of a gravitational anomaly. This anomaly can be interpreted either as a diffeomorphism anomaly, which leads to non-covariant conservation of the stress tensor, or as a local Lorentz anomaly, which results in a non-symmetric stress tensor [175, 182].[12] For our purposes, we express

[12] For a concise summary of the different notions of stress tensors, see [183].

the gravitational anomaly in terms of the diffeomorphism anomaly. This choice allows us to define the stress tensor as the variation of the action with respect to the metric,

$$\delta I = \frac{1}{2}\int d^2x\sqrt{-g_{\text{2D}}}\,T_{ab}\,\delta g^{ab}_{\text{2D}}\ . \tag{4.122}$$

The Ward identities, which are the conformal and trace anomalies, are now

$$\begin{aligned}\nabla_a T^{ab} &= -\frac{\bar{c}}{24\pi}g^{ab}\epsilon^{cd}\partial_e\partial_c\Gamma^e_{ad}\ ,\\ T^a_{\ a} &= \frac{c}{24\pi}R^{(2)} + \frac{\bar{c}}{12\pi}E^a_{\ a}\ .\end{aligned} \tag{4.123}$$

This form of writing the Ward identities in the presence of the diffeomorphism anomaly is consistent with the Wess-Zumino consistency conditions. The violation of covariant conservation of the stress tensor is parameterized by the central charge $\bar{c}$, while the Weyl anomaly is parameterized by the central charge c. These are expressed in terms of the right and left central charges of the CFT_2 as follows:

$$c = \frac{c_L + c_R}{2}\ , \qquad \bar{c} = \frac{c_L - c_R}{2}\ . \tag{4.124}$$

In the Ward identities (4.123), $R^{(2)}$ and Γ^e_{ad} represent the Ricci scalar and the Christoffel connection of the background geometry, respectively. Additionally, the non-tensorial quantity E_{ab} is defined as:

$$E_{ab} = \frac{1}{4}\epsilon^{cd}\nabla_c\partial_d g_{ab} - \frac{1}{8}\epsilon_a^{\ c}\epsilon_b^{\ d}\epsilon^{ef}\nabla_d\partial_e g_{fc} - \frac{1}{8}\epsilon_b^{\ c}\epsilon_a^{\ d}\epsilon^{ef}\nabla_d\partial_e g_{fc}\ . \tag{4.125}$$

Here, ϵ_{ab} is the Levi-Civita tensor normalized $\sqrt{-g}\epsilon_{01} = 1$. We note the terms accompanying the central charge $\bar{c}$ in the Ward identities (4.123) are local expressions of the background geometry.

With this, now we can make some more explicit choices for the non-trivial two-dimensional background. We adopt the same background metric as in our previous discussion of CFT_2 in Sec. 4.3.1, as this choice remains unaffected by the gravitational anomaly, which reads

$$ds^2_{\text{2D}} = -\alpha^2 \mathrm{d}u^2 + \nu^2(\mathrm{d}\theta + \mu \mathrm{d}u)^2 \ , \tag{4.126}$$

where $\alpha(u)$, $\nu(u)$ and $\mu(u)$ are three arbitrary functions. A key advantage of choosing the stress tensor (4.122) in a manner consistent with the variational principle in the presence of the gravitational anomaly is that it enables us to apply a decomposition similar to that used in Sec. 4.3.1 to our current case:

$$\begin{aligned} T_{\theta\theta} &= \nu\, \mathcal{O}^{\text{TMG}}_{\theta} \ , \\ T_{u\theta} &= \alpha\, \mathcal{O}^{\text{TMG}}_{j} + \mu\, T_{\theta\theta} \ , \\ T_{uu} &= \mu^2 \nu\, \mathcal{O}^{\text{TMG}}_{\theta} + 2\mu\alpha\, \mathcal{O}^{\text{TMG}}_{j} - \frac{\alpha^2}{\nu} \mathcal{O}^{\text{TMG}}_{u} \ . \end{aligned} \tag{4.127}$$

From the variation of the generating function (4.122), we obtain a pairing between the sources and operators given by

$$\delta I = \int \mathrm{d}x^2 \Big(- \mathcal{O}^{\text{TMG}}_{j} \nu \delta\mu + \mathcal{O}^{\text{TMG}}_{\theta} \frac{\alpha}{\nu} \delta\nu + \mathcal{O}^{\text{TMG}}_{u} \delta\alpha \Big) \ . \tag{4.128}$$

Finally, with this parametrization, the Ward identities (4.123) now read

$$\begin{aligned} (\partial_u - \mu\partial_\theta)\mathcal{O}^{\text{TMG}}_{u} - \mathcal{O}^{\text{TMG}}_{\theta} \frac{\partial_u \nu}{\nu} + \frac{\alpha}{\nu} \partial_\theta \mathcal{O}^{\text{TMG}}_{j} &= -\frac{\bar{c}}{24\pi} \frac{\alpha}{2\nu\partial_u\nu} \partial_u \left(\left(\frac{\nu \partial_u \nu}{\alpha^2} \right)^2 \partial_u \mu \right) \ , \\ (\partial_u - \mu\partial_\theta)\mathcal{O}^{\text{TMG}}_{j} + \mathcal{O}^{\text{TMG}}_{j} \frac{\partial_u \nu}{\nu} + \frac{\alpha}{\nu} \partial_\theta \mathcal{O}^{\text{TMG}}_{u} &= \frac{\bar{c}}{24\pi} \frac{1}{2\nu} \partial_u^2 \left(\frac{\nu \partial_u \nu}{\alpha^2} \right) \ , \\ \mathcal{O}^{\text{TMG}}_{\theta} + \mathcal{O}^{\text{TMG}}_{u} &= \frac{c}{24\pi} \frac{2}{\alpha} \partial_u \left(\frac{\partial_u \nu}{\alpha} \right) - \frac{\bar{c}}{24\pi} \frac{1}{2\alpha} \partial_u \left(\frac{\nu^2 \partial_u \mu}{\alpha^2} \right) \ . \end{aligned} \tag{4.129}$$

The right-hand side of these equations consists of local functions of the sources, arising from the curvature terms in (4.123).

Finally, it is useful to construct explicitly conserved charges in this case. Due to the presence of the diffeomorphism anomaly, the generating function is not invariant under diffeomorphisms, i.e., $\delta_\xi I \neq 0$ for an arbitrary diffeomorphism ξ^a. As a consequence, the stress tensor is not covariantly conserved, as expressed in the Ward identity (4.123). Nevertheless, conserved charges can still be defined under certain conditions. In particular, let us consider diffeomorphisms that preserve the gauge choice of the background metric (4.126). In this case, the transformation of the sources is given by:

$$\delta\alpha = \partial_u(\epsilon\alpha) + \alpha\sigma \ , \quad \delta\nu = \epsilon\delta\nu + \nu\sigma \ , \quad \delta\mu = \delta_u(\epsilon\mu + \varphi) \ . \tag{4.130}$$

Here, ϵ, φ and σ represent time-reparameterization, θ-reparameterization, and a Weyl transformation, respectively. The conformal killing vectors (CKVs) are determined by imposing $\delta_{\text{CKV}}\alpha = \delta_{\text{CKV}}\mu = \delta_{\text{CKV}}\nu = 0$. This leads to the following solutions for the infinitesimal transformations:

$$\epsilon = \xi_1\frac{\nu}{\alpha} \ , \quad \sigma = -\xi_1\frac{\partial_u(\nu)}{\alpha} \ , \quad \varphi = \xi_2 - \xi_1\frac{\nu}{\alpha}\mu \ , \tag{4.131}$$

where ξ_1 and ξ_2 are arbitrary constants. Substituting these conformal transformations into the generating function, we obtain

$$\delta_{\text{CKV}} I = \int \mathrm{d}x^2(-\mathcal{O}_j^{\text{TMG}}\nu\delta_{\text{CKV}}\mu + \mathcal{O}_\theta^{\text{TMG}}\frac{\alpha}{\nu}\delta_{\text{CKV}}\nu + \mathcal{O}_u^{\text{TMG}}\delta_{\text{CKV}}\alpha) = 0 \ , \tag{4.132}$$

Now, assuming that the operators $(\mathcal{O}_u^{\text{TMG}}, \mathcal{O}_j^{\text{TMG}}, \mathcal{O}_\theta^{\text{TMG}})$ are independent of θ, we apply the

equations of motion (4.129) along with integration by parts to derive

$$0 = \int \mathrm{d}x^2 \Bigg[-\xi_2 \partial_u \left(\nu \mathcal{O}_j^{\text{TMG}} - \frac{\bar{c}}{48\pi} \partial_u \left(\frac{\nu \partial_u \nu}{\alpha^2} \right) \right) + \xi_1 \partial_u \left(\nu \mathcal{O}_u^{\text{TMG}} - \frac{c}{24\pi} \left(\frac{\partial_u \nu}{\alpha} \right)^2 + \frac{\bar{c}}{24\pi} \frac{\nu^2 \partial_u \nu \partial_u \mu}{\alpha^3} \right) \Bigg] . \tag{4.133}$$

Here, prime means derivative with respect to time u. Since the constants ξ_1 and ξ_2 are arbitrary, we identify two conserved charges, given by

$$\begin{aligned} E &= -\int \mathrm{d}\theta \left(\nu \mathcal{O}_u^{\text{TMG}} - \frac{c}{24\pi} \left(\frac{\partial_u \nu}{\alpha} \right)^2 + \frac{\bar{c}}{24\pi} \frac{\nu^2 \partial_u \nu \partial_u \mu}{\alpha^3} \right) , \\ J &= \int \mathrm{d}\theta \left(\nu \mathcal{O}_j^{\text{TMG}} - \frac{\bar{c}}{48\pi} \partial_u \left(\frac{\nu \partial_u \nu}{\alpha^2} \right) \right) . \end{aligned} \tag{4.134}$$

J represents the angular momentum, while E denotes the energy of the system. Note that they agree with (4.88) when $\bar{c} = 0$ ($c_L = c_R$). In the general case where the operators depend on θ, these charges are not conserved. However, they remain useful quantities to consider.

4.4.2 TMG reduced phase space

In three dimensions, the Einstein-Hilbert action supplemented by a gravitational Chern-Simons term defines the topological massive gravity (TMG) theory [184, 185, 186], and we will mostly follow the conventions of [183]. The action is given by

$$S_{\text{CS}} = \frac{1}{2\kappa_3^2} \int \mathrm{d}^3x \sqrt{-g} \Big(R + \frac{2}{\ell_3} \Big) + \frac{1}{4\kappa_3^2 \boldsymbol{\mu}} \int \mathrm{d}^3x \sqrt{-g} \epsilon^{\alpha\nu\gamma} \left(\Gamma^{\mu}_{\alpha\nu} \partial_\xi \Gamma^{\xi}_{\gamma\mu} + \frac{2}{3} \Gamma^{\mu}_{\alpha\xi} \Gamma^{\xi}_{\nu\sigma} \Gamma^{\sigma}_{\gamma\mu} \right) . \tag{4.135}$$

In this action, $\boldsymbol{\mu}$ is a real coupling constant with the dimensions of mass; we adopt the convention that the three-dimensional Levi-Civita tensor is $\sqrt{-g}\epsilon_{012} = 1$. The equations

of motion of TMG are

$$R_{\mu\nu} - \frac{1}{2} g_{\mu\nu} R - \frac{1}{\ell_3^2} g_{\mu\nu} = -\frac{1}{\boldsymbol{\mu}} C_{\mu\nu} \ , \tag{4.136}$$

where $C_{\mu\nu}$ is the Cotton tensor,

$$C_{\mu\nu} = \epsilon_{\mu}{}^{\gamma\lambda} \nabla_{\gamma} \left(R_{\lambda\nu} - \frac{1}{4} g_{\lambda\nu} R \right) \ . \tag{4.137}$$

Despite the presence of the connection $\Gamma^{\gamma}_{\alpha\nu}$ in the action, the equations of motion remain covariant. Moreover, all locally AdS_3 solutions have a vanishing Cotton tensor $C_{\mu\nu} = 0$, making them solutions of TMG, as seen in (4.136). For a nonzero Cotton tensor, $C_{\mu\nu} \neq 0$, TMG admits new solutions, a subclass of which corresponds to warped AdS_3 spacetimes, including warped black holes [187, 188, 189]. These asymptotically warped AdS_3 geometries do not satisfy the Brown-Henneaux boundary conditions and will not be considered here.

In what follows, we focus exclusively on locally AdS_3 solutions with a vanishing Cotton tensor, $C_{\mu\nu} = 0$. In this case, it is well-known that the dictionary with the dual CFT_2 leads to [175]

$$c_L = \frac{3\ell_3}{2G_3} \left(1 + \frac{1}{\boldsymbol{\mu}\ell_3} \right) \ , \quad c_R = \frac{3\ell_3}{2G_3} \left(1 - \frac{1}{\boldsymbol{\mu}\ell_3} \right) \ . \tag{4.138}$$

Alternatively, via (4.124), we have

$$c = \frac{3\ell_3}{2G_3} \ , \quad \bar{c} = \frac{1}{\boldsymbol{\mu}\ell_3} \frac{3\ell_3}{2G_3} \ . \tag{4.139}$$

The reduced phase space will again be given by (4.90)-(4.92). The key difference is how metric functions in (4.92) are mapped to CFT_2 variables in Sec. 4.4.1, which affects

(4.93). The simplest way to proceed is to write

$$\begin{aligned} F_1(u,\theta) &= 2\frac{\kappa_3^2}{z_1}\frac{\alpha^2}{\nu^2}\int \mathrm{d}u\,\alpha\left(\bar{\mathcal{O}}_\theta + \bar{\mathcal{O}}_u\right)\,, \\ F_0(u,\theta) &= 2\ell_3\kappa_3^2\frac{\alpha^2}{\nu}\bar{\mathcal{O}}_u - z_1\ell_3^2\frac{\partial_u\nu^2}{\nu^2} - \Phi_0 f_1(u,\theta)\,, \\ F_{-2}(u,\theta) &= \ell_3\kappa_3^2\,\alpha(u)\,\bar{\mathcal{O}}_j\,. \end{aligned} \tag{4.140}$$

where in these expressions, we have introduced the barred operators $(\bar{\mathcal{O}}_u, \bar{\mathcal{O}}_\theta, \bar{\mathcal{O}}_j)$, which serve as auxiliary variables dependent on the physical operators. A tedious but straightforward analysis gives

$$\begin{aligned} \bar{\mathcal{O}}_j &\equiv z_1\mathcal{O}_j^{\text{TMG}} + z_2\mathcal{O}_u^{\text{TMG}} - \frac{z_1\bar{c}}{24\pi}\left[\frac{1}{2\nu}\partial_u\left(\frac{\nu\partial_u\nu}{\alpha^2}\right) + \frac{(\partial_u\nu)^2}{\alpha^2\nu}\right] + \frac{z_2\bar{c}}{24\pi}\frac{\nu\partial_u\nu}{\alpha^3}\partial_u\mu\,, \\ \bar{\mathcal{O}}_u &\equiv z_1\mathcal{O}_u^{\text{TMG}} + z_2\mathcal{O}_j^{\text{TMG}} + \frac{z_1\bar{c}}{24\pi}\frac{\nu\partial_u\nu}{\alpha^3}\partial_u\mu - \frac{z_2\bar{c}}{24\pi}\frac{1}{2\nu}\partial_u\left(\frac{\nu\partial_u\nu}{\alpha^2}\right)\,, \\ \bar{\mathcal{O}}_\theta &\equiv z_1\mathcal{O}_\theta^{\text{TMG}} - z_2\mathcal{O}_j^{\text{TMG}} + \frac{z_1\bar{c}}{24\pi}\left(-\frac{\nu^2}{\alpha^4}\partial_u\alpha\partial_u\mu + \frac{\nu^2}{2\alpha^3}\partial_u^2\mu\right) + \frac{z_2\bar{c}}{24\pi}\frac{1}{2\nu}\partial_u\left(\frac{\nu\partial_u\nu}{\alpha^2}\right)\,, \end{aligned} \tag{4.141}$$

where the parameters z_1 and z_2 are defined as

$$z_1 = \frac{c^2}{c^2-\bar{c}^2}, \quad z_2 = \frac{c\bar{c}}{c^2-\bar{c}^2}\,. \tag{4.142}$$

It is straightforward to verify that in the limit $\bar{c}\to 0$—corresponding to equal left and right central charges—the parameters approach $z_1 \to 1$ and $z_2 \to 0$. In this limit, the TMG phase space described by equations (4.140) and (4.141) reduces to the AdS_3 phase space constructed in Section 4.3.2.

BTZ black hole in TMG

The line element for BTZ is still given by (4.96). The main difference in this case arises from the modifications to the stress tensor and other conserved quantities. In TMG, the

identification between the horizons $r_\pm$, and the mass M_{TMG} and angular momentum J_{TMG} is given by

$$\begin{aligned} \ell_3 M_{\text{TMG}} + J_{\text{TMG}} &= \left(1 - \frac{1}{\boldsymbol{\mu}\ell_3}\right) \frac{(r_+ + r_-)^2}{8G_3\ell_3} \ , \\ \ell_3 M_{\text{TMG}} - J_{\text{TMG}} &= \left(1 + \frac{1}{\boldsymbol{\mu}\ell_3}\right) \frac{(r_+ - r_-)^2}{8G_3\ell_3} \ . \end{aligned} \tag{4.143}$$

Furthermore, the energy M_{TMG} and angular momentum J_{TMG} are related to the operators $(\mathcal{O}_\theta^{\text{TMG}}, \mathcal{O}_u^{\text{TMG}}, \mathcal{O}_j^{\text{TMG}})$ via

$$\begin{aligned} \mathcal{O}_u^{\text{TMG}} = -\mathcal{O}_\theta^{\text{TMG}} &= -\frac{M_{\text{TMG}}}{2\pi} \ , \\ \mathcal{O}_j^{\text{TMG}} &= \frac{J_{\text{TMG}}}{2\pi\ell_3} \ . \end{aligned} \tag{4.144}$$

The Hawking temperature T and angular velocity Ω are

$$T = \frac{r_+^2 - r_-^2}{2\pi\ell_3^2 r_+} \ , \qquad \Omega = \frac{r_+}{\ell_3 r_-} \ , \tag{4.145}$$

which remains unchanged relative to (4.99). The semi-classical Wald entropy of the black hole is

$$S_{\text{TMG}} = \frac{\pi}{6\ell_3}\left(c_L(r_+ - r_-) + c_R(r_+ + r_-)\right) \ , \tag{4.146}$$

which receives a contribution from the gravitational Chern-Simons term in addition to the area-law [190, 191, 174, 192, 193].

Near-extremal Thermodynamics: At extremality, we again have $r_+ = r_- = r_0$ and zero temperature. In this limit, we have the relation between mass and angular momentum is

$$J_{\text{TMG}} = M_{\text{TMG}}\ell_3 = \frac{c_R}{6\ell_3^2} r_0^2 \ . \tag{4.147}$$

The linear response in temperature of the energy ΔM_{TMG} and entropy ΔS_{TMG}, at fixed J_{TMG}, results in

$$\Delta M_{\text{TMG}} = \frac{\pi \ell_3 c_L}{12} T^2 \ , \qquad \Delta S_{\text{TMG}} = \frac{\pi \ell_3 c_L}{6} T \ . \tag{4.148}$$

The right sector controls the notion of extremality, as we can see from (4.147). On the other hand, the linear response around extremality is only controlled by the left sector, as seen from (4.148). The presence of the gravitational anomaly in TMG disentangles the role of the right and left degrees of freedom of the CFT_2 [183].

Finally, for later comparison, we note from equation (4.148) that $\ell_2 = \ell_3/2$. Accordingly, the normalized heat capacity C_H is given by:

$$C_H^{\text{TMG}} = \frac{c_L}{6\ell_3} = \frac{2\pi}{\kappa_3^2}\left(1 + \frac{1}{\boldsymbol{\mu}\ell_3}\right) . \tag{4.149}$$

4.4.3 Off-shell decoupling limit

We now proceed to implement the decoupling limit for the TMG phase space described by equation (4.140). The procedure closely parallels the $\text{AdS}_3/\text{CFT}_2$ case discussed in Section 4.3.3, so we will present it only briefly here. As before, to control the expansion associated with the decoupling limit, we require that the charge J, defined in equation (4.134), remains finite as $\lambda \to 0$. The appropriate prescription for TMG is given by

$$\mathcal{O}_j^{\text{TMG}} = \frac{\mathcal{O}_j^{(-1)}}{\lambda} + \mathcal{O}_j^{(1)}\lambda, \tag{4.150}$$

where both $\mathcal{O}_j^{(-1)}$ and $\mathcal{O}_j^{(1)}$ are held fixed. The presence of the $\mathcal{O}_j^{(1)}$ term—arising from the compensating contribution due to the diffeomorphism anomaly in equation (4.134)—marks one of the key differences from the $\text{AdS}_3/\text{CFT}_2$ case analyzed in Section 4.3.3.

The prescription for the decoupling limit in TMG is to scale the source ν as

$$\nu = \lambda\tilde{\nu} \ , \qquad \lambda \to 0 \ , \tag{4.151}$$

while keeping $\tilde{\nu}$ fixed, in conjunction with (4.150). This procedure introduces divergences in the geometry, which we handle by expanding the remaining operators as

$$\mathcal{O}_i^{\text{TMG}} = \frac{\mathcal{O}_i^{(-1)}}{\lambda} + \mathcal{O}_i^{(0)} + \mathcal{O}_i^{(1)}\lambda + \mathcal{O}_i^{(2)}\lambda^2 + ..., \qquad i \in (u, \theta) \ . \tag{4.152}$$

The expansion of operators starts at order $1/\lambda$, as dictated by dimensional analysis of the line element (4.140). Requiring regularity of the geometry as $\lambda \to 0$ yields

$$\begin{aligned} \mathcal{O}_j^{(-1)} = \mathcal{O}_\theta^{(-1)} = -\mathcal{O}_u^{(-1)} = \frac{c_R}{12\pi\ell_3}\frac{\Phi_0^2}{\lambda\tilde{\nu}} \ , \\ \mathcal{O}_u^{(0)} = \mathcal{O}_\theta^{(0)} = 0 \ , \\ \mu = \tilde{\mu} - \frac{\alpha}{\lambda\tilde{\nu}} \ . \end{aligned} \tag{4.153}$$

The first two equations are equivalent to the extremality conditions (4.147) derived from the thermodynamic analysis, upon identifying $\tilde{\nu} = \ell_3$ and $\Phi_0 = r_0$.

With the redefinitions (4.151), and taking the limit $\lambda \to 0$ while keeping $(\tilde{\nu}, \tilde{\mu}, \alpha)$, Φ_0, and $\mathcal{O}_i^{\text{2D}}$ fixed, the line element (4.140) remains smooth and well-defined. In this way, we obtain the following IR effective lapse function and vector potential:

$$\begin{aligned} f_{\text{IR}} = \frac{\alpha^2 r^2}{(\ell_3/2)^2} + 2r\frac{\alpha^2}{\tilde{\nu}}\frac{\kappa_3^2}{\ell_3}\int \mathrm{d}u\, \alpha \left(\mathcal{O}_\theta^{(1)} + \mathcal{O}_u^{(1)} + \frac{\bar{c}}{24\pi}\frac{1}{2\alpha}\partial_u\left(\frac{\tilde{\nu}^2}{\alpha^2}\partial_u\left(\frac{\alpha}{\tilde{\nu}}\right)\right)\right) \\ + 2\frac{\alpha^2}{\tilde{\nu}}\ell_3\kappa_3^2\frac{c}{c_L}(\mathcal{O}_u^{(1)} - \mathcal{O}_j^{(1)}) + \frac{\ell_3^2}{2}\frac{\bar{c}}{c_L}\partial_u\left(\frac{\partial_u\tilde{\nu}}{\tilde{\nu}}\right) - \ell_3^2\frac{c}{c_L}\left(\frac{\partial_u\tilde{\nu}}{\tilde{\nu}}\right)^2 \ , \end{aligned} \tag{4.154}$$

$$A_{\text{IR}} = \tilde{\mu} - \frac{2r\alpha}{\ell_3\Phi_0} \ . \tag{4.155}$$

The IR vector potential $A_{\rm IR}$ is identical to that of the $\mathrm{AdS}_3/\mathrm{CFT}_2$ case with $c_L = c_R$. On the other hand, the lapse function $f_{\rm IR}$ is more intricate, as it involves the operator $\mathcal{O}_j^{(1)}$. It is important to emphasize that the equations of motion (4.129) were *not* used to obtain the expressions above.

We now turn to the effect of this decoupling limit on the dynamics of the system. Substituting the decoupling limit into (4.129), and expanding to leading order in λ, we find

$$\begin{aligned} \partial_\theta \mathcal{O}_s^{(-1)} = \partial_u(\tilde{\nu}\mathcal{O}_s^{(-1)}) = 0 \ , \quad s \in \{u, \theta, j\} \ , \\ \partial_\theta \mathcal{O}_i^{(1)} = 0 \ , \quad i \in \{u, \theta\} \ , \end{aligned} \tag{4.156}$$

$$\begin{aligned} \mathcal{O}_\theta^{(1)} + \mathcal{O}_u^{(1)} &= \frac{c}{24\pi}\frac{2}{\alpha}\partial_u\left(\frac{\partial_u\tilde{\nu}}{\alpha}\right) - \frac{\bar{c}}{24\pi}\frac{1}{2\alpha}\partial_u\left(\frac{\tilde{\nu}^2\partial_u(\alpha/\tilde{\nu})}{\alpha^2}\right) \ , \\ \partial_u\mathcal{O}_u^{(1)} - \mathcal{O}_\theta^{(1)}\frac{\partial_u\tilde{\nu}}{\tilde{\nu}} &= -\frac{\bar{c}}{24\pi}\frac{\alpha}{2\tilde{\nu}\partial_u\tilde{\nu}}\partial_u\left(\left(\frac{\tilde{\nu}\partial_u\tilde{\nu}}{\alpha^2}\right)^2\partial_u(\alpha/\tilde{\nu})\right) \ , \\ \partial_u\mathcal{O}_j^{(1)} + \mathcal{O}_j^{(1)}\frac{\partial_u\tilde{\nu}}{\tilde{\nu}} &= \frac{\bar{c}}{24\pi}\frac{1}{2\tilde{\nu}}\partial_u^2\left(\frac{\tilde{\nu}\partial_u\tilde{\nu}}{\alpha^2}\right) \ . \end{aligned} \tag{4.157}$$

Hence, the decoupling limit removes all θ-dependence from the operators, effectively reducing the dynamics to one dimension. The last two equations reflect the presence of the original diffeomorphism anomaly. However, we observe that the diffeomorphism symmetry and the associated conservation law can be restored by performing the following field redefinitions:

$$\begin{aligned} \mathcal{O}_u^{\rm IR} &= \mathcal{O}_u^{(1)} - \mathcal{O}_j^{(1)} + \frac{\bar{c}}{48\pi}\frac{\tilde{\nu}}{\alpha^2}\partial_u\left(\frac{\partial_u\tilde{\nu}}{\tilde{\nu}}\right) \ , \\ \mathcal{O}_\phi^{\rm IR} &= \mathcal{O}_\Phi^{(1)} + \mathcal{O}_j^{(1)} - \frac{\bar{c}}{48\pi}\frac{\tilde{\nu}}{\alpha^2}\partial_u\left(\frac{\partial_u\tilde{\nu}}{\tilde{\nu}}\right) + \frac{\bar{c}}{48\pi}\frac{1}{\alpha}\partial_u\left(\frac{\tilde{\nu}^2}{\alpha^2}\partial_u\left(\frac{\alpha}{\tilde{\nu}}\right)\right) \ . \end{aligned} \tag{4.158}$$

These field redefinitions are induced by the following local counterterm, which can be

added to the generating functional:

$$I_{\rm CT} = -\frac{\bar{c}}{48\pi}(2\pi)\int \mathrm{d}u \frac{\tilde{\nu}}{\alpha}\partial_u\Big(\frac{\partial_u\tilde{\nu}}{\tilde{\nu}}\Big)\ , \tag{4.159}$$

As discussed in Section 4.4.1, when $c_L \neq c_R$, a diffeomorphism anomaly arises in the CFT_2, manifested through the non-conservation of the stress tensor. While the counterterm in (4.159) is not covariant under one-dimensional diffeomorphisms, its inclusion restores the invariance of the generating functional under such transformations.

In terms of these variables (4.158), the IR lapse function becomes

$$f_{\rm IR} = \frac{\alpha^2 r^2}{(\ell_3/2)^2} + 2r\frac{\alpha^2}{\tilde{\nu}}\frac{\kappa_3^2}{\ell_3}\int du\alpha(\mathcal{O}_u^{\rm IR}+\mathcal{O}_\theta^{\rm IR}) + \left(\frac{\alpha^2}{\tilde{\nu}}\frac{2\ell_3\kappa_3^2}{\Big(1+\frac{1}{\ell_3\boldsymbol{\mu}}\Big)}\mathcal{O}_u^{\rm IR} - \frac{\ell_3^2}{\Big(1+\frac{1}{\ell_3\boldsymbol{\mu}}\Big)}\frac{\partial_u\tilde{\nu}^2}{\tilde{\nu}^2}\right)\ . \tag{4.160}$$

Similarly, the IR Ward identities are given by

$$\begin{aligned} \partial_u\mathcal{O}_u^{\rm IR} - \mathcal{O}_\theta^{\rm IR}\frac{\partial_u\tilde{\nu}}{\tilde{\nu}} &= 0\ , \\ \mathcal{O}_\theta^{\rm IR}+\mathcal{O}_u^{\rm IR} &= \frac{c}{24\pi}\frac{2}{\alpha}\partial_u\left(\frac{\partial_u\tilde{\nu}}{\alpha}\right)\ . \end{aligned} \tag{4.161}$$

The operator $\mathcal{O}_j^{(1)}$ drops out of the dynamics, as it is effectively absorbed into the prescription given in (4.150), which satisfies its equation of motion (4.157). Finally, applying the decoupling limit directly to the generating functional (4.128) yields

$$\delta I^{\rm IR} = 2\pi\lambda\int du\left(\mathcal{O}_\theta^{\rm IR}\frac{\alpha}{\tilde{\nu}}\delta\tilde{\nu} + \mathcal{O}_u^{\rm IR}\delta\alpha\right) + \delta I_{\rm CT}\ . \tag{4.162}$$

To obtain this expression, we use the regularity conditions (4.153) and the change of variables (4.158). From now on, we set $\lambda = 1$, as this bookkeeping parameter will no longer play a role in the analysis that follows.

Comparison with JT gravity. We now observe that many aspects of the decoupling limit in TMG reproduce features of JT gravity discussed in Section 4.2. In particular, the lapse function in (4.160) resembles that of (4.4), and the equations of motion (4.161) are compatible with (4.12a)–(4.12b). We will now make this correspondence precise, taking into account the ambiguities encountered in Sec. 4.2.

Our first step is to identify the JT dilaton as follows:

$$\Phi - \Phi_0 = \frac{\tilde{\nu}}{l_3} r \equiv \phi \Longrightarrow \phi = \frac{\nu}{l_2} r \ , \tag{4.163}$$

where ℓ_2 and ν denote the AdS radius and the source of JT gravity, respectively. These are related to the corresponding quantities in TMG in the same manner than AdS_3 via:

$$l_2 = \frac{l_3}{2} \ , \quad \nu = \frac{\tilde{\nu}}{2} \ , \tag{4.164}$$

which is a consequence that these identifications are more geometrical in nature, and not relying on the action of a given theory. That is why the same identifications hold for AdS_3 and TMG.

With this identification, the IR lapse function $f_{\rm IR}$ from equation (4.160) can be rewritten as:

$$f_{\rm IR} = \frac{\alpha^2 r^2}{\ell_2^2} + 2r \frac{\alpha^2}{4\nu} \frac{\kappa_3^2}{\ell_2} \int \mathrm{d}u \, \alpha (\mathcal{O}_\theta^{\rm IR} + \mathcal{O}_u^{\rm IR}) + \left(\frac{\alpha^2}{\nu} \frac{2\ell_2 \kappa_3^2}{\left(1 + \frac{1}{\ell_3 \boldsymbol{\mu}}\right)} \mathcal{O}_u^{\rm IR} - \frac{4\ell_2^2}{\left(1 + \frac{1}{\ell_3 \boldsymbol{\mu}}\right)} \left(\frac{\partial_u \nu}{\nu} \right)^2 \right) \ . \tag{4.165}$$

By comparing this expression with equations (4.11) in Section 4.2, we recognize that the decoupling limit in TMG yields the identifications $\omega^2 = \gamma^{-2} = \frac{4}{\left(1 + \frac{1}{\ell_3 \boldsymbol{\mu}}\right)}$, provided we

relate the operators as:

$$\kappa_2^2\mathcal{O}_u = \frac{\kappa_3^2}{\left(1+\frac{1}{\ell_3\boldsymbol{\mu}}\right)}\mathcal{O}_u^{\rm IR}\ , \quad \kappa_2^2\mathcal{O}_\phi = \frac{\kappa_3^2}{\left(1+\frac{1}{\ell_3\boldsymbol{\mu}}\right)}\mathcal{O}_\theta^{\rm IR}\ . \tag{4.166}$$

Applying this relation to the IR generating functional $I_{\rm 3D}^{\rm IR}$ defined in (4.162), we find:

$$\delta I^{\rm IR} - \delta I_{\rm CT} = 2\pi\Big(1+\frac{1}{\ell_3\boldsymbol{\mu}}\Big)\frac{\kappa_2^2}{\kappa_3^2}\int {\rm d}u\Big(\mathcal{O}_u\,\delta\alpha + \frac{\alpha}{\nu}\mathcal{O}_\phi\,\delta\nu\Big) = \delta I_\omega\ . \tag{4.167}$$

Here we used the fact that $2\pi\left(1+\frac{1}{\ell_3\boldsymbol{\mu}}\right)\kappa_2^2/\kappa_3^2 = 1$, in accordance with the definition of the heat capacity in (4.149). We note that this relation does not follow from dimensional reduction, which would instead yield the naive estimate $2\pi\kappa_2^2/\kappa_3^2 \sim 1$. The reason behind this discrepancy is that TMG is a higher-derivative theory. For instance, to compute the black hole entropy in TMG, one must use the Wald entropy formula rather than the standard Bekenstein–Hawking formula, which holds only for two-derivative theories. Our off-shell construction of the decoupling limit properly captures this subtlety.

Thus, for TMG, we obtain the following mapping:

$$I_{\rm JT} = I_\omega + (1-\omega^2)\frac{\ell_2}{2\kappa_2}\int du\sqrt{-h_b}\nu^{-1}h_b^{-1}(\partial_u\nu)^2\ , \quad \omega^2 = \frac{4}{\left(1+\frac{1}{\ell_3\boldsymbol{\mu}}\right)}\ . \tag{4.168}$$

From this point, the Schwarzian action can be derived via the canonical transformation given in (4.79). In conclusion, we have recovered the Schwarzian dynamics as the outcome of our off-shell construction of the decoupling limit.

In nAdS$_2$/nCFT$_1$, the normalized heat capacity is given by $C_H = \frac{1}{\kappa_2}$, which, according to our mapping, corresponds to $C_H = \frac{c_L}{6\ell_3}$. Therefore, the dynamics of JT gravity is controlled solely by the left-movers, while the right-movers are frozen in the near-extremal regime [183]. Our off-shell construction of the decoupling limit reproduces this feature

without issue, highlighting its flexibility in accommodating different UV parent theories underlying the IR Schwarzian dynamics.

4.5 Near-extremality at the boundary of AdS_4/CFT_3

In this section, we introduce a novel construction of the decoupling limit within the AdS_4/CFT_3 correspondence, where we can track how the near-extremal dynamics is imprinted on the UV data on both the gravitational and CFT sides by matching the appropriate phase spaces in the IR and UV. The gravitational analysis will be done for Einstein-Maxwell theory with a negative cosmological constant, and the reduced phase space we construct is a non-trivial gravitational dressing around the Reissner-Nordström AdS_4 black hole. On the CFT_3, this corresponds to a configuration with a non-trivial stress tensor and a $U(1)$ current placed on a curved manifold of topology $\mathbb{R} \times M_2$.

Nevertheless, the situation in this section is substantially more intricate relative to AdS_3/CFT_2. First, unlike in two-dimensional CFTs, in three dimensions, there are no anomalies. This makes a possible connection with the Schwarzian dynamics more elusive. We will address this by making contact with the counterterm ambiguity discussed in Sec. 4.2.4.

Second, on the gravity side, the presence of local degrees of freedom prevents the complete characterization of solutions in the Einstein equations with a fixed boundary metric. To address this challenge, we focus on a specific subsector of Einstein-Maxwell theory with a negative cosmological constant: a generalization of the Robinson-Trautman (RT) family of algebraically special solutions originally discovered in [194]. RT solutions have gained attention in holography [195, 196, 197, 198, 199, 200], particularly in studies of out-of-equilibrium physics in AdS/CFT correspondence, and their corresponding flat limit has been discussed in [201]. Further recent investigations into different aspects of

RT solutions include [202, 203, 204, 205].

4.5.1 CFT$_3$ Ward identities on curved backgrounds

In this portion, we will characterize the Ward identities of a three-dimensional CFT that possesses a $U(1)$ global symmetry. The relevant currents in this case are the stress tensor, T^{ab}, and a U(1) current, J^a. If we place the theory on a curved background and turn on a background gauge field, we can read off these currents through the variation of the generating function $I[g, \mathcal{A}]$ with respect to the corresponding source, namely

$$\delta I = \int \mathrm{d}^3x\sqrt{-g}\Big(\frac{1}{2}T^{ab}\delta g_{ab} + J^b\delta\mathcal{A}_b\Big) \ . \tag{4.169}$$

The Ward identities that these operators satisfy follow from the invariance of $I[g, \mathcal{A}]$ under diffeomorphisms, U(1) gauge, and local Weyl transformations of the background sources. Respectively, they take the form

$$\nabla_a T^{ab} + J_a\mathcal{F}^{ab} = 0 \ , \quad \nabla_b J^b = 0 \ , \quad T^a_a = 0 \ , \tag{4.170}$$

where $\mathcal{F} = d\mathcal{A}$. A key difference between the two-dimensional CFTs discussed above is that there is no possibility of a Weyl or gravitational anomaly in this case.

We will place the CFT on a curved background g of the form $\mathbb{R} \times M_2$ and turn on a background gauge field $\mathcal{A}_a$. We will parametrize the metric as

$$ds^2_{\text{3D}} = -\alpha^2\mathrm{d}u^2 + 2\nu^2 e^{2\chi}\mathrm{d}z\mathrm{d}\bar{z} \ , \tag{4.171}$$

where $\alpha = \alpha(u)$, $\nu = \nu(u)$ depend only on the time u, while $\chi = \chi(u, z, \bar{z})$ depends on

all three coordinates. The background gauge field is

$$\mathcal{A} = \mu\,\mathrm{d}u + \mathcal{A}_z \mathrm{d}z + \mathcal{A}_{\bar{z}}\mathrm{d}\bar{z}\ , \tag{4.172}$$

where $\mu = \mu(u)$ and the spatial components are arbitrary for now. This shares various features of the two-dimensional background in (4.81). The components α and ν will play the same role as in two dimensions: α acts as time dilation, while ν is a Weyl factor for M_2. However, now the angular potential is traded for chemical potential, hence, μ here enters as a component of the background gauge field. The geometry of M_2, i.e., $2e^{2\chi}\mathrm{d}z\mathrm{d}\bar{z}$, will be held fixed.

On this background, we decompose the stress tensor and current such that their components are tied directly to the appropriate sources we have introduced: (α, ν, μ). Thus, we have

$$\begin{aligned} T_{uu} &= -\frac{\alpha^2}{\nu^2}\mathcal{O}_u^{\text{3D}}\ , \quad T_{z\bar{z}} = \frac{1}{2}\mathcal{O}_{z\bar{z}}^{\text{3D}} e^{2\chi}\ , \\ T_{uz} &= \frac{\alpha}{\nu^2} t_{uz}\ , \quad T_{zz} = \frac{1}{\alpha} t_{zz}\ , \end{aligned} \tag{4.173}$$

plus the appropriate barred components. Here, $\mathcal{O}_u^{\text{3D}} = \mathcal{O}_u^{\text{3D}}(u, z, \bar{z})$, and $\mathcal{O}_{z\bar{z}}^{\text{3D}} = \mathcal{O}_{z\bar{z}}^{\text{3D}}(u, z, \bar{z})$. The components t_{uz} and t_{zz} (and barred components) also depend on the local coordinates, however, they will not be treated as dynamical operators. As we will see in the AdS_4 construction, these components are sourced by the curvature of the background (4.171). The $U(1)$ current is decomposed as

$$J = -\frac{\alpha}{\nu}\mathcal{O}_e^{\text{3D}}\mathrm{d}u + \frac{j_z}{\alpha}\mathrm{d}z + \frac{j_{\bar{z}}}{\alpha}\mathrm{d}\bar{z}\ , \tag{4.174}$$

where $\mathcal{O}_e^{\text{3D}} = \mathcal{O}_e^{\text{3D}}(u, z, \bar{z})$ controls the electric charge carried by the current, and the spatial components j_z also depend on $(u, z, \bar{z})$. In this notation, turning on a magnetic

charge corresponds to setting

$$\mathcal{F}_{z\bar{z}} = \nu e^{2\chi}\mathcal{O}_m^{\text{3D}} \ . \tag{4.175}$$

In this way, the variation of the generating function is given by paring the sources with their respective operators[13]

$$\delta I = \int \mathrm{d}^3x \left(e^{2\chi}\left(\mathcal{O}_{z\bar{z}}^{\text{3D}} \frac{\alpha}{\nu}\delta\nu + \mathcal{O}_u^{\text{3D}}\delta\alpha + \mathcal{O}_e^{\text{3D}}\nu\delta\mu \right) + j_z\delta\mathcal{A}_{\bar{z}} + j_{\bar{z}}\delta\mathcal{A}_z \right) \ . \tag{4.176}$$

Finally, with this notation, the Ward identities (4.170) take the form

$$\begin{aligned} \partial_u(e^{2\chi}\mathcal{O}_u^{\text{3D}}) - \frac{1}{2\nu^2}\partial_u(\nu^2 e^{2\chi})\mathcal{O}_{z\bar{z}}^{\text{3D}} &= \frac{1}{\alpha}(\mathcal{F}_{uz}j_{\bar{z}} + \mathcal{F}_{u\bar{z}}j_z) - \frac{\alpha}{\nu^2}(\partial_{\bar{z}}t_{uz} + \partial_z t_{u\bar{z}}) \ , \\ \partial_z\mathcal{O}_{z\bar{z}}^{\text{3D}} + 2\frac{\nu}{\alpha}\mathcal{F}_{uz}\mathcal{O}_e^{\text{3D}} &= \frac{2}{\alpha}e^{-2\chi}\left(\mathcal{F}_{z\bar{z}}j_z - \partial_{\bar{z}}t_{zz} + \partial_u(e^{2\chi}t_{uz}) \right) \ , \\ \partial_{\bar{z}}\mathcal{O}_{z\bar{z}}^{\text{3D}} + 2\frac{\nu}{\alpha}\mathcal{F}_{u\bar{z}}\mathcal{O}_e^{\text{3D}} &= \frac{2}{\alpha}e^{-2\chi}\left(\mathcal{F}_{\bar{z}z}j_{\bar{z}} - \partial_z t_{\bar{z}\bar{z}} + \partial_u(e^{2\chi}t_{u\bar{z}}) \right) \ , \end{aligned} \tag{4.177}$$

which correspond to the conservation equation of the stress tensor, while the $U(1)$ conservation and trace conditions give

$$\partial_u(\nu e^{2\chi}\mathcal{O}_e^{\text{3D}}) = -\partial_z j_{\bar{z}} - \partial_{\bar{z}}j_z \ , \tag{4.178}$$

and

$$\mathcal{O}_u^{\text{3D}} + \mathcal{O}_{z\bar{z}}^{\text{3D}} = 0 \ . \tag{4.179}$$

4.5.2 Generalised Robinson-Trautman phase space

In this section we will construct a reduced phase space in AdS_4 which has the operators $\mathcal{O}_u^{\text{3D}}$, $\mathcal{O}_{z\bar{z}}^{\text{3D}}$, $\mathcal{O}_e^{\text{3D}}$ turned on, and carries also the sources (α, ν, μ). The simplest gravitational

[13] The components T_{uz} and T_{zz} are inert in our discussion. In particular, we are not turning on sources in the background metric for those components. This is motivated by the step up we will have in AdS_4, however, appropriate modifications to turn on those sources are straightforward.

theory that contains these ingredients is a four-dimensional Maxwell-Einstein theory with a negative cosmological constant, where our conventions are

$$S = \frac{1}{2\kappa_4^2}\int \mathrm{d}^4x\sqrt{-g}\,(R-2\Lambda) - \frac{1}{4}\int \mathrm{d}^4x\sqrt{-g}F^2 \ , \tag{4.180}$$

with $\Lambda = -3/\ell_4^2$ and $\kappa_4^2 = 8\pi G_4$. A useful way to construct the phase space is to consider a generalisation of Robinson-Trautman (RT) solutions of this theory. The RT family of algebraically special solutions describes spacetimes with a null geodesic congruence that has vanishing shear and rotation but nonzero expansion [194]. These solutions exactly satisfy the radial component of the Einstein equations, while the transverse dynamics follow a Calabi flow [196]. The extension of the RT solutions to include a negative cosmological constant and electric/magnetic charges was found [206]. Here, we generalise RT solutions such that the three-dimensional metric (4.171) matches the boundary metric of the bulk spacetime. We will also make sure that the equations of motion of the four-dimensional Maxwell-Einstein theory are identified with CFT_3 Ward identities (4.177). In particular, the traceless condition of the boundary stress tensor will correspond to an equation of motion, which is a new feature in our construction.

We will work in a Bondi-like gauge, where we have

$$ds^2_{\text{4D}} = -f(x)\mathrm{d}u^2 - 2\alpha(u)\big(1+B(x)\big)\mathrm{d}u\mathrm{d}r + 2\Phi^2(u,r)\big(1+B(x)\big)e^{2\chi}\mathrm{d}z\mathrm{d}\bar{z} \ . \tag{4.181}$$

Similar to AdS_3 cases in previous sections, the scalar Φ controls the size of the transverse manifold with metric $2e^{2\chi}\mathrm{d}z\mathrm{d}\bar{z}$ and chosen to be

$$\Phi(u,r) = \nu(u)\frac{r}{\ell_4} + \Phi_0 \ , \tag{4.182}$$

where Φ_0 is constant. The field strength components are

$$\begin{aligned} F_{ur} &= -\frac{\alpha\nu(\mathcal{O}_q^{3D}+\mathcal{O}_{\bar{q}}^{3D})}{\Phi^2} \ , \quad F_{z\bar{z}} = \nu e^{2\chi}(\mathcal{O}_q^{3D}-\mathcal{O}_{\bar{q}}^{3D}) \ , \\ F_{uz} &= j_z + \frac{\ell_4\alpha}{\Phi}\partial_z\mathcal{O}_q^{3D} \ , \quad F_{u\bar{z}} = j_{\bar{z}} + \frac{\ell_4\alpha}{\Phi}\partial_{\bar{z}}\mathcal{O}_{\bar{q}}^{3D} \ , \end{aligned} \tag{4.183}$$

with $\mathcal{O}_q^{3D} = \mathcal{O}_q^{3D}(u,z)$, $\mathcal{O}_{\bar{q}}^{3D} = \mathcal{O}_{\bar{q}}^{3D}(u,\bar{z})$, while we have j_z and $j_{\bar{z}}$ functions of $(u,z,\bar{z})$. In the following, we will show how the bulk equations of motion translate to Ward identities in the CFT_3.

The dynamics of the gauge field are the simplest to analyze first. Imposing the Bianchi identity and Maxwell's equations on the background (4.181)-(4.183) gives

$$\begin{aligned} \partial_u\left(\nu e^{2\chi}\mathcal{O}_q^{3D}\right) &= -\partial_{\bar{z}} j_z \ , \\ \partial_u\left(\nu e^{2\chi}\mathcal{O}_{\bar{q}}^{3D}\right) &= -\partial_z j_{\bar{z}} \ . \end{aligned} \tag{4.184}$$

From the perspective of the CFT_3, the appropriate map of the bulk variables to the boundary is

$$\mathcal{O}_e^{3D} = \mathcal{O}_q^{3D} + \mathcal{O}_{\bar{q}}^{3D} \ , \qquad \mathcal{O}_m^{3D} = \mathcal{O}_q^{3D} - \mathcal{O}_{\bar{q}}^{3D} \ , \tag{4.185}$$

and also have the boundary background field strength is

$$\mathcal{F}_{z\bar{z}} = \nu e^{2\chi}(\mathcal{O}_q^{3D}-\mathcal{O}_{\bar{q}}^{3D}) \ , \quad \mathcal{F}_{uz} = j_z \ , \quad \mathcal{F}_{u\bar{z}} = j_{\bar{z}} \ . \tag{4.186}$$

With this, it is clear that the bulk equations (4.184) map to the Ward identity (4.178).

Imposing the Einstein equation is more involved. We will first solve for the radial profile of the metric functions. Based on the form of the RT solutions, an appropriate

decomposition of the metric function $f(x)$ and $B(x)$ in (4.181) is

$$\begin{aligned} f(x) &= \frac{\alpha^2}{\nu^2}\Phi^2 + 2\ell_4\frac{\alpha}{\nu}\left(\partial_u\Phi + \Phi\partial_u\chi\right) - \frac{\ell_4^2\alpha^2}{\nu^2}\Delta\chi + \frac{f_{-1}(u,z,\bar{z})}{\Phi} + \frac{f_{-2}(u,z,\bar{z})}{\Phi^2} \ , \\ B(x) &= \frac{f_{-3}(u,z,\bar{z})}{\Phi^3} \ , \end{aligned} \tag{4.187}$$

where $\Delta = 2e^{-2\chi}\partial_z\partial_{\bar{z}}$. The functions $f_i(u,z,\bar{z})$ are related to the one-point function of the boundary stress tensor and $U(1)$ current. With respect to the notation in (4.176), and with some hindsight, we write

$$\begin{aligned} f_{-1}(u,z,\bar{z}) &= \frac{1}{2}\ell_4\kappa_4^2\frac{\alpha^2}{\nu}(\mathcal{O}_u^{3\text{D}} - \mathcal{O}_{z\bar{z}}^{3\text{D}}) + \frac{1}{12}\ell_4\kappa_4^2\frac{\alpha^2}{\nu}(\mathcal{O}_u^{3\text{D}} + \mathcal{O}_{z\bar{z}}^{3\text{D}}) \ , \\ f_{-2}(u,z,\bar{z}) &= 2\ell_4^2\kappa_4^2\alpha^2\mathcal{O}_q^{3\text{D}}\mathcal{O}_{\bar{q}}^{3\text{D}} \ , \\ f_{-3}(u,z,\bar{z}) &= -\frac{1}{12}\ell_4^2\kappa_4^2\nu(\mathcal{O}_u^{3\text{D}} + \mathcal{O}_{z\bar{z}}^{3\text{D}}) \ , \end{aligned} \tag{4.188}$$

which controls the boundary value of T_{uu} and $T_{z\bar{z}}$, and currents. In addition, this background also ignites the following boundary components,

$$t_{uz} = -\frac{\ell_4^2}{2\kappa_4^2}\partial_z\Delta\chi \ , \quad t_{zz} = \frac{\ell_4^2}{\kappa_4^2}\partial_u(e^{\chi}\partial_z^2(e^{-\chi})) \ , \tag{4.189}$$

and the appropriate barred version. With this, the Einstein's equations of motion imply

$$\begin{aligned} e^{-3\chi}\partial_u\left(e^{3\chi}\mathcal{O}_u^{3\text{D}}\right) + \mathcal{O}_u^{3\text{D}}\frac{\partial_u\nu}{\nu} &= \frac{\alpha}{\nu^2}\frac{\ell_4^2}{2\kappa_4^2}\Delta^2\chi + \frac{2}{\alpha}e^{-2\chi}j_z j_{\bar{z}} \ , \\ \partial_z\mathcal{O}_u^{3\text{D}} - 4\frac{\nu}{\alpha}\mathcal{O}_{\bar{q}}^{3\text{D}}j_z &= 0 \\ \partial_{\bar{z}}\mathcal{O}_u^{3\text{D}} - 4\frac{\nu}{\alpha}\mathcal{O}_q^{3\text{D}}j_{\bar{z}} &= 0 \\ \mathcal{O}_u^{3\text{D}} + \mathcal{O}_{z\bar{z}}^{3\text{D}} &= 0 \ . \end{aligned} \tag{4.190}$$

Using (4.185), (4.186) and (4.189), we identify these equations with the Ward identities

(4.177) and (4.179). Note that these equations also imply that

$$\partial_{\bar{z}}\left(\mathcal{O}_{\bar{q}}^{3\mathrm{D}} j_z\right) = \partial_z\left(\mathcal{O}_{q}^{3\mathrm{D}} j_{\bar{z}}\right) \ . \tag{4.191}$$

This is an additional restriction on the j_z and $j_{\bar{z}}$ that support this background, which arises as an integrability condition on $\mathcal{O}_u^{3\mathrm{D}}$.

The family of solutions constructed here represents a subset of the most general phase space of the CFT_3, as it can be viewed from the specificity in (4.185), (4.186), (4.189) and (4.191). Some of these choices have a natural interpretation. The boundary stress tensor dual to the RT spacetimes can be decomposed as [195]

$$T_{ab} = T_{ab}^{PF} + Z_{ab} \ , \tag{4.192}$$

where T_{ab}^{PF} is the perfect fluid stress tensor

$$T_{ab}^{PF} = p(g_{ab} + U_a U_b) + \epsilon U_a U_b \tag{4.193}$$

Here, $U = \alpha du$ is a time-like vector, while the density energy ϵ and pressure p are given respectively

$$\epsilon = -\frac{\mathcal{O}_u^{3\mathrm{D}}}{\nu^2} \ , \qquad p = \frac{\mathcal{O}_{z\bar{z}}^{3\mathrm{D}}}{2\nu^2} \ . \tag{4.194}$$

The conformal equation of state, $\epsilon = 2p$, is satisfied, reflecting the traceless stress tensor of a CFT_3. The symmetric tensor Z_{ab} is defined as

$$Z_{ab} \equiv \frac{\ell_4^2}{\kappa_4^2}(\delta_a^d - U_a U^d) C_{dbc} U^c \ . \tag{4.195}$$

In this expression, C_{abc} is the Cotton tensor associated with the boundary background

metric g_{ab}. This reproduces the components (4.189).[14] The presence of a nonzero Cotton tensor C_{abc} has been argued to encode gravitational radiation in the CFT_3 [207], in addition to the electromagnetic radiation captured by the U(1) current J given in (4.174). Furthermore, a nonzero Cotton tensor C_{abc} can also be interpreted as a measure of the deviation of spacetime from conformal flatness [195].

Vector potential in RT: We have postponed the discussion of the vector potential A, defined via $F = dA$, since its treatment in this phase space is particularly subtle. The electromagnetic field given in (4.184) does not trivially satisfy the Bianchi identity. As a result, the equations in (4.184) must be understood as linear combinations of the Maxwell equation $\nabla_\mu F^{\mu\nu} = 0$ and Bianchi identity $\nabla_\mu \tilde{F}^{\mu\nu} = 0$. This means that constructing an explicit expression for the vector potential A requires invoking one of the equations of motion, which is somewhat unsatisfactory. Nevertheless, we choose to express A as follows:

$$A(x) = \left[-\frac{(\mathcal{O}_q^{\text{3D}} + \mathcal{O}_{\bar{q}}^{\text{3D}})\ell_4 \alpha}{\Phi} + \mu \right] \mathrm{d}u + \Big(- \int \mathrm{d}\bar{z} \nu e^{2\chi} \mathcal{O}_q^{\text{3D}} \Big) \mathrm{d}z + \Big(- \int \mathrm{d}z \nu e^{2\chi} \mathcal{O}_{\bar{q}}^{\text{3D}} \Big) \mathrm{d}\bar{z} \ . \tag{4.196}$$

Here, $\mu = \mu(u)$ is the dual source for the electric charge operator $\mathcal{O}_e^{\text{3D}} = \mathcal{O}_q^{\text{3D}} + \mathcal{O}_{\bar{q}}^{\text{3D}}$. In this expression for A, the magnetic charge operator $\mathcal{O}_m^{\text{3D}} = \mathcal{O}_q^{\text{3D}} - \mathcal{O}_{\bar{q}}^{\text{3D}}$ does not appear explicitly. We emphasize that this subtlety is well known in the literature on Robinson–Trautman spacetimes and is entirely unrelated to our generalization of this phase space.

[14] It is important to note that the combination $(\delta_a^d - U_a U^d)$ does not act as a projector orthogonal to U^a due to its relative "wrong" sign.

AdS Reissner-Nordström black hole

In this portion, we will describe the dyonic AdS_4 Reissner-Nordstrom black holes using the Bondi-like gauge introduced above. The metric is given by

$$ds^2 = -f(r)\mathrm{d}u^2 - 2\mathrm{d}u\mathrm{d}r + \frac{4r^2}{(1+z\bar{z})^2}\mathrm{d}z\mathrm{d}\bar{z} \ , \tag{4.197}$$

where the blackening factor is

$$f(r) = \frac{r^2}{\ell_4^2} + 1 - \frac{2MG_4}{r} + \frac{(Q^2+P^2)G_4}{4\pi r^2} \ , \tag{4.198}$$

and the gauge field reads

$$A = \left(-\frac{1}{4\pi}\frac{Q}{r} + \mu_0\right)\mathrm{d}u + \frac{P}{4\pi}\left(\frac{\mathrm{d}z}{z} - \frac{\mathrm{d}\bar{z}}{\bar{z}}\right)\frac{i}{(1+z\bar{z})} \ . \tag{4.199}$$

The factor of $\frac{1}{4\pi}$ in front charges comes from our conventions for the Einstein-Maxwell action (4.180). In relation to the above notation, here we have set $\alpha = 1$, $\nu = \ell_4$ and $\Phi_0 = 0$, which gives $\Phi = r$. The metric on M_2 is set to

$$2e^{2\chi}\mathrm{d}z\mathrm{d}\bar{z} = \frac{4}{(1+z\bar{z})^2}\mathrm{d}z\mathrm{d}\bar{z} \ , \tag{4.200}$$

which describes a round 2-sphere, and $j_z = j_{\bar{z}} = 0$. The one-point functions are

$$\begin{aligned} \mathcal{O}_u^{\text{3D}} &= -\mathcal{O}_{z\bar{z}}^{\text{3D}} = -\frac{M}{4\pi} \ , \\ \mathcal{O}_q^{\text{3D}} &= \frac{1}{8\pi\ell_4}(Q+iP) \ , \\ \mathcal{O}_{\bar{q}}^{\text{3D}} &= \frac{1}{8\pi\ell_4}(Q-iP) \ . \end{aligned} \tag{4.201}$$

In order to describe the thermodynamics in a simple manner, we rewrite the blackening factor in terms of its roots, i.e.,

$$f(r) = \frac{1}{r^2\ell_4^2}(r - r_+)(r - r_-)(r + r_1)(r + r_2) \ , \tag{4.202}$$

where r_1 and r_2 are defined through the following relations

$$r_1 + r_2 = r_+ + r_-, \quad r_1 r_2 = \ell_4^2 + r_+^2 + r_-^2 + r_- r_+ \ . \tag{4.203}$$

Here, r_+ is the outer horizon, and r_- the inner horizon; $r_{1,2}$ are unphysical roots of $f(r)$. In terms of $r_\pm$, the mass M, and charges Q, P are

$$\begin{aligned} MG_4 &= \frac{(r_+ + r_-)}{2}\left(1 + \frac{(r_+^2 + r_-^2)}{\ell_4^2}\right) \ , \\ (Q^2 + P^2)\frac{G_4}{4\pi} &= r_+ r_- \left(1 + \frac{(r_+^2 + r_-^2 + r_- r_+)}{\ell_4^2}\right) \ . \end{aligned} \tag{4.204}$$

The Hawking temperature T, and black hole entropy S are given by

$$\begin{aligned} T &= \frac{(r_+ - r_-)}{4\pi}\frac{(\ell_4^2 + 3r_+^2 + r_-^2 + 2r_- r_+)}{\ell_4^2 r_+^2} \ , \\ S &= \frac{\pi r_+^2}{G_4} \ . \end{aligned} \tag{4.205}$$

The electric potential μ_e and magnetic potential μ_m are controlled by the gauge field (4.199). Demanding regularity at the horizon sets

$$\mu_e = \frac{Q}{4\pi r_+} \ , \quad \mu_m = \frac{P}{4\pi r_+} \ . \tag{4.206}$$

With this, we have the standard first law: $dM = TdS + \mu_e dQ + \mu_m dP$.

Near-extremal Thermodynamics: At extremality, $r_+ = r_- = r_0$, the mass and charges satisfy the constraint

$$G_4 M_0 = r_0 \left(1 + \frac{2r_0^2}{\ell_4^2}\right) , \quad \frac{(P_0^2 + Q_0^2)G_4}{4\pi} = r_0^2 \left(1 + \frac{3r_0^2}{\ell_4^2}\right) . \tag{4.207}$$

At zero temperature, the Smarr law relates the extremal mass M_0 and charges Q_0, P_0 as follows[15]

$$M_0 - (\mu_{e,0} Q_0 + \mu_{m,0} P_0) = -\frac{8\pi}{\kappa_4^2} \frac{r_0^3}{\ell_4^2} . \tag{4.208}$$

This expression will play an important role in the subsequent discussion. Finally, the extremality conditions (4.207) written in terms of CFT_3 variables are

$$\mathcal{O}_u^{\text{3D},*} = -\frac{2r_0}{\kappa_4^2} \left(1 + \frac{2r_0^2}{\ell_4^2}\right) , \quad \mathcal{O}_q^{\text{3D},*} \mathcal{O}_{\bar{q}}^{\text{3D},*} = \frac{r_0^2}{2\kappa_4^2 \ell_4^2} \left(1 + \frac{3r_0^2}{\ell_4^2}\right) . \tag{4.209}$$

To study the low-temperature regime, we expand linearly around the extremality as $r_\pm = r_0 \pm \delta r$ at fixed P_0 and Q_0, giving [208]

$$T = \frac{\delta r}{2\pi \ell_2^2} , \quad \ell_2^2 = \frac{\ell_4^2 r_0^2}{6r_0^2 + \ell_4^2} . \tag{4.210}$$

Here, we recognize the effective AdS_2 as ℓ_2 given by the expression above. The linear response in energy ΔM and entropy ΔS are

$$\Delta M = 2\pi^2 \ell_2^2 \left(\frac{8\pi r_0}{\kappa_4^2}\right) T^2 , \quad \Delta S = 4\pi^2 \ell_2^2 \left(\frac{8\pi r_0}{\kappa_4^2}\right) T . \tag{4.211}$$

From here, we recognize the normalized heat capacity C_H as

$$C_H = \frac{8\pi r_0}{\kappa_4^2} = \frac{1}{\kappa_2^2} . \tag{4.212}$$

[15] For a recent analysis of the Smarr law in the context of the AdS/CFT correspondence, see [52].

4.5.3 Off-shell decoupling limit

We now proceed to implement the decoupling limit for the Robinson–Trautman phase space described in Section 4.5.2. The procedure closely parallels the cases discussed in previous sections. To ensure control over the decoupling limit, we require that the operators $\mathcal{O}_q^{\text{3D}}$ and $\mathcal{O}_{\bar{q}}^{\text{3D}}$ remain finite in the limit $\lambda \to 0$. The conservation of the $U(1)$ current can be expressed as: $\partial_u \left(e^{2\chi}\nu\mathcal{O}_q^{\text{3D}}\right) = -\partial_{\bar{z}} j_z$. From this, we deduce that the operators $\mathcal{O}_q^{\text{3D}}$ and $\mathcal{O}_{\bar{q}}^{\text{3D}}$ must scale as

$$\mathcal{O}_q^{\text{3D}} = \frac{\mathcal{O}_q^{(-1)}}{\lambda} \ , \quad \mathcal{O}_{\bar{q}}^{\text{3D}} = \frac{\mathcal{O}_{\bar{q}}^{(-1)}}{\lambda} \ , \tag{4.213}$$

with $\mathcal{O}_q^{(-1)}$ and $\mathcal{O}_{\bar{q}}^{(-1)}$ held fixed. This also implies that j_z is a holomorphic function, completely independent of the decoupling parameter λ.

The defining feature of the decoupling limit is to scale

$$\nu = \lambda\tilde{\nu} \ , \qquad \lambda \to 0 \ , \tag{4.214}$$

while keeping $\tilde{\nu}$ fixed, along with the scaling in (4.213). As in previous cases, this procedure introduces divergences into the geometry, so we expand the remaining operators as

$$\mathcal{O}_i^{\text{3D}} = \frac{\mathcal{O}_i^{(-1)}}{\lambda} + \mathcal{O}_i^{(0)} + \mathcal{O}_i^{(1)}\lambda + \mathcal{O}_i^{(2)}\lambda^2 + ..., \qquad i \in (u, z\bar{z}) \ . \tag{4.215}$$

We note that the expansion of $\mathcal{O}_i^{\text{3D}}$ starts at order $1/\lambda$, as inferred from dimensional analysis of the line element (4.181)–(4.187). Imposing regularity of the lapse function

$f(x)$ in equation (4.187) as $\lambda \to 0$ yields the constraints

$$\begin{aligned} \mathcal{O}_q^{(-1)}\mathcal{O}_{\bar{q}}^{(-1)} &= \frac{3\Phi_0^4}{2\ell_4^2\kappa_4^2\tilde{\nu}^2} - \frac{\Phi_0^2}{2\kappa_4^2\tilde{\nu}^2}\Delta\chi \ , \\ \mathcal{O}_u^{(-1)} = -\mathcal{O}_{z\bar{z}}^{(-1)} &= -\frac{4\Phi_0^3}{\ell_4\kappa_4^2\tilde{\nu}} + \frac{2\ell_4\Phi_0}{\kappa_4^2\tilde{\nu}}\Delta\chi \ , \\ \mathcal{O}_u^{(0)} = -\mathcal{O}_{z\bar{z}}^{(0)} &= -\frac{2\Phi_0^2}{\kappa_4^2\alpha}\partial_u\chi \ . \end{aligned} \tag{4.216}$$

To ensure regularity of the vector potential $A(x)$ from equation (4.196), we must, in addition to (4.216), implement the shift

$$\mu = \tilde{\mu} + \frac{1}{\lambda}\frac{\ell_4\alpha(\mathcal{O}_q^{(-1)} + \mathcal{O}_{\bar{q}}^{(-1)})}{\Phi_0} \tag{4.217}$$

With the redefinitions (4.214)–(4.217) and in the limit $\lambda \to 0$, where $(\tilde{\nu}, \tilde{\mu}, \alpha)$, Φ_0, and $\mathcal{O}_i^{\text{3D}}$ are kept fixed, the line element (4.181) remains smooth and well-defined. In particular, we find the following IR expressions for the lapse function and the vector potential:

$$\begin{aligned} f_{\text{IR}}(x) &:= \lim_{\lambda\to 0} f(x) \\ &= \frac{\alpha^2 r^2}{\left(\frac{\ell_4^2\Phi_0^2}{6\Phi_0^2 - \ell_4^2\Delta\chi}\right)} + 2r\left(2\alpha\partial_u\chi + \frac{\alpha\partial_u\tilde{\nu}}{\tilde{\nu}}\right) + \frac{\ell_4\kappa_4^2(\mathcal{O}_u^{(1)} - \mathcal{O}_{z\bar{z}}^{(1)})\alpha^2}{2\Phi_0\tilde{\nu}} \ . \end{aligned} \tag{4.218}$$

$$\begin{aligned} A_{\text{IR}}(x) &:= \lim_{\lambda\to 0} A(x) \\ &= \left[\frac{(\mathcal{O}_q^{(-1)} + \mathcal{O}_{\bar{q}}^{(-1)})\alpha\tilde{\nu}r}{\Phi_0^2} + \tilde{\mu}\right] du + \Big(-\int \mathrm{d}\bar{z}\tilde{\nu}e^{2\chi}\mathcal{O}_q^{(-1))}\Big)\mathrm{d}z + \Big(-\int \mathrm{d}z\tilde{\nu}e^{2\chi}\mathcal{O}_{\bar{q}}^{(-1))}\Big)\mathrm{d}\bar{z} \ . \end{aligned} \tag{4.219}$$

In contrast to the lower-dimensional examples discussed previously, the resulting geometry exhibits a more intricate dependence on the transverse coordinates z and $\bar{z}$. We emphasize once again that this decoupling limit is entirely off-shell in directions transverse to the radial coordinate, as we have not imposed the equations of motion (4.190).

Applying the decoupling limit to the equations of motion (4.190) yields the following set of equations:

$$\begin{aligned} \Delta^2\chi &= 0 \ , \\ e^{-3\chi}\partial_u(e^{3\chi}\mathcal{O}_u^{(-1,1)}) - \mathcal{O}_{z\bar{z}}^{(-1,1)}\frac{\partial_u\tilde{\nu}}{\tilde{\nu}} &= 0 \ , \\ e^{-3\chi}\partial_u(e^{3\chi}\mathcal{O}_u^{(0)}) - \mathcal{O}_{z\bar{z}}^{(0)}\frac{\partial_u\tilde{\nu}}{\tilde{\nu}} &= e^{-2\chi}\frac{2}{\alpha}j_z j_{\bar{z}} \ , \\ \partial_z\mathcal{O}_u^{(-1,1)} = 0, \quad \partial_z\mathcal{O}_u^{(0)} &= 4\mathcal{O}_{\bar{q}}^{(-1)}j_z\frac{\tilde{\nu}}{\alpha} \ . \end{aligned} \tag{4.220}$$

Requiring consistency between these equations and the regularity conditions (4.216) imposes additional constraints.[16]

$$\begin{aligned} \mathcal{O}_u^{(0)}(u,z,\bar{z}) = j_z = j_{\bar{z}} = \partial_u\chi &= 0 \ , \\ \chi &= \log\left(\frac{\sqrt{2}}{1+z\bar{z}}\right) \ . \end{aligned} \tag{4.221}$$

With these simplifications, the regularity conditions (4.216) reduce to:

$$\begin{aligned} \mathcal{O}_q^{(-1)}\mathcal{O}_{\bar{q}}^{(-1)} &= \frac{\Phi_0^2}{2\kappa_4^2\tilde{\nu}^2}\left(1+\frac{3\Phi_0^2}{\ell_4^2}\right) \ , \\ \mathcal{O}_u^{(-1)} &= -\frac{2\Phi_0}{\kappa_4^2}\frac{\ell_4}{\tilde{\nu}}\left(1+\frac{2\Phi_0^2}{\ell_4^2}\right) \ , \end{aligned} \tag{4.222}$$

which match the extremality conditions obtained from thermodynamics in (4.209) upon identifying $\tilde{\nu} = \ell_4$ and $\Phi_0 = r_0$.

Similarly, the lapse function $f_{\rm IR}$ and vector potential $A_{\rm IR}$ simplify to:

$$f_{\rm IR} = \frac{\alpha^2 r^2}{\left(\frac{\ell_4^2\Phi_0^2}{6\Phi_0^2+\ell_4^2}\right)} + 2r\frac{\alpha\partial_u\tilde{\nu}}{\tilde{\nu}} + \frac{\ell_4\kappa_4^2(\mathcal{O}_u^{(1)} - \mathcal{O}_{z\bar{z}}^{(1)})\alpha^2}{2\Phi_0\tilde{\nu}} \ , \tag{4.223}$$

[16] To solve the Laplace equation, we assume a trivial topology for the transverse space. This excludes accelerating AdS black holes, which are also valid solutions in AdS Robinson–Trautman spacetimes [202].

$$A_{\rm IR} = \left[\frac{(\mathcal{O}_q^{(-1)} + \mathcal{O}_{\bar{q}}^{(-1)})\alpha\tilde{\nu}r}{\Phi_0^2} + \tilde{\mu}\right] du + \frac{\tilde{\nu}(\mathcal{O}_q^{(-1)} - \mathcal{O}_{\bar{q}}^{(-1)})i}{(1+z\bar{z})}\left(\frac{dz}{z} - \frac{d\bar{z}}{\bar{z}}\right) . \tag{4.224}$$

In these expressions, all dependence on z and $\bar{z}$ has disappeared. To obtain the simplified form of the gauge field $A_{\rm IR}$, a gauge transformation is performed to remove irrelevant terms. This explicitly exposes the presence of both electric and magnetic charges, defined respectively as

$$\mathcal{O}_e^{(-1)} = \mathcal{O}_q^{(-1)} + \mathcal{O}_{\bar{q}}^{(-1)} , \quad \mathcal{O}_m^{(-1)} = \mathcal{O}_q^{(-1)} - \mathcal{O}_{\bar{q}}^{(-1)} . \tag{4.225}$$

In what follows, we focus solely on the electric charge and set $\mathcal{O}_m^{(-1)} = 0$. For magnetic black holes, the Euclidean on-shell action leads to a mixed ensemble—grand canonical in both electric and magnetic charges [209]. In our case, however, we work in Lorentzian signature and within a nonstationary spacetime, where the inclusion of magnetic charges renders the mixed ensemble technically challenging. Conceptually, though, there is no obstruction to incorporating magnetic charges. Hence, the IR vector potential relevant for the subsequent analysis is given by:

$$A_{\rm IR} = \left[\frac{\mathcal{O}_e^{(-1)}\alpha\tilde{\nu}r}{\Phi_0^2} + \tilde{\mu}\right] du . \tag{4.226}$$

Furthermore, after all the simplifications, the non-trivial Ward identities are

$$\partial_u \mathcal{O}_u^{(1)} - \mathcal{O}_{z\bar{z}}^{(1)} \frac{\partial_u \tilde{\nu}}{\tilde{\nu}} = 0 , \quad \mathcal{O}_{z\bar{z}}^{(1)} + \mathcal{O}_u^{(1)} = 0 , \tag{4.227}$$

Thus, after taking the decoupling limit, all radiation in this spacetime disappears. The geometry settles into a simplified phase space, consistent with the interpretation of Robinson–Trautman spacetimes as duals of far-from-equilibrium fluids [195, 196, 197, 198, 199, 200]. After a sufficiently long evolution, the fluid equilibrates and asymptotically ap-

proaches "near" global equilibrium.

Finally, applying the decoupling limit directly to the generating functional (4.176) yields:

$$\delta I^{\rm IR} = \int d^3x e^{2\chi}\Big(\lambda\left[\mathcal{O}^{(1)}_{z\bar{z}}\frac{\alpha}{\tilde{\nu}}\delta\tilde{\nu} + \mathcal{O}^{(1)}_{u}\delta\alpha + \mathcal{O}^{(-1)}_{e}\tilde{\nu}\delta\tilde{\mu}\right] + \frac{1}{\lambda}\delta\left(\frac{2\Phi_0^3}{\ell_4\kappa_4^2}\frac{\alpha}{\tilde{\nu}}\right)\Big)\ , \tag{4.228}$$

where the regularity conditions from (4.222) have been used. At first glance, the $\lambda \to 0$ limit appears singular due to the last term, which arises from the Smarr relation at zero temperature (4.208). However, this term is a total variation and does not obstruct the definition of the generating functional; it can be removed by adding a local counterterm.

To understand better why the divergence arises from the Smarr relation, let us recall the pressure (4.194) at zero temperature:

$$p = \frac{\mathcal{O}^{(-1)}_{z\bar{z}}}{2\lambda^2\tilde{\nu}^2} = \frac{\Phi_0}{\kappa_4^2}\frac{\ell_4}{\lambda^3\tilde{\nu}^3}\Big(1+\frac{2\Phi_0^2}{\ell_4^2}\Big)\ . \tag{4.229}$$

To apply the generalized Euler relation (3.47), which we reproduce here for the reader's convenience,

$$\epsilon + p = sT + \mu q + y\frac{\partial p}{\partial y}\ . \tag{4.230}$$

we need to express $p = p(s,\mu,y)$. The chemical potential $\mu^{(-1)}$, the entropy density s, and the geometrical variable y are given by

$$\begin{aligned}\mu_{(-1)} &= \frac{\ell_4\alpha}{\lambda\tilde{\nu}}\left(\frac{2}{\kappa_4^2}\Big(1+\frac{3\Phi_0^2}{\ell_4^2}\Big)\right)^{1/2}\\ y &= \frac{\ell_4}{\lambda\tilde{\nu}}\ ,\\ s &= \frac{S}{V} = \frac{\Phi_0^2}{4G_4\lambda^2\tilde{\nu}^2}\ .\end{aligned} \tag{4.231}$$

Here, we used the fact that the volume of the 2-sphere is $V = 4\pi\nu^2 = 4\pi\lambda^2\tilde{\nu}^2$. In this

way, the pressure at zero temperature is

$$p = \frac{1}{2\kappa^2 \ell_4}\left[(4G_4 s)^{3/2} + (4G_4 s)^{1/2}\left(y^2 + \frac{\kappa_4^2}{2\alpha^2}\mu_{(-1)}^2\right)\right] \tag{4.232}$$

This expression holds at both finite and zero temperature since it is not a function of T.[17] At zero temperature, the Smarr relation becomes

$$\epsilon - \mu_{(-1)} q = -p + y\frac{\partial p}{\partial y} = -\frac{2\Phi_0^3}{\ell_4 \kappa_4^2}\frac{1}{\lambda \tilde{\nu}^3} \ , \tag{4.233}$$

which is the local version of the Smarr relation at zero temperature given in (4.208) (with zero magnetic charge). Finally, integrating this expression,

$$\int dx^3 \sqrt{-g}(\epsilon - \mu q) = -\int d^3x e^{2\chi}\left(\frac{2\Phi_0^3}{\ell_4 \kappa_4^2}\frac{\alpha}{\lambda \tilde{\nu}}\right) \ , \tag{4.234}$$

we recover the divergence under consideration. Hence, this divergence is expected from general considerations of a charged perfect fluid at zero temperature.

To proceed, we perform a Legendre transformation that replaces the source $\tilde{\mu}$ with its conjugate variable $\mathcal{O}_e^{(-1)}\tilde{\nu}$, which is a conserved charge. As a result, the term $\tilde{\mu}\delta(\mathcal{O}_e^{(-1)}\tilde{\nu})$ drops out. The final form of the generating functional simplifies to:

$$\delta I^{\rm IR} = 4\pi \int du \left(\mathcal{O}_{z\bar{z}}^{(1)}\frac{\alpha}{\tilde{\nu}}\delta\tilde{\nu} + \mathcal{O}_u^{(1)}\delta\alpha\right) \ , \tag{4.235}$$

where we have integrated over the transverse space, yielding the factor of 4π. Here, we have set $\lambda = 1$, as it will not play a role in the analysis that follows.

[17] In this chapter, we are using a different convention for the electromagnetic sector compared to Chapter 3; that is why there is a factor of $\frac{\kappa^2}{2}$ in front of the chemical potential.

Comparison with JT gravity. We can see now that many portions of our decoupling limit reproduce the features of JT gravity described in Sec.4.2. In particular, the blackening factor (4.223) resembles (4.4), and the equations of motion (4.227) are similar to (4.12a)–(4.12b), though the system appears to be free of anomalies, as would be expected from its parent CFT_3 theory. We will now explain how the anomaly of Schwarzian dynamics shows up, taking into account the ambiguities that we encountered in Sec.4.2.

Our first step is to identify the JT dilaton as follows:

$$\Phi - \Phi_0 = \frac{\tilde{\nu}}{l_4} r \equiv \phi \Longrightarrow \phi = \frac{\nu}{l_2} r \ , \tag{4.236}$$

where ℓ_2 and ν denote the AdS radius and the source of JT gravity, respectively. These are related to the corresponding quantities in AdS_4 via:

$$\ell_2 = \ell_4 \sqrt{\frac{\Phi_0^2}{6\Phi_0^2 + \ell_4^2}} \ , \quad \nu = \tilde{\nu} \sqrt{\frac{\Phi_0^2}{6\Phi_0^2 + \ell_4^2}} \ . \tag{4.237}$$

With this identification, the lapse function f_{IR} from equation (4.223) can be rewritten as:

$$f_{\text{IR}} = \frac{\alpha^2 r^2}{\ell^2} + \frac{r}{\ell_2}\Big(\frac{2\ell_2 \alpha \partial_u \nu}{\nu}\Big) + \frac{\ell_2 \kappa_4^2 (\mathcal{O}_u^{(1)} - \mathcal{O}_{z\bar{z}}^{(1)})\alpha^2}{2\Phi_0 \nu} \ . \tag{4.238}$$

By comparing this expression with equations (4.11) from Sec. 4.2, we recognize that the decoupling limit in the generalized Robinson-Trautman solutions yields the identifications $\omega = \gamma = 0$, provided we relate the operators as:

$$\kappa_2^2 \mathcal{O}_u = \frac{\kappa_4^2}{2\Phi_0} \mathcal{O}_u^{(1)} \ , \quad \kappa_2^2 \mathcal{O}_\phi = \frac{\kappa_4^2}{2\Phi_0} \mathcal{O}_{z\bar{z}}^{(1)} \ . \tag{4.239}$$

Applying this relation to the IR generating functional I_{3D}^{IR} defined in (4.235), we find:

$$\delta I^{IR} = 4\pi(2\Phi_0)\frac{\kappa_2^2}{\kappa_4^2}\int \mathrm{d}u\Big(\mathcal{O}_u\,\delta\alpha + \frac{\alpha}{\nu}\mathcal{O}_\phi\,\delta\nu\Big) = \delta I_\omega\ . \tag{4.240}$$

Here, we have used the relation $8\pi\Phi_0\kappa_2^2/\kappa_3^2 = 1$, which is consistent with the thermodynamic considerations summarized in the heat capacity expression C_H given in (4.212). Accordingly, we arrive at the following mapping:

$$I_{JT} = I_{\omega=0} + \frac{\ell_2}{2\kappa_2}\int du\sqrt{-h_b}\nu^{-1}h_b^{-1}(\partial_u\nu)^2\ . \tag{4.241}$$

Again, from I_{JT}, the Schwarzian action can be derived via the canonical transformation given in (4.79).

In conclusion, we began with a CFT_3 that is free of Weyl anomalies, encapsulated in the generating functional $I_{\omega=0}$. Through our off-shell construction of the decoupling limit, we derived the Schwarzian dynamics, which exhibits an associated Weyl anomaly. The key mechanism underlying this construction is that the anomaly arises from a local counterterm that exists only in one dimension. In higher dimensions, it is not possible to modify the Weyl anomaly in this way, as there is no covariant counterterm available to modify it.

4.6 Discussion

In this work, we have presented a novel generalization of the decoupling limit that allows us to track the evolution of the Ward identities of higher-dimensional holographic CFTs along the RG flow and connect them to Schwarzian dynamics. In Section 4.5, we provide an explicit derivation of the anomalous dynamics characteristic of the Schwarzian theory from a CFT_3 that is free of Weyl anomalies. The key conceptual insight behind this

construction is that the very notion of a Weyl anomaly in one dimension is inherently ambiguous—in stark contrast to its higher-dimensional counterparts. As a result, a covariant counterterm exists that relates the UV generating functional of Ward identities, once the decoupling limit is applied, with that of the Schwarzian theory.

In Sections 4.3 and 4.4, we analyze the AdS_3/CFT_2 correspondence and TMG, respectively. In particular, the dual field theory of TMG exhibits a boundary diffeomorphism anomaly, while the gravitational theory includes higher-derivative terms. Our off-shell decoupling construction systematically addresses these technical challenges, illustrating the versatility of the framework introduced here. This level of generality suggests that extending our method to gravitational phase spaces involving rotating black holes should be conceptually straightforward. However, in the case of a purely rotating black hole with no additional charges beyond angular momentum, the absence of other physical parameters implies that there is no separation of scales between superradiance and the effects associated with the Schwarzian theory. As a result, it becomes inherently difficult to isolate the Schwarzian dynamics from superradiant effects.

It is important to acknowledge that the one-dimensional covariant counterterm—used to match the Schwarzian generating functional with the effective generating functional derived from a higher-dimensional CFT—can, in principle, also be used to eliminate the anomalous part of the Schwarzian theory. This would effectively reduce it to a dynamically simpler boundary theory. Such a possibility carries significant physical implications. While the tree-level thermodynamics of JT gravity remains unaffected by the addition of covariant counterterms, the one-loop contribution would vanish, as the boundary theory would no longer be governed by the Schwarzian action—the Weyl anomaly having been canceled by the counterterm. It is conceivable that a general principle forbids this scenario, but we have not identified such an argument within the scope of this work. However, in the specific case of the RG flow from AdS_3 to JT gravity, there is supporting

evidence from bootstrap arguments that the anomalous Schwarzian dynamics is realized at very low temperatures [170, 172]. In higher dimensions, however, the situation remains less clear, as similar bootstrap analyses are technically more challenging and have not yet been fully developed.

The existence of finite entropy in non-supersymmetric extremal black holes has long posed a conceptual puzzle, as there is no underlying symmetry that protects a ground-state degeneracy in these cases. In contrast, the finite entropy of supersymmetric black holes is naturally accounted for by the degeneracy of BPS states, which is preserved by supersymmetry. Such conclusions emerge from classical thermodynamic considerations, which predict finite entropy even at zero temperature, regardless of supersymmetry [210].

The $\mathrm{nAdS}_2/\mathrm{nCFT}_1$ correspondence provides a resolution to this puzzle by incorporating quantum corrections that lift the apparent ground-state degeneracy in non-supersymmetric settings. At very low temperatures, one-loop effects governed by Schwarzian dynamics dominate over the classical thermodynamics, leading to the characteristic $T^{3/2}$ scaling of the black hole partition function [171, 211, 212, 213]. Crucially, these quantum contributions ensure that the entropy of non-supersymmetric extremal black holes vanishes in the zero-temperature limit, resolving the inconsistency between classical predictions and the absence of symmetry protection.

Given this context, one may ask whether it is possible to go beyond the near-horizon approximation and instead use the full black hole geometry at low temperatures to compute the quantum effects responsible for the characteristic $T^{3/2}$ scaling of the partition function. In spirit, this is the same question that motivates the present work: if we understand the emergence of Schwarzian dynamics from the parent CFT, this insight may enable us to explore the $T^{3/2}$ behavior of the partition function directly from the perspective of the UV CFT, particularly in the very low-temperature regime.

Notably, previous efforts have attempted to address this question. In the context of

superconformal field theory, the work of [214] identified the Schwarzian contribution to the free energy in a particular limit of $U(N)$ $\mathcal{N} = 4$ SYM theory on $\mathbb{R} \times S^3$. However, in that case, the presence of fermions modifies the result, and the $T^{3/2}$ scaling does not appear. On the gravitational side, the works [215, 216] used the full geometry of non-supersymmetric black holes in AdS_3 to compute the gravitational path integral and successfully reproduce the $T^{3/2}$ scaling of the partition function. Notably, [216] also provides preliminary numerical evidence for analogous behavior in AdS_4, where a fully analytical treatment remains unavailable.

We believe that our construction of the off-shell decoupling limit may provide a useful framework for analytically studying the logarithmic corrections associated with the $T^{3/2}$ scaling of the partition function for AdS_4 black holes using the full geometry. Specifically, by employing our construction of the gravitational phase space in a Bondi-like gauge, one can treat it as a kind of superspace approximation for performing the gravitational path integral and then take the low-temperature limit. Nonetheless, this approach faces technical challenges, primarily due to the fact that the Bondi gauge explicitly breaks covariance. In contrast, gravitational path integrals for Euclidean black holes—and the quantum corrections derived from them—are typically formulated in covariant gauges. Moreover, the analytic continuation of a Bondi-like gauge to Euclidean signature is subtle, since this gauge is intrinsically tied to the Lorentzian causal structure of spacetime. Addressing these difficulties is a necessary step toward the rigorous application of our method in this setting.

Chapter 5

Chaotic LLM Billiards

We study null geodesics of the ten-dimensional LLM geometries. In particular, we show that there are a subset of these null geodesics that are confined to the LLM plane. The effective dynamics of these in-plane geodesics is that of a Hamiltonian system with two degrees of freedom (a phase space of dimension 4). We show that these are chaotic. In the two-coloring of the LLM plane, if they start in the empty region, they cannot penetrate the filled region and viceversa. The dynamical problem is therefore very similar to that of a billiards problem with fixed obstacles. We study to what extent LLM geometries with many droplets may be treated as an incipient black hole and draw analogies with the fuzzball proposal. We argue that for in-plane null geodesics deep in the interior of a region with a lot of droplets, in order to exit towards the AdS boundary they will need to undergo a process that resembles diffusion. This mechanism can account for signals getting lost in the putative black hole for a very long time.

5.1 Introduction to the chapter

What is a black hole? In the classical theory of general relativity, the notion of a black hole has a precise definition. Colloquially, it is the region of spacetime situated behind a horizon from which no information can escape. Usually, there is also a singularity in the future of any infalling observer.

Once we include quantum mechanics, especially in view of the gauge/gravity duality [29], describing the notion of a black hole is harder. Noting that semi-classical stationary black holes have a temperature [12], one can associate black holes with a particular class of thermal states. This serves us well in equilibrium. Outside of equilibrium, however, it is very hard to extract in general the notion of a horizon from a quantum field theory dual computation. Part of the reason is that the notion of a horizon in general relativity is teleological. It is tied to future infinity: the horizon for an AdS black hole is the surface that divides the events that a future asymptotic observer on the boundary of AdS space might be able to see, versus the ones that are invisible to them. The horizon might also depend on how we choose to act on the quantum system on the boundary later on. This requires a notion of time in the bulk. We are thinking here of the spacetime being foliated by Cauchy slices labelled by a parameter that we choose to call the time variable. We want that time variable to coincide with the time variable on the boundary of AdS. So long as we can make different choices later on, a portion of spacetime at an instant of time might be situated behind the horizon or not, depending on some event that has not happened yet. In that sense, the field theory dual of a classical horizon is not an observable.

Nevertheless, the presence or absence of a horizon can be used as an order parameter distinguishing two phases of matter: confinement and deconfinement [14]. This is simplest in a static setting with large black holes where one can Wick rotate the theory to a

Euclidean geometry. The reason to choose large black holes is that they are thermodynamically stable [74]. Namely, they have positive specific heat. The Hawking-Page first order phase transition is identified with the confinement/deconfinement transition. The deconfined phase, in this case, has a different topology of the Wick rotated Euclidean spacetime than the confined phase. It should be noted that the same Euclidean topology is assigned to small black holes in AdS space. These are black holes that behave like Schwarzschild black holes in flat space: they have negative specific heat. Reasoning by similarity, small black holes have been argued to be a partially deconfined phase [217, 218] (see also the earlier [219]), where only a subset of the color gauge group is deconfined. Their entropy is of order ϵN^2, with $\epsilon \lesssim 1$. Usually, ϵ is very small but finite, so there is not enough energy in the system to excite most of the color degrees of freedom (this would require an energy strictly larger than an order one constant times N^2 in free field theory). To solve the problem of the thermodynamic instability of these black holes one needs to work in the microcanonical ensemble: one fixes the mass, not the temperature. Since the horizon can become arbitrarily small, when these black holes are sufficiently small they can evaporate rapidly into the bulk. The question of whether there is a black hole or not becomes harder to analyze. There is no clear dividing line in the quantum gravity theory between spacetimes with black holes and spacetimes without them, essentially because black holes can evaporate.

More to the point, there are many examples of geometric solutions of Einstein's equations that are horizon free, stationary and have the same asymptotic behavior as a black hole with the same quantum numbers. These solutions have bubbles (they have different topologies with many non-contractible cycles with fluxes through them) and many times only start to differ significantly from a corresponding black hole solution near the region where the horizon would have been located. These solutions usually arise from states that satisfy a supersymmetric bound between their charges and the

mass (they are BPS states). The corresponding black hole is extremal and has zero temperature. The fuzzball proposal [47] (see also [48] for an overview of these ideas) states that the black hole is just a coarse-grained version of these possible microstate geometries. Moreover, the horizon appears due to our lack of knowledge of what is occurring on the *inside region*, broadly speaking. The proposal states that "horizons and singularities are artifacts of attempting to describe gravity using a theory that has too few degrees of freedom to resolve the physics" [220].

More precisely, these extremal black hole solutions have a well defined throat region and it is in this throat region where the differences between the different geometries appear. In this case, the right question to ask is how can any of the typical microstate geometries seem to us as if it were a black hole?

That question is addressed by throwing observers (matter) into the black hole and asking what they see (seeing what comes out). The answer to the question becomes phenomenological: can an individual microstate behave qualitatively similar to a black hole? For example, do signals generally take a long time to get out? Are there large tidal forces that rip objects apart? If such tidal forces exist, the fuzzballs would appear to destroy information to an outside observer. These questions are computable: given details of the microstate geometry, one can throw matter inside and follow its motion in the interior. One can then wait until the matter comes out again.

Our goal in this chapter is to understand a similar set of questions for half-BPS geometries in $AdS_5 \times S^5$. These geometries, constructed by Lin, Lunin and Maldacena [49], which we will call LLM geometries, have similar properties to the fuzzball microstates. They are horizon free geometries, they have bubbles and fluxes and come in large families. These solutions can have different topologies. Part of their simplicity is that their dual states in the boundary CFT are easy to describe. The geometries are dual to a very simple sector of $\mathcal{N} = 4$ SYM that can be described in terms of 2D incompressible

droplets of free fermions [50]. The droplet picture also arises directly from the supergravity solutions, so one can actually have a two-dimensional picture of the spacetime that encodes all the data necessary to recover the ten-dimensional geometry [49]. We will call this two-dimensional surface the LLM plane.

These solutions do not admit black holes and have no Wick rotated Euclidean geometry related to them. They can still be coarse-grained. When one does so, the droplets become grey: they can be a statistical ensemble of filled or unfilled regions of the LLM plane, so the local droplet density on the LLM plane instead of being zero or one can be any number in between. The corresponding greyscale supergravity solutions have naked singularities. Essentially, there are not enough half-BPS states to give an entropy of order N^2 and generate a horizon with an area of the right size in geometric units. One can think of these as incipient black holes [221] and put a stretched horizon around the singular locus. It should also be noted that in these geometries the topology of the spacetime is not a quantum observable. The topology of LLM geometries can be changed by the superposition of a very large number of states [222]. This fact guarantees that the topology is not a quantum observable [223]. The notion of topology depends on the coarse-graining, but for large enough bubbles this is not a major issue. This is similar to arguing that the topology of the Euclidean spacetime is not characterized by a *conserved* quantum number, as we can take extreme limits where the small black holes evaporate and change topology.

Armed with explicit solutions of the LLM geometries, we aim to ask to what extent an individual LLM microstate might behave as a black hole. The whole point is to argue that being a black hole in the dual theory is more a matter of degree, rather than an expression of the quantum numbers of the state. Therefore, even in these cases where one barely has a notion of an incipient black hole, where even the notion of the horizon is not available, it is interesting to ask if light gets trapped. We also want to come to

a simplified picture of what is responsible for the *trapping mechanism* and ask about the existence of tidal forces that might pull objects apart [224, 225, 226, 227] (see also [228, 229, 230, 231]).

To test if light is trapped, we consider solving for the null geodesics of the LLM geometries. A particularly useful observation we have in this chapter is that there are null geodesics whose motion is restricted to lie in the LLM plane. The motion is that of a particle in two dimensions in the presence of non-trivial magnetic fields. These are restricted to be either in the filled or empty region of the LLM plane.

The picture that appears is very appealing. For geodesics in the empty region, the droplets are obstacles in the path of the null geodesics that they need to avoid. Essentially, the geodesics are reflected from the droplets, similar to a problem of chaotic billiards. The fact that we see chaos in the dynamics can be used as an analogue of strong tidal forces: nearby null geodesics will separate exponentially fast from each other. A notion of the trapping mechanism can be extrapolated to the case where there are many droplets. The null particles in that case are better thought of as moving through a dense medium with multiple scattering centers. A typical microstate can be argued to have many droplets of random shapes. If the results of collisions are fairly random, the process of getting outside a region is analogous to diffusion. This mechanism can explain simply why something that falls in might take a very long time to get out. Some such geodesics might be completely encircled so they can never get out. Such modes could in principle become internal excitations of the putative incipient black hole that are very hard to tease out by an outside observer.

The chapter is organized as follows. In section 5.2 we briefly summarize the ten-dimensional LLM geometries to establish notation. In section 5.3, we describe the dynamical system of our interest. We turn the problem of studying null geodesics into a Hamiltonian dynamics problem in very few variables. The main reason to do so is that

the LLM geometries have multiple symmetries that lead to conserved quantities. In the Hamiltonian formulation, these constants of motion are angular momenta and can be frozen to reduce the dimensionality of the problem. We will also end up studying a subset of the geodesics that lie in the LLM plane. In section 5.4, we describe the geodesic motion in vacuum $AdS_5 \times S^5$, where the LLM data is one round disk case as a warm-up. Part of the purpose is to later compare with a geometry with more droplets. In section 5.5 we present numerical results that characterize the chaotic behavior of the three disks configuration. Because the work we do is numerical, we study a configuration with three disks as an example, but the main results are expected to be generic.

5.2 LLM geometries

In this section, we briefly review the bubbling AdS geometries constructed in [49] to establish notation.

Motivated by the AdS/CFT correspondence, Lin, Lunin and Maldacena (LLM) explored asymptotically $AdS_5 \times S^5$ half-BPS IIB supergravity solutions. These solutions preserve an SO(4)×SO(4) × $\mathbf{R}$ symmetry. This residual symmetry of configurations is easiest to understand in the dual CFT formulation [50], where only one of the complex scalars of $\mathcal{N} = 4$ is excited. The field theory is analyzed in the $S^3 \times \mathbb{R}$ cylinder, whose ground state is dual to $AdS_5 \times S^5$ in global coordinates. The unbroken R-symmetry is $SO(4)$ and the configuration is also spherically symmetric on the spatial S^3 of the boundary. The BPS constraint adds one extra conserved charge, identified with $\mathbf{R}$.

The upshot of the field theory analysis is that the half-BPS configurations of the SYM theory are described in the weak coupling limit in terms of eigenvalues of a complex matrix (the Gauss' law constraint turns the matrix variable describing the half-BPS states into a normal matrix). The real and imaginary parts of the eigenvalues are conjugate variables

to each other. The measure terms from gauge fixing make these eigenvalues behave like fermions. The effective system describing the dynamics of this reduced set of states is that of droplets of fermions in the presence of a magnetic field, when reduced to the lowest Landau level. Correlators in the half-BPS sector can be computed exactly for these states by combinatorial methods [232]. More recently, other tools have been used to simplify how these results can be obtained [233] by using coherent state methods and integral representations that can be evaluated by localization.

With these symmetry considerations Lin, Lunin and Maldacena found the following general solution, in type IIB supergravity, for the metric,

$$h^2 ds^2 = -(dt + V_a dx^a)^2 + h^4(d\xi^2 + dx_a dx^a) + \left(\frac{1}{2} - z\right) d\tilde{\Omega}_3^2 + \left(\frac{1}{2} + z\right) d\Omega_3^2. \quad (5.1)$$

The $SO(4) \times SO(4) \times \mathbf{R}$ symmetry is manifest, with all functions being independent of t and the $SO(4)$ symmetries realized by isometries of the two 3-spheres $\tilde{\Omega}_3$ and Ω_3. The functions z and h depend only on the three variables $\xi, x^{1,2}$.

The h function is related to z by,

$$h^2 = \frac{1}{\xi}\sqrt{\frac{1}{4} - z^2}, \quad (5.2)$$

while the V_a functions obey the following equations in terms of z and ξ,

$$\partial_\xi V_a = \frac{\epsilon_{ab}\, \partial_b z}{\xi}, \qquad \partial_a V_b = \frac{\epsilon_{ab}\, \partial_\xi z}{\xi} + \partial_b V_a. \quad (5.3)$$

This means that the solution is completely characterized by the single function $z = z(\xi, x, y)$, where $x^a = \{x, y\}$ and the range of the coordinates is $\xi \in (0, \infty)$ and $x^a \in (-\infty, \infty)$. That is, the domain of the z function is an upper half space in three dimensions.

Besides the metric, the background is supported by a five-form in the RR sector, which together with the metric (5.1) is a solution of type IIB supergravity if the following linear PDE for z is satisfied,

$$\partial_a \partial_a z + \xi \partial_\xi \left(\frac{\partial_\xi z}{\xi} \right) = 0. \tag{5.4}$$

The solutions are tuned with precise boundary conditions, $z \to \pm 1/2$ as $\xi \to 0$, in such a way that the metric ds^2 does not contain conical singularities. One gets a 'Black' and 'White' colouring xy-plane for each geometry defined by,

$$\text{White:} \quad \lim_{\xi \to 0} z(\xi, x, y) = \frac{1}{2}, \qquad \text{Black:} \quad \lim_{\xi \to 0} z(\xi, x, y) = -\frac{1}{2}. \tag{5.5}$$

The convention of colors can also be thought of as 'White' being a region with no fermions and 'Black' a filled region with the maximum density of fermions that is allowed. This $\xi = 0$ surface will be called the LLM plane and is parametrized by $x^{1,2}$. The smoothness restriction arises because we need h to be finite in the LLM plane. More precisely, it is $\lim_{\xi \to 0} h^{-1} \neq 0$ that must be non-vanishing. Otherwise, both spheres shrink to zero size at $\xi = 0$. The boundary between the two saturated color regions is allowed as there the metric becomes that of a non-singular plane wave [49]. The two coloring of the LLM plane is that of an incompressible fluid and reproduces exactly the $\mathcal{N} = 4$ free fermion picture.

Notice that the boundary conditions of z on the $\xi = 0$ plane play an important role as it describes the size of the two 3-spheres. In the $z \to -1/2$ regions the 3-sphere Ω_3 shrinks to zero as $\xi \to 0$, whilst in the $z \to +1/2$ regions the 3-sphere $\tilde{\Omega}_3$ shrinks to zero as $\xi \to 0$. These are easy to see in (5.1) if h is finite. The radii of the spheres have additional factors of $1/2 \pm z$ in the metric.

Note that these boundary conditions ensure smoothness of the solution (5.1) in the

entire space. If one accepts greyscale solutions, the limit $\xi \to 0$ has singularities. The function z is then in the range $(-1/2, 1/2)$. These are the only values that are compatible with causality [234] (other values lead to closed timelike curves). The effective reason for these bounds in the dual $\mathcal{N} = 4$ SYM is that the fermions must satisfy the Fermi exclusion principle. The density of fermions has an upper bound, and similarly, cannot be negative.

5.2.1 The one disk and multi disks geometries

The simplest configuration is the geometry described by the $AdS_5 \times S^5$ spacetime itself. In the LLM plane, this is described by a single disk. This solution is described by the following z function,

$$z = \frac{r^2 + \xi^2 - R^2}{2\sqrt{(r^2 + \xi^2 + R^2)^2 - 4r^2R^2}}, \qquad \text{with} \qquad z(\xi \to 0) = \begin{cases} -\frac{1}{2} & r < R, \\ \frac{1}{2} & r > R, \end{cases} \tag{5.6}$$

where $r^2 = x^2 + y^2$ and R is the radius of the disk. When we consider more general disk configurations at the boundary $\xi \to 0$, the rotational symmetry in the x_a plane is lost.

We can easily find generalizations to geometries with n-disks. We do this by summing solutions for various disks. This is where the fact that we need to solve a linear PDE does its work: we just superpose (sum) solutions and fix a constant so that the empty region is at the right value of z. We write these geometries in Cartesian coordinates and the z_T function is obtained as the sum of each individual z_i function,

$$\begin{aligned} z_i &= \frac{r_i^2 + \xi^2 - R_i^2}{2\sqrt{(r_i^2 + \xi^2 + R_i^2)^2 - 4r_i^2R_i^2}}, \\ \text{with} \quad z_T &= \sum_i^n \left(z_i + \frac{1-n}{2n} \right) \quad \text{and } z_T(\xi \to 0) = \begin{cases} -\frac{1}{2} & r < R, \\ \frac{1}{2} & r > R, \end{cases} \end{aligned} \tag{5.7}$$

where n is the number of disks and the subscript i labels the ith-disk. The ith-disk has its center at coordinates at $\{x_i, y_i\}$ and radius R_i, and we define $r_i^2 = (x-x_i)^2+(y-y_i)^2$. The constant factor $\frac{1-n}{2n}$ guarantees that the boundary conditions $z = \pm 1/2$ are satisfied.

The V_a functions that solve the equations (5.3) with the z_T function given by (5.7) are,

$$V_a = \frac{\epsilon_{ba}}{2}\sum_i^n \frac{(r_i^2+\xi^2+R_i^2)}{\sqrt{(r_i^2+\xi^2+R_i^2)^2-4r_i^2R_i^2}}\partial_{x_b}(\log r_i). \tag{5.8}$$

This way, we have a readily available explicit list of interesting geometries to consider.

5.3 General dynamics of the system

In order to study the dynamics of the system we compute the Hamiltonian from the metric (5.1). We call the null geodesic affine time parameter of the dynamical problem τ. We start from the Lagrangian

$$L = \frac{1}{2}g_{\mu\nu}\dot{x}^\mu\dot{x}^\nu \tag{5.9}$$

and compute the Legendre transform. Null geodesics are interpreted as the geometric limit of massless particles. In the type IIB string theory, these massless particles are all part of the gravity multiplet in 10 dimensions, so they are captured by all the possible supergravity modes. Any statement about null geodesics has consequences for wave solutions in supergravity.

The spherical symmetry in Ω_3 and $\tilde{\Omega}_3$ automatically lets us introduce conserved angular momenta $L, \tilde{L}$. Also, the time translation invariance in the t variable lets us introduce E as the conserved conjugate momenta of t. The null geodesic constraint will have the Hamiltonian function vanishing ($\mathcal{H} = 0$). The Hamiltonian (rescaled by h^2) for the

dynamics of the remaining three variables is the following

$$2h^2\,\mathcal{H} = P_\xi^2 + (P_x + EV_x)^2 + (P_y + EV_y)^2 + h^4\left(\frac{2L^2}{(1+2z)} + \frac{2\tilde{L}^2}{(1-2z)} - E^2\right), \quad (5.10)$$

where the two coordinates x^a have been renamed to x, y and the third coordinate ξ of the LLM metric has remained the same. The $P_{x,y}$ are conjugate to x, y and P_ξ is conjugate to ξ.

We want to study geodesics that reach the incipient black hole region $\xi \simeq 0$. One can check that the geodesics that reach the LLM plane $\xi \to 0$ must have an angular momentum vanishing in one of the two possible spheres. Which angular momentum vanishes depends on which sphere goes to zero size at the intersection. This mathematical fact generates an angular momentum repulsion barrier. Also notice that the $\xi = 0$ region is a locus of unbroken rotation symmetry for one of the two spheres, depending on which sphere degenerates. This indicates that it is possible to find solutions to the equations of motion that stay completely in this locus. These will have $P_\xi = 0$ and $\xi = 0$ and one of the angular momenta vanishing. Our main computational effort will be to study this subset of solutions to the null geodesics that are strictly confined to the LLM plane.

In such limit, the system is reduced to a four-dimensional phase space with the following Hamiltonian,

$$\mathcal{H}_0 = \frac{1}{2h^2}\left((P_x + EV_x)^2 + (P_y + EV_y)^2 + h^4\left(L^2 - E^2\right)\right)\Big|_{\xi\to 0}. \quad (5.11)$$

where both L, E are constants of motion. Therefore, the interesting dynamics takes place only in the x, y coordinates.

Null geodesics then satisfy the following constraint,

$$(P_x + EV_x)^2 + (P_y + EV_y)^2 + h^4 \left(L^2 - E^2\right)\big|_{\xi\to 0} = 0, \tag{5.12}$$

which can be expressed in terms of the velocities in a quite simple way as,

$$E^2 - L^2 = \dot{x}^2 + \dot{y}^2. \tag{5.13}$$

This form of the constraint suggests that the motion should be very simple. The constraint tells us that $E > L$ (this is a classical limit of the BPS constraint). When $E = L$, there is no motion in the x, y coordinates. There is one of these stationary solutions for any empty point in the LLM plane.[1]

The equations of motion derived from the Hamiltonian (5.11) that satisfy the requirement (5.12) are,

$$\begin{aligned} \dot{x_a} &= \frac{P_{x_a} + E\, V_a}{h^2}\bigg|_{\xi\to 0}, \\ \dot{P}_{x_a} &= (E^2 - L^2)\partial_{x_a} h^2 - \frac{E}{h^2}\left((P_x + EV_x)\partial_{x_a} V_x + (P_y + EV_y)\partial_{x_a} V_y\right)\bigg|_{\xi\to 0}, \end{aligned} \tag{5.14}$$

for $x_a = (x, y)$. The h^2 and V_a functions in the $\xi \to 0$ limit are given by the following explicit expressions

$$h^2\big|_{\xi\to 0} = \sqrt{\sum_{i=1}^{n}\left(\frac{R}{|r_i^2 - R^2|}\right)^2}, \qquad V_a\big|_{\xi\to 0} = \frac{1}{2}\epsilon_{ba}\sum_{i=1}^{n}\frac{(r_i^2 + R^2)}{|r_i^2 - R^2|}\partial_{x_b}(\log r_i). \tag{5.15}$$

One can see that the explicit equations of motion in this limit are somewhat unwieldy, suggesting that finding analytical solutions to this system of differential equations be-

[1] These are also related to the zero size limit of BPS open strings discussed in [236].

comes a complicated task. The quantities EV_x, EV_y in equation (5.11) act as an effective magnetic field potential on the LLM plane. The dynamical system is that of particles subject to a non trivial metric, a non-trivial potential proportional to $L^2 - E^2$ and a non-trivial magnetic field that is time independent.

This low dimensionality of the problem makes it easier in the end to visualize the solutions. In the next section we will show a numerical analysis of our system.

5.4 The global $AdS_5 \times S^5$ geometry

In order to contrast with more elaborate configurations, in this section we present the dynamics of the simplest case in the LLM geometries: the $AdS_5 \times S^5$ vacuum itself. The main idea is to understand the null geodesics of interest to us in the LLM coordinates, rather than the more conventional global AdS coordinates. The geometry here is determined by one disk with radius R. The disk on the LLM plane has rotational symmetry, which is associated with the conserved angular momentum P_θ. There is also the conserved energy of the particle E in these coordinates. In the plane wave limit geometry [235], the quantity E is identified with $E = \Delta - J$, where Δ is the global energy (the one that measures anomalous dimensions of operators) and J is the R-charge carried by the LLM geometry. This is a true statement in general. The LLM geometries satisfy the constraint $E_{back} = \Delta - J = 0$. This is the BPS constraint. The geometries have vanishing energy with respect to the LLM time variable. This is also part of the dual field theory setup [50]. The P_θ momentum is the additional amount of R-charge J carried by the null particle whose geodesic motion we are analyzing.

The general Hamiltonian (5.11) mapped to polar coordinates for this particular case

is

$$\mathcal{H}_0 = \frac{1}{2h^2}\left(P_r^2 + \frac{(P_\theta + EV_\theta)^2}{r^2} + h^4\left(L^2 - E^2\right)\right)\Big|_{\xi\to 0}. \tag{5.16}$$

The canonical momenta are given by

$$P_r = h^2\dot{r}, \quad h^2 E = \dot{t} + V_\theta\dot{\theta}, \quad P_\theta = -EV_\theta + h^2 r^2\dot{\theta}. \tag{5.17}$$

The additional rotational symmetry on the LLM plane transforms this problem into a one-dimensional system, as P_θ is conserved. Furthermore, since the Hamiltonian is time-independent, then the system is integrable. This result is also true for generic concentric circle geometries. The integrability is for null geodesics inside the LLM plane, which is the reduction we are studying in this chapter.

In turn, the null constraint (5.12), which is also $\mathcal{H}_0 = 0$, can be recast as a condition over the domain of r, as P_r must be real. We can solve for P_r as follows:

$$P_r = \pm\sqrt{h^4\left(E^2 - L^2\right) - \frac{(P_\theta + EV_\theta)^2}{r^2}}. \tag{5.18}$$

All the terms on the right hand side depend on r and the constants of motion. Notice that, for certain values of the conserved momenta (L, E, P_θ), the quantity P_r vanishes, giving us turning points for r.

In the $\xi \to 0$ limit, one can also determine the explicit form of functions h^2 and V_θ in polar coordinates,

$$h^2\big|_{\xi\to 0} = \frac{R}{|r^2 - R^2|}, \quad V_\theta|_{\xi\to 0} = \frac{1}{2}\left(\frac{r^2 + R^2}{|r^2 - R^2|} - 1\right). \tag{5.19}$$

In Figure 5.1 we show a set of orbits where we consider a disk centered at the origin

with radius $R = 5$. We consider geodesics with $E = 20$ and $L = 5$, but with different values for initial positions and momenta.

Notice also that there exist trivial analytic solutions in the LLM plane with $E = L$ (the general BPS solutions we argued in the previous section). These solutions have a nontrivial angular momentum $P_\theta = -EV_\theta$ and $P_r = 0$. In these coordinates, these null geodesics are all stationary, but they still move in the time direction t on the one 3-sphere on which they have angular momentum.

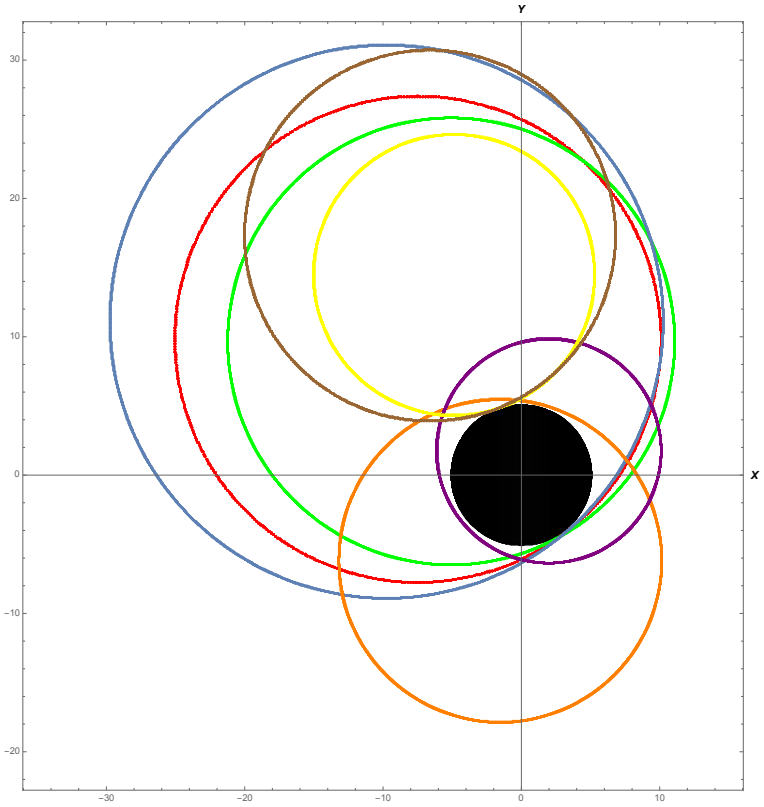


Figure 5.1: The disk of $R = 5$ centered at the origin is represented by a black circular region. The rest of the circles with different colors represent geodesics with different initial conditions. Each orbit has a circle-like shape, but are not exactly circular orbits. Some of the geodesics (brown and yellow) do not orbit the central black disk.

5.5 Numerical results and graphs for one example: three disks

Now we are ready to study a more general case. In general, black holes are expected to lead to chaotic behavior in the dynamics [237, 238]. One would expect that for an LLM geometry to behave similarly to a black hole, a prerequisite is to have the geodesic solutions be chaotic. Given the high degree of symmetry of the solutions, this is not guaranteed in general. The results of [239] suggest that most LLM geometry solutions will lead to a non-integrable system, even for null geodesics. These arguments are based on the separability of the associated Hamilton-Jacobi problem. Here we verify explicitly that there is chaos. This fact by itself does not mean that a system behaves as a black hole, but it serves as a prerequisite for that statement to be true. For example, in the $AdS_5 \times T^{1,1}$ geometry, there is chaos for string motions [240], but the geodesic problem itself is integrable. Clearly, there is no black hole. In this section, we want to verify explicitly the claim of the existence of chaos in one simple configuration with multiple disks.

Because we expect chaos, we will verify the presence of chaos numerically. We choose one example of a geometry with enough features to be interesting, but with the expectation that some of the features of motion are generic.

We consider one example of a configuration with three disks of the same radius $R = 5$, whose centers are located at the following positions in the LLM plane

$$(x_1, y_1) = (0, 0), \qquad (x_2, y_2) = (20, 0), \qquad (x_3, y_3) = (10, 20). \tag{5.20}$$

Our initial setup considers geodesics of energy $E = 20$ and angular momentum $L = 5$. These are chosen to be of order one. The only parameter that physically matters is L/E,

as solutions of null geodesics have a rescaling property: the Hamiltonian is a purely quadratic function of momenta. The null geodesics with momenta all rescaled by the same factor will follow the same trajectory in the position coordinates, but they will evolve faster or slower in the affine parameter τ.

Figure 5.2 shows an orbit plot for a given generic initial condition in position and momenta. We see the location of the three disks demarcated in the plot by the region that the null geodesics are avoiding. Comparison with Figure 5.1 shows that this new orbit is significantly more complicated than in the one disk case. The rotational symmetry on the xy-plane from before is now lost due to the additional disks. We see that the motion is highly irregular: the orbit spends most of its time circling around a single disk, but jumps occasionally to motion around the other disks. Less frequently, the orbit travels far outside of all of the disks, as seen in the figure.

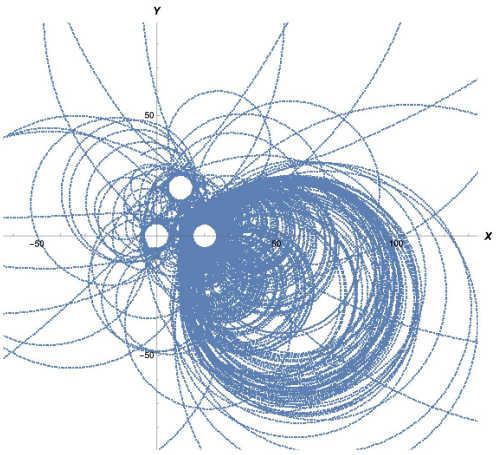
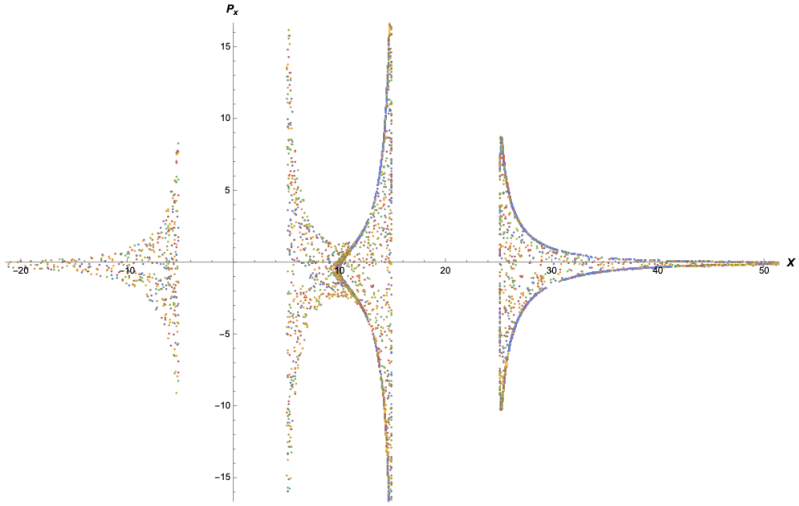


Figure 5.2: The orbit followed by a single null geodesic in the three disk geometry projected to the LLM plane.

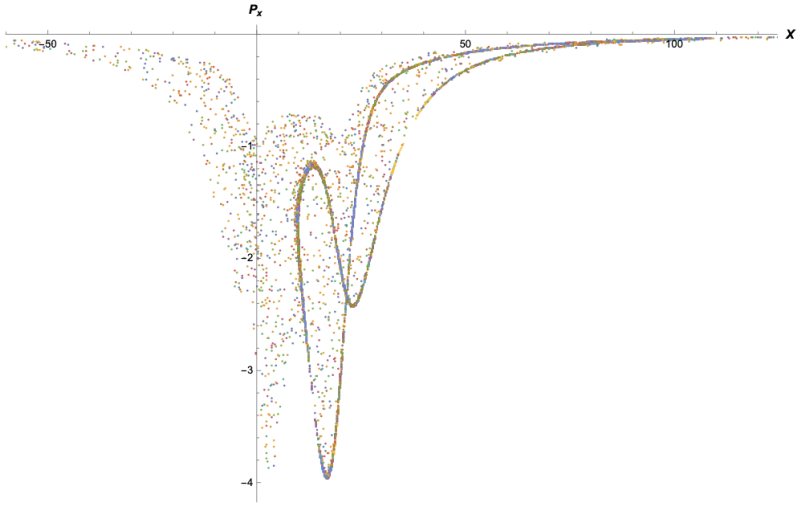
The orbits are prevented from reaching the inside of the disks by the angular momentum L. As we explained earlier, the two 3-spheres degenerate in the LLM plane and there is an angular momentum repulsion from the filled disk region. In that sense, we can think of the disks as impenetrable obstacles that the trajectory must be reflected from. This is similar to a billiards problem. The main difference is that there is also an effective magnetic field present. This effective magnetic field arises because the metric is not static in the t coordinate.

The trajectory appears to bounce off these disks. Some parts of the trajectory also travel far out in the radial direction, closer to the boundary of AdS. Since the trajectory only has angular momentum in the $SO(4)$ rotational group of the S^3 on the boundary, these can in principle reach infinity if they stop carrying angular momentum with respect to the $U(1)$ charge of rotations in the LLM plane. That is, if P_θ becomes very small (the angular momentum P_θ is not conserved, but should become an adiabatic invariant in trajectories of the region very far from the disks). The rotational breaking of symmetry makes it in principle possible to do this (we can have jumps in P_θ between different portions of a geodesic).

Since the rotational symmetry on the plane is lost, the system that was originally integrable for one disk becomes chaotic for three disks. Due to the low effective dimension of the problem (a two-dimensional phase space), we can visualize chaos with the aid of Poincaré sections. In Figure 5.3, the Poincaré sections with the y variable fixed are shown. They clearly display chaos.



(a) Poincaré section for $y = 0$.



(b) Poincaré section for $y = -8$.

Figure 5.3: Poincaré sections, x vs P_x, for some values of y. The exterior white regions represent the region disallowed by the null constraint, where the position x is roughly inversely proportional to the momentum P_x. The points fill out completely the allowed region in the phase space as we expect for chaotic motion. In the first plot, the two vertical white strips represent the locations of the two disks at $y = 0$, which are forbidden. In the second plot, the two vertical white lines are gone since the cut is moved to $y = -8$.

The main characteristic of chaotic dynamics is the butterfly effect [237]: exponential sensitivity to initial conditions. This is checked by demonstrating that the system has a non-trivial Lyapunov spectrum (Lyapunov exponents that don't vanish). To compute Lyapunov exponents, we choose the following initial conditions $(x^{(0)}, y^{(0)}) = (10, 3)$ and $(P_x^{(0)}, P_y^{(0)}) = (\frac{152785}{856086}, \frac{25\sqrt{1695}}{616})$, so that we can have arbitrary precision if necessary. Since the three disks configuration has a four-dimensional phase space, we report the four Lyapunov exponents associated with the configuration, checking that they are numerically in accordance with the following pattern numerically $\lambda_1 > \lambda_2 > -\lambda_2 > -\lambda_1$, and that $\lambda_2 \simeq 0$ due to there being a constant of motion. The pattern arises because the chaotic motions respect the symplectic structure of phase space. Computing the exponents numerically, we find that

$$\{\lambda_i\} = \{0.4484, 0.02104, -0.02109, -0.4483\}. \tag{5.21}$$

The maximum Lyapunov exponent is positive and $\lambda_{max} \sim 0.4484$ is represented by the blue data in Figure 5.4. We can use the difference from zero of the Lyapunov exponents as an error bar. This method would indicate that one expects the largest exponent to have an error of order 5%. We expect two of the Lyapunov exponents to vanish. This is supported by our analysis with two of the exponents slowly converging toward zero. The slow convergence comes from the form of the differential equations we are integrating. The equations become stiff near disk boundaries, setting limits as to how far we can integrate up to.

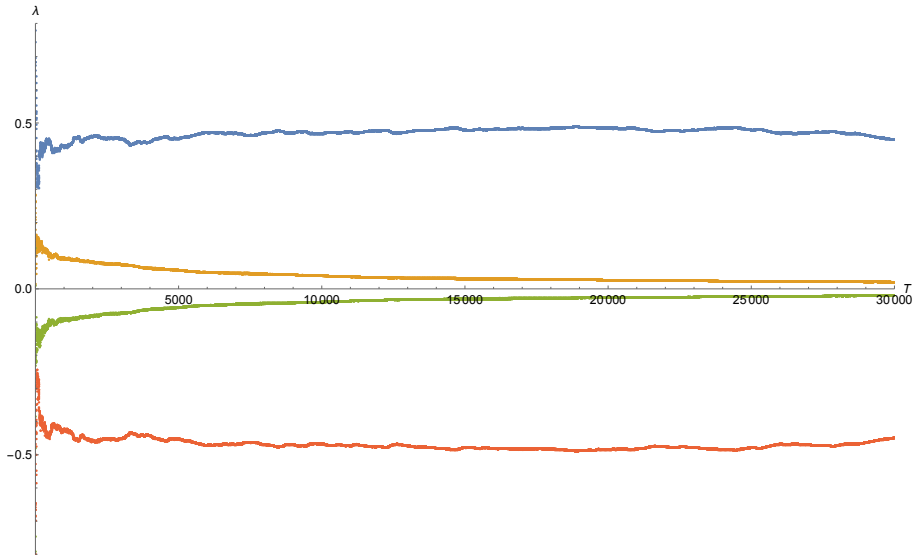


Figure 5.4: The maximum Lyapunov exponent $\lambda_{max} = 0.4484$ is represented by the blue line.

5.5.1 Geodesics trapped in the interior region formed by the disks

The goal of our analysis is to observe trajectories that are almost trapped and take a very long time to escape to infinity. One way to create this behavior is to make the exits of some regions very narrow by placing our disks close to each other. Due to the angular momentum repulsion effect, this causes a trajectory to bounce back and get trapped for an extended period. For our setup, we choose the same center locations for three disks as before (see (5.20)), but we increase the radius of the disks such that they are almost touching each other. This causes a geodesic starting in the interior region formed by the three disks to get effectively trapped. We choose $R = \frac{9999}{1000}$ for each disk. The energy is kept the same at $E = 20$, but the angular momentum is changed to $L = 19$. This is close to the BPS limit. The initial condition of the representative trajectory is $(x_0, y_0) = (10, 3)$ and $v_{x_0} = 1$, $v_{y_0} > 0$. We only show some points for a very long time

trajectory. If we filled the points of the trajectory, the region where the null geodesic is trapped would seem filled.

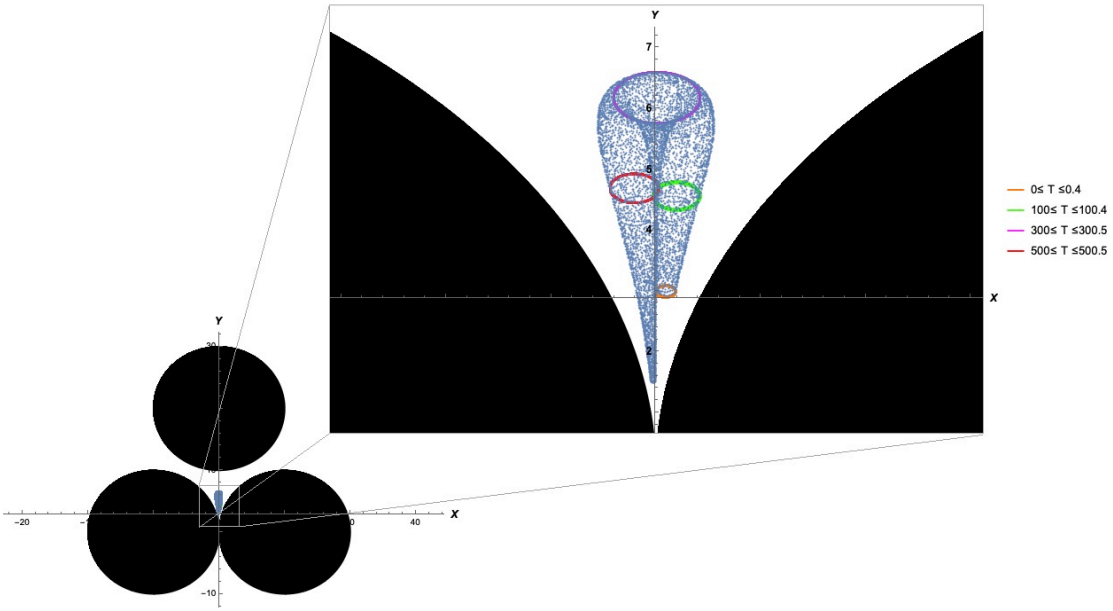


Figure 5.5: In this plot, we can see how the geodesic is trapped in the interior region formed by the three disks. Segments of trajectory associated to very short periods of time evolution have been marked with different colors. The blue dots are the positions of the particle sampled at long intervals.

The evaluated trajectory is shown in Figure 5.5. We see that the geodesic gets effectively trapped. In order to clarify how the motion looks for small time periods, we have highlighted short intervals with separate colors. These oscillations look like a particle in the presence of a magnetic field, and it is clear that these motions are repelled

from the black disks. More precisely, the characteristic oscillation period of the trapped geodesics is very small with respect to the total time of numerical evolution T. Given the numerical evolution T, the geodesic has many oscillations that look as if they are filling the interior region. These show how the trajectory appears to be drifting slowly between different, almost integrable magnetically trapped orbits. The total time evolution of the geodesic is represented by the blue color in Figure 5.5.

We remark that the plot does not have the same scale in the x and y axes in order to better display the orbit of the geodesics. Because of this, the black regions that represent the locations of the disks are distorted. The Lyapunov exponents of this trajectory are all small and in our tests are consistent with values of zero. See the Appendix 5.7.

To more easily see that this orbit is actually chaotic, in Figures 5.6 and 5.7, we present three-dimensional projections of the dynamics where we can see that the system is slowly filling the available phase space. This is accomplished by coloring different portions of the evolution in different colors and superposing them on top of each other. If the system were integrable, the trajectory would only fill a 2-torus, rather than a 3d volume. This would be readily apparent. The long trajectory has not had enough time to fill its available phase space in 5.5. Because of this, our Lyapunov exponent computation does not make complete sense: in the numerical limit defining the Lyapunov exponents, one assumes that the orbit has approximately explored all of its available phase space before one believes that the numerical value of the exponent has converged.

In these 3d plots, we see that the null geodesic is filling out the phase space. Hence, we conclude that the system is chaotic, but with a small Lyapunov exponent (we deal with this in the Appendix 5.7), as the system seems to be quasi-adiabatically exploring the available phase space.

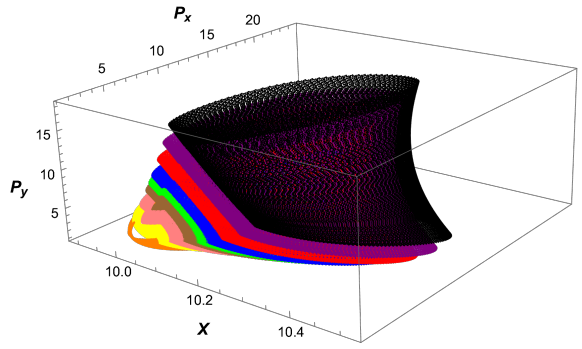


Figure 5.6: 3d projection of the phase space x, P_x, P_y.

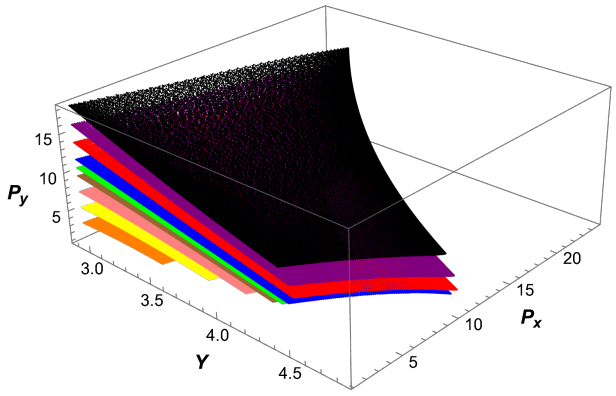


Figure 5.7: 3d projection of the phase space y, P_x, P_y.

5.6 Conclusion

In this chapter, we have studied a special set of null geodesics in the general LLM geometries. These null geodesics are restricted to motion in the LLM plane. The reason that such geodesics stay in the LLM plane is that the LLM plane is a degeneration locus of symmetry (one of the two 3-spheres goes to zero radius) and this fact guarantees that solutions that preserve the symmetry must stay confined to the LLM plane. Because we are at a degeneration locus, the angular momentum associated to the shrunken sphere vanishes. The null geodesics are allowed to carry an angular momentum L with respect to the remaining $SO(4)$. In our case, we have focused on situations where the angular momentum that is turned on is associated to the spatial symmetry of the boundary

S^3, rather than the R-charge. After the conserved quantities are taken into account, the effective motion is in two-dimensions and the corresponding phase space is four-dimensional. The motion is restricted to the region where the R-symmetry sphere is of zero size (the white region in our black and white coloring of the LLM geometries). There are some special solutions of LLM geometries that preserve an additional $U(1)$ symmetry of rotations of the LLM plane. In these cases, the null geodesics restricted to the LLM plane are integrable.

When we studied particular cases where the rotational symmetry is broken, we found that the null geodesics exhibited chaotic behavior. Also, in general, we found that solutions that minimize the LLM energy after fixing the angular momentum satisfy the constraint $E = L$, stay at a fixed position in the LLM plane, and can be located arbitrarily on the allowed locus of the LLM plane (the white region). These are associated with states that satisfy a BPS constraint. This degeneration is similar to that of a classical particle in the lowest Landau level in a magnetic field. When we increase the energy, the orbit precesses. In some situations, the orbit's center moves slowly in the LLM plane, as depicted in Figure 5.5, where $(E - L)/E$ is small.

Let us consider what are the possible consequences of our observations. First, null geodesics are a geometric optics limit of massless wave equations on the LLM geometry. We expect that there should a large class of BPS modes of supergravity fluctuations associated with these geodesics that do not move. The fact that they are classically soluble suggests that they may also be found analytically in the ten-dimensional geometry.

Secondly, the fact that these in-plane geodesics are chaotic is indicative that the non-BPS protected modes in the LLM geometry can only be solved numerically. The modes associated with chaotic motion should display level statistics typical of chaotic systems. It becomes interesting to ask to what extent they display the eigenstate thermalization hypothesis properties. Solving these issues can provide interesting thermalization

dynamics on these geometries.

More generally, we explored to what extent a generic LLM geometry might start looking like an incipient black hole. The interesting observation we have made is that the problem of solving these null geodesics becomes similar to a problem of chaotic billiards scattering in two dimensions. We expect that as we add more droplets the classical problem of *getting out of the black hole region* should resemble a problem of diffusive dynamics. Considering that we will eventually want to solve wave equations in these systems, one should try to understand to what extent other phenomena like Anderson localization due to the effective random potential might make certain modes much harder to probe than others.

These questions, once all symmetries are taken into account, should correspond to an eigenvalue problem of partial differential equations in three dimensions (the LLM plane variables x, y plus the extra ξ direction) that seem more tractable than other similar problems associated with fuzzball geometries, [241, 242, 243, 244, 245, 246, 247, 248, 249, 250]. Moreover, it would be interesting to study more elaborated frameworks, for instance the simplest nontrivial LLM geometry: the annulus, or configurations that involve geodesics outside of the LLM plane. We hope to tackle some of these problems in the near future.

5.7 Appendix: Small Lyapunov exponents

In this Appendix, we study numerically the effectively trapped geodesic discussed in section 5.5.1. Our goal is to measure the Lyapunov exponents. The maximum Lyapunov exponent is measured by taking an infinitesimal deformation δ in phase space and

checking how quickly it grows. The Lyapunov exponent is defined as

$$\lambda_{max} = \lim_{T\to\infty} \frac{1}{T} \log(|\delta(T)|/|\delta(0)|). \tag{5.22}$$

The natural question to ask is if the total time T is long enough to see that the maximum Lyapunov exponent is different from zero.

In an integrable system, the growth of the maximal stretching direction is linear in time T (the angle variables evolve linearly). The growth would therefore behave for large times as $\log(aT)$ and the Lyapunov exponent would only vanish in the $T \to \infty$ limit, decaying as $\log(T)/T$. We contrast the system we have with an integrable system by testing with a fit to $\log(T)/T$ in Figure 5.8.

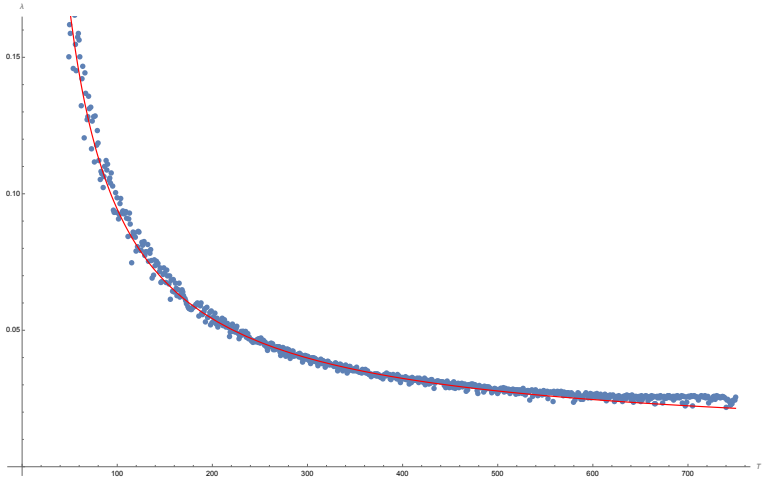


Figure 5.8: We plot the logarithm $\log(|\delta(T)|/|\delta(0)|)/T$ with respect to time. We show a fit of the corresponding quantity given by $0.00707 + 4.1227/T + \log(T)/T$ where $\lambda_{max} \simeq 0.00707$ is interpreted as the maximum Lyapunov exponent. The other parts of the fit serve to correct for the quasi-adiabatic almost integrable behavior for short time scales.

It is clear that since the fit to an integrable system is fairly good, we cannot yet distinguish the system from an integrable system: the Lyapunov exponents have not converged yet. The infinite time limit of the fit would go to zero and this is indicated by the maximum numerically evaluated Lyapunov exponent decaying slowly due to the

logarithmic contribution. The fit gets worse at later times, indicating that there is a small Lyapunov exponent that will remain nonzero in the infinite time limit. However, this exponent is much smaller than what we were able to compute with this extended trajectory.

Bibliography

[1] MICROSCOPE Collaboration, *MICROSCOPE mission: final results of the test of the Equivalence Principle*, Phys.Rev.Lett. 129 (2022) 12, 121102, arXiv:2209.15487 [gr-qc].

[2] M. Hassaine, J. Zanelli, *Chern-Simons (super) Gravity*, World Scientific, 2016.

[3] R. Arnowitt, S. Deser, C. Misner, *The Dynamics of General Relativity*, Gen.Rel.Grav. 40 (2008) 1997-2027, arXiv:gr-qc/0405109.

[4] H. Bondi, M. van der Burg, A. Metzner, *Gravitational waves in general relativity. 7. Waves from axisymmetric isolated systems*, Proc.Roy.Soc.Lond.A 269 (1962) 21-52.

[5] R. Sachs, *Asymptotic symmetries in gravitational theory*, Phys.Rev. 128 (1962) 2851-2864.

[6] J. Brown, M. Henneaux, *Central charges in the canonical realization of asymptotic symmetries: An example from three dimensional gravity*, Commun.Math.Phys. 104 (1986) 207-226.

[7] H. Nicolai, K. Peeters, M. Zamaklar *Loop quantum gravity: an outside view*, Class.Quant.Grav. 22 (2005) R193, arXiv:hep-th/0501114.

[8] J. Donoghue, *General relativity as an effective field theory: The leading quantum corrections*, Phys.Rev.D 50 (1994) 3874-3888, arXiv:gr-qc/9405057.

[9] R. Percacci, *An Introduction to Covariant Quantum Gravity and Asymptotic Safety*, World Scientific, 2017.

[10] S. Dimopoulos, S. Raby, F. Wilczek, *Supersymmetry and the scale of unification*, Phys.Rev.D 24 (1981) 1681-1683.

[11] J. Bekenstein, *Black holes and entropy*, Phys.Rev.D 7 (1973) 2333-2346.

[12] S. Hawking, *Particle Creation by Black Holes*, Commun.Math.Phys. 43 (1975) 199-220.

[13] G. Gibbons, S. Hawking, *Action Integrals and Partition Functions in Quantum Gravity*, Phys.Rev.D 15 (1977) 2752-2756.

[14] E. Witten, *Anti-de Sitter Space, Thermal Phase Transition, And Confinement In Gauge Theories*, Adv.Theor.Math.Phys. 2 (1998) 505-532, arXiv:hep-th/9803131.

[15] C. Stephens, G. 't Hooft, B. Whiting, *Black hole evaporation without information loss*, JHEP 03 (2003) 046, arXiv:gr-qc/9310006.

[16] L. Susskind, *The World as a hologram*, J.Math.Phys. 36 (1995) 6377-6396, arXiv:hep-th/9409089.

[17] A. Shomer, *A Pedagogical explanation for the non-renormalizability of gravity*, arXiv:0709.3555 [hep-th].

[18] D. Tong, *Lectures on String Theory*, arXiv:0908.0333 [hep-th].

[19] C. Maccaferri, F. Marino, B. Valsesia, *Introduction to String Theory*, SciPost Phys.Lect.Notes 90 (2025) 1, SciPost Phys.Lect.Notes 2025 (2025) 90, arXiv:2311.18111 [hep-th].

[20] M. Greene, J. Schwarz, *Anomaly Cancellation in Supersymmetric D=10 Gauge Theory and Superstring Theory*, Phys.Lett.B 149 (1984) 117-122.

[21] D. Gross, J. Harvey, E. Martinec, R. Rohm, *The Heterotic String*, Phys.Rev.Lett. 54 (1985) 502-505.

[22] T. Ortin, *Gravity and Strings*, 2nd ed. Cambridge University Press; 2015.

[23] H. Nastase, *Introduction to Supergravity and its Applications*, Cambridge University Press; 2024.

[24] I. Papadimitriou, *Aspects of the gauge gravity duality and holography*, PhD thesis; 2005.

[25] G. Horowitz, A. Strominger, *Black strings and P-branes*, Nucl.Phys.B 360 (1991) 197-209.

[26] J. Polchinski, *Dirichlet Branes and Ramond-Ramond charges*, Phys.Rev.Lett. 75 (1995) 4724-4727, arXiv:hep-th/9510017.

[27] A. Strominger, C. Vafa, *Microscopic Origin of the Bekenstein-Hawking Entropy*, Phys.Lett.B 379 (1996) 99-104, arXiv:hep-th/9601029.

[28] G. 't Hooft, *A Planar Diagram Theory for Strong Interactions*, Nucl.Phys.B 72 (1974) 461.

[29] J. Maldacena, *The Large N limit of superconformal field theories and supergravity*, Int.J.Theor.Phys. 38 (1999) 1113-1133 (reprint), Adv.Theor.Math.Phys. 2 (1998) 231-252, arXiv:hep-th/9711200 [hep-th].

[30] D. Berenstein, J. Maldacena, H. Nastase, *Strings in flat space and pp waves from $\mathcal{N}$=4 Super Yang Mills*, JHEP 04 (2002) 013, arXiv:hep-th/0202021.

[31] C. Herzog, D. Son, *Schwinger-Keldysh Propagators from AdS/CFT Correspondence*, JHEP 03 (2003) 046, arXiv:hep-th/0212072.

[32] D. Son, A. Starinets, *Minkowski space correlators in AdS / CFT correspondence: Recipe and applications*, JHEP 09 (2002) 042, arXiv:hep-th/0205051.

[33] K. Skenderis, S. Solodukhin, *Quantum effective action from the AdS/CFT correspondence*, Phys.Lett.B 472 (2000) 316-322, arXiv:hep-th/9910023.

[34] P. Kraus, F. Larsen, *Holographic Gravitational Anomalies*, JHEP 01 (2006) 022, arXiv:hep-th/0508218.

[35] S. Gubser, I. Klebanov, A. Polyakov, *Gauge theory correlators from noncritical string theory*, Phys.Lett.B 428 (1998) 105-114, arXiv:hep-th/9802109 [hep-th].

[36] E. Witten, *Anti-de Sitter space and holography*, Adv.Theor.Math.Phys. 2 (1998) 253-291, arXiv:hep-th/9802150 [hep-th].

[37] S. de Haro, K. Skenderis, S. Solodukhin, *Holographic Reconstruction of Spacetime and Renormalization in the AdS/CFT Correspondence*, Commun.Math.Phys. 217 (2001) 595-622, arXiv:hep-th/0002230.

[38] J. Deutsch, *Quantum statistical mechanics in a closed system*, Phys. Rev. A 43, 2046.

[39] M. Srednicki, *Chaos and Quantum Thermalization*, Phys.Rev.E 50 888, arXiv:cond-mat/9403051.

[40] R. Myers, T. Sierens, W. Witczak-Krempa, *A Holographic Model for Quantum Critical Responses*, JHEP 05 (2016) 073, arXiv:1602.05599 [hep-th].

[41] M. Grinberg, J. Maldacena, *Proper time to the black hole singularity from thermal one-point functions*, JHEP 03 (2021) 131, arXiv:2011.01004 [hep-th].

[42] V. Hubeny, S. Minwalla, M. Rangamani, *The fluid/gravity correspondence*, TASI (2010) 817-860, arXiv:1107.5780 [hep-th].

[43] F. Haehl, R. Loganayagam, M. Rangamani, *The Fluid Manifesto: Emergent symmetries, hydrodynamics, and black holes*, JHEP 01 (2016) 184, arXiv:1510.02494 [hep-th].

[44] P. Glorioso, H. Liu, *Lectures on non-equilibrium effective field theories and fluctuating hydrodynamics*, PoS TASI 2017 (2018) 008, arXiv:1805.09331 [hep-th].

[45] J. Maldacena, D. Stanford, Z. Yang, *Conformal symmetry and its breaking in two dimensional Nearly Anti-de-Sitter space*, PTEP 2016 (2016) 12, 12C104, arXiv:1606.01857 [hep-th].

[46] G. Sárosi, *AdS_2 holography and the SYK model*, PoS Modave2017 (2018) 001, arXiv:1711.08482 [hep-th].

[47] S. Mathur, *The Fuzzball proposal for black holes: An Elementary review*, Fortsch.Phys. 53 (2005) 793-827, arXiv:hep-th/0502050.

[48] I. Bena, E. Martinec, S. Mathur, N. Warner, *Fuzzballs and Microstate Geometries: Black-Hole Structure in String Theory*, arXiv:2204.13113 [hep-th].

[49] H. Lin, O. Lunin, J. Maldacena, *Bubbling AdS space and 1/2 BPS geometries*, JHEP 10 (2004) 025, arXiv:hep-th/0409174.

[50] D. Berenstein, *A Toy model for the AdS/CFT correspondence*, JHEP 07 (2004) 018, arXiv:hep-th/0403110.

[51] D. Berenstein, R. Mancilla, *Aspects of thermal one-point functions and response functions in AdS black holes*, Phys. Rev. D 107 (2023) 12, arXiv:2211.05144 [hep-th].

[52] R. Mancilla, *Generalized Euler Equation from Effective Action: Implications for the Smarr Formula in AdS Black Holes*. arXiv:2410.06605 [hep-th].

[53] A. Castro, R. Mancilla, I. Papadimitriou, *Near-extremal dynamics away from the horizon*. arXiv:2505.XXXX [hep-th].

[54] D. Berenstein, E. Maderazo, R. Mancilla, A. Ramirez, *Chaotic LLM billiards*, JHEP 08 (2024) 056, arXiv:2305.19321 [hep-th].

[55] D. Marolf, *States and boundary terms: Subtleties of Lorentzian AdS/CFT*, JHEP 05 (2005) 042, arXiv:hep-th/0412032.

[56] D. Berenstein, A. Miller, *Conformal perturbation theory, dimensional regularization, and AdS/CFT correspondence*, Phys.Rev.D 90 (2014) 8, 086011, arXiv:1406.4142 [hep-th].

[57] D. Berenstein, A. Miller, *Logarithmic enhancements in conformal perturbation theory and their real time interpretation*, Int.J.Mod.Phys.A 35 (2020) 29, 2050184, arXiv:1607.01922 [hep-th].

[58] D. Berenstein, R. Corrado, W. Fischler, J. Maldacena, *The Operator product expansion for Wilson loops and surfaces in the large N limit*, Phys.Rev.D 59 (1999) 105023, arXiv:hep-th/9809188.

[59] G. Horowitz, J. Santos, D. Tong, *Optical Conductivity with Holographic Lattices*, JHEP 07 (2012) 168, arXiv:1204.0519 [hep-th].

[60] G. Horowitz, J. Santos, D. Tong, *Further Evidence for Lattice-Induced Scaling*, JHEP 11 (2012) 102, arXiv:1209.1098 [hep-th].

[61] A. Donos, J. Gauntlett, *Holographic Q-lattices*, JHEP 04 (2014) 040, arXiv:1311.3292 [hep-th].

[62] S. Hartnoll, J. Santos, *Disordered horizons: Holography of randomly disordered fixed points*, Phys.Rev.Lett. 112 (2014) 231601, arXiv:1402.0872 [hep-th].

[63] D. Son, A. Starinets, *Minkowski space correlators in AdS/CFT correspondence: Recipe and applications*, JHEP 09 (2002) 042, arXiv:hep-th/0205051.

[64] M. Dodelson, A. Grassi, C. Iossa, D. Panea Lichtig, A. Zhiboedov, *Holographic thermal correlators from supersymmetric instantons*, SciPost Phys. 14 (2023) 5, 116, SciPost Phys. 14 (2023) 116, arXiv:2206.07720 [hep-th].

[65] A. Bhatta, T. Mandal, *Exact thermal correlators of holographic CFTs*, JHEP 02 (2023) 222, arXiv:2211.02449 [hep-th].

[66] M. Bianchi, D. Consoli, A. Grillo, J. Morales, *More on the SW-QNM correspondence*, JHEP 01 (2022) 024, arXiv:2109.09804 [hep-th].

[67] J. Barragán Amado, B. Carneiro Da Cunha and E. Pallante, *Scalar quasinormal modes of Kerr-AdS$_5$*, Phys.Rev.D 99 (2019) 10, 105006, arXiv:1812.08921 [hep-th].

[68] G. Aminov, A. Grassi, Y. Hatsuda, *Black Hole Quasinormal Modes and Seiberg–Witten Theory*, Annales Henri Poincare 23 (2022) 6, 1951-1977, arXiv:2006.06111 [hep-th].

[69] G. Bonelli, C. Iossa, D. Panea Lichtig, A. Tanzini, *Exact solution of Kerr black hole perturbations via CFT$_2$ and instanton counting: Greybody factor, quasinormal modes, and Love numbers*, Phys.Rev.D 105 (2022) 4, 044047, arXiv:2105.04483 [hep-th].

[70] G. Bonelli, C. Iossa, D. Panea Lichtig, A. Tanzini, *Irregular Liouville Correlators and Connection Formulae for Heun Functions*, Commun.Math.Phys. 397 (2023) 2, 635-727, arXiv:2201.04491 [hep-th].

[71] M. Blake, R. A. Davison and D. Vegh, *Horizon constraints on holographic Green's functions*, JHEP 01 (2020) 077, arXiv:1904.12883 [hep-th].

[72] D. Grabovsky, *Heavy States in 3d Gravity and 2d CFT*, JHEP 07 (2024) 287, arXiv:2403.13757 [hep-th].

[73] J. Maldacena, *Eternal Black Holes in AdS*, JHEP 04 (2003) 021, arXiv:hep-th/0106112.

[74] S. Hawking and D. Page, *Thermodynamics of Black Holes in anti-De Sitter Space*, Commun.Math.Phys. 87 (1983) 577.

[75] A. Karch, B. Robinson, *Holographic Black Hole Chemistry*, JHEP 12 (2015) 073, arXiv:1510.02472 [hep-th].

[76] S. Bhattacharyya, V. Hubeny, S. Minwalla, M. Rangamani, *Nonlinear Fluid Dynamics from Gravity*, JHEP 02 (2008) 045, arXiv:0712.2456 [hep-th].

[77] M. Rangamani, *Gravity and Hydrodynamics: Lectures on the fluid-gravity correspondence*, Class.Quant.Grav. 26 (2009) 224003, arXiv:0905.4352 [hep-th].

[78] A. Awad, C. Johnson, *Holographic Stress Tensors for Kerr-AdS Black Holes*, Phys.Rev.D 61 (2000) 084025, arXiv:hep-th/9910040.

[79] A. Awad, C. Johnson, *Higher Dimensional Kerr-AdS Black Holes and the AdS/CFT Correspondence*, Phys.Rev.D 63 (2001) 124023, arXiv:hep-th/0008211.

[80] S. Dubovsky, T. Gregoire, A. Nicolis, R. Rattazzi, *Null energy condition and superluminal propagation*, JHEP 03 (2006) 025, arXiv:hep-th/0512260.

[81] D. Nickel, D. Son, *Deconstructing holographic liquids*, New J.Phys. 13 (2011) 075010, arXiv:1009.3094 [hep-th].

[82] S. Dubovsky, L. Hui, A. Nicolis, D. Son, *Effective field theory for hydrodynamics: thermodynamics, and the derivative expansion*, Phys.Rev.D 85 (2012) 085029, arXiv:1107.0731 [hep-th].

[83] N. Banerjee, J. Bhattacharya, S. Bhattacharyya, S. Jain, S. Minwalla, T. Sharma, *Constraints on Fluid Dynamics from Equilibrium Partition Functions*, JHEP 09 (2012) 046, arXiv:1203.3544 [hep-th].

[84] K. Jensen, M. Kaminski, P. Kovtun, R. Meyer, A. Ritz, A. Yarom, *Towards hydrodynamics without an entropy current*, Phys.Rev.Lett. 109 (2012) 101601, arXiv:1203.3556 [hep-th].

[85] M. Crossley, P. Glorioso, H. Liu, *Effective field theory of dissipative fluids*, JHEP 09 (2017) 095, arXiv:1511.03646 [hep-th].

[86] M. Crossley, P. Glorioso, H. Liu, *Effective field theory of dissipative fluids (II): classical limit, dynamical KMS symmetry and entropy current*, JHEP 09 (2017) 096, arXiv:1701.07817 [hep-th].

[87] F. Haehl, R. Loganayagam, M. Rangamani, *Topological sigma models and dissipative hydrodynamics*, JHEP 04 (2016) 039, arXiv:1511.07809 [hep-th].

[88] F. Haehl, R. Loganayagam, M. Rangamani, *Schwinger-Keldysh formalism I: BRST symmetries and superspace*, JHEP 06 (2017) 069, arXiv:1610.01940 [hep-th].

[89] F. Haehl, R. Loganayagam, M. Rangamani, *Schwinger-Keldysh formalism II: Thermal equivariant cohomology*, JHEP 06 (2017) 070, arXiv:1610.01941 [hep-th].

[90] K. Jensen, R. Marjieh, N. Pinzani-Fokeeva, A. Yarom, *An entropy current in superspace*, JHEP 01 (2019) 061, arXiv:1803.07070 [hep-th].

[91] D. Kastor, S. Ray, J. Traschen, *Enthalpy and the Mechanics of AdS Black Holes*, Class.Quant.Grav. 26 (2009) 195011, arXiv:0904.2765 [hep-th].

[92] M. Cvetic, G. Gibbons, D. Kubiznak, C. Pope, *Black Hole Enthalpy and an Entropy Inequality for the Thermodynamic Volume*, Phys.Rev.D 84 (2011) 024037, arXiv:1012.2888 [hep-th].

[93] B. Dolan, *The cosmological constant and the black hole equation of state*, Class.Quant.Grav. 28 (2011) 125020, arXiv:1008.5023 [gr-qc].

[94] B. Dolan, *Pressure and volume in the first law of black hole thermodynamics*, Class.Quant.Grav. 28 (2011) 235017, arXiv:1106.6260 [gr-qc].

[95] B. Dolan, *Where is the PdV term in the first law of black hole thermodynamics?*, 2012 by INTECH, arXiv:1209.1272 [gr-qc].

[96] M. Visser, *Holographic thermodynamics requires a chemical potential for color*, Phys.Rev.D 105 (2022) 10, 106014, arXiv:2101.04145 [hep-th].

[97] Z. Gao, L. Zhao, *Restricted phase space thermodynamics for AdS black holes via holography*, Class.Quant.Grav. 39 (2022) 7, 075019, arXiv:2112.02386 [gr-qc].

[98] M. Ahmed, W. Cong, D. Kubizňák, R. Mann, M. Visser, *Holographic dual of extended black hole thermodynamics*, Phys.Rev.Lett. 130 (2023) 18, 181401, arXiv:2302.08163 [hep-th].

[99] R. Mann, *Recent Developments in Holographic Black Hole Chemistry*, JHAP 4 (2024) 1, 1-26, arXiv:2403.02864 [hep-th].

[100] Hai-Shan Liu, H. Lu, C. Pope, *Generalised Smarr Formula and the Viscosity Bound for Einstein-Maxwell-Dilaton Black Holes*, Phys.Rev.D 92 (2015) 064014, arXiv:1507.02294 [hep-th].

[101] J. Alfaro, R. Mancilla, *Thermodynamics of Graviton Condensate*, Eur.Phys.J.C 81 (2021) 10, 871, arXiv:2010.13225 [gr-qc].

[102] D. Kastor, *Komar Integrals in Higher (and Lower) Derivative Gravity*, Class.Quant.Grav. 25 (2008) 175007, arXiv:0804.1832 [hep-th].

[103] D. Kastor, S. Ray, J. Traschen, *Smarr Formula and an Extended First Law for Lovelock Gravity*, Class.Quant.Grav. 27 (2010) 235014, arXiv:1005.5053 [hep-th].

[104] T. Ortín, *Komar integrals for theories of higher order in the curvature and black-hole chemistry*, JHEP 08 (2021) 023, arXiv:2104.10717 [gr-qc].

[105] D. Mitsios, T. Ortín, D. Pereñíguez, *Komar integral and Smarr formula for axion-dilaton black holes versus S duality*, JHEP 08 (2021) 019, arXiv:2106.07495 [hep-th].

[106] R. Ballesteros, T. Ortin, *Generalized Komar charges and Smarr formulas for black holes and boson stars*, arXiv:2409.08268 [gr-qc].

[107] V. Balasubramanian, P. Kraus, *A Stress Tensor for Anti-de Sitter Gravity*, Commun.Math.Phys. 208 (1999) 413-428, arXiv:hep-th/9902121.

[108] R. Emparan, C. Johnson, R. Myers, *Surface Terms as Counterterms in the AdS/CFT Correspondence*, Phys.Rev.D 60 (1999) 104001, arXiv:hep-th/9903238.

[109] M. Henningson, K. Skenderis, *The Holographic Weyl anomaly*, JHEP 07 (1998) 023, arXiv:hep-th/9806087.

[110] M. Natsuume, *AdS/CFT Duality User Guide*, Lect.Notes Phys. 903 (2015) pp.1-294, arXiv:1409.3575 [hep-th].

[111] G. Basar, *Recent developments in relativistic hydrodynamic fluctuations*, arXiv:2410.02866 [hep-th].

[112] M. Knysh, H. Liu, N. Pinzani-Fokeeva, *New horizon symmetries, hydrodynamics, and quantum chaos*, JHEP 09 (2024) 162, arXiv:2405.17559 [hep-th].

[113] G. Ballesteros, D. Comelli, L. Pilo, *Thermodynamics of perfect fluids from scalar field theory*, Phys.Rev.D 94 (2016) 2, 025034, arXiv:1605.05304 [hep-th].

[114] I. Papadimitriou, K. Skenderis, *Thermodynamics of Asymptotically Locally AdS Spacetimes*, JHEP 08 (2005) 004, arXiv:hep-th/0505190.

[115] A. Frassino, J. Pedraza, A. Svesko, M. Visser, *Higher-dimensional origin of extended black hole thermodynamics*, Phys.Rev.Lett. 130 (2023) 16, 161501, arXiv:2212.14055 [hep-th].

[116] D. Kubiznak, R. Mann, M. Teo, *Black hole chemistry: thermodynamics with Lambda*, Class.Quant.Grav. 34 (2017) 6, 063001, arXiv:1608.06147 [hep-th].

[117] R. Mann, *The (Holographic) Chemistry of Black Holes*, Springer Proc.Phys. 392 (2024) 97-132.

[118] D. Kubiznak, R. Mann, *P-V criticality of charged AdS black holes*, JHEP 07 (2012) 033, arXiv:1205.0559 [hep-th].

[119] N. Altamirano, D. Kubiznak, R. Mann, Z. Sherkatghanad, *Kerr-AdS analogue of triple point and solid/liquid/gas phase transition*, Class.Quant.Grav. 31 (2014) 042001, arXiv:1308.2672 [hep-th].

[120] C. Johnson, *Holographic Heat Engines*, Class.Quant.Grav. 31 (2014) 205002, arXiv:1404.5982 [hep-th].

[121] D. Kastor, S. Ray, J. Traschen, *Chemical Potential in the First Law for Holographic Entanglement Entropy*, JHEP 11 (2014) 120, arXiv:1409.3521 [hep-th].

[122] I. Papadimitriou, *Holographic renormalization as a canonical transformation*, JHEP 11 (2010) 014, arXiv:1007.4592 [hep-th].

[123] I. Papadimitriou, *Lectures on Holographic Renormalization*, Springer Proc.Phys. 176 (2016) 131-181.

[124] J. de Boer, M. Heller, N. Pinzani-Fokeeva, *Effective actions for relativistic fluids from holography*, JHEP 08 (2015) 086, arXiv:1504.07616 [hep-th].

[125] M. Crossley, P. Glorioso, H. Liu, Y. Wang, *Off-shell hydrodynamics from holography*, JHEP 02 (2016) 124, arXiv:1504.07611 [hep-th].

[126] K. Jensen, *Chaos in AdS_2 holography*, Phys.Rev.Lett. 117 (2016) 11, 111601, arXiv:1605.06098 [hep-th].

[127] J. Cotler, K. Jensen, *A theory of reparameterizations for AdS_3 gravity*, JHEP 02 (2019) 079, arXiv:1808.03263 [hep-th].

[128] K. Nguyen, *Holographic boundary actions in AdS_3/CFT_2 revisited*, JHEP 10 (2021) 218, arXiv:2108.01095 [hep-th]

[129] H. Lu, Y. Pang, C. Pope, *AdS Dyonic Black Hole and its Thermodynamics*, JHEP 11 (2013) 033, arXiv:1307.6243 [hep-th]

[130] M. Cárdenas, O. Fuentealba, J. Matulich, *On conserved charges and thermodynamics of the AdS4 dyonic black hole*, JHEP 05 (2016) 001, arXiv:1603.03760 [hep-th]

[131] J. Koga, *Asymptotic symmetries on Killing horizons*, Phys.Rev.D 64 (2001) 124012, arXiv:gr-qc/0107096.

[132] M. Hotta, K. Sasaki, T. Sasaki, *Diffeomorphism on horizon as an asymptotic isometry of Schwarzschild black hole*, Class.Quant.Grav. 18 (2001) 1823-1834, arXiv:gr-qc/0011043.

[133] M. Hotta, *Holographic Charge Excitations on Horizontal Boundary*, Phys.Rev.D 66 (2002) 124021, arXiv:hep-th/0206222.

[134] L. Donnay, G. Giribet, H. Gonzalez, M. Pino, *Supertranslations and Superrotations at the Black Hole Horizon*, Phys.Rev.Lett. 116 (2016) 9, 091101, arXiv:1511.08687 [hep-th].

[135] L. Donnay, G. Giribet, H. Gonzalez, M. Pino, *Extended Symmetries at the Black Hole Horizon*, JHEP 09 (2016) 100, arXiv:1607.05703 [hep-th].

[136] L. Ciambelli, C. Marteau, A. Petkou, P. Petropoulos, K. Siampos, *Covariant Galilean versus Carrollian hydrodynamics from relativistic fluids*, Class.Quant.Grav. 35 (2018) 16, 165001, arXiv:1802.05286 [hep-th].

[137] L. Ciambelli, C. Marteau, A. Petkou, P. Petropoulos, K. Siampos, *Flat holography and Carrollian fluids*, JHEP 07 (2018) 165, arXiv:1802.06809 [hep-th].

[138] J. de Boer, J. Hartong, N. Obers, W. Sybesma, S. Vandoren, *Carroll symmetry, dark energy and inflation*, Front.in Phys. 10 (2022) 810405, arXiv:2110.02319 [hep-th],

[139] A. Petkou, P. Petropoulos, D. Rivera Betancour, K. Siampos, *Relativistic fluids, hydrodynamic frames and their Galilean versus Carrollian avatars*, JHEP 09 (2022) 162, arXiv:2205.09142 [hep-th].

[140] L. Freidel, P. Jai-akson, *Carrollian hydrodynamics from symmetries*, Class.Quant.Grav. 40 (2023) 5, 055009, arXiv:2209.03328 [hep-th].

[141] A. Bagchi, K. Kolekar, A. Shukla, *Carrollian Origins of Bjorken Flow*, Phys.Rev.Lett. 130 (2023) 24, 241601, arXiv:2302.03053 [hep-th].

[142] J. de Boer, J. Hartong, N. Obers, W. Sybesma, S. Vandoren, *Carroll stories*, JHEP 09 (2023) 148, arXiv:2307.06827 [hep-th].

[143] J. Armas, E. Have, *Carrollian fluids and spontaneous breaking of boost symmetry*, Phys.Rev.Lett. 132 (2024) 16, 161606, arXiv:2308.10594 [hep-th].

[144] C. Eling, Y. Oz, *On the Membrane Paradigm and Spontaneous Breaking of Horizon BMS Symmetries*, JHEP 07 (2016) 065, arXiv:1605.00183 [hep-th].

[145] C. Eling. *Spontaneously Broken Asymptotic Symmetries and an Effective Action for Horizon Dynamics*, JHEP 02 (2017) 052, arXiv:1611.10214 [hep-th].

[146] R. Penna, *Near-horizon BMS symmetries as fluid symmetries*, JHEP 10 (2017) 049, arXiv:1703.07382 [hep-th].

[147] L. Donnay, C. Marteau, *Carrollian Physics at the Black Hole Horizon*, Class.Quant.Grav. 36 (2019) 16, 165002, arXiv:1903.09654 [hep-th].

[148] W. Donnelly, L. Freidel, S. Moosavian, A. Speranza, *Gravitational Edge Modes, Coadjoint Orbits, and Hydrodynamics*, JHEP 09 (2021) 008, arXiv:2012.10367 [hep-th].

[149] A. Almheiri, J. Polchinski, *Models of AdS_2 Backreaction and Holography*, JHEP 11 (2015) 014, arXiv:1402.6334 [hep-th].

[150] J. Engelsöy, T. Mertens, H. Verlinde, *An Investigation of AdS2 Backreaction and Holography*, JHEP 07 (2016) 139, arXiv:1606.03438 [hep-th].

[151] V. Godet, C. Marteau, *New boundary conditions for AdS_2*, JHEP 12 (2020) 020, arXiv:2005.08999 [hep-th].

[152] R. Ruzziconi, C. Zwikel, *Conservation and Integrability in Lower-Dimensional Gravity*, JHEP 04 (2021) 034, arXiv:2012.03961 [hep-th].

[153] A. Sen, *Quantum Entropy Function from AdS_2/CFT_1 Correspondence*, Int.J.Mod.Phys.A 24 (2009) 4225-4244, arXiv:0809.3304 [hep-th].

[154] A. Sen, *Entropy Function and AdS_2/CFT_1 Correspondence*, JHEP 11 (2008) 075, arXiv:0805.0095 [hep-th].

[155] A. Sen, *Microscopic and Macroscopic Entropy of Extremal Black Holes in String Theory*, Gen.Rel.Grav. 46 (2014) 1711, arXiv:1402.0109 [hep-th].

[156] J. Preskill, P. Schwarz, A. Shapere, S. Trivedi, F. Wilczek, *Limitations on the statistical description of black holes*, Mod.Phys.Lett.A 6 (1991) 2353-2362.

[157] J. Maldacena, J. Michelson, A. Strominger, *Anti-de Sitter fragmentation*, JHEP 02 (1999) 011, arXiv:9812073 [hep-th].

[158] M. Cvetic, I. Papadimitriou, *AdS_2 Holographic Dictionary*, JHEP 12 (2016) 008, JHEP 01 (2017) 120 (erratum), arXiv:1608.07018 [hep-th].

[159] T. Mertens, G. Turiaci, *Solvable Models of Quantum Black Holes: A Review on Jackiw-Teitelboim Gravity*, Living Rev.Rel. 26 (2023) 1, 4, arXiv:2210.10846 [hep-th].

[160] G. Turiaci, *Les Houches lectures on two-dimensional gravity and holography*, arXiv:2412.09537 [hep-th].

[161] P. Chaturvedi, I. Papadimitriou, W. Song, B. Yu, *AdS3 gravity and the complex SYK models*, JHEP 05 (2021) 142, arXiv:2011.10001 [hep-th].

[162] E. Witten, *Coadjoint Orbits of the Virasoro Group*, Commun.Math.Phys. 114 (1988) 1.

[163] A. Cabo-Bizet, U. Kol, L. Pando Zayas, I. Papadimitriou, V. Rathee, *Entropy functional and the holographic attractor mechanism*, JHEP 05 (2018) 155, arXiv:1712.01849 [hep-th].

[164] A. Castro, F. Larsen, I. Papadimitriou, *5D Rotating Black Holes and the $nAdS_2/nCFT_1$ Correspondence*, JHEP 10 (2018) 042, arXiv:1807.06988 [hep-th].

[165] M. Geiller, C. Goeller, C. Zwikel, *3d gravity in Bondi-Weyl gauge: charges, corners, and integrability*, JHEP 09 (2021) 029, arXiv:2107.01073 [hep-th].

[166] R. McNees, C. Zwikel, *Finite Charges from the Bulk Action*, JHEP 08 (2023) 154, arXiv:2306.16451 [hep-th].

[167] M. Bañados, *Three-dimensional quantum geometry and black holes*, AIP Conf.Proc. 484 (1999) 1, 147-169, arXiv:hep-th/9901148.

[168] M. Bañados, C. Teitelboim, J. Zanelli, *The Black Hole in Three Dimensional Space Time*, Phys.Rev.Lett. 69 (1992) 1849-1851, arXiv:hep-th/9204099.

[169] M. Bañados, M. Henneaux, C. Teitelboim, J. Zanelli, *Geometry of the 2+1 Black Hole*, Phys.Rev.D 48 (1993) 1506-1525, arXiv:hep-th/9302012.

[170] A. Ghosh, H. Maxfield, G. Turiaci, *A universal Schwarzian sector in two-dimensional conformal field theories*, JHEP 05 (2020) 104, arXiv:1912.07654 [hep-th].

[171] M. Heydeman, L. Iliesiu, G. Turiaci, W. Zhao, *The statistical mechanics of near-BPS black holes*, J.Phys.A 55 (2022) 1, 014004, arXiv:2011.01953 [hep-th].

[172] S. Pal, J. Qiao, *Lightcone Modular Bootstrap and Tauberian Theory: A Cardy-like Formula for Near-extremal Black Holes*, Annales Henri Poincare 26 (2025) 3, 787-844, Annales Henri Poincare 25 (2024), arXiv:2307.02587 [hep-th].

[173] S. Deser and B. Tekin, *Massive, topologically massive, models*, Class.Quant.Grav. 19 (2002) L97-L100.

[174] S. Solodukhin, *Holographic Description of Gravitational Anomalies*, JHEP 07 (2006) 003, arXiv:0512216 [hep-th].

[175] P. Kraus, F. Larsen, *Holographic gravitational anomalies*, JHEP 01 (2006) 022, arXiv:0508218 [hep-th].

[176] W. Li, W. Song, A. Strominger, *Chiral Gravity in Three Dimensions*, JHEP 04 (2008) 082, arXiv:0801.4566 [hep-th].

[177] K. Hotta, Y. Hyakutake, T. Kubota, H. Tanida, *Brown-Henneaux's Canonical Approach to Topologically Massive Gravity*, JHEP 07 (2008) 066, arXiv:0805.2005 [hep-th].

[178] K. Skenderis, M. Taylor, B. van Rees, *Topologically Massive Gravity and the AdS/CFT Correspondence*, JHEP 09 (2009) 045, arXiv:0906.4926 [hep-th].

[179] W. Li, W. Song, and A. Strominger, *Comment on 'Cosmological Topological Massive Gravitons and Photons*, arXiv:0805.3101 [hep-th].

[180] D. Grumiller, N. Johansson, *Instability in cosmological topologically massive gravity at the chiral point*, JHEP 07 (2008) 134, arXiv:0805.2610 [hep-th].

[181] A. Maloney, W. Song, A. Strominger, *Chiral Gravity, Log Gravity and Extremal CFT*, Phys.Rev.D 81 (2010) 064007, arXiv:0903.4573 [hep-th].

[182] S. Solodukhin, *Holography with gravitational chern-simons term*, Phys.Rev.D 74 (2006) 024015, arXiv:0509148 [hep-th].

[183] A. Castro, B. Mühlmann, *Gravitational Anomalies in $nAdS_2/nCFT_1$*, Class.Quant.Grav. 37 (2020) 14, 145017, arXiv:1911.11434 [hep-th].

[184] S. Deser, R. Jackiw, S. Templeton, *Topologically massive gauge theories*, Annals Phys. 140 (1982) 372-411.

[185] S. Deser, R. Jackiw, S. Templeton, *Three-Dimensional Massive Gauge Theories*, Phys.Rev.Lett. 48 (1982) 975-978.

[186] S. Deser, X. Xiang, *Canonical formulations of full nonlinear topologically massive gravity*, Phys.Lett.B 263 (1991) 39-43.

[187] K. Moussa, G. Clement, C. Leygnac, *The black holes of topologically massive gravity*, Class.Quant.Grav. 20 (2003) L277-L283.

[188] A. Bouchareb, G. Clement, *Black hole mass and angular momentum in topologically massive gravity*, Class.Quant.Grav. 24 (2007) 5581-5594, arXiv:0706.0263 [hep-th].

[189] D. Anninos, W. Li, M. Padi, W. Song, and A. Strominger, *Warped ads_3 black holes*, JHEP 03 (2009) 130, arXiv:0807.3040 [hep-th].

[190] H. Saida, J. Sod, *Statistical entropy of BTZ black hole in higher curvature gravity*, Phys.Lett.B 471 (2000) 358-366, arXiv:gr-qc/9909061.

[191] P. Kraus, F. Larsen, *Microscopic black hole entropy in theories with higher derivatives*, JHEP 09 (2005) 034, arXiv:0506176 [hep-th].

[192] B. Sahoo, A. Sen, *BTZ Black Hole with Chern-Simons and Higher Derivative Terms*, JHEP 07 (2006) 008, arXiv:0601228 [hep-th].

[193] Y. Tachikawa, *Black hole entropy in the presence of Chern-Simons terms*, Class.Quant.Grav. 24 (2007) 737-744, arXiv:0611141 [hep-th].

[194] I. Robinson, A. Trautman, *Some spherical gravitational waves in general relativity*, Proc.Roy.Soc.Lond.A 265 (1962) 463-473.

[195] G. Bernardi de Freitas, H. Reall, *Algebraically special solutions in AdS/CFT*, JHEP 06 (2014) 148, arXiv:1403.3537 [hep-th].

[196] I. Bakas, K. Skenderis, *Non-equilibrium dynamics and AdS_4 Robinson-Trautman*, JHEP 08 (2014) 056, arXiv:1404.4824 [hep-th].

[197] J. Gath, A. Mukhopadhyay, A. Petkou, P. Petropoulos, K. Siampos, *Petrov Classification and holographic reconstruction of spacetime*, JHEP 09 (2015) 005, arXiv:1506.04813 [hep-th].

[198] I. Bakas, K. Skenderis, B. Withers, *Self-similar equilibration of strongly interacting systems from holography*, Phys.Rev.D 93 (2016) 10, 101902, arXiv:1512.09151 [hep-th].

[199] K. Skenderis, B. Withers, *Robinson-Trautman spacetimes and gauge/gravity duality*, PoS CORFU2016 (2017) 097, arXiv:1703.10865 [hep-th].

[200] L. Ciambelli, A. Petkou, P. Petropoulos, K. Siampos, *The Robinson-Trautman spacetime and its holographic fluid*, PoS CORFU2016 (2017) 076, arXiv:1707.02995 [hep-th].

[201] R. Fareghbal, I. Mohammadi, *Flat-space holography and correlators of Robinson–Trautman stress tensor*, Annals Phys. 411 (2019) 167960, arXiv:1802.05445 [hep-th].

[202] M. Nozawa, *Supersymmetry of the Robinson-Trautman solution*, JHEP 10 (2024) 201, arXiv:2408.04848 [hep-th].

[203] H. Adami, A. Parvizi, M. Sheikh-Jabbari, V. Taghiloo, *Heisenberg soft hair on Robinson-Trautman spacetimes*, JHEP 05 (2024) 191, arXiv:2402.17658 [hep-th].

[204] M. Nozawa, T. Torii, *Robinson–Trautman solutions with scalar hair and Ricci flow*, Class.Quant.Grav. 41 (2024) 6, 065016, arXiv:2310.05460 [hep-th].

[205] M. Adak, T. Dereli, Y. Senikoglu, *Non-riemannian description of robinson–trautman spacetimes in brans–dicke theory of gravity*, Int.J.Mod.Phys.D 28 (2019) 04, 1950070, arXiv:1807.07981 [hep-th].

[206] M. Ortaggio, J. Podolsky, M. Zofka, *Static and radiating p-form black holes in the higher dimensional Robinson-Trautman class*, JHEP 02 (2015) 045, arXiv:1411.1943 [hep-th].

[207] L. Ciambelli, S. Pasterski, E. Tabor, *Radiation in Holography*, arXiv:2410.06605 [hep-th].

[208] A. Almheiri, B. Kang, *Conformal Symmetry Breaking and Thermodynamics of Near-Extremal Black Holes*, JHEP 10 (2016) 052, arXiv:1606.04108 [hep-th].

[209] S. Hawking, S. Ross, *Duality between electric and magnetic black holes*, Phys.Rev.D 52 (1995) 5865-5876, arXiv:hep-th/9504019.

[210] D. Page, *Thermodynamics of near extreme black holes*, arXiv:0012020 [hep-th].

[211] L. Iliesiu, S. Murthy, G. Turiaci, *Revisiting the Logarithmic Corrections to the Black Hole Entropy*, arXiv:2209.13608 [hep-th].

[212] L. Iliesiu, S. Murthy, G. Turiaci, *Black hole microstate counting from the gravitational path integral*, arXiv:2209.13602 [hep-th].

[213] G. Turiaci, *New insights on near-extremal black holes*, arXiv:2307.10423 [hep-th].

[214] A. Cabo-Bizet, *The Schwarzian from gauge theories*, arXiv:2404.01540 [hep-th].

[215] D. Kapec, Y. Albert Law, C. Toldo, *Quasinormal Corrections to Near-Extremal Black Hole Thermodynamics*, arXiv:2409.14928 [hep-th].

[216] M. Kolanowski, D. Marolf, I. Rakic, M. Rangamani, G. Turiaci, *Looking at extremal black holes from very far away*, JHEP 04 (2025) 020, arXiv:2409.16248 [hep-th].

[217] D. Berenstein, *Submatrix deconfinement and small black holes in AdS*, JHEP 09 (2018) 054, arXiv:1806.05729 [hep-th].

[218] M. Hanada, G. Ishiki, H. Watanabe, *Partial Deconfinement*, JHEP 03 (2019) 145, JHEP 10 (2019) 029 (erratum), arXiv:1812.05494 [hep-th].

[219] C. Asplund, D. Berenstein, *Small AdS black holes from SYM*, Phys.Lett.B 673 (2009) 264-267, arXiv:0809.0712 [hep-th].

[220] I. Bena, E. Martinec, S. Mathur, N. Warner, *Snowmass White Paper: Micro- and Macro-Structure of Black Holes*, arXiv:2203.04981 [hep-th].

[221] V. Balasubramanian, D. Berenstein, A. Lewkowycz, A. Miller, O. Parrikar, C. Rabideau, *Emergent classical spacetime from microstates of an incipient black hole*, JHEP 01 (2019) 197, arXiv:1810.13440 [hep-th].

[222] D. Berenstein and A. Miller, *Superposition induced topology changes in quantum gravity*, JHEP 11 (2017) 121, arXiv:1702.03011 [hep-th].

[223] D. Berenstein and A. Miller, *Can Topology and Geometry be Measured by an Operator Measurement in Quantum Gravity?*, Phys.Rev.Lett. 118 (2017) 26, 261601, arXiv:1605.06166 [hep-th].

[224] A. Tyukov, R. Walker and N. Warner, *Tidal Stresses and Energy Gaps in Microstate Geometries*, JHEP 02 (2018) 122, arXiv:1710.09006 [hep-th].

[225] I. Bena, E. J. Martinec, R. Walker and N. Warner, *Early Scrambling and Capped BTZ Geometries*, JHEP 04 (2019) 126, arXiv:1812.05110 [hep-th].

[226] I. Bena, A. Houppe, N. Warner, *Delaying the Inevitable: Tidal Disruption in Microstate Geometries*, JHEP 02 (2021) 103, arXiv:2006.13939 [hep-th].

[227] E. Martinec, N. Warner, *The Harder They Fall, the Bigger They Become: Tidal Trapping of Strings by Microstate Geometries*, JHEP 04 (2021) 259, arXiv:2009.07847 [hep-th].

[228] F. C. Eperon, H. S. Reall, J. E. Santos, *Instability of supersymmetric microstate geometries*, JHEP 10 (2016) 031, arXiv:1607.06828 [hep-th].

[229] D. Marolf, B. Michel, A. Puhm, *A rough end for smooth microstate geometries*, JHEP 05 (2017) 021, arXiv:1612.05235 [hep-th].

[230] F. Eperon, *Geodesics in supersymmetric microstate geometries*, Class.Quant.Grav. 34 (2017) 16, 165003, arXiv:1702.03975 [gr-qc].

[231] I. Bena, F. Eperon, P. Heidmann, N. Warner, *The Great Escape: Tunneling out of Microstate Geometries*, JHEP 04 (2021) 112, arXiv:2005.11323 [hep-th].

[232] S. Corley, A. Jevicki, S. Ramgoolam, *Exact correlators of giant gravitons from dual N=4 SYM theory*, Adv.Theor.Math.Phys. 5 (2002) 809-839, arXiv:hep-th/0111222.

[233] D. Berenstein and S. Wang, *BPS coherent states and localization*, JHEP 08 (2022) 164, arXiv:2203.15820 [hep-th].

[234] M. Caldarelli, D. Klemm and P. Silva, *Chronology protection in anti-de Sitter*, Class.Quant.Grav. 22 (2005) 3461-3466, arXiv:hep-th/0411203.

[235] D. Berenstein, J. M. Maldacena and H. S. Nastase, *Strings in flat space and pp waves from N=4 superYang-Mills*, JHEP 04 (2002) 013, arXiv:hep-th/0202021.

[236] D. Berenstein and A. Holguin, *Open giant magnons on LLM geometries*, JHEP 01 (2021) 080, arXiv:2010.02236 [hep-th].

[237] S. Shenker and D. Stanford, *Black holes and the butterfly effect*, JHEP 03 (2014) 067, arXiv:1306.0622 [hep-th].

[238] J. Maldacena, S. H. Shenker and D. Stanford, *A bound on chaos*, JHEP 08 (2016) 106, arXiv:1503.01409 [hep-th].

[239] Y. Chervonyi and O. Lunin, *(Non)-Integrability of Geodesics in D-brane Backgrounds*, JHEP 02 (2014) 061, arXiv:1311.1521 [hep-th].

[240] P. Basu and L. Pando Zayas, *Chaos rules out integrability of strings on $AdS_5 \times T^{1,1}$*, Phys.Lett.B 700 (2011) 243-248, arXiv:1103.4107 [hep-th].

[241] V. Cardoso, A. Miranda, E. Berti, H. Witek and V. Zanchin, *Geodesic stability, Lyapunov exponents and quasinormal modes*, Phys.Rev.D 79 (2009) 6, 064016, arXiv:0812.1806 [hep-th].

[242] I. Bena, D. Turton, R. Walker and N. Warner, *Integrability and Black-Hole Microstate Geometries*, JHEP 11 (2017) 021, arXiv:1709.01107 [hep-th].

[243] M. Bianchi, D. Consoli and J. Morales, *Probing Fuzzballs with Particles, Waves and Strings*, JHEP 06 (2018) 157, arXiv:1711.10287 [hep-th].

[244] M. Bianchi, D. Consoli, A. Grillo and J. Morales, *The dark side of fuzzball geometries*, JHEP 05 (2019) 126, arXiv:1811.02397 [hep-th].

[245] M. Bianchi, A. Grillo and J. Morales, *Chaos at the rim of black hole and fuzzball shadows*, JHEP 05 (2020) 078, arXiv:2002.05574 [hep-th].

[246] M. Bianchi, D. Consoli, A. Grillo, J. Morales, *Light rings of five-dimensional geometries*, JHEP 03 (2021) 210, arXiv:2011.04344 [hep-th].

[247] F. Bacchini, D. Mayerson, B. Ripperda, J. Davelaar, H. Olivares, T. Hertog, B. Vercnocke, *Fuzzball Shadows: Emergent Horizons from Microstructure*, Phys.Rev.Lett. 127 (2021) 17, 171601, arXiv:2103.12075 [hep-th].

[248] A. Addazi, S. Capozziello, S. Odintsov, *Chaotic solutions and black hole shadow in $f(R)$ gravity*, Phys.Lett.B 816 (2021) 136257, arXiv:2103.16856 [hep-th].

[249] P. Heidmann, I. Bah, E. Berti, *Imaging topological solitons: The microstructure behind the shadow*, Phys.Rev.D 107 (2023) 8, 084042, arXiv:2212.06837 [hep-th].

[250] M. Emelin, S. Massai, *A note on integrability loss in fuzzball geometries*, Fortsch.Phys. 71 (2023) 8-9, 2300120, arXiv:2305.11793 [hep-th].